Wave Propagation in Flexible Tubes

A thesis submitted for the degree for Doctor of Philosophy

by

Jiling Feng

School of Engineering and Design
and Institute of Bioengineering
Brunel University

May 2008

Abstract

Wave dissipation was previously investigated intensively in the frequency domain, in which the dissipation of waves is described as attenuation of pressure pulse decay with respect to the frequency or harmonics. In this thesis, wave dissipation, including decay of pressure pulse, peak of wave intensity and wave energy, is investigated in the time domain using wave intensity analysis (WIA). Wave intensity analysis benefits to this research in several aspects including: **1)** WIA allows for wave dissipation investigated in the time domain; **2)** WIA does not make any assumptions about the tube's wall non-linearity and the analysis takes into account the effects of the vessel's wall viscoelastic properties, convective, frictional effects and fluid viscosity; **3)** WIA offers a technique (separation) to study wave dissipation in one direction whilst taking into account the effect of reflections from the opposite direction; **4)** The physical meaning of wave intensity provides a convenient method to study the dissipation of energy carried by the waves along flexible tubes.

In this research, it is found that the degree of dissipation in flexible tube were not only affected by the mechanical properties of the wall property and viscosity of liquid but also by the other factors including initial pressure and pumping speed of piston as well as direction of wave in relation to direction of flow.

Also an new technique to separate waves into forward and backward directions only using diameter and velocity might potentially be used to separate the waves in both directions non-invasively based on the non-invasive measurement of diameter (wall movement) available.

Table of Content

Chapter 1 Introduction 1
1.1 Background 1
1.2 Historical and clinical review 1
1.2.1. Wave propagation in frequency domain 1
1.2.2. Wave propagation in time domain 5
1.2.3 Arrival time of reflected wave 7
1.2.4 Wave speed 7
1.3 Motivation 9
1.4 Aims 12
Figures 13

Chapter 2 Theoretical Analysis 14
2.1 Introduction 14
2.2 Governing equations 17
2.3 Wave separation 21
2.4 Wave Intensity Analysis 22
2.5 Wave speed determined by PU-loop 22
2.6 Reflected waves 23
2.6.1 The type of reflection sites 23
2.6.2 Types of reflected wave 23
Figures 25

Chapter 3 Methods and instrumentation 30
3.1 Experimental setup 30
3.2 Measurements 32
3.3 Calibration 32
3.4 Static property test 33
3.5 Reproducibility 34
3.6 Statistics methods 35
3.6.1 Normalization 35
3.6.2 Curve fitting 35
Figures 37

Chapter 4 Wave dissipation in time domain 43
4.1 Wave dissipation in the different sized tubes 43
4.1.1 Introduction 43
4.1.2 Results 44
4.1.2.1 Wave speed and the static compliance 44
4.1.2.2 Dissipation of pressure wave 44
4.1.2.3 Dissipation of wave intensity and wave energy 45
4.1.2.4 The effect of the tube size on wave dissipation 45
4.2 Wave dissipation at different experimental conditions 47
4.2.1 Introduction 47
4.2.3 Results 48
4.2.3.1 The effect of initial pressure on wave dissipation 48
4.2.3.2 The effect of pumping speed of piston on wave dissipation 50

4.3 Effect of viscosity of liquid on wave dissipation 51
4.3.1. Introduction 51
4.3.2. Results 52
4.3.2.1 Effect of viscosity on wave speed 52
4.3.2.2 The effect of viscosity on wave dissipation 53
4.4 The effect of tube wall on wave dissipation 53
4.4.1 Introduction 53
4.4.2 Result 55
4.4.2.1 Wave speed, compliance and distensibility 55
4.4.2.2 Effect of stiffness of tube wall on wave dissipation 55
4.5 Discussion 56
4.5.1 Dissipation of the separated pressure waveforms 57
4.5.2 Dissipation of wave energy 58
4.5.3 Effect of size on wave dissipation 59
4.5.4. Effect of experimental conditions on wave dissipation 60
4.5.5 Effect of viscosity 61
4.5.6 Effect of property of tube wall 62
4.5.7 Sources of wave dissipation 63
4.5.8The limitation 64
Figures 65

Chapter 5 Dissipation of waves during pushing and pulling actions 94
5.1 Clinical background of the wave with pulling effect 94
5.2 Methods 95
5.2.1 Experiment setup 96
5.2.2 Instrumentation 96
5.3 Analysis 97
5.3.1 Waves with the pushing and pulling action 97
5.3.2 Compression and expansion waves 97
5.3.3 Wave intensity analysis (WIA) 98
5.4 Results 99
5.4.1 Wave speed 99
5.4.2 The amplitude of measured pressure and velocity 100
5.4.3 The forward pressure: 100
5.4.4 Wave intensity and energy: dI_+ and I_+ 101
5.5 Discussion 102
Figures 118

Chapter 6 Determination of wave speed and separation of waves using diameter and velocity 120
6.1 Introduction 120
6.2 Theory 123
6.2.1 Separation of wave using diameter and velocity 123
6.2.2 Determination of wave intensity using diameter and velocity 125
6.2.3 DU-loop method 125
6.3 Method 125
6.3.1 Experimental setup 126
6.3.2 Instrumentation 127
6.3.3 Analysis 127

6.4 Results 128
6.4.1 Wave speed determined by PU-loop and DU-loop 128
6.4.2 Arrival time of reflected waves (Trw) 129
6.4.3 Timing of key points 130
6.4.4 Comparison of P and D 131
6.4.5 Peak values at key points 131
6.5 Discussion 132
6.5.1 Significance of DU-loop determining wave speed 134
6.5.2 Importance of WI determined by diameter and velocity 134
Figures 138

Chapter 7 Discussion and conclusions 157
Future Work: 161
List of publications 162
Reference 163

Acknowledgement

Firstly, I would like to express my sincere gratitude to Dr Ashraf Khir for his excellent supervision, support and patience. Thanks to his knowledge on biomechanics engineering, I start to understand propagation of blood wave in human body.

Secondly, I would like to express my deep thanks to Professor Colin Clark for his constant support and helpful discussions throughout my study.

In addition, I would like to offer my thanks to my family for their faithful support in all respects. I would like to give my deep thankfulness and respect to my parents, who always care about my study and life although they are very far away from me.

I also would like to thank all the biofluid group members (Chloe page, Christina Kolyva, Marcel Swalen, Giovanni Biglino, Francesco Clavica, Karnal Patel, Ye Li) for their help and friendship.

Chapter 1

Introduction

1.1 Background

The character of the arterial pulse has long been an important part of the clinical evaluation of patients with cardiovascular diseases (Murgo et al., 1980). The features of pressure and flow wave propagation along the aorta, including amplification of pressure wave and steeping of the wave front, has also been well recognized (Murgo et al. 1980, 1981), **Figure1.1**. Several mechanisms that have been suggested to explain these features are (1) dissipation of waves; (2) effect of reflected waves; (3) effect of the increasing elastic stiffness; (4) tapering of aorta and (5) non-linear elastic behaviour of arteries (Mcdonald 1974). Wave attenuation, a parameter is used to express decay of pressure pulse against the frequencies, received little attention. The knowledge of relative contribution of these factors to the shape of pressure and flow waveform along the aorta, including wave dissipation, would offer valuable information to the diagnosis of cardiovascular diseases. This project is mainly concerned with the pattern of wave dissipation, including pressure pulse, wave intensity and wave energy, along the travelled distance. Also, this project aims to investigate the effect of reflected waves, elastic property of vessel wall and experimental conditions on wave dissipation.

1.2 Historical and clinical review

1.2.1. Wave propagation in frequency domain

Wave propagation in flexible tubes and arteries has been studied extensively (Westerhof et al., 1972; Bertram, 1980; Taylor, 1959; Bergel, 1961). Previous work was mostly carried out in the frequency domain through impedance approach using Fourier transform, in which the complex propagation coefficient that varies with frequency was used to describe both pulse wave velocity and attenuation (Mcdonald et al., 1968, Taylor, 1959).

Bergel made the first predictions of attenuation using the measurement of the complex elastic properties of excised vessels (Bergel, 1961a, b). However, the direct measurement of this parameter in arteries in vivo is difficult due to the presence of reflected waves (Mcdonald et al., 1968). To determine the complex elastic properties in the presence of reflected waves, the three-point method was proposed by Taylor (1959) and then was extended by McDonald and Gessner(1968). This technique has also been used by Learoyd and Taylor (1966) and extended to the study of arteries in vivo by Gow and Taylor (1968). However, the limitation of this technique lies in its experimental difficulty of the placement and precise matching of three manometers in the arteries, which restricted the investigation of the attenuation using three-point method throughout the arterial tree (Mcdonald,1974). The results from Bergel (1961b) were compared to the results from three-point method in the thoracic and also compared to the attenuation expected when only the viscosity of liquid was considered. All the results demonstrated that the measured attenuation in the artery is much higher than that expected when only viscosity of the blood was considered (Pedley, 1980).

Milnor and Nichols devised a method only requiring two observation sites with measurement of pressure and flow to investigate the propagation of blood flow (Milnar and Nichols, 1975). Milnor and Bertram also investigated the relation between arterial viscoelasticity and wave propagation in the canine femoral artery in vivo using their own method, which was introduced by Milnor and Nichols in 1975, and concluded that the dissipation is greater than that predicted by the linear models in a blood vessel of given dimensions and viscoelasticity (Milnor and Nichols, 1978). Newman and Greenwald also carried out experimental work on wave propagation and found that impulse waves attenuated along the distance travelled as an approximately mono-exponential function in both latex rubber tubes and the aorta of dogs (Newman et al. 1981; Greenwald, et al.,1985).

Anliker and his colleagues (Anliker et al., 1968a; 1968b; 1969; 1971; Histand et al., 1973; Moritz et al., 1974) studied the dispersion and attenuation of small artificial pressure waves in the canine arteries and veins by using finite sine waves trains superimposed on the naturally pressure fluctuations. They found for the frequency range considered that amplitude of small waves attenuated exponentially with the distance travelled.

Theoretical analysis on the complex properties of visco-elastic wall facilitates the comparison between the mathematical simulation and experimental results. Horsten studied the dissipation of pulsatile waves in viscoelastic tubes using a one-dimensional linear model and found that the viscoelastic behaviour of the tube's wall dominate the damping of the pressure pulse (Horsten et al., 1989). By comparing his experimental results with linear and non-linear modelling results, Reuderink found that disregarding the

viscoelastic properties of the tube's wall results in an underestimation in the damping (Reuderink et al. 1989). They also found that the linear viscoelastic Womersley model (Womersley, 1957) describes the pulse wave dissipation of the non-linear system satisfactorily.

It appears that there is still a considerable disparity in estimating the degree of wave dissipation, despite the extensive work on wave dissipation. To investigate the causes of disparity on the estimation of wave dissipation coefficient, Ursino and Bertram compared different methods, which were employed to determining wave propagation coefficient, but arrived to different conclusions (Ursino, et al.1992, 1994; Bertram et al. 1997). Ursino argued that the experimental methods, such as the three-point method, proposed by Taylor (1959) and used by Mcdonald and Gessner (1968), are the sources of inaccuracy of the attenuation values. Bertram however, concluded that the discrepancy is not caused by the experimental methods, but rather by the experimental conditions, such as blood pressure and the placement position of pressure transducers (Bertram, et al. 1997).

In addition, there is also a disagreement regarding the cause of wave dissipation. Bertram studied the energy dissipation and pulse wave attenuation in the canine carotid artery and concluded that wall viscoelasticity contributes relatively little to energy dissipation per cardiac cycle and pulse wave attenuation (Bertram, et al. 1980). More recently, Bertram concluded that "Relative contribution to energy dissipation of wall viscoelasticity and viscous shear depend strongly on the size of vessels"(Bertram, et al. 1997). He also implied in this study that the main sources of dissipation of bigger sizes of tube was viscoelastic vessels, while viscosity of blood was mostly the cause of wave

dissipation for small-sized vessels. However, three main causes accounting for the attribution of waves dissipation were suggested in Anliker's study (1) dissipation mechanisms in the vessel wall; (2) radiation of energy into the surrounding tissue or vascular bed; and (3) viscosity of blood. They also demonstrated experimentally that the effect of surrounding medium play a minor role in their study and demonstrated theoretically that the viscosity of the blood can account for only a small fraction of the observed attenuation for the frequency range in their study (Jones and Anliker, 1971a; 1971b). Therefore, they concluded that the dissipation of pressure waves must be attributed primarily to viscosity of vessel wall.

Most of work carried out in investigating wave dissipation to date used only the measured pressure waves. However, it is well accepted that the measured pressure is made of the interaction between the incident and reflected waves (Westerhof, et al., 1972). Therefore, studying the dissipation of waves travelling in one direction using the measured pressure will almost certainly be affected by the waves travelling in the other direction, which may lead to inaccuracies in determining the pattern by which waves dissipate along a specific direction. Bertram investigated the pulse wave attenuation measurement in nonlinearly elastic tubes using linear and nonlinear method (Bertram, et al. 1999). In his research, he found the separation of the measured pulse into forward and backward waves by either linear or non-linear means produced similar results; for the forward-going waves (downstream) the attenuation values were comparable to those found by the linear methods but the backward-going waves gave physically unreasonable attenuation results.

1.2.2. Wave propagation in time domain

As discussed above, arterial wave propagation had been mainly assessed in the frequency domain using impedance approach, the results of which are normally interpreted as a function of harmonics. A new analysis tool, wave intensity analysis (WIA), proposed by Parker and Jones (1988), allows for assessment of arterial wave in time domain, which is more intuitively than impedance approach and other techniques such as three points method in frequency domain. In addition, using WIA, the measured pressure and flow wave can be separated into forward and backward elements in time domain (Parker and Jones, 1990).

The concept of wave intensity (WI) is the analogue of the acoustic intensity in the theory of sound waves (Jones et al., 1994). WI is the measure of the energy flux transported by waves in the cardiovascular system and carry the information about both upstream and downstream events when it is measured at a given sites of arteries. Although WI is very small compared with total power of the ventricle, it can provide the important information about the change of working condition of heart as it acts with arterial system. Since the WI was introduced to the cardiovascular studies (Parker and Jones, 1988), it has been proven to be useful and regarded as a hemodynamic index in studying waves in the aorta (Koh et al., 1998; Khir and Parker, 2005), in the coronary arteries (Sun et al. 2003; Davies et al. 2006) and in the carotid artery (Niki et al, 1999, 2002).

The propagation of arterial pressure wave in the cardiovascular system and the mechanism of arterial pressure waveform has been investigated in time domain by a few bio-scientists using WIA. Parker studied arterial pressure wave propagation in the aorta and concluded that non-linearity of arterial tree is

mainly responsible for the profile of arterial pressure waveform (Jones, et al. 1992). Wang also studied wave propagation in the circulation using a complex numerical model and concluded that the complex pattern of wave propagation is a dominant factor to determine the aortic pressure and velocity waveforms (Wang, et al., 2004). Up to date the dissipation of wave in the arterial system has not been studied either in vitro or in vivo with time domain techniques.

1.2.3 Arrival time of reflected wave

The pressure waveform recorded in the arteries can be described as the sum of the forward pressure wave generated by the heart and the backward reflected pressure wave from the peripheral arteries (Nichols, W.W. and O'Rourke, M.F., 2005). The arrival time of reflected waves to the ascending aorta is of physiological importance (Ueda et al. 2004). Several methods have been proposed to identify the arrival time of reflected waves. Westerhof used the input impedance to calculate the distance to the apparent reflection site, from which, they determined the arrival time of reflected waves (Westerhof et al, 1972). Murgo suggested that the temporal difference from the initial pressure upstroke to the pressure inflection point is the time that it takes the wave to run forward, be reflected and arrive back (Murgo et al. 1980). Parker and Jones introduced wave intensity analysis (WIA) for studying travelling waves in arteries, which allows for the separation of waves into their forward and backward directions (Parker et al. 1990). Onset of backward wave can be used as the arrival time of reflected wave because of the WIA is a time domain technique.

1.2.4 Wave speed

The determination of arrival time of the reflected wave usually required the knowledge of wave speed. It is known that wave speed is one of key factors describing the wave propagation of blood flow in arteries. Local wave speed is mainly related to the elastic property of arterial wall (Milnor,1989). With the increase of age, wave speed in the arteries increases with an increase in blood pressure, due to the stiffer of arterial wall. Increase of wave speed is associated with cardiovascular diseases such as atherosclerosis and arteriosclerosis (Benetos *et al*. 2002).

Wave speed is the speed by which disturbance travels along the medium. In frequency domain, wave speed is described as phase velocity, C_p, which is function of harmonics and determined by the difference of phase angles of the individual harmonics of two pressure recordings taken at two locations. Wave speed determined by phase angle might be affected by the reflected wave, which limited the accuracy of this technique (Latham *et al*, 1988).

Theoretically, wave speed in the thin walled elastic tube can be determined by Moens-Kortweg equation, $c = \sqrt{\frac{Eh}{\rho D}}$, if the fluid is assumed to be incompressible (Kortweg, 1878; Moens, 1878), where, c is the wave speed, E is the Young's modules of tube wall, h is the wall thickness, ρ is density of liquid and D is the diameter of tube

The conventional way to measure wave speed is based on foot-to-foot method. This method has been used extensively and the results confirm that the wave speed in the aorta is not uniform; a significant increase is observed

distally (Latham *et al.,* 1985). Several methods have been used to determine local wave speed at the measurement site. Latham used the characteristic impedance to determine the local wave speed (Latham et al. 1987). Khir proposed PU-loop method to determine the wave speed using one-point measurements of pressure and velocity (Khir, et al. 2001). Harada also use the principle of the water-hammer equation to determine the wave speed online (Harada, et al., 2002). In addition, Harada derived wave speed from the stiffness parameter of the artery. Davies introduced a new technique for determining local wave speed also based on the measurements of the pressure and flow at the same site (Davies et al. 2006).

1.3 Motivation

Historical review reveals that the following issues remain to be unsolved:

(1) Despite the fact that wave dissipation was studied extensively, there is still considerable disparity on the estimation of its degree. Firstly, there is always scatter, which is quantified by error bars (Bertram et al., 1995). Secondly, there is a disagreement between the results achieved by different groups. For example, the source of disparity on degree of dissipation given by Ursino (1994) is opposite to that given by Bertram (1997).

(2) The dissipation predicted theoretically is not quantitatively consistent with that measured experimentally (Bertram, et al. 1999).

(3) There is also disparity regarding the source of dissipation, although most research groups tends to accept that viscoelastic of wall dominate wave dissipation (Pedley, 1980), which is based on the underestimation of dissipation if only viscosity is considered.

(4) Previous works on wave dissipation were mainly investigated in the frequency domain using Fourier analysis (Bertram, 1997, 1999, Anliker, 1971, 1973). The deficiency of Fourier analysis is that it considers system under investigation in a steady state and difficult to be used to examine the transient events. In addition, the assumption of linear relationship between pressure and flow in Fourier analysis is also unrealistic.

(5) Using only measured pressure wave to examine the dissipation without taking account of the reflected wave would probably lead to misleading results. Hence, it is required that waves are separated into forward and backward directions for the investigation of wave dissipation.

(6) Mostly, measuring wave dissipation to date required at least four measurements simultaneously, such as three-point method, which required measuring the pressure at three points and flow in the middle position. Milnor-Nichole method requires simultaneous measurements of pressure and flow at two different sites in the blood vessels.

(7) It was pointed out that "The energy dissipation during wave travel, which is expressed as attenuation is probably the most important parameter in arterial haemodynamics" (Mcdonald, 1974). The energy dissipation here indicates the attenuation against the frequencies. The physical meaning of wave intensity, which is wave energy flux per cross-sectional area, also dissipated along the travelling distance. To date, the dissipation of the energy carried by the travelling wave, which is expressed as decay of wave intensity, have not been investigated. ,

(8) The wave dissipation was only investigated for the waves with "pushing effect" although the waves with "pulling effect" are important in the

cardiovascular system. As much as explored insofar, propagation of wave with "pulling effect" has not been thoroughly studied in either in vitro or in vivo regardless of time or frequency domain.

To measure the wave dissipation reliably, the technique of separation of wave into forward and backward direction is necessary. Westerhof et al. (1972) proposed the impedance method for separation of waves and Pythoud et al. (1996 a, b) also use the linear and non-linear methods to separate the waveforms in frequency domain. WIA allows for separation of waves into forward and backward directions in the time domain using the characteristic solution for one-dimensional flow in elastic tube. The approach of WIA has several benefits to this research, which will be discussed in the Chapter 2.

In general, WIA provides an approach to analyse wave dissipation in the time domain rather than in the frequency domain, therefore, the results interpreted in terms of time and space would be more understandable. Furthermore, the dissipation displayed in both forward and backward direction would be valuable and reliable.

In addition, as discussed, the arrival time of reflected wave is physiologically important. WIA allows us to determine the arrival time of reflected waves using backward waveforms. Furthermore, as is known, separation of waves into forward and backward directions using WIA is based on measurement of pressure and velocity, where, the pressure was usually measured invasively. Therefore, we consider developing a method to separate waves using diameter and velocity, which might be potentially used to separate the wave non-invasively.

1.4 Aims

The aims of this thesis therefore are: (1) to investigate wave propagation (wave speed and dissipation) in flexible tube in time domain under the different conditions using WIA; (2) to compare the propagation of wave during pushing and pulling effect; (3) to develop a mathematic method determining the wave speed and separation of wave using the measured diameter and velocity directly and then the arrival time of reflected wave will be potentially determined non-invasively.

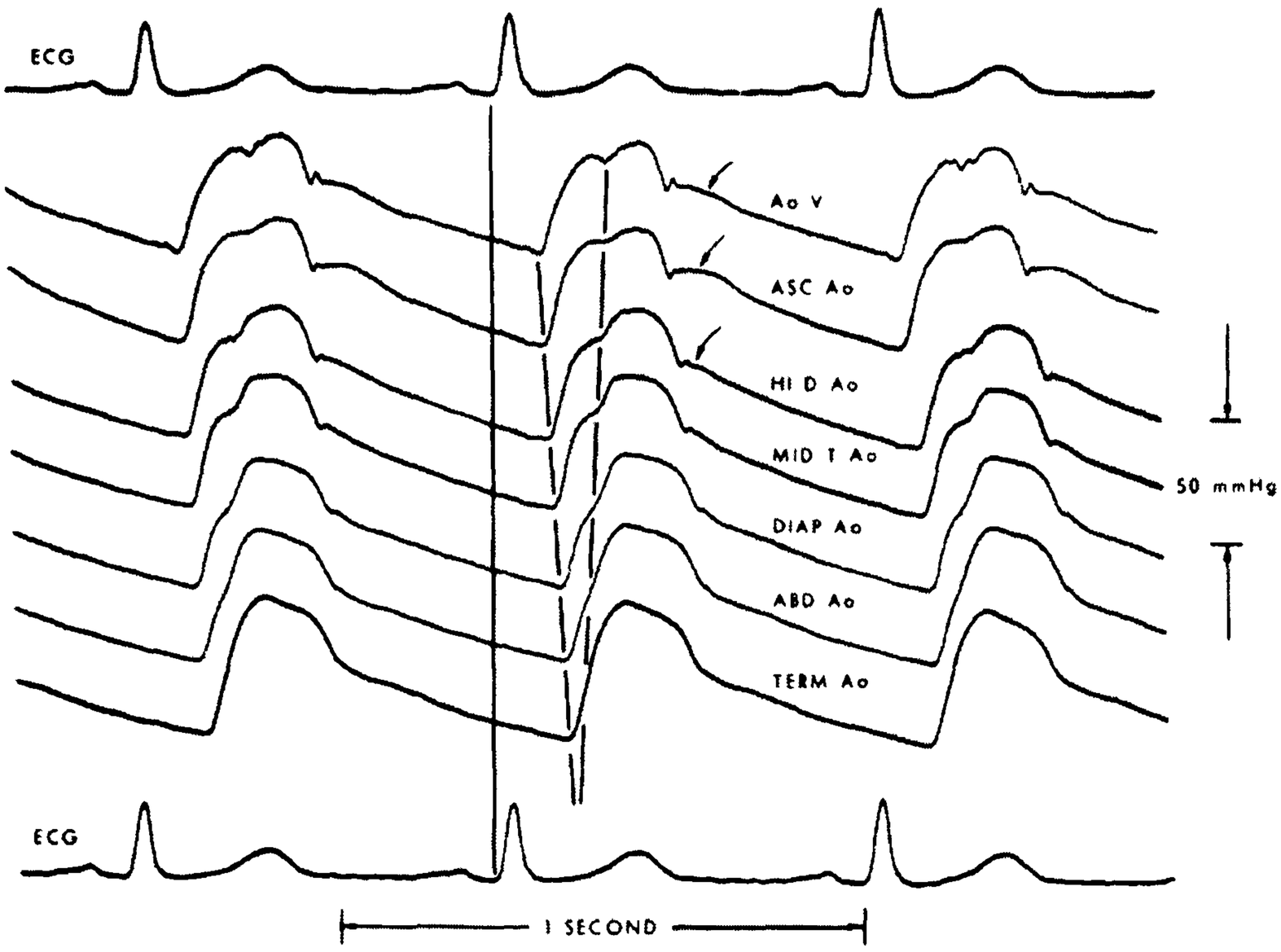

FIGURE 7. *Pressure wave forms as a function of location from the ascending aorta to the iliac bifurcation in one patient. Figure constructed from single or pairs of pulses selected from cardiac cycles with equal RR intervals and from similar phases of respiration. AoV = sensor just above aortic valve; Asc Ao = ascending aorta; Hi D.Ao = high descending aorta; Mid T.Ao = midthoracic aorta; Diap Ao = diaphragmatic aorta; Abd Ao = abdominal aorta; Term Ao = terminal abdominal aorta just before iliac bifurcation. See text for discussion.*

Figure1.1 The pressure wave forms from the ascending aorta to the iliac bifurcation (copy from Murgo, 1980)

Chapter 2

Theoretical Analysis

2.1 Introduction

Euler introduced his one-dimensional analysis of flow in distensible tube, which is still used today and considered the oldest theory of blood flow in arteries (Euler, 1775). The equation derived by Euler mathematically quantitative remained unsolved until Riemann introduced the method of characteristics in 1860. WIA, based on the solution of the Euler's mathematical model and equations using the method of characteristics, made it possible to consider the arterial waves as wavefronts where a wavefront is composed of infinitesimal wavelets (Parker and Jones, 1990).

The investigation of propagation of blood wave in the arterial system has been dominated by the impedance method previously. Essentially, the approach of the impedance method considers a solution using Fourier transforms under the assumption of linearity of equation for flow (Womersley, 1957). Compared with impedance method, WIA has several advantages to study the propagation of blood waves in the arterial system, which are explained as follows:

(1) The impedance method presents the results in the frequency domain, which is not intuitive clinically. In contrast, WIA is a time domain approach, which allows for the interpretation of wave propagation in the arterial system or elastic tubes as a function of time and space. Therefore, the results can be directly related to physiological events. In addition, analysis in the frequency

domain can lead to the implicit assumption that the arterial flow is a steady oscillation, which imply that the arterial system will remain oscillating even when the ejection from the heart is stopped (Sherwin, 2003). This is not in accordance with physiological statues when the heart is blocked; during this periods neither flow nor pressure shows any hint of the "periodic" behaviour.

(2) The impedance method considered arterial waveform as wave trains, which means that each waveform of a heart beat is similar to those of previous beats. However, there are differences between the shape of waveforms in different cycles due to the variation of the arterial system (for example: constriction and dilatation) and variation of output of the heart (for example: inspiration and expiration). In addition, the impedance method assumes a linear relationship between pressure and flow. In contrast, WIA does not make any assumptions about the tube's wall linearity or periodicity.

Furthermore, the data analysed using WIA take into account the effects of the vessel wall's viscoelastic properties, convective and frictional effects and fluid viscosity.

Apart from the advantages mentioned above, WIA has the other strengths for this study:

(1) WIA provides a method to separate pressure and velocity waves travelling in the forward and backward directions from the measured pressure and velocity waveforms. Thus, the analysis offers a technique to study wave dissipation in one direction whilst taking into account the effect of reflections from the opposite direction.

(2) The physical meaning of WI is the flux of energy carried by the wave per unit cross-sectional area. Therefore, WI provides a convenient method to study the dissipation of energy carried by the waves along flexible tubes.

There are two assumptions to be made when one-dimensional flow equations are applied in the circulation. The reasons and suitability of these two assumptions are discussed as follows:

1) **The validation of one-dimensional model:**

If the flow in arteries were assumed as one-dimensional model, the measured pressure and flow can be expressed as the function of distance and time, that is $P = P(x,t)$ and $Q = Q(x,t)$. It has been reported that under normal conditions velocity distribution in the arteries tends to be axisymmetrical (Schultz et al. 1969). It is also been stated that axial flow is dominant in the aortic arch (Pedley, 1980). Lighthill stated that arterial radius expands and contracts by only a few percent of its undisturbed value, requiring radial motions negligible small compared with the longitudinal motion, which suggested that the one-dimensional theory is quite a reasonable and accurate enough to analyse the blood flow in the arterial system(Lighthill, 1978).

2) Blood is treated as an incompressible fluid:

Pedley suggested that the blood can be approximately treated as incompressible liquid (Pedley, 1980). Lighthill also stated that the compressibility of the blood is negligibly small compared to the large distensibility of the arterial wall (Lighthill,1978).

2.2 Governing equations

Blood flow in the arterial system follows the laws of conservation for mass and momentum. Based on the two assumptions above, the blood flow in the arterial system can be analysed using one-dimensional equation of flow in an uniform elastic tube:

$$A_t + (UA)_x = -q \tag{2.1}$$

$$U_t + UU_x = -P_x / \rho + F \tag{2.2}$$

Where

A : Cross-sectional area of tube

U : The mean velocity across the cross-sectional area.

P : The mean pressure across the cross section.

ρ : The density of the fluid.

q: The volume flow rate per unit length out of the tube.

F : Frictional force between fluid and tube wall.

x : The distance along the tube.

t : The time.

The subscripts denote partial differentiation.

Equation (2.1) describes the law of conservation of mass. The left side of the equation expresses the rate of flow into the tube and the right side of the equation indicates the rate of flow seepage out of the tube. Equation (2.2) follows the law of the conservation of the momentum. The left side of equation express the rate of momentum per mass and the right side of equation describes the difference of pressure with respect to the distance, x, and the friction dissipation.

Under the assumption of viscous losses is negligible and the tube wall is impermeable, the equations (2.1) and (2.2) can be simplified as:

$$A_t + (UA)_x = 0 \tag{2.3}$$

$$U_t + UU_x = -P_x / \rho \tag{2.4}$$

There are three variables, P, U, A, in these two equations. Therefore, it is required to add another equation to get a solution.

As the wave propagates in the elastic tube, the cross-section area is a function of pressure, while the pressure is also function of distance, x, and time, t.

$$A = A(P(x,t)) \tag{2.5}$$

The change in the cross sectional area with respect to time and distance can be written:

$$A_t = \frac{dA}{dP} P_t \quad \text{and} \quad A_x = \frac{dA}{dP} P_x \tag{2.6}$$

Substitution of equation (2.6) into (2.3) gives:

$$\frac{dA}{dP} P_t + U \frac{dA}{dP} P_x + AU_x = 0 \tag{2.7}$$

Dividing (2.7) by $\frac{dA}{dP}$ and rearranging

$$P_t + UP_x + \frac{A}{\frac{dA}{dP}} U_x = 0 \tag{2.8}$$

The distensibility of the arterial vessel wall, D, can be defined as the relevant change of cross sectional area per the change of the pressure compared to initial area:

$$D = \frac{1}{A} \frac{dA}{dP} \tag{2.9}$$

Substitute (2.9) into (2.8) gives,

$$P_t + UP_x + \frac{1}{D}U_x = 0 \tag{2.10}$$

Equation (2.4) and (2.8) can be written in the matrix form:

$$\omega_t + \Omega\omega_x = 0 \tag{2.11}$$

where, $\omega = \begin{bmatrix} P \\ U \end{bmatrix}$ and $\Omega = \begin{bmatrix} U & \frac{1}{D} \\ \frac{1}{\rho} & U \end{bmatrix}$

These equations are hyperbolic and amenable to solution by the method of characteristics. The eigenvalues, λ, of the matrix can be determined from the equation $|\Omega - \lambda I| = 0$ and we can write:

$$(U - \lambda)^2 = \frac{1}{\rho D} \tag{2.12}$$

If we define the right item of equation (2.12) as c^2,

$$c^2 = \frac{1}{\rho D} \tag{2.13}$$

then, $(U - \lambda)^2 = c^2$ and the eigenvalues of the matrix are:

$$\lambda_{\pm} = U \pm c \tag{2.14}$$

The physical meaning of the term c is the local wave speed. In equation (2.14), the positive sign, "+" indicates the forward direction and the negative sign "-" indicates the backward direction. Usually in the arterial system, the forward direction means that the wave is running from ventricle to the peripheral arteries and the backward direction means that the wave is running from the peripheral arteries to the ventricle. In this thesis, the forward wave refers the flow from inlet to outlet and the backward wave refers the wave from outlet to inlet of the tube.

The method of characteristics relies on the observation that the waves run in the space-time plane along the characteristics direction, which are

$$\frac{dx}{dt} = U \pm c \tag{2.15}$$

Along the characteristic directions the partial differential equations (2.11) can be reduced to the ordinary differential equations

$$\frac{dU}{dt} \pm \frac{1}{\rho c}\frac{dP}{dt} = 0 \tag{2.16}$$

Along the characteristics direction the equation (2.16) can be written in terms of the Riemann function,

$$R_{\pm} = U \pm \int_{P_0}^{P} \frac{dP}{\rho c} \tag{2.17}$$

Where, P_0 is initial pressure, the differential form of equation (2.17) can be written:

$$dR_{\pm} = dU \pm \frac{dP}{\rho c} = 0 \tag{2.18}$$

In equation (2.18) the difference operator, d, is defined as the change across the characteristic. The physical meaning of this equation is that any change in pressure and velocity imposed on the flow will cause a change in the Riemann functions, which will propagate along the characteristic direction. As shown in **Figure 2.1**, at each point (t,x), the local pressure and velocity can be determined at the intersection of forward and backward Riemann values.

Rewriting equation (2.18) along the characteristic directions gives the water-hammer equation:

$$dP = \pm \rho c dU \tag{2.19}$$

2.3 Wave separation

If we assumed that the changes in pressure and velocity are the linear summation of increments of pressure and velocity in forward and backward directions,

$$dP = dP_+ + dP_- \tag{2.20}$$

$$dU = dU_+ + dU_- \tag{2.21}$$

Substitution of equation (2.20) and (2.21) into (2.19) arrives at the forward and backward change of pressure and velocity,

$$\begin{aligned} dP_+ &= \frac{1}{2}(dP + \rho c dU) \\ dP_- &= \frac{1}{2}(dP - \rho c dU) \end{aligned} \tag{2.22}$$

$$\begin{aligned} dU_+ &= \frac{1}{2}(dU + \frac{dP}{\rho c}) \\ dU_- &= \frac{1}{2}(dU - \frac{dP}{\rho c}) \end{aligned} \tag{2.23}$$

Summation of forward and backward changes of pressure, $dP_\pm$, and velocity, $dU_\pm$, respectively, gives the forward and backward pressure, $P_\pm$, and velocity, $U_\pm$,

$$P_+ = P_0 + \sum_{t=0}^{t} dP_+ \ , \ P_- = \sum_{t=0}^{t} dP_- \tag{2.24}$$

$$U_+ = \sum_{t=0}^{t} dU_+ \ \ U_- = \sum_{t=0}^{t} dU_- \tag{2.25}$$

where P_0 is an initial static pressure and t is the time. An example of measured pressure and velocity waveform and their separated forward and backward pressure and velocity are shown in **Figure 2.2.** Also, the detailed relationship of the measured pressure and its separated forward and backward elements are

shown in **Figure 2.3a,** from which one can see the measured pressure are summation of forward and backward pressure.

2.4 Wave Intensity Analysis

Wave Intensity, $dI = dPdU$, is the flux of energy carried by the waves per unit area, having units of W/m^2. Also, dI can be separated into forward wave intensity, $dI_+ = dP_+ dU_+$, and backward wave intensity, $dI_- = dP_- dU_-$, which can be obtained from measurement of P and U, and knowledge of wave speed:

$$dI_\pm = \pm\frac{1}{4\rho c}(dP \pm \rho c dU)^2 \tag{2.26}$$

Equation (2.26) shows that forward wave intensity is always positive and backward wave intensity is always negative. A typical example of separated wave intensity is shown in **Figure2.3b**.

Furthermore, the forward and backward wave energy can be obtained by integration of $dI_\pm$ with respect to time,

$$I_\pm = \int_0^T dI_\pm dt \tag{2.27}$$

Inherently, the I_+ have units of J/m^2.

2.5 Wave speed determined by PU-loop

The separation of pressure and wave intensity into their forward and backward directions, $P_\pm$ and $dI_\pm$, requires knowledge of wave speed, which can be determined using the PU-loop method (Khir et al., 2001). The water hammer equation (2.19) can be used to determine the wave speed only if waves passing by the measurement site are running in one direction. Therefore, plotting the measured pressure against the measured velocity over the cycle we obtain a

PU-loop (**Figure 2.4**), whose slope during the very early part of the cycle, when wave are running only in the forward direction, equals ρc. It has been accepted that local wave speed is mainly depended on the local elastic properties (Milnor, 1989). Wave speed determined using PU-loop method only needs the measurements of pressure and flow at one point, hence directly associated with the local properties of tube wall. Wave speed determined using this method has been proven to be sensitive to the properties of tube wall (Feng, 2008).

2.6 Reflected waves

2.6.1 The type of reflection sites

In this thesis, wave propagation was investigated in single long tubes. Generally, reflection sites in single long tubes can be positive or negative and reflection coefficient can be determined by $R = \frac{P_r}{P_i}$, where P_r is reflected pressure wave and P_i is incident pressure wave. The types of reflection sites can be classified as following:

Positive reflection sites: $0 < R < 1$;

Negative reflection sites: $-1 < R < 0$;

No reflection: $R=0$.

Close end: $R=1$.

Open end: $R=-1$.

2.6.2 Types of reflected wave

Waves can be classified into compression or expansion wave according to their effect on pressure. A compression wave causes an increase but an

expansion wave causes a decrease in pressure. The type of backward wave is depended on the incident wave and reflection sites. If the reflection site is positive, then the type of backward wave is the same as the forward wave is. For example, if the forward compression waves encounter the positive reflection sites, then a backward compression wave will be produced, but if a forward expansion wave encounters the positive reflection sites, then a backward expansion wave will be produced. In contrast to the positive reflection sites, negative reflection sites have the opposite effect; that is to say, the forward compression wave will be reflected by the negative reflection sites as the backward expansion wave and forward expansion wave will be reflected as the backward compression wave. The close-end reflection site is a typical of positive reflection, with value R=1, and the open-end reflection site is a typical of negative reflection, with value R=-1. The relation of formation of forward and backward wave and reflection sites type are summarized in **Table 2.1.**

Table2.1. Comparison of type of backward wave and type of reflection sites

Forward			Backward (Positive Reflection)			Backward (Negative Reflection)		
Comp*	dP (+)	dU (+)	Comp*	dP (+)	dU (-)	Exp*	dP (-)	dU (+)
Exp*	dP (-)	dU (-)	Exp*	dP (-)	dU (+)	Comp*	dP (+)	dU (-)

Note: * Comp and Exp indicate the compression and expansion wave, respectively;

"+" and "-" indicate the positive and negative

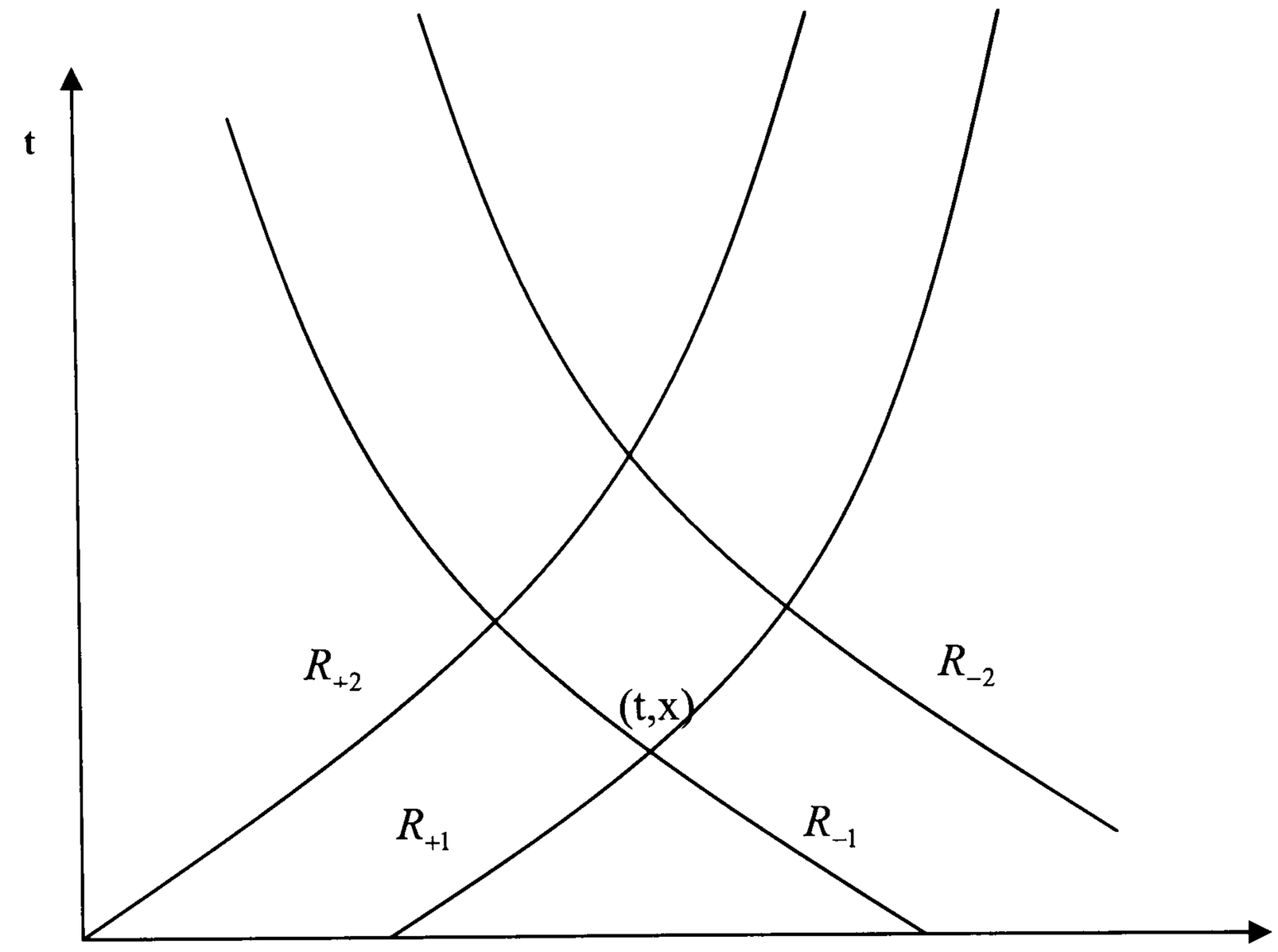

Figure 2.1 In the distance-time plane, the change of pressure and velocity at point (t,x) are determined by the intersection of pair of forward and backward charateristic line.

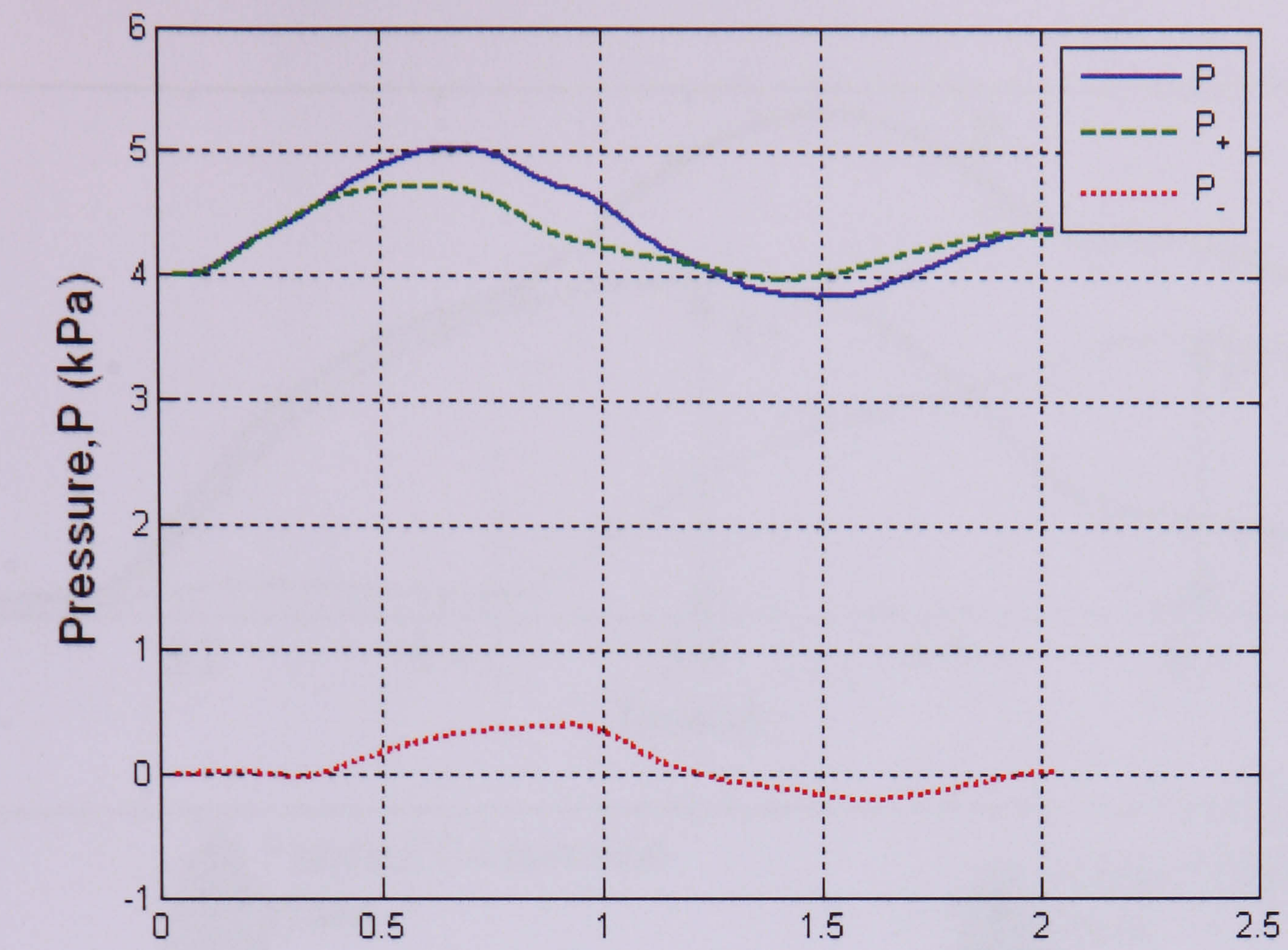

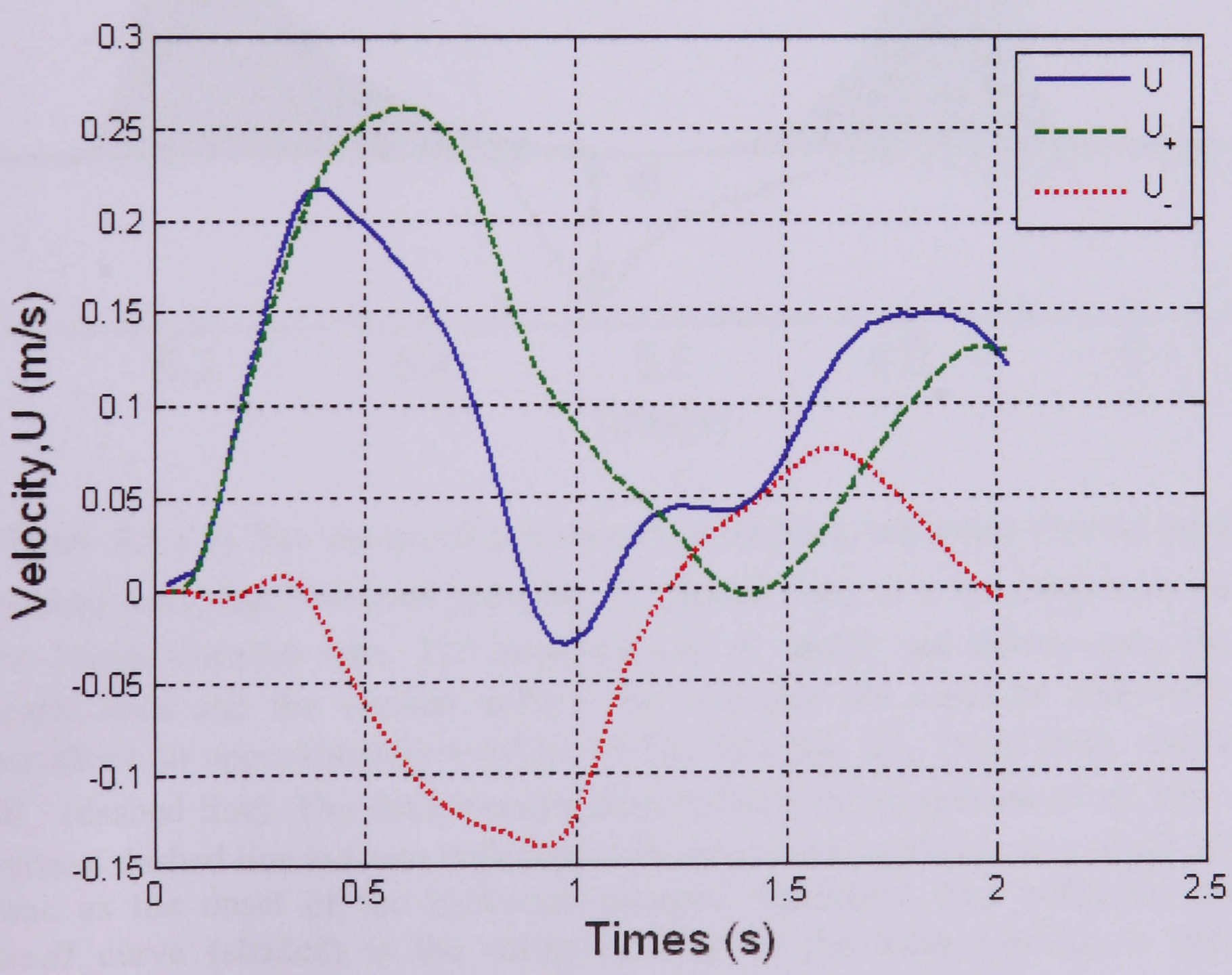

Figure 2.2 The measured pressure, P ,and velocity, U ,(solid line), separated forward pressure , P_+, and velocity, U_+ (dashed line), and backward pressure, P_-, velocity, U_- (dotted line), at 1.5m away from the inlet in 16mm diameter tube.

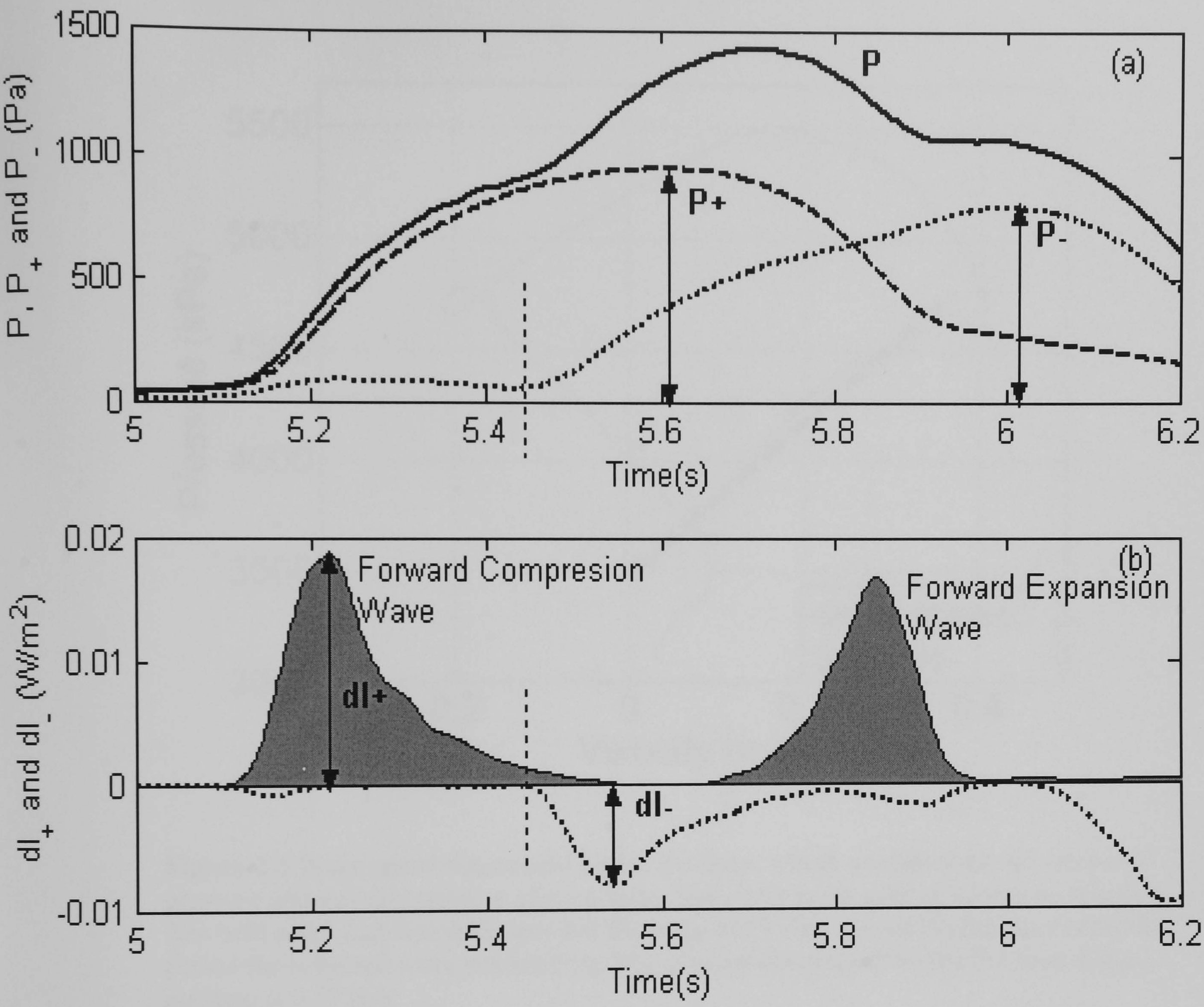

Figure 2.3 : a) The measured pressure, P (solid line), separated forward pressure, P_+ (dashed line), and backward pressure, P_- (dotted line), at 1.3m away from the inlet of the 16mm diameter tube. The amplitudes of P_+ and P_- are shown using the double-arrow lines and the vertical dashed line indicates the onset of backward pressure waveform at approximately t=5.45s. **b)** The forward, dI_+ (solid line), and backward, dI_- (dashed line). The double-arrow lines indicate the magnitude of dI_+ and dI_-, and vertical dashed line indicate the onset of the backward wave intensity which is the same time as the onset of the backward pressure waveform. The integrated area under the dI_+ curve (shaded) is the energy carried by the wave running in the forward direction, I_+. Note this area is composed of the forward compression wave due to the increase in pressure (first half of the pressure wave), and a forward expansion wave due to the decrease in pressure (second half of the pressure wave).

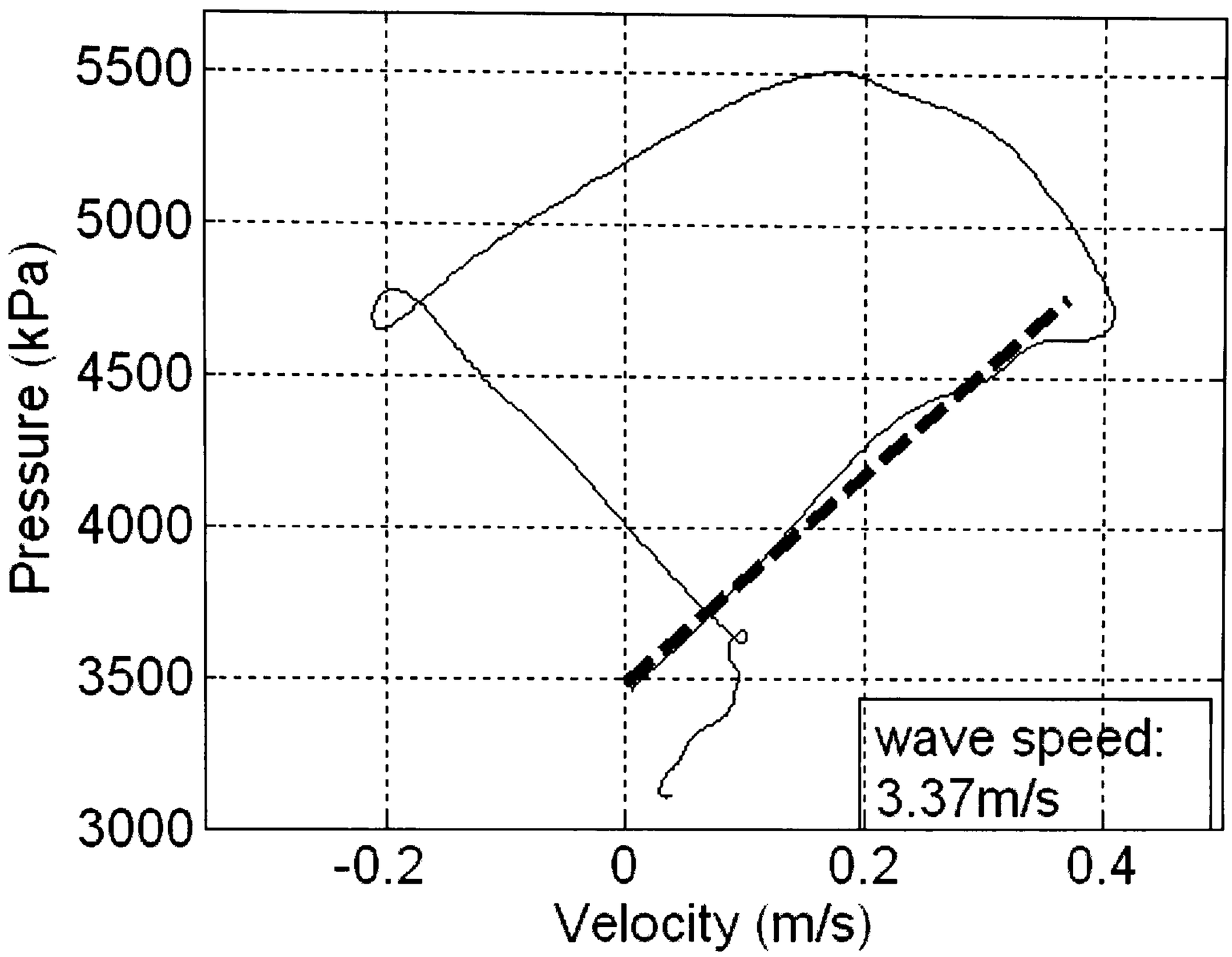

Figure 2.4 Wave speed determined by the PU-loop, which is made from the measured pressure and velocity pulse at 150 cm away from inlet in the tube of 16 mm in diameter. The bald solid dash line indicates that the slope of PU-loop in the beginning, during this period the reflected wave not arriving. Wave speed determined by the PU-loop at this position is 3.37 m/s.

Chapter 3

Methods and instrumentation

Features of the general experimental setup and instrumentation are introduced in this chapter, which includes the experimental setup, the calibration procedure, static properties test and statistics analysis. Further description for each specific experiment will be discussed in Chapter 4, 5, 6, where a variation of the general experimental setup and instrumentation was needed.

3.1 Experimental setup

The general experimental setup used in the work carried out in this thesis is shown in **Figure 3.1**. A semi-sinusoidal wave was produced at the inlet of the tube. The pressure and flow measurements were made at known distances to observe the decay of the magnitude of waves. The followings are the components used.

a. Tubes

We investigated wave dissipation in four sizes of latex tubes, whose diameters and wall thicknesses are given in **Table 3.1,** and each of the tubes is uniform in both dimension and mechanical properties along its 2m in length. This length was chosen to represent the distance that the wave would have to run from the heart to the feet, reflected and returned in an average human. The tubes were fully merged into a water tank, where the water level was approximately 1 cm above the tubes. Each tube was carefully mounted and kept in the horizontal position.

b. Pump

The inlet of the tube was connected to a piston pump, which produced an approximately semi-sinusoidal single pulse wave with the piston moving forward from the bottom to the top dead centre. The cylinder of the pump is of 5 cm in diameter and the stroke of the piston is 2 cm; giving a displaced volume of approximately 40ml. We used an 11 Watts graphite brushes DC motor (Maxon 110937, A-max , Sachseln, Switzerland) to drive the pump. The motor used a constant DC power supply of 5.5 Volts. The characteristics of this motor reveal that speed of motor will reduce when the load increase for a fixed Voltage of power supply.

c. Reservoirs

The inlet and outlet of each tube were connected to the inlet and outlet reservoirs, respectively. The height of the fluid in the reservoirs was adjusted to 30 cm above the longitudinal axis of the tube; producing an initial hydrostatic pressure of 3 kPa. We note that although the transmural pressure for the different-sized tubes will vary, this variation was ignored as it was not significant and its effect was expected to be minimal. The inlet and outlet reservoirs were interconnected and their connections to the tube were made using rigid polyurethane tubing; hence a strong reflection site was expected at the exit of the latex tubes.

d. Valve

One-way valve was placed between inlet of the tubes and the inlet reservoir as illustrated in **Figure 3.1**. The function of this valve was to prevent any portion of the displaced volume of water at inlet flow into the reservoir.

3.2 Measurements

Simultaneous pressure and flow waveforms were measured at the same sites, sequentially in time, every 5cm along the tubes. Pressure was measured using a 6F pressure transducer tipped catheter (Gaeltec, Scotland, UK), which was inserted into the tube through a Y-junction at the inlet of the tube or outlet of the tube. Due to the limited length of catheter of pressure transducer, no measurements were made at the position of 85, 90 and 95cm away from the inlet of the tubes. Flow was measured using ultrasound flow probes (Transonic System Inc, Itheca, NY, USA). The static external diameter and wall thickness of each tube were measured using a digital calliper, and the internal diameters were obtained by the subtraction of thickness from external diameters and then were used with the flow rate to calculate the velocity at each site; assuming a flat flow velocity profile over the cross sectional area.

The data of pressure and flow rate were acquired at 500Hz using Labview (National Instruments, Austin, Texas, USA), and analysed subsequently using programs in Matlab (The Mathworks, Natick, MA, USA).

3.3 Calibration

Before all measurements were taken, the pressure transducers and ultrasonic flow cuffs were calibrated.

a. Pressure

The pressure transducers were calibrated using the water-column methods. The pressure in Volt was recorded up to the tip of catheter was advanced into the water at interval of 10 cm up to 1 m deep. The pressures in

water-column were converted into the kilo Pascal. The correlation of pressures in voltage with that in kilo Pascal was assessed using regression line and the equation of regression line is used to convert voltage into kilo Pascal (**Figure 3.2 a**).

b. Flow and velocity

The flow can be calibrated by the flow meter itself. For the varied size of flow probes, the flows were calibrated using the corresponding coefficient. For example, for the 8 mm flow probe the flow in 1V is equal to 200 ml/min. The calibration coefficient for 4 sized flow probes was shown in the **Table 3.1**.

The velocity was calculated from the flow divided by the internal cross-sectional area.

In addition, the accuracy of flow calibration using the coefficient of flow meter was also inspected by calculation of the volume within one cycle of wave. In our case, the displacement in volume, 40 ml, by the pump is expected and only a single wave is generated, therefore, the integration of flow with respect to time for one cycle is expected to be equal to the displacement in volume by pump, 40 ml. The inspection for each sized flow probe reveals that the integration of flow within one cycle is approximately 39.4 ml, which is very close to the expected value.

3.4 Static property test

The static properties of tube wall were determined from the static pressure-diameter relationship just before the dynamic measurements starts. The change of static pressure was established by either increase or decrease the height of water in the reservoirs. To eliminate the dynamic effect, the measurements for

both pressure and diameter at each stage were taken 2 minutes later after the level of liquid in the reservoirs was either increased or decreased. **Figure 3.3 a, b, c and d** show that the relationship of pressure and diameter when the head of water in the reservoirs was increased at intervals of 5 cm from 30 cm to 55 cm and then decreased at the same intervals from 55 cm to 30 cm. The pressure was measured using 6F pressure transducer tipped catheter and the diameter of tube is measured with the digital vernier calliper.

The internal cross-sectional area can be calculated from the measured diameter using equation, $A = \frac{\pi}{4} D^2$, where A is the cross-section area and D is internal diameter of the tube, under the reasonable assumption of circular cross-sectional area of tube. To assess the wall properties of each tube, we measured the static compliance. The static compliance of each size of tube can be established using the changes of internal cross-section area of the tube and the change of pressure at each step, $C_s = \frac{dA}{dP}$, where C_s indicates the static compliance, dA is the change of cross-sectional area and dP is the change of static pressure when the level of liquid in the reservoirs either increase or decrease every 5 cm. The average of static compliance for each size of tube is shown in the **Table 3.1**.

3.5 Reproducibility

To examine the reproducibility of data, measurements of the pressure at sites of 0.3 m and 1.5 m away from the inlet were repeated 10 times, **Figure 3.4**. The maximum of the measured pressure at 0.3 m was $6217 \pm 23Pa$, and at 1.5m

was $6805 \pm 18Pa$. The data are highly reproducible with a standard deviation of less than 0.5%.

3.6 Statistics methods

3.6.1 Normalization

The same volume of flow, 40ml, was ejected into each of the four sizes of tubes. To examine the effect of tube sizes and the other parameters, such as initial pressure and pumping speed of pump, on wave dissipation, the results were normalized. The normalisation was expressed as the ratio of the value at each site along the tube compared to the value at the inlet of the tube. For example, the normalised P_+ is expressed as $\frac{P_+}{P_{+i}}$, where P_+ is forward pressure at the measurement site and P_{+i} is forward pressure at inlet of the tube. Similarly, dI_+ and I_+ were normalized as $\frac{dI_+}{dI_{+i}}$ and $\frac{I_+}{I_{+i}}$. The percentages of dissipation of the pressure wave at any specific site was calculated as $1-\frac{P_+}{P_{+i}}$. Similarly, the percentage of dissipation of dI_+ and I_+ were determined using $1-\frac{dI_+}{dI_{+i}}$ and $1-\frac{I_+}{I_{+i}}$.

3.6.2 Curve fitting

The dissipation curves were constructed using the data best-fit function of Matlab. The power of the exponential equation was used to compare the decay of the forward pressure, forward wave intensity and forward wave energy, between the 4 tube sizes. The dissipation exponential equations are

expressed as $e^{-x/\lambda}$, where x is the distance away from the inlet of the tube and λ is the inverse of the power of the exponential equation. This allows the calculation of the dissipation at any given distance away from the inlet of the tube.

Table3.1 Dimensions and properties of the 4 different sized latex tubes.

Unstressed diameters D (mm)	4	8	12	16
Wall thicknesses t (mm)	0.1	0.15	0.2	0.2
Initial external diameters (mm)	4.2	8.8	12.53	16.6
Flow meter calibration coefficient (L/min/V)	0.2	2	4	10
Compliance (dA/dP) ($10^{-8}m^2Pa^{-1}$)	0.024	0.872	1.98	4.55

The initial external diameter was measured when the hydrostatic pressure in the tube is 3 kPa.

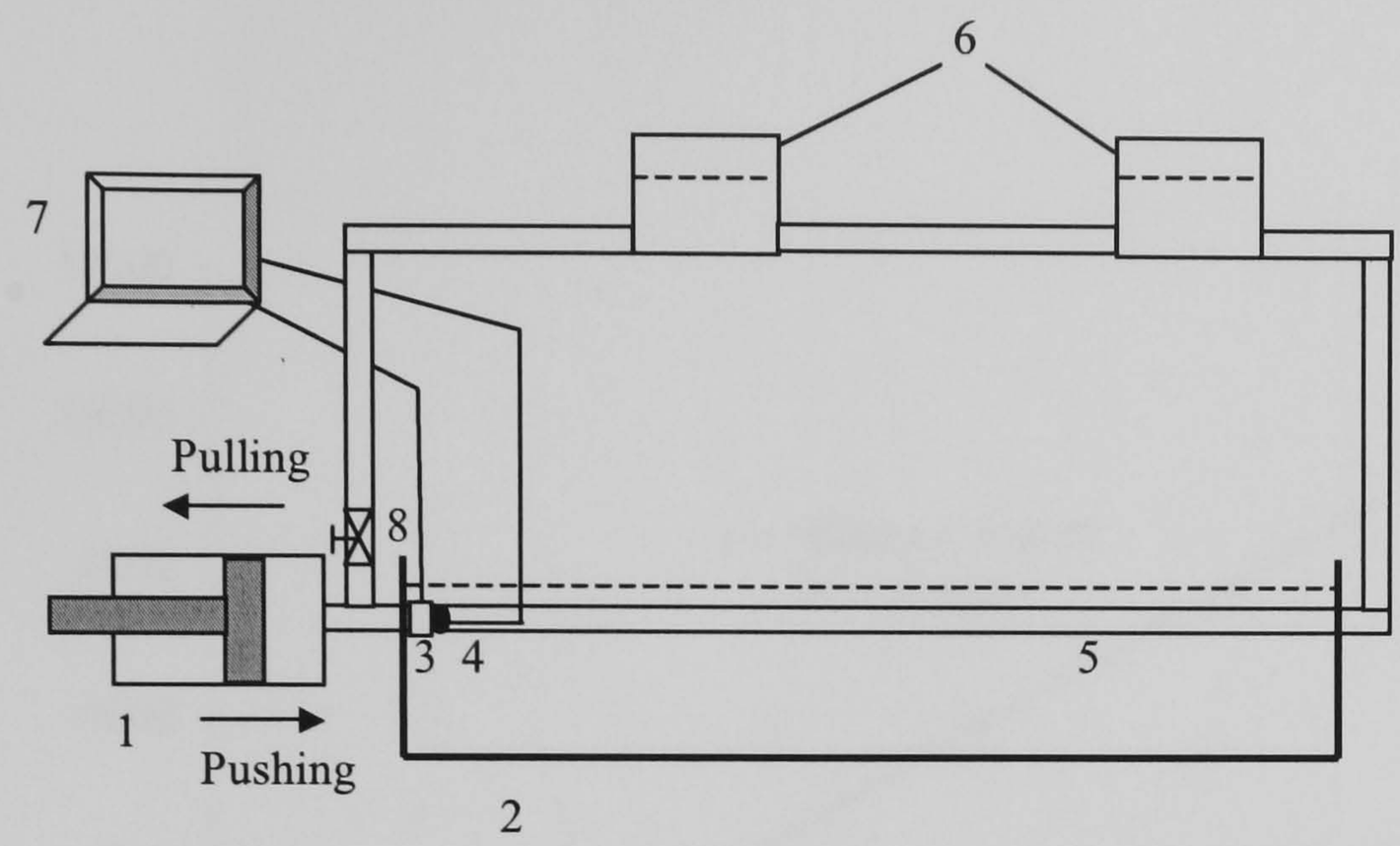

Figure3.1 A schematic of experiment setup. 1, pump; 2, tank with water; 3 and 4, flow probe and catheter tipped pressure transducer; 5, latex tubes; 6, two reservoirs; 7, personal computer; 8, valve. Arrows indicates the directions of piston moving when the pump produced the wave with pushing or pulling effect. Horizontal dashed line indicates that level of water in the tank and reservoirs.

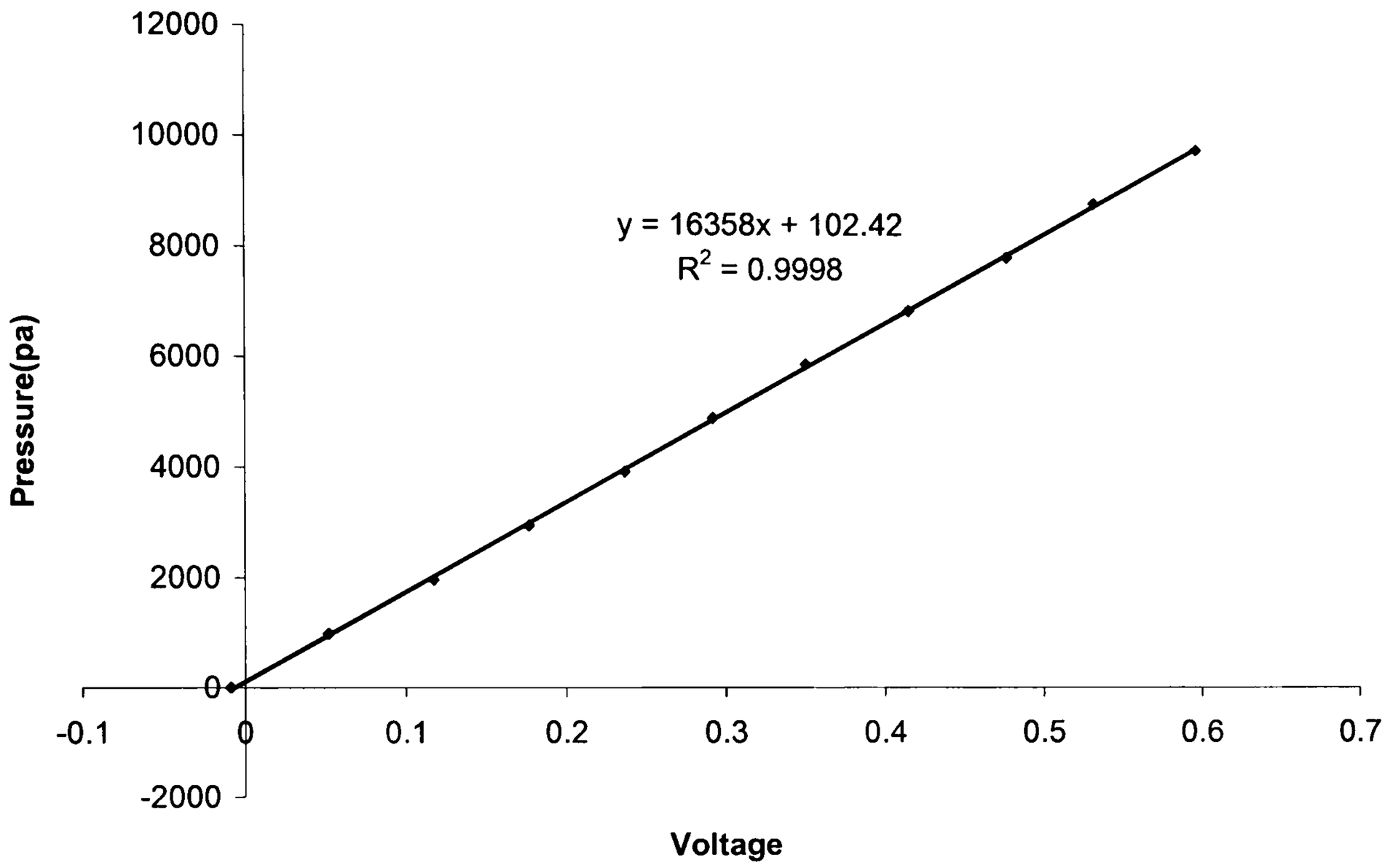

Figure 3.2 Calibration from Voltage to Pascal using water-column method; Abscissa denotes the readings in voltage from pressure transducer and vertical coordinate denotes the pressure in Pascal at depth in the water, where pressure transducer are placed. The equation of regression line is used to conversion from the measurement of pressure in Voltage to that in Pascal.

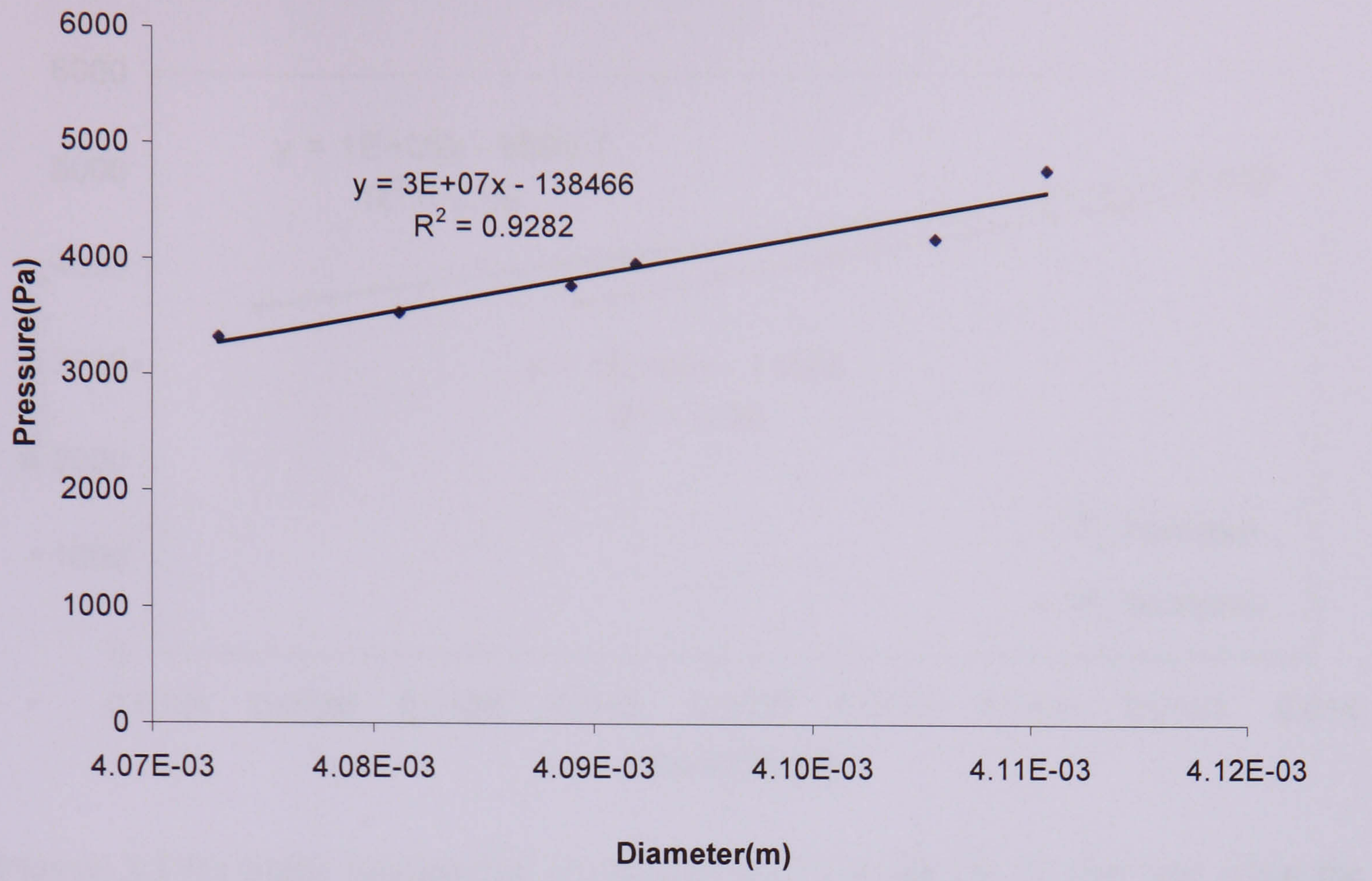

Figure 3.3 (a) Static relationship of pressure and diameter for 4 mm tube when the hydrostatic pressure (level of water in the reservoirs) increases (blue squares) at each step of 2.5 cm ($\Delta p = 1000 \times 9.81 \times 2.5/100 = 245 Pa$).

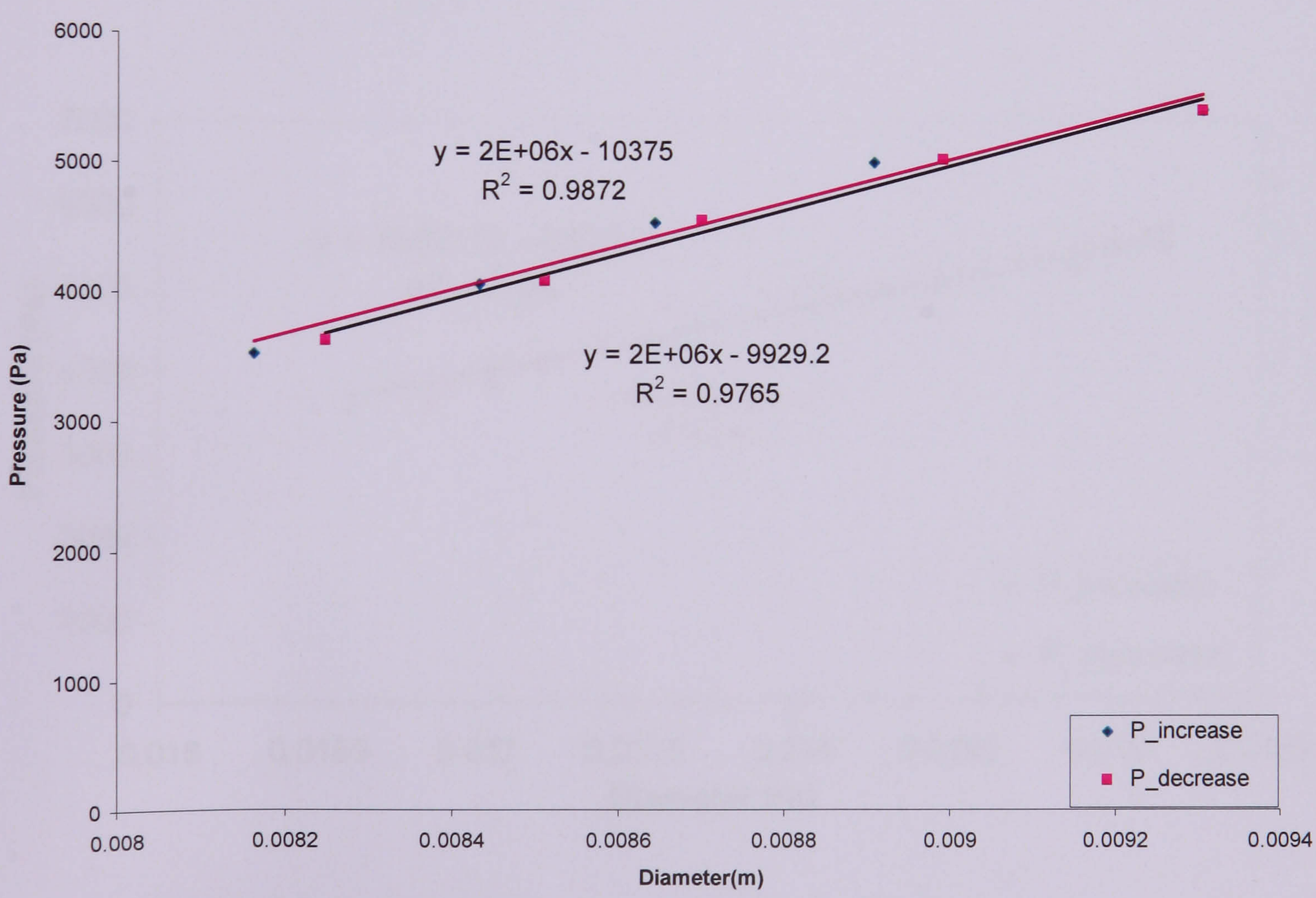

Figure 3.3 (b) Static relationship of pressure and diameter for 8 mm tube when the hydrostatic pressure (level of water in the reservoirs) either increases (blue squares) or decrease (pink squares) at each step of 5 cm ($\Delta p = 1000 \times 9.81 \times 5/100 = 490 Pa$).

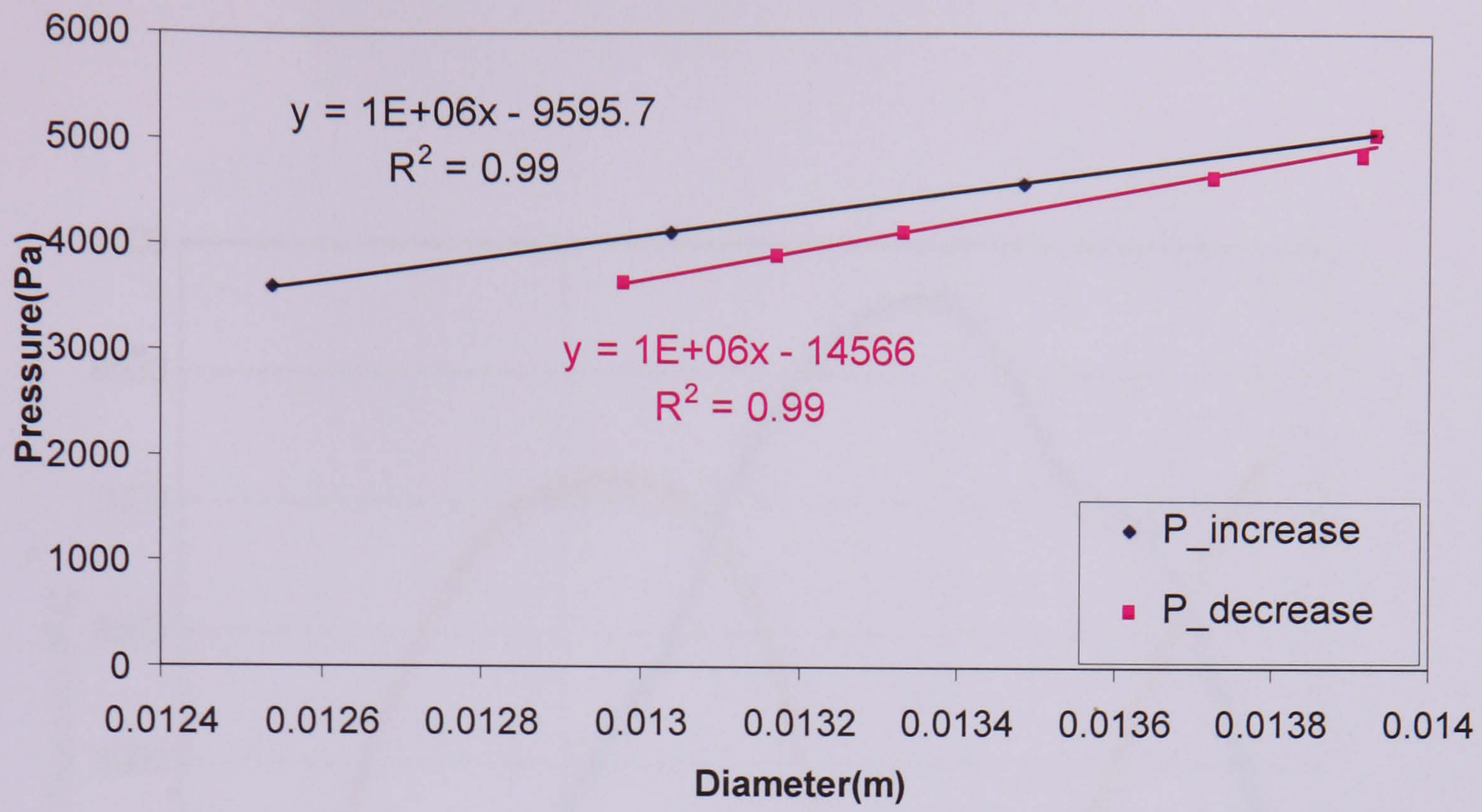

Figure 3.3 (c) Static relationship of pressure and diameter for 12 mm tube when the hydrostatic pressure (level of water in the reservoirs) either increases (blue squares) or decrease (pink squares) at each step of 5 cm. ($\Delta p = 1000 \times 9.81 \times 5/100 = 490 Pa$).

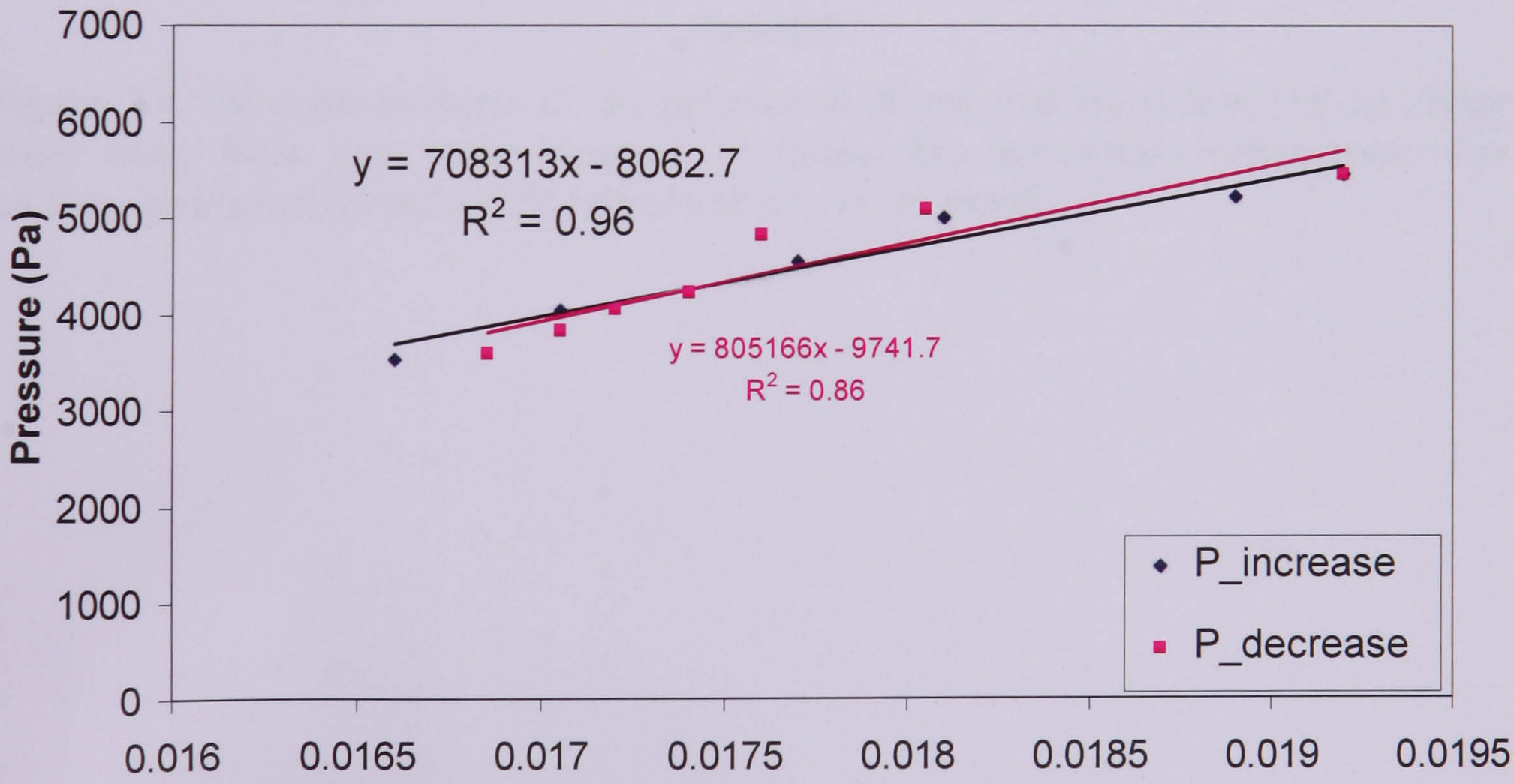

Figure 3.3 (d) Static relationship of pressure and diameter for 16 mm tube when the hydrostatic pressure (level of water in the reservoirs) either increases (blue squares) or decrease (pink squares) at each step of 5 cm ($\Delta p = 1000 \times 9.81 \times 5/100 = 490 Pa$).

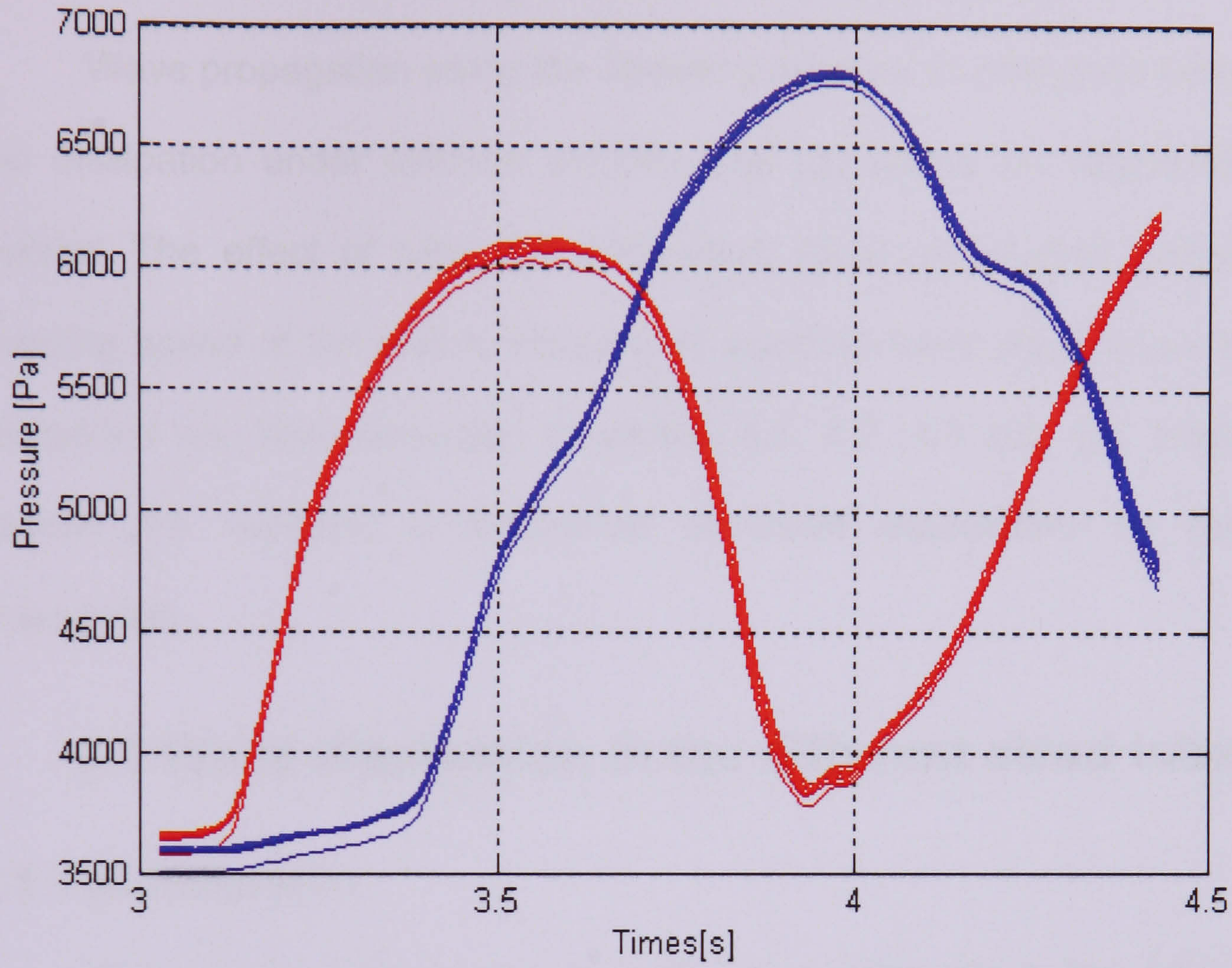

Figure 3.4 The measurements of the pressure at 30 cm (red lines) and 150 cm (Blue lines) away from inlet were repeated 10 times. The waveforms superimpose one another, giving confidence of the reproducibility of the pump.

Chapter 4

Wave dissipation in time domain

Wave propagation along the travelling distance including the wave speed and dissipation under different experimental conditions are described in this chapter. The effect of tube size (diameter), initial undisturbed pressure, the pumping speed of the piston, viscosity of liquid and wall property on the wave dissipation are also discussed in section 4.1, 4.2, 4.3 and 4.4, respectively. Section 4.5 contains a discussion of these parameters on the wave propagation.

4.1 Wave dissipation in the different sized tubes

4.1.1 Introduction

The experimental setup is described in the Chapter 3. The effect of size of tube (diameter) on wave dissipation is investigated in four sized tubes. The tube size and the corresponding thickness are listed in **Table 4.1**. The local wave speed was determined using PU-loop method, which is discussed in Chapter 2. The degree of dissipation of the wave was assessed according to the amplitude of separated forward and backward pressure, peak of forward and backward intensity and forward wave energy, respectively, which is presented in the results section.

4.1.2 Results

4.1.2.1 Wave speed and the static compliance

Table 4.1 shows the average of wave speed and the static compliance in the different sized tubes. One can see from this table that the average of wave speed in 4 mm tube is highest, which is approximately 7.1 m/s and in 16 mm tube it is approximately 3.5 m/s. In addition, the static compliance of tube wall is the smallest in the 4 mm tube and the biggest in the 16 mm tube, which is approximately $4.55\times10^{-8} m^2 Pa^{-1}$.

4.1.2.2 Dissipation of pressure wave

Typical pressure and velocity waveforms measured along the length of 12 mm diameter tube are shown in **Figure 4.1 a & b.** The peak of the measured pressure waveform initially decreased along the tube, then start to increase as the measurement site moved distally approaching the exit of the tube due to the effect of arrival of the reflected wave. However, the peak of the measured velocity waveform decreased along the length of the tube and then continued to decrease sharply as the measurement site moved toward the exit of the tube also due to the arrival of the reflected wave, **Figure 4.1b.**

Amplitude of forward pressure dissipated exponentially along the distance travelled in the different four-sized tubes, as shown in Figure 4.2. In the smaller-sized tube the amplitude of forward pressure dissipated is greater than that in the bigger-sized tube, **Figure 4.2**.

Typical forward and backward pressure waveforms calculated using WIA are shown in **Figure 4.1c,d,** where P_+ and P_- continued to decrease along the

length of the tube. It is noted that the earlier arrival of the foot of the separated backward pressure wave as the measurement site moved away from the inlet of the tube due to the measurement sites close to the reflection site (outlet)The peaks of P_+ and P_- decreased in a similar exponential way with the travelling distance, although in a different directions, **Figure 4.3**. **Table 4.2** includes the exponential decay function of normalized peak of P_+ for each of the four tubes.

4.1.2.3 Dissipation of wave intensity and wave energy

The peak of dI_+ decreased exponentially along the length of the tube as shown in **Figure 4.4a**, while the peak of dI_- also decreased exponentially along the length of the tube (in the backward direction), **Figure 4.4b.** We also note the gradual earlier arrival of the reflected wave as determined by the onset of dI_- while the measurement sites moved closer to the end of the tube, **Figure 4.4b.**

The dissipation of I_+ followed a similar pattern of dissipation to that of dI_+, decreased exponentially along the tube and this observation was consistent in all four-sized of tubes, **Figure 4.5 a & b.**

Similar to P_+ and P_-, the peaks of dI_+ and dI_- also decreased exponentially in opposite directions in a similar way, **Figure 4.6.**

Table 4.2 includes the exponential decay function of normalised peak of dI_+, and normalised I_+ for each of the four tubes.

4.1.2.4 The effect of the tube size on wave dissipation

The same volume of flow (40ml) was ejected into each of the four tube sizes and as we expected, a bigger pulse pressure was observed in the smaller tubes compared to that in the bigger size tubes. For example, at 20 cm away

from inlet, in 12 mm and 16 mm tube the pressure pulse is approximately 1.85 kPa and 0.8 kPa, respectively, **Figure 4.7.** The greatest pulse pressure was found in the 4 mm diameter tube, approximately 6.5 kPa, while the smallest was found in the 16 mm diameter tube, approximately 0.8 kPa.

The effect of the tube size on wave dissipation was investigated using the normalized values. The normalized values were calculated as described in the section 3.6.

As described above, the exponential dissipation equations shown in **Table 4.2** are written as $e^{-x/\lambda}$, where *x* is the distance away from inlet of the tube and **λ** is the inverse of the power of the exponential decay. Obviously, the smaller the **λ** the greater the dissipation.

The results in **Table 4.2** show that the greater dissipation of P_+ occurs in the smaller-sized tubes. For example, the peak of P_+ dissipated by 40%, 36%, 29% and 17% in the 4 mm, 8 mm, 12 mm and 16 mm diameter tubes, respectively, at approximately 1.8 m away from the inlet of the tube. dI_+ and I_+ followed a similar pattern and greater dissipation was observed at the smaller tube sizes. For example, I_+ dissipated by 67% in 8 mm diameter tube at 1 m away from inlet, where it dissipated by only 43% in the 16 mm diameter tube at the same distance away from the inlet. The results shown in **Table 4.2** demonstrate that the smaller size tubes cause greater dissipation than those observed in the larger size tubes.

4.2 Wave dissipation at different experimental conditions

4.2.1 Introduction

The general experimental set-up (**Figure 3.1**) introduced in Chapter 3 is used for this set of experiments. However, only two sized tubes were used in this experiment, which are 12 mm and 16 mm in diameter.

The aim of this experiment is to investigate effect of twonon-walled parameters, which are not related to wall properties, including initial pressure (undisturbed) and speed of piston pumping, on wave dissipation in flexible tubes. Hence, the operation of change of initial pressure and pumping speed of piston are also introduced in this section as follows:

Initial pressure: The effect of initial pressure on wave dissipation was investigated when the initial pressure was set as 4 kPa and 5 kPa, respectively. The varied initial pressure is provided by changing the level of water in the reservoirs. Input volume (displacement of pump) is set as 40 ml and the pumping speed of piston is controlled by the power of motor of pump, which was fixed at 5.5 V.

Pumping speed of piston: The effect of pumping speed of piston on wave dissipation was also investigated. This experiment aims to simulate the effect of increased heart rate on wave dissipation. The varied pumping speed of piston was controlled by increasing the voltage of power driving the DC motor, operating the pump from 5.5 V to 8 V. The corresponding pumping speed of

piston was approximately 2.2 cm/s and 4 cm/s, respectively. The initial pressure for this experiment was set as 4 kPa and the input volume was set as 40 ml.

It is worth noting that study of the effect of each parameter on wave dissipation required keeping the other parameter unchanged. That is to say, when the initial pressure was varied, the voltage of DC motor was kept fixed, and so on. The parameters are listed in **Table 4.3**.

4.2.3 Results

4.2.3.1 The effect of initial pressure on wave dissipation

The pressure, velocity pulse and peak of WI: The greater pressure and velocity pulse occurs when the initial pressure is lower, which is consistent in two sized tubes. An example of pressure and velocity pulse at inlet in 12 mm tube under the initial pressure of 4 kPa and 5 kPa are shown in **Figure 4.8**. This figure shows that the pressure pulse when the initial pressure is 4 kPa is bigger than that when the initial pressure is 5 kPa (1.85 vs. 1.3 kPa). The measured, forward and backward pressure pulse at the measurement sites of 150 cm away from inlet when the initial pressures is 4 kPa are slightly bigger than those when the initial pressures is 5 kPa, **Figure 4.9 a, b.** The measured and forward velocity pulses when the initial pressure is 4 kPa are also slightly bigger than those when the initial pressure is 5 kPa. However, a difference of backward velocity pulse between these two cases is not obvious, **Figure 4.9 c, d**. The difference for the peak of forward wave intensity between initial pressure at 4 and 5 kPa was not noticeable, **Figure 4.9 e, f.**

The measured pressure, velocity waveforms of 16 mm tube in the space-time when the initial pressure was 4 kPa is shown in **Figure 4.10 a, c** and 5 kPa

is shown, **Figure 4.10 b, d,** respectively. The pulses of the measured pressure when the initial pressure was 4 kPa are slightly bigger than that when the initial pressure was 5 kPa. The pulses of the measured pressures for both cases decreased first and then increased due to the effect of reflected waves. The pulses of the measured velocity when the initial pressure is 4 kPa are similar to that when the initial pressure is 5 kPa. The pulses of the measured velocity for both cases decreased first and then continued to decrease sharply due to the effect of reflected waves.

The separated forward pressure and wave intensity waveforms in the 16 mm tube in the space-time are shown in **Figure 4.11 a, b, c, d**. The pulses of separated forward pressure decreased gradually along the length of the tube regardless of the initial pressure although the pulses of separated forward pressure when the initial pressure was 4 kPa are slightly bigger than those when the initial pressure was 5 kPa. Similar pattern also occurs with the separated forward wave intensity.

Dissipation of the forward pressure, wave intensity and wave energy: The normalized values for all measurements of 16 mm tube show that forward pressure, peak of forward wave intensity and forward wave energy dissipated exponentially along the distance regardless of whether the initial pressure was 4 kPa or 5 kPa. The normalized forward pressure, wave intensity and wave energy when the initial pressure is 4 kPa dissipated more than that when the initial pressure is 5 kPa, which can be judged by the indices of power of exponential equation of regression line, **Figure 4.12 a, b, c**.

Wave dissipation under the lower initial pressure is greater than that under the higher pressure occurs consistently in two sized tubes, which can be

judged by the indices of power of exponential equation for regression line, **Table 4.3.**

4.2.3.2 The effect of pumping speed of piston on wave dissipation

The pressure, velocity pulse and peak of WI: With the initial pressure and input volume are constant, the greater pressure and velocity pulse occurs when the pumping speed of piston is faster. For example, at 5 cm away from inlet in 12 mm tube the pressure pulse when the pumping speed is 4 cm/s (voltage of power is set as 8 V) is approximately 30% greater than that when the pumping speed is 2.2 cm/s (or voltage of power is set as 5.5 V) (2.4 vs 1.85 kPa), **Figure 4.13**. Meanwhile, the greater measured, separated forward and backward pressure and velocity pulse occurs when the pumping speed is fast, **Figure 4.14 a, b, c, d**. There is a considerable difference for the peak of wave intensity between when the piston was pumping slow and fast, **Figure 4.14 e, f**.

The measured pressure, velocity waveforms in the 16 mm tube in the space-time plane when the pumping speed of piston is 2.2 cm/s and 4 cm/s are shown in **Figure 4.15 a, b, c, d,** respectively. The amplitudes of the measured pressure when the pumping speed of piston was 2.2 cm/s are smaller than that when the pumping speed of piston was 4 cm/s. The amplitudes of the measured pressures for both cases decreased first and then increased due to the effect of reflected waves. The amplitude of the measured velocity when the pumping speed is 2.2 cm/s is smaller than that when the pumping speed is 4 cm/s. The amplitudes of the measured velocity for both cases decreased first and then continued decrease sharply also due to the effect of reflected waves.

The separated forward pressure and wave intensity waveforms in the 16 mm tube in the space-time are shown in **Figure 4.16 a, b, c, d**. The amplitude

of separated forward pressure decreased slowly along the length of the tube for both cases although the amplitude of separated forward pressure when the pumping speed of piston is 2.2 cm/s is smaller than those when the pumping speed of piston is 4 cm/s. The peak of forward wave intensity when the pumping speed of piston is 2.2 cm/s is much smaller than those when the pumping speed of piston is 4 cm/s. The peak of forward wave intensity decreased sharply along the length of tube for both cases, **Figure 4.16**.

Dissipation of the forward pressure, wave intensity and wave energy: The normalized values for all measurements of 16 mm tube show that forward pressure, peak of forward wave intensity and forward wave energy dissipated exponentially along the distance regardless of whether the pumping speed are at 2.2 or 4 cm/s, **Figure 4.17**. A greater dissipation of forward pressure and wave energy occurs when the piston is pumping faster is consistent in the two sized tube but dissipation of wave intensity was less when the piston was moving faster than that when the piston is moving slower, **Figure 4.17 and Table 4.3**.

4.3 Effect of viscosity of liquid on wave dissipation

4.3.1. Introduction

The experimental setup described in Chapter 3, which is shown in **Figure 3.1,** was used to carry out this experiment. Three sized tubes were used to test the effect of viscosity on wave dissipation. The main aim of this experiment is to investigate the wave dissipation in the latex tubes when viscosity of liquid was varied. In this work, we used 16% and 36% of glycerol-

water solution in volume to change the viscosity from 1.48cS to 2.84cS and density from 1.036 kg/l to 1.088 kg/l (Weast, 1981-1982). The degree of wave dissipation in the three sized latex tubes with these two types of glycerol solution will be compared.

4.3.2. Results

4.3.2.1 Effect of viscosity on wave speed

Wave speed in the 16% of glycerol-solution is similar to that in the 36% of glycerol water solution, which is consistent in the three sized tubes. For example, at inlet of 12 mm tube, the local wave speed determined by PU-loop is 3.26 m/s in the 16% and 3.04 m/s in the 36% of glycerol-water solution, **Figure 4.18**.

The average of wave speeds in the three sized tubes in the 16% of solution is also similar to that of 36% of glycerol-water solution, **Figure 4.19 a, b and c**. For example, the average of wave speed along the 12 mm tube for 16% of the glycerol-water solution is approximately 3.88 ±0.76 m/s and for the 36% of the glycerol-water solution is approximately 3.85 ±0.96 m/s.

The average of wave speed when the tube is filled with water is slightly greater than that when the tube is filled with glycerol solution, **Table 4.1 and Figure 4.19 a, b, c**. For example, the average of wave speed along the 8 mm tube when the tube is filled with water is 5.0±0.5 m/s but it is 3.83 ±0.73 m/s when the tube is filled with 16% glycerol-water solution.

4.3.2.2 The effect of viscosity on wave dissipation

The greater dissipation occurs when the liquid in the tube is more viscous. For example, in the 16 mm tube, the forward wave energy dissipated approximately 60% at 1 m away from inlet, compared to that at inlet in the 16% of the glycerol-water solution. While, in the 36% of the glycerol-water solution the forward wave energy dissipated around 80% at the same position. As shown in the **Figure 4.20 a, b, c**, the forward pressure, wave intensity and wave energy with the 36% of glycerol solution dissipate more than those with the 16% of glycerol solution, judged by the power of regression line of normalized value for all measurements of 16 mm tube. **Table 4.4** lists the exponential equations of decay of normalized forward pressure, forward wave intensity and forward wave energy in three sizes tube. Overall, greater dissipation occurs in the 36% of glycerol-water solution than that in the 16% of glycerol-water solution.

4.4 The effect of tube wall on wave dissipation

4.4.1 Introduction

Experiment setup: Experiment setup is based on the general experimental setup described in Chapter 3, **Figure 3.1**. Most of the components used in this experiment are the same as those used before with the exception of pump and tubes. In this experiment, the pulse wave is produced by an artificial heart pump, BCM, (Cardialcare, Minneapolis, MN, U.S.A), driven by the Intra-aortic-balloon-pump (IABP) rather than by a piston pump driven by a DC motor. The two sized tubes, 16 mm in diameter with 2 m in length and 24 mm in diameter with 1 m in length, were used to investigate the effect of wall property on wave dissipation. The wall property was modified by inserting the latex tube

into a nylon tube, diameter and length of which are the same as latex tube. The wall of nylon tube is much stiffer than that of latex tube is.

Measurements: The simultaneous measurements of pressure, flow and diameter were taken at the same position at interval of 5 cm along the length of tube. Pressure is measured using Millar-Mikro tip catheter pressure transducer (Millar Instruments, INC, Houston, Texas, 77023, USA) and flow is measured using ultrasonic flow probe (Transonic System, Inc, Ithaca, NY, USA). The diameter is measured using Sonometric ultrasonic paired crystals (Sonometric Cooperation , 500 Nottinghill London, ONT, N6K 3P1, Canada).

Millar pressure transducer was calibrated using standard calibration tool generating 0, 25, 100 and 125 mmHg to establish the relationship of pressure in mmHg and in Voltage, whose slope constitutes the calibration factor.

Dynamic compliance and distensibility: This experiment aims to investigate the effect of stiffness of tube wall on wave dissipation. Therefore, we also investigate the pattern of wave speed, dynamic compliance and distensibility along the tubes with and without Nylon sleeves. The wave speed was established using PU-loop and the dynamic compliance can be obtained using the following equation,

$$C = dA / dP \qquad (m^2 Pa^{-1}) \qquad (4.1)$$

where, C is the local dynamic compliance. dP denotes the changes of the measured pressure when the wave arrives the measurement sites and dA is the changes of cross-sectional area related to the change of dP. Under the assumption of the circular cross-section of tube, the cross-sectional area can be calculated from the measured diameter, $A = \frac{\pi}{4} D_m^{\,2}$, where A is the cross-

sectional area of the tube and D_m is the measured diameter. Dynamic distensibility, D, can be established by the dynamic compliance dividing by the undisturbed cross-sectional area, A

$$D = dA / AdP \qquad (Pa^{-1}) \tag{4.2}$$

4.4.2 Result

4.4.2.1 Wave speed, compliance and distensibility

As expected, local wave speed in the tube with sleeves is greater than that without sleeves in the 16 mm tube, **Figure 4.21.** The average wave speed in the 16 mm tube with sleeves is approximately 30% greater than that without the sleeves when the outliers are taken out (4.92±1.1 vs. 3.42±0.54). Similarly, the wave speed in the 24 mm tube with sleeves is also greater than that without sleeves.

It is noticeable that the compliance and distensibility of tube with sleeves is less than those without sleeves in the 16 mm tube, **Figure 4.22, 4.23**. In addition, the compliance and distensibility is lowest in the middle part of tube and then increase toward to both ends. Lower compliance and distensibilities are also found in the 24 mm tube with sleeves, **Figure 4.24, 4.25.** In the 24 mm tube the compliances and ditensibilities decreased along the tube regardless of with and without sleeves.

4.4.2.2 Effect of stiffness of tube wall on wave dissipation

The latex tube wall was stiffening due to it be inserted into a Nylon sleeves, which increase the wave dissipation. For example, the dissipation of

peak of forward wave intensity and forward wave energy in the 16 mm tube with sleeve is greater than that without sleeves, **Figure 4.26, Figure 4.27**.

4.5 Discussion

There is growing evidence that the interaction between the forward and backward arterial waves have real prognostic value for cardiovascular patients in the clinic (Asmar et al. 2001; Bleasdale, et al. 2003). Adopting the methods discussed in this Chapter for studying the dissipation of waves both in the forward and backward travelling directions could provide information on the up- and downstream arterial mechanical conditions, which could potentially be used clinically for the diagnosis of vascular patients.

In this work, WIA was used to investigate the dissipation of waves in elastic tubes. This analysis has been tested *in vitro* (Khir and Parker, 2002), and proved to be useful in studying waves in the aorta (Koh et al., 1998; Khir and Parker, 2005), in the coronary arteries (Sun et al. 2003; Davies et al. 2006) and in the carotid artery (Sugawara, et al. 2002). WIA benefits this research in several respects: **1)** WIA is a time domain technique allowing for wave dissipation in elastic tubes to be studied and the results presented as a function of time and space; **2)** WIA does not make any assumptions about the tube's wall nonlinearity, although the solution of one-dimensional equations along the characteristic directions involving the water hammer equation is linearised expression. Also, This analysis takes into account the effects of the vessel's wall viscoelastic properties, convective, frictional effects and fluid viscosity; **3)** WIA provides a method to separate pressure and velocity waves travelling in

the forward and backward directions from the measured pressure and velocity waveforms. Thus, the analysis offers a technique to study wave dissipation in one direction whilst taking into account the effect of reflections from the opposite direction. **4)** The physical meaning of wave intensity is the flux of energy carried by the wave per unit cross-sectional area. This provides a convenient method to study the dissipation of energy carried by the waves along flexible tubes.

4.5.1 Dissipation of the separated pressure waveforms

It is widely accepted that measured arterial waves could be regarded as the linear summation of the incident pressure wave generated by the contracting left ventricle, and the reflected waves generated at the various reflection sites along the arterial bed (Parker and Jones, 1990). Also, it has been long established that the magnitude of the measured pressure increases downstream in arteries, which is thought of due to reflected waves (Nichols and O'Rourke, 1998). It is therefore rather difficult to investigate the dissipation of the measured pressure waves alone, as it will almost certainly be affected by the existence of the reflected waves, especially if the measurement and reflection sites are close. We therefore believe that investigating wave dissipation requires the separation of the forward and backward waveforms from the measured waveform. The significance of using WIA in this study is to allow for investigating the dissipation of waves travelling in the forward and backward directions separately and independently from each other, hence eliminating the effect of wave reflections on the magnitude of the measured waveforms.

Figure 4.1a shows a typical example of P ,which is the summation of P_+ generated upstream by the pump and P_- generated downstream by the reflection site at the exit of the tube. The peak of P initially decreased gradually as the measurement site moved away from the inlet of the tube, then started to increase due to the arrival of reflected waves, obscuring the pattern of dissipation. **Figure 4.1c,d** show the propagation of P_+ and P_- in time and space, where the peaks of P_+ and P_- can be seen steadily decreasing with the travelling distance, highlighting the importance of wave separation in the study of wave dissipation. **Figure 4.1d,** shows the feet of the P_- waves indicating the time of arrival of reflected waves at each site, and since this line is in the time-distance plane, its slope could be used for verifying wave speed.

4.5.2 Dissipation of wave energy

The peak of wave intensity, dI_+, and integration of wave intensity with respect to time over one cycle, I_+, dissipated exponentially along the distance travelled, as shown in **Figure 4.5a** and **Figure 4.5b**. We note that there are some scatters in the beginning part of the 4 mm tube. It is speculated that these scatter occurred due to great difference of diameter between the 4 mm tube and rigid connector at inlet. The regression line fits well with the most of the measured value with the exception of the first 6 points.

The peaks of dI_+ and dI_- decreased as an exponential function with the travelling distance as shown in **Figure 4.6.** The exponential decay of dI_- was nearly equal to that of dI_+. The concurrence of the degree of dissipation demonstrates that wave dissipation in uniform elastic tubes has a strong similarity between the forward and backward directions. This finding agrees with

that of Histand and Anliker (1973). They found that the "wave travelling in either direction exhibited similar exponential decay patterns for their amplitudes". Although, they found that the retrograde waves appear to dissipate faster than the down-stream travelling waves, this difference was related to the tapering of the aorta. In our work, the difference between the exponential decay of wave dissipation in the forward and backward directions is very small, approximately 5% of which is in the order of the experimental noise.

4.5.3 Effect of size on wave dissipation

Fung pointed out the different relationship of change of pressure and diameter between the loading and unloading of the vessel wall as the wave passes through the measurement site, reveals a hysteresis in the stress-strain plot (Fung, 1981). He suggested that the area of this hysteresis could be used as a means for quantifying energy dissipation. A possible explanation for the greater dissipation observed in our experiments in the smaller sized tubes is that those tubes may have a greater hysteresis area compared to the bigger sized tubes. This may be due to the increased wall stiffness owing to the greater pulse pressure, thus affecting the viscoelastic properties of the wall. Due to the lack of measurement of diameter for 4 mm tube, we are not able to examine the effect of hysteresis area on wave dissipation quantitatively. However, it is speculated that bigger hysteresis area in the smaller sized tube could be aroused from greater pressure pulse.

Further, Bertram suggested that the relative contribution to energy dissipation of wall viscoelasticity and viscous shear depends strongly on the size of vessels, where it was implicit that the main cause of dissipation in the bigger tube sizes is the viscoelastic properties of the vessels, while viscosity of

blood was the main cause of wave dissipation in the small vessel sizes (Bertram, et al., 1997). The exact description of the effect of tube size on wave dissipation is not yet fully understood.

4.5.4. Effect of experimental conditions on wave dissipation

Pulsatile energy in the circulation system (which is an index of energy losses of circulation system) might be affected by many factors such as blood pressure, cardiac output, and heart rates (O'Rourker, 1967). Further, Bertram suggested that different experimental conditions such as pressure might attribute to the discrepancy of a previous study (Ursino, et al., 1993), which implies experimental conditions might affect noticeably the degree of wave dissipation (Bertram, et al. 1997).

The investigation of effect of initial pressure and pumping speed of piston on wave propagation aimed to mimic relevant clinical conditions such as increased blood pressure and heart rate.

Initial pressure: The smaller pressure pulse occurs when the initial pressure is higher might be caused by the stiffer of tube wall due to the higher pressure. The greater wave dissipation occurs at the lower initial pressure, which might be caused by the greater hysteresis area due to the greater pressure pulse.

Pumping speed of piston: The greater wave dissipation as the piston pumping faster is also consistent with what is expected. This finding is consistent the statement by Macdonald (Macdonald, 1974), in which it is believed that the higher frequencies damped out first.

Ursino investigated experimentally the wave propagation in the latex tube with different pressure signals and found that increasing the amplitude of

pressure evidently increase the attenuation per wavelength (Ursino, et al., 1993). In general, the results in this research agreed with the founding by Ursino. For example, the greater pulse when piston is moving faster is accompanied with the greater dissipation. Further, the greater pressure pulse at lower initial pressure also cause the greater dissipation.

4.5.5 Effect of viscosity

In 12 mm and 16 mm tube, the effect of viscosity on wave speed is not noticeable, which is consistent with the prediction by Womersley curve (Mcdonald, 1974), in which they found that effect of viscosity on wave speed is relatively small in larger vessels. However, the results in 8 mm tube in our experiment that wave speed is higher at lower viscosity glycerol-solution is not reasonable, which is also dissimilar to the predication using Wonersley method. These unreasonable results are speculated to be the density of glycerol-solution. In our experiment, the latex tubes are supported by the water in the tank. However, the latex tubes filled with the glycerol-solution appear bending due to the difference of density between water in the tank and glycerol solution in the tube. In this case, the middle part of latex tube is lower than its ends in the water, which cause the varied transmural pressure along the length of the tube. Therefore, these unreasonable results probably resulted from the added effect of transmural pressure and gravity.

The greater wave dissipation occurs in the more viscous glycerol solution is consistent in three sized tubes although in large sized tube it is less marked than it is in smaller sized tube. This finding is consistent with the early work by Bertram about the viscosity of blood is more important in the smaller sized vessels (Bertram, et al., 1997).

4.5.6 Effect of property of tube wall

Aortic stiffness is an independent predictor of cardiovascular mortality in hypertensive patients. Stiffening the tube wall has the effect of increasing the damping and wave speed (Mcdonald, 1974). In this thesis, the tube wall was stiffened by inserting the latex tube into nylon tube. It is very clear that stiffening of tube wall increase the wave speed approximately 30% in the 16 mm tube. The dynamic compliance and distensibility decreased as expected due to the stiffening of tube wall.

It is worth noting that the tubes of 16 mm in diameter and 2 m in length are produced using the tube in 1 m length, which is not exactly uniform due to the dipping method used in manufacturing these tubes. It is found that the smallest wall thickness we measured was about 0.15 mm at one end and gradually increases to the largest at the other end of approximately 0.2 mm. Each tube of 16 mm in diameter and 2 m in length were constructed by gluing the thicker ends of two tubes of 1 m using liquid latex. Therefore, it is reasonable to deduce that the overlapped part of connecting the two tubes was inevitably slightly stiffer and thicker than the other parts of the 2 m long tube. This variation in wall thickness and mechanical properties might be the source of difference in the local wave speed, compliance and distensibilities along the tube; giving the highest values around the middle of the tube.

The variation of local wave speed along the tube length, which is associated with the changes of wall thickness, provides evidence to the sensitivity of PU-loop method to local changes. The increase of wave speed along the length of 24 mm tube was caused by the thickness of tube wall decrease from inlet to outlet. Likewise, the gradually reduction of thickness of

tube wall along the tube also results in the gradual decrease of compliance and distensibility.

Furthermore, as expected, greater dissipation occurs in the modified tube also due to stiffness of tube wall.

4.5.7 Sources of wave dissipation

Although attempts by researchers have been made to find the sources of wave dissipation, a general consensus has not been reached. The relative large contribution of viscous element in the wall to dissipation was suggested due to the greater dissipation in arteries than was predicted only from the viscous dissipation (Mcdonald and Gessner, 1968). Bertram et al. (1980) stated that wall viscoelasticity contributes relatively little to energy dissipation per cardiac cycle and pulse wave attenuation. In our experiments, effect of the viscosity of the liquid on wave dissipation is more marked in the large sized tube than it is in the smaller sized tube. Stiffening of tube wall increase the degree of dissipation probably due to the viscoelastic effect of tube wall increasing.

In addition, the energy imparted to the surroundings might also contribute to dissipation. As described in the experimental setup section, the tube is fully emerged in water. As the wave travels in the tube, part of the kinetic energy imparted from the wave to the wall of the tube will generate waves in the water of the tank outside the tube. Given that the cross-sectional area of the tank is much larger than that of any of the tubes, and that the tank is open to the atmosphere, the waves generated in the tank are expected to be relatively small in magnitude. Using the reasonable assumption that the energy transported outside of the tube would not be restored again to inside of the tube indicates this energy must be accounted for as part of the energy dissipated from the

waves inside the tube. We can therefore extrapolate that the boundary conditions may play a role in the dissipation of waves in elastic tubes.

4.5.8 The limitation

The limitations of this investigation are that wave dissipation was examined in uniform tubes rather than tapered tubes. We acknowledge that using tapered tubes might have given different dissipation results in the forward and backward direction. However, using cross sectional uniform tubes as the first step is useful to provide the basic understanding, and then study the wave dissipation in tapered tube in the future. Thin walled latex tubes (commercial available) used in this investigation can not sustain as high pressure as physiological pressure. Therefore we consciously restricted the pressure inside the tubes to be 3kPa to avoid rupture or bulging. Consequently, in order to avoid external deformation to the tubes' wall we chose water height above the tube to be 1 cm.

Table 4.1 **Dimensions and properties of the 4 different sized latex tubes.**

Unstressed diameters D (mm)	4	8	12	16
Wall thicknesses t (mm)	0.1	0.15	0.2	0.2
Initial external diameters (mm)	4.2	8.8	12.53	16.6
Wave speed (m/s)	7.1±0.9	5.0±0.5	4.0±0.5	3.5±0.4
Compliance (dA/dP) ($10^{-8}m^2Pa^{-1}$)	0.024	0.872	1.98	4.55

Wave speed was determined using the PU-loop method and the initial external diameter was measured when the hydrostatic pressure in the tube is 3Kpa.

Table 4.2 Wave dissipation in 4 sized tubes.

	Tube Diameter (mm)			
	4	**8**	**12**	**16**
Normalised Peak Pressure ($\frac{P_+}{P_{+i}}$)				
Peak pressure dissipation equation	$1.00e^{-x/4.46}$	$0.97e^{-x/4.54}$	$1.00e^{-x/6.72}$	$0.91e^{-x/15.9}$
Correlation Coefficient (r^2)	0.81	0.64	0.78	0.42
Normalised Peak Wave Intensity ($\frac{dI_+}{dI_{+i}}$)				
Peak wave intensity dissipation equation	$0.74e^{-x/1.03}$	$0.81e^{-x/1.21}$	$0.84e^{-x/2.74}$	$0.77e^{-x/3.36}$
Correlation Coefficient (r^2)	0.92	0.84	0.78	0.74
Normalised Wave Energy ($\frac{I_+}{I_{+i}}$)				
Wave energy dissipation equation	$0.78e^{-x/1.11}$	$0.86e^{-x/1.55}$	$1.01e^{-x/2.29}$	$0.82e^{-x/3.83}$
Correlation Coefficient (r^2)	0.94	0.76	0.73	0.67

The exponential equations for normalised values of forward pressure, $\frac{P_+}{P_{+i}}$, forward wave intensity, $\frac{dI_+}{dI_{+i}}$ and forward wave energy $\frac{I_+}{I_{+i}}$ in four different sized tubes. Dissipation is expressed as an exponential function $e^{-x/\lambda}$, where x is the distance away from inlet and λ is the inverse of the power of the exponential decay, allowing for calculating the dissipation at any distance away from the inlet of the tube. We note that $1-\frac{P_+}{P_{+i}}$ indicates the dissipation percentage of P_+, $1-\frac{dI_+}{dI_{+i}}$ is the dissipation percentages of dI_+, and $1-\frac{I_+}{I_{+i}}$ is the dissipation percentages of I_+. The greater the value of λ the lower value of dissipation, which is highest for 4 mm tube and lowest for 16 mm tube.

Table 4.3 The effect of non-walled parameters on wave dissipation

Non-walled parameters				
Power of pump (Voltage)		5.5 V	5.5 V	8 V
Displacement in volume (pump) (ml)		40 ml	40 ml	40 ml
Initial undisturbed pressure (kPa)		4 kPa	5 kPa	4 kPa
Exponential equations of best fit curve for all measurements				
12 mm	Peak of forward pressure, P_+/P_{+i}	$e^{-x/9.1}$	$e^{-x/10.8}$	$e^{-x/5.9}$
	Correlation Coefficient (r^2)	0.93	0.89	0.90
	Peak of forward wave intensity, dI_+/dI_{+i}	$e^{-x/1.85}$	$e^{-x/2.27}$	$e^{-x/1.9}$
	Correlation Coefficient (r^2)	0.87	0.84	0.88
	Forward wave energy, I_+/I_{+i}	$e^{-x/2.44}$	$e^{-x/2.5}$	$e^{-x/2.17}$
	Correlation Coefficient (r^2)	0.93	0.93	0.9
16 mm	Peak of forward pressure, P_+/P_{+i}	$e^{-x/10.5}$	$e^{-x/12.3}$	$e^{-x/7.1}$
	Correlation Coefficient (r^2)	0.71	0.58	0.83
	Peak of forward wave intensity, dI_+/dI_{+i}	$e^{-x/2}$	$e^{-x/2.2}$	$e^{-x/2.7}$
	Correlation Coefficient (r^2)	0.89	0.69	0.84
	Forward wave energy, I_+/I_{+i}	$e^{-x/2.9}$	$e^{-x/3.6}$	$e^{-x/2.5}$
	Correlation Coefficient (r^2)	0.8	0.79	0.80

The exponential equations for normalised values of forward pressure, $\frac{P_+}{P_{+i}}$, forward wave intensity, $\frac{dI_+}{dI_{+i}}$ and forward wave energy $\frac{I_+}{I_{+i}}$ in two different sized tubes when the two parameters (pumping speed of piston controlled by the voltage and initial hydrostatic undisturbed pressure) varied independently. Dissipation is expressed as an exponential function $e^{-x/\lambda}$, where x is the distance away from inlet and λ is the inverse of the power of the exponential decay, allowing for calculating the dissipation at any distance away from the inlet of the tube.

Table 4.4 The effect of viscosity of liquid on wave dissipation

Diameter		16% Glycerol-water solution	36%Glycerol-water solution
8 mm	Peak of forward pressure, P_+/P_{+i}	$e^{-x/23}$	$e^{-x/3.03}$
	Correlation coefficient, r^2	0.044	0.83
	Peak of forward wave intensity, dI_+/dI_{+i}	$e^{-x/1.136}$	$e^{-x/0.79}$
	Correlation coefficient r^2	0.88	0.94
	Forward wave energy, I_+/I_{+i}	$e^{-x/2.08}$	$e^{-x/1.43}$
	Correlation coefficient , r^2	0.64	0.89
12 mm	Peak of forward pressure, P_+/P_{+i}	$e^{-x/4.2}$	$e^{-x/4.1}$
	r^2	0.7	0.53
	Peak of forward wave intensity, dI_+/dI_{+i}	$e^{-x/1.43}$	$e^{-x/1.35}$
	r^2	0.72	0.72
	Forward wave energy, I_+/I_{+i}	$e^{-x/2.86}$	$e^{-x/2}$
	Correlation coefficient , r^2	0.89	0.76
16 mm	Peak of forward pressure, P_+/P_{+i}	$e^{-x/9.8}$	$e^{-x/3.57}$
	Correlation coefficient , r^2	0.34	0.77
	Peak of forward wave intensity, dI_+/dI_{+i}	$e^{-x/1.05}$	$e^{x/0.82}$
	Correlation coefficient , r^2	0.83	0.78
	Forward wave energy, I_+/I_{+i}	$e^{-x/1.82}$	$e^{-x/1.2}$
	Correlation coefficient ,r^2	0.81	0.77

Table 4.4 The exponential equations for the forward pressure, forward wave intensity and forward wave energy in three sized tubes (8 mm, 12 mm and 16 mm in diameter) when liquid inside of tube are 16% and 36% glycerol-water solution, respectively.

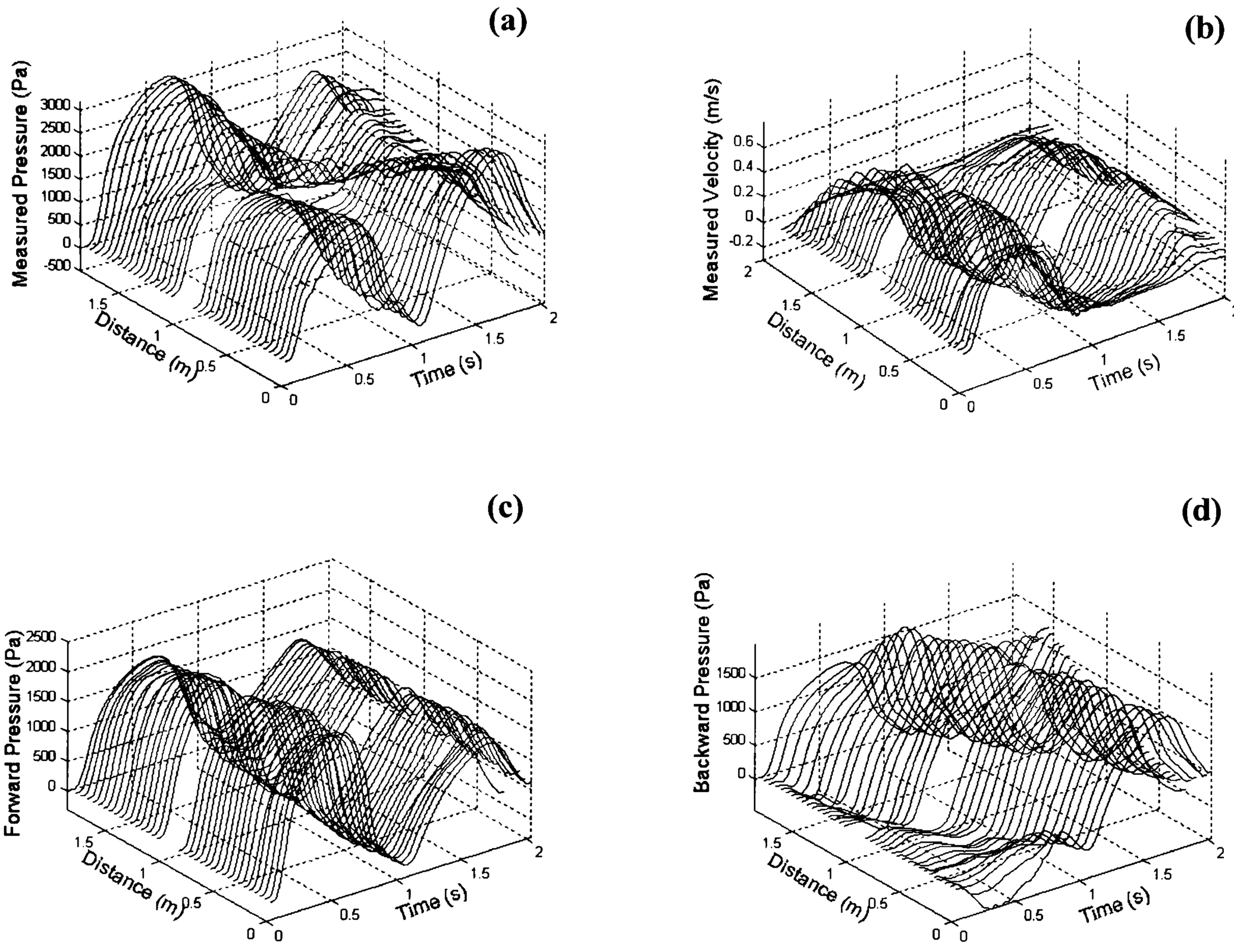

Figure 4.1 The pressure and velocity waveform measured in the 12mm diameter tube at 5cm intervals along the length of the tube **(a,b).** The calculated forward and backward pressure waveforms are also shown varying with time and distance **(c,d).**

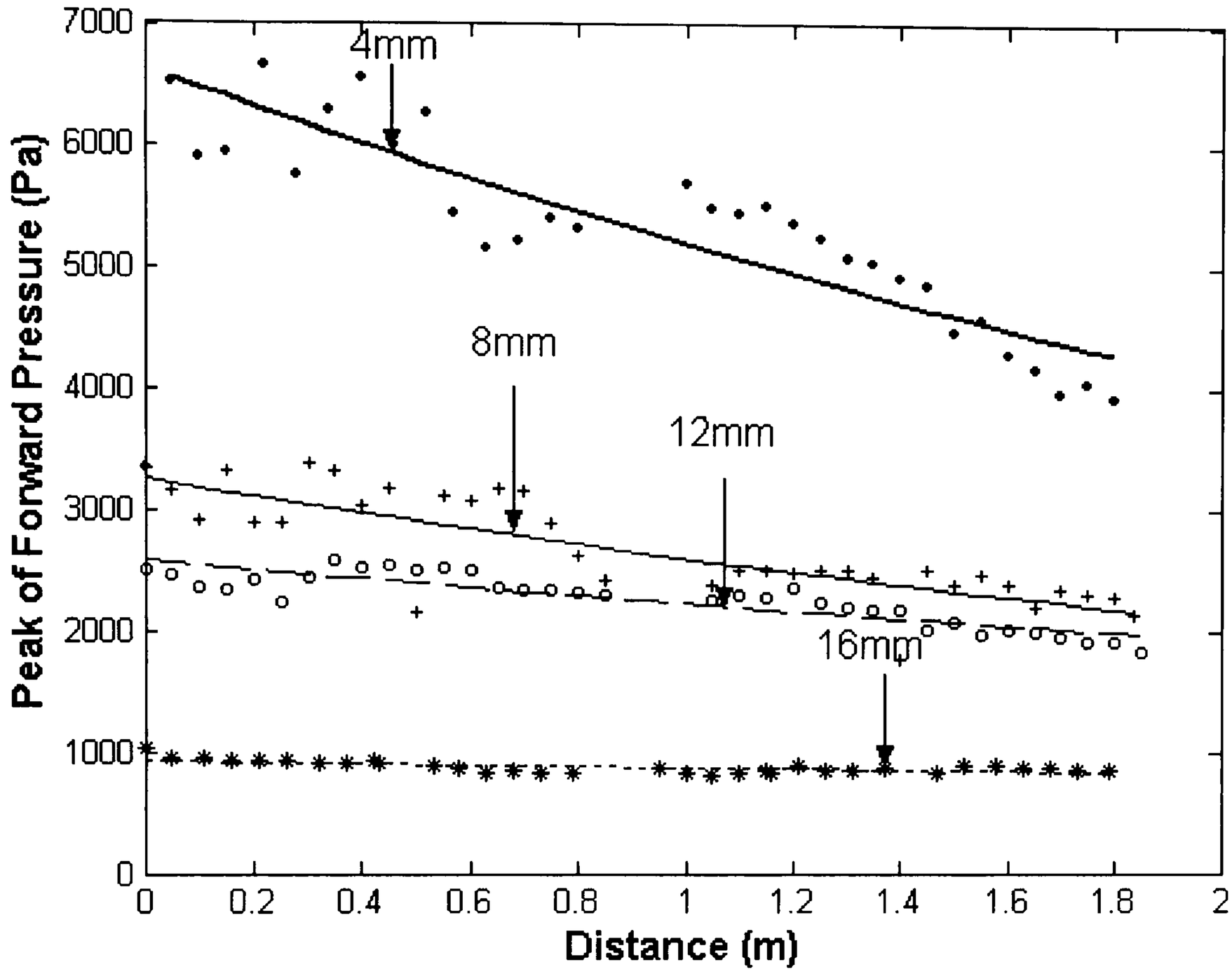

Figure 4.2 The peak of the forward pressure wave is plotted against the distance travelled by the wave. This peak is dissipating exponentially with distance, which was consistent in all four tube sizes.

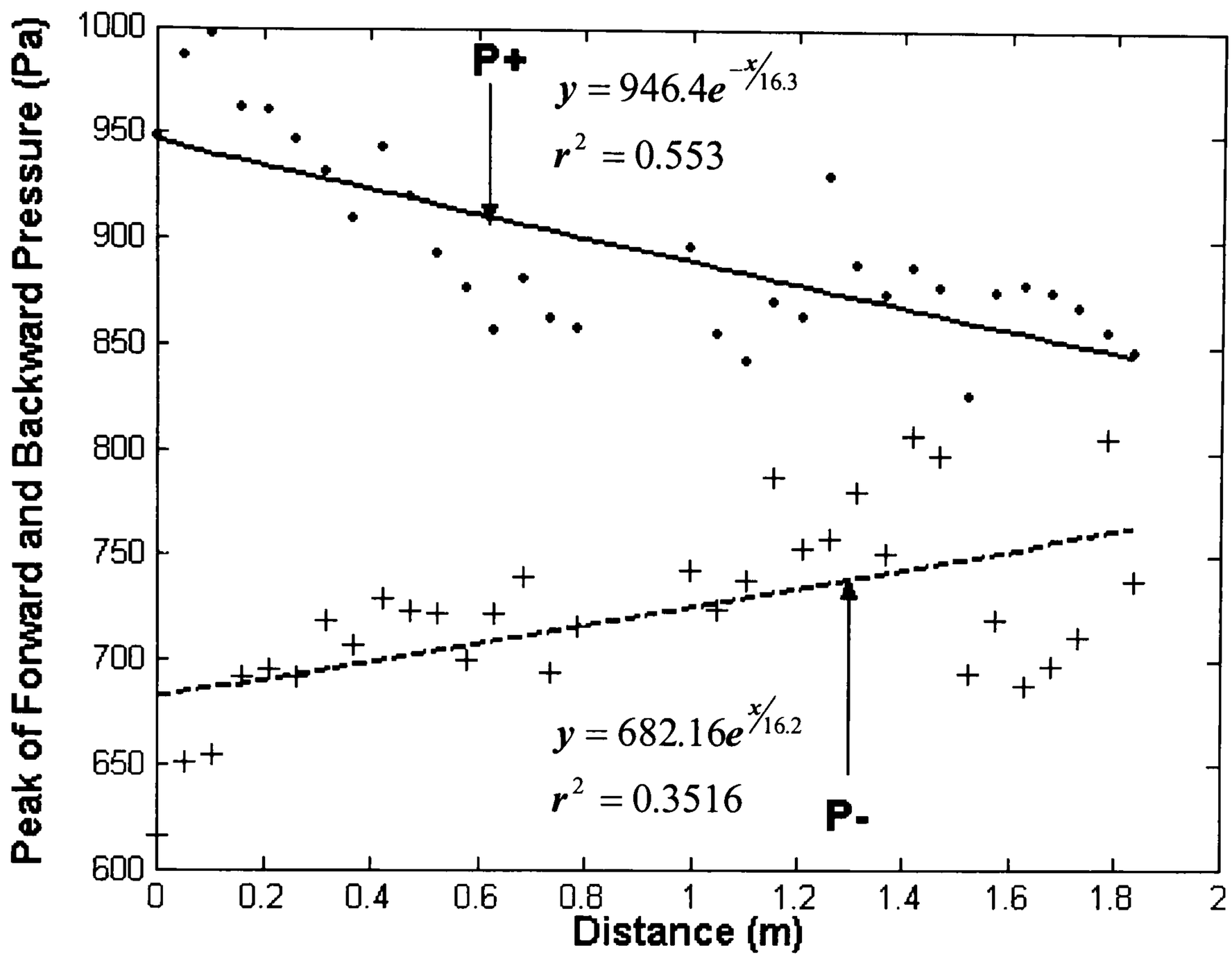

Figure 4.3 The peak of P_+ and P_- against the distance in the 16mm diameter tube. The corresponding regression equations are provided where y denotes P_+ or P_- and x denotes the travelling distance. Note that although the dissipation of P_+ is in the opposite direction of the dissipation of P_-, the power of the exponential equation of both curves is almost identical (16.3 and 16.2) indicating that waves dissipate in a similar pattern in the forward and backward directions in uniform flexible tubes.

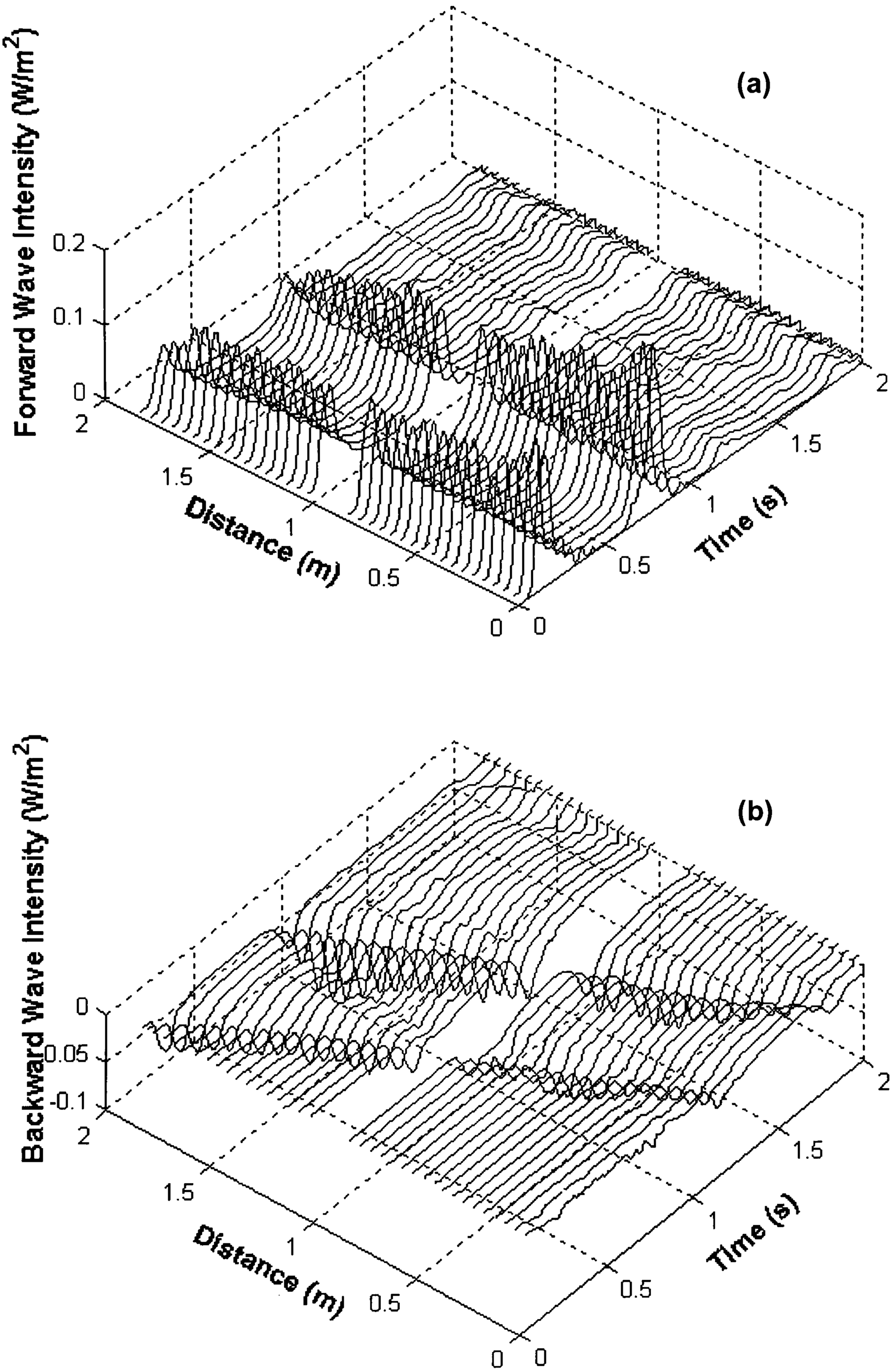

Figure 4.4. Forward **(a)** and backward **(b)** wave intensity in the 12mm diameter tube are shown varying in time and space. The peak of dI_+ is shown decreasing with distance and $dI\_$ is also decreasing with distance but in the opposite direction.

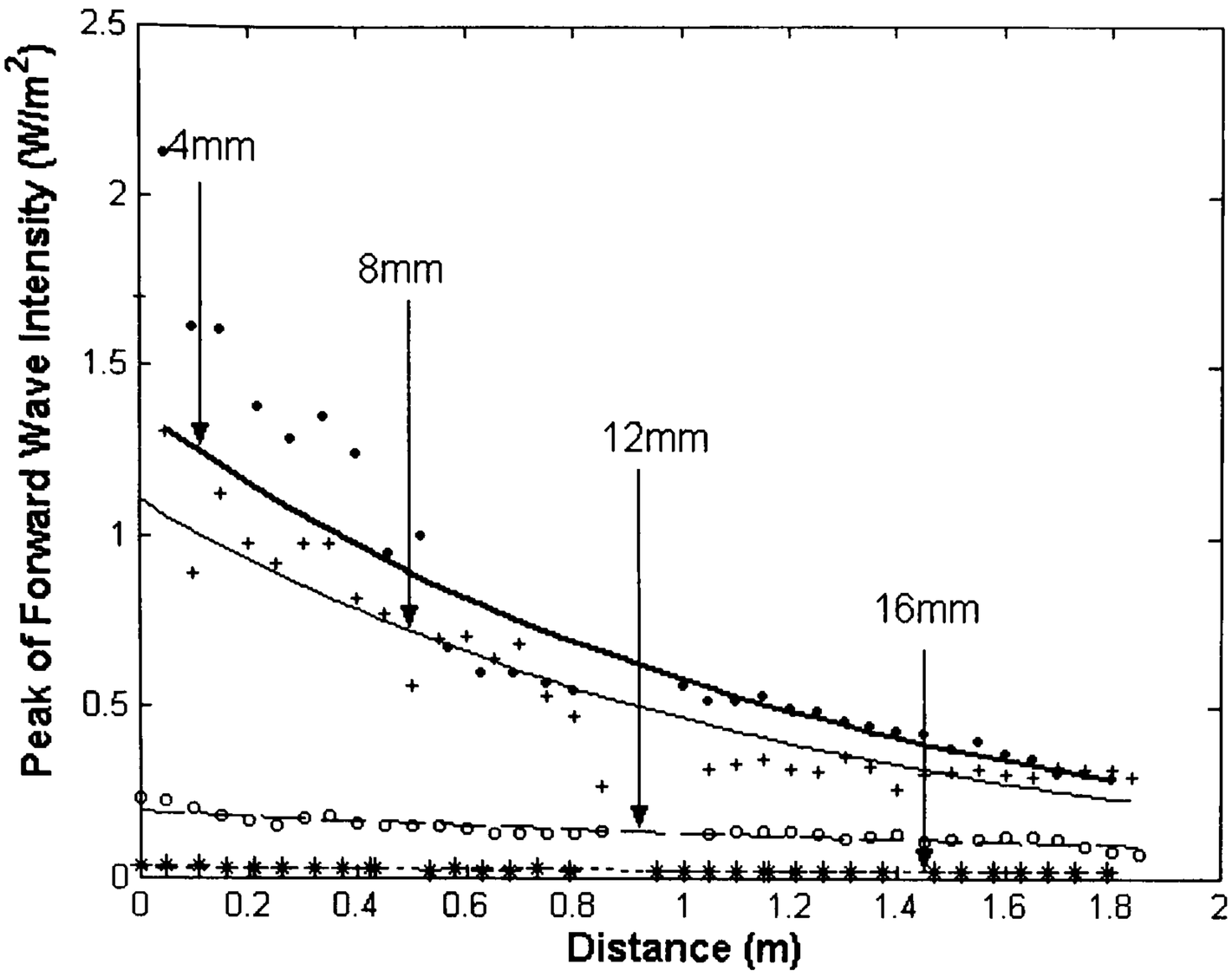

(a)

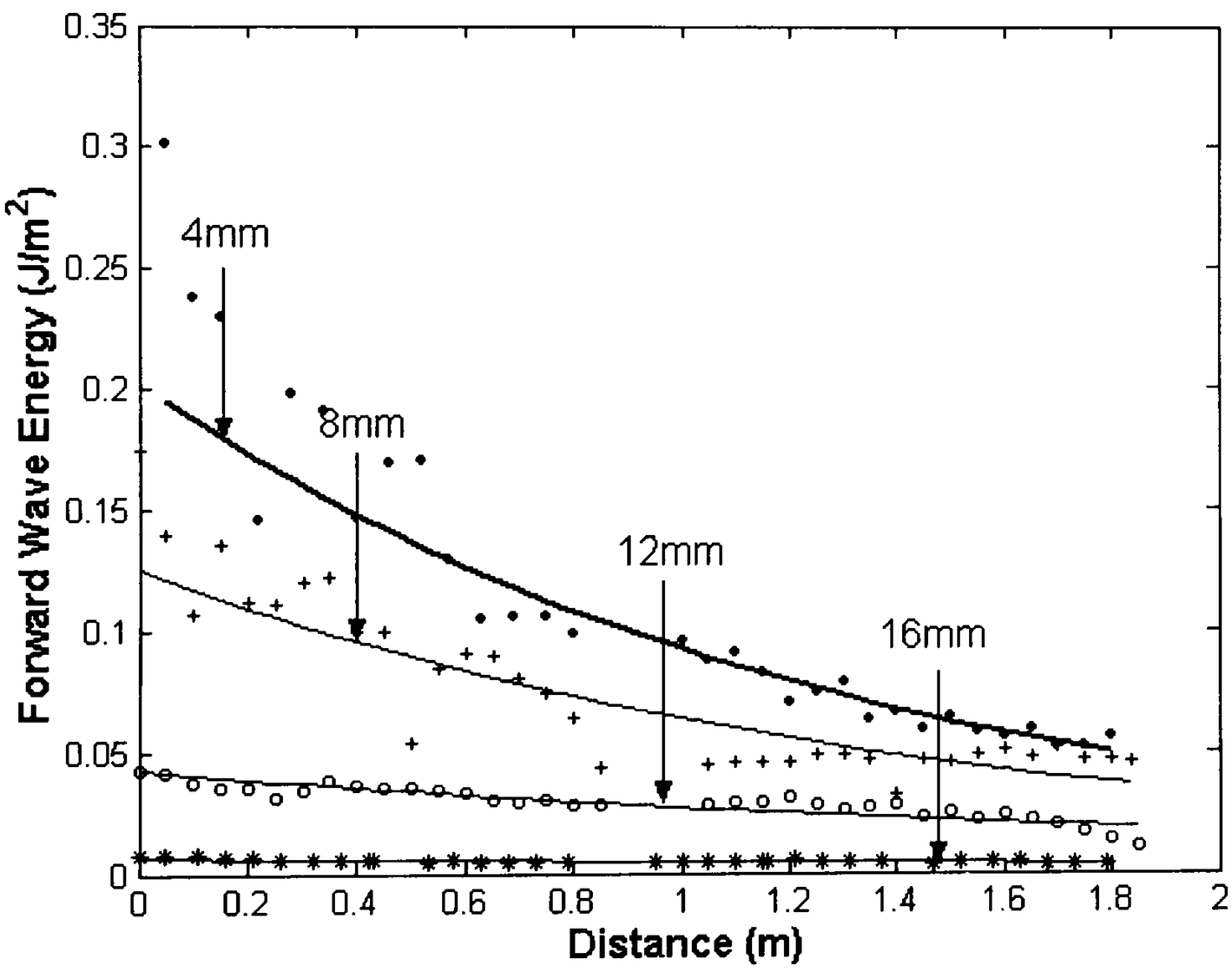

(b)

Figure 4.5 The peak of dI_+ **(a)** and I_+ **(b)** varying with distance in the four tube sizes. This peak is dissipating exponentially with distance, which was consistent in all four tube sizes.

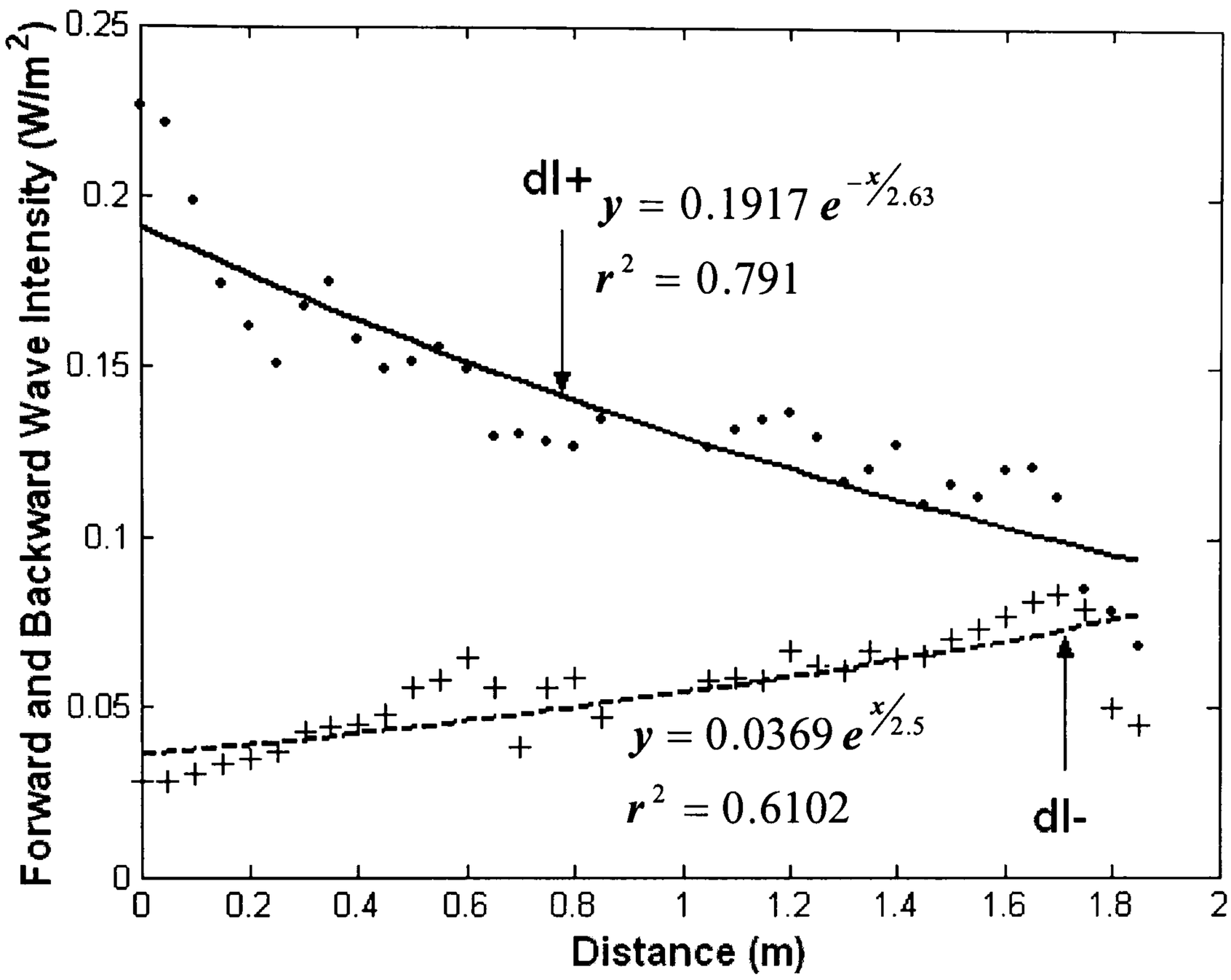

Figure4.6 The peak of the forward dI_+ and dI_- vary with distance in the 12mm diameter tube. Note that although the dissipation of dI_+ is in the opposite direction of the dissipation of dI_-, the power of the exponential equation for both curves is very close (2.63 and 2.5) indicating that wave intensity dissipates in a similar pattern in the forward and backward directions in uniform flexible tubes.

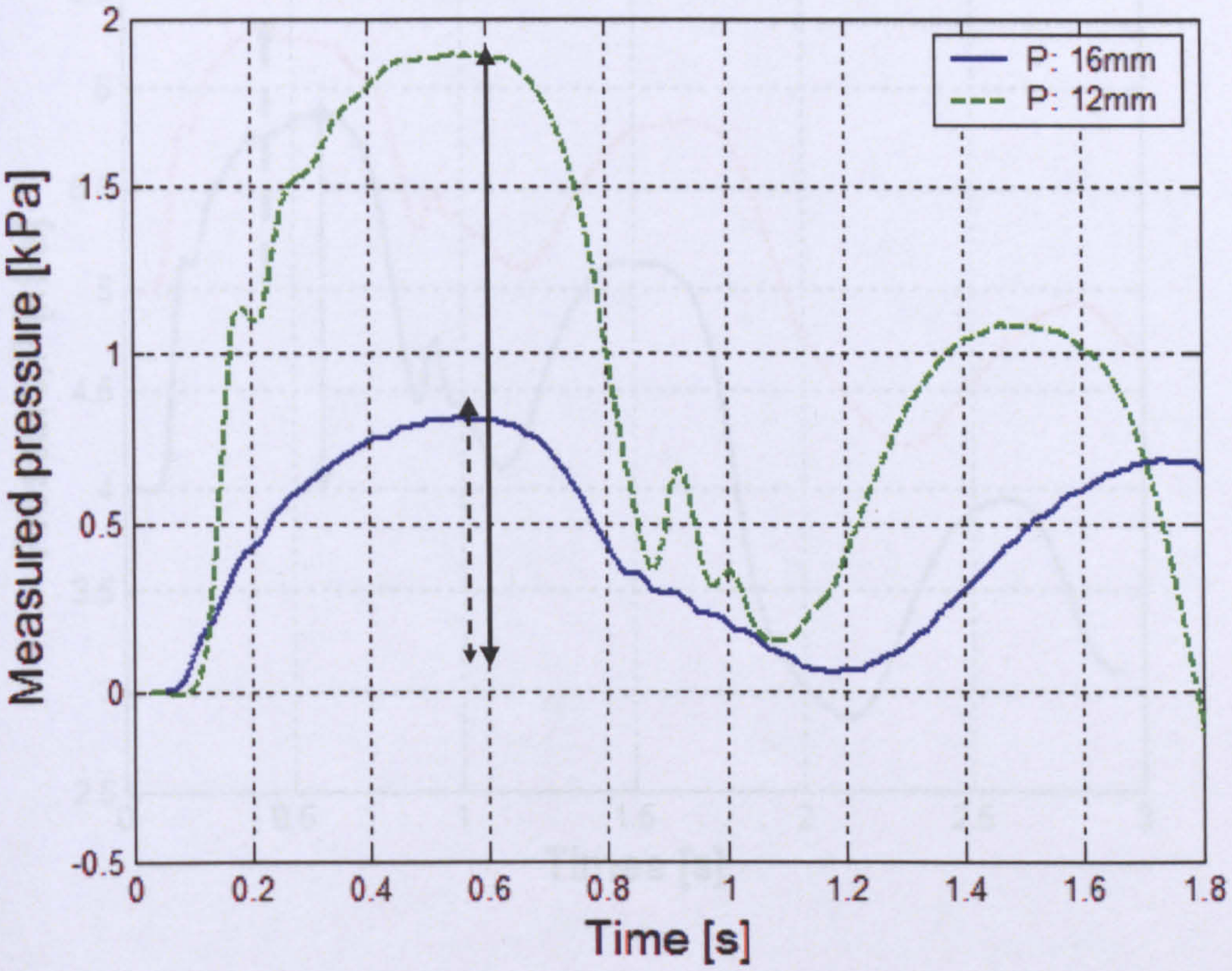

Figure 4.7 The pressure pulse measured at 20 cm away from inlet in the 12 mm and 16 mm tube, respectively. Vertical double arrow (solid) indicates the pressure pulse in the 12 mm tube and Vertical double arrow (dash line) indicates the pressure pulse in the 16 mm tube.

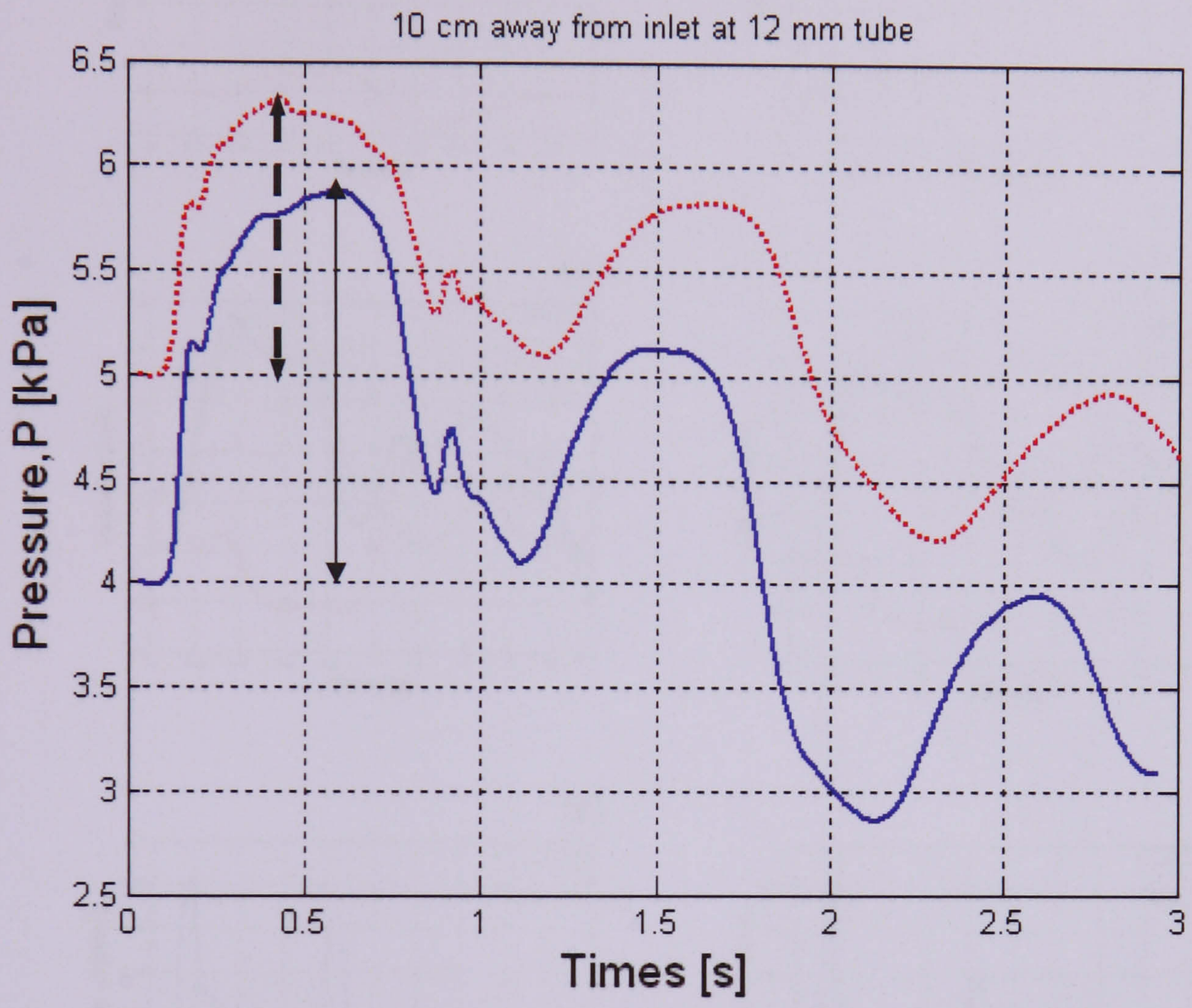

Figure 4.8 The pressure waves were measured at 10cm away from inlet in 12mm tube when initial pressure is 4 kPa (Blue solid) and 5 kPa (Red dotted line), respectively. Solid double way arrow indicates the pressure pulse when initial pressure is 4 kPa, which is approximately 1.85 kPa. The pressure pulse with the initial pressure of 5 kPa is around 1.3 kPa.

Initial pressure: 4 kPa

Initial pressure: 5 kPa

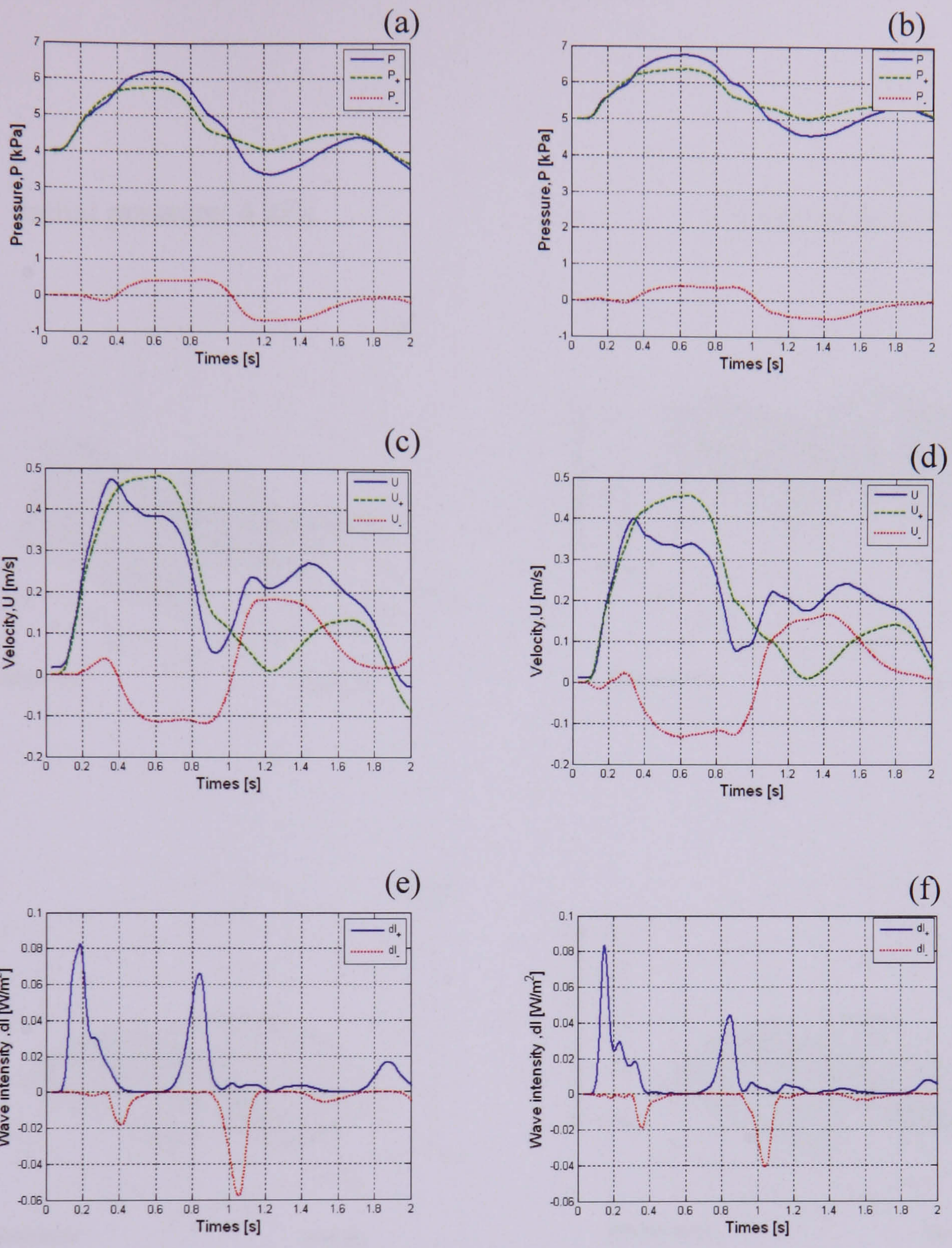

Figure 4.9 (a) & (b) show that the measure, forward and backward pressure wave when the initial pressures are 4 and 5 kPa, respectively, at the site of 150 cm away from inlet; **(c) & (d)** show the measured, forward and backward velocity at the same site and same experimental conditions; **(e) & (f)** show the forward and backward wave intensity at the same sites and same experimental conditions.

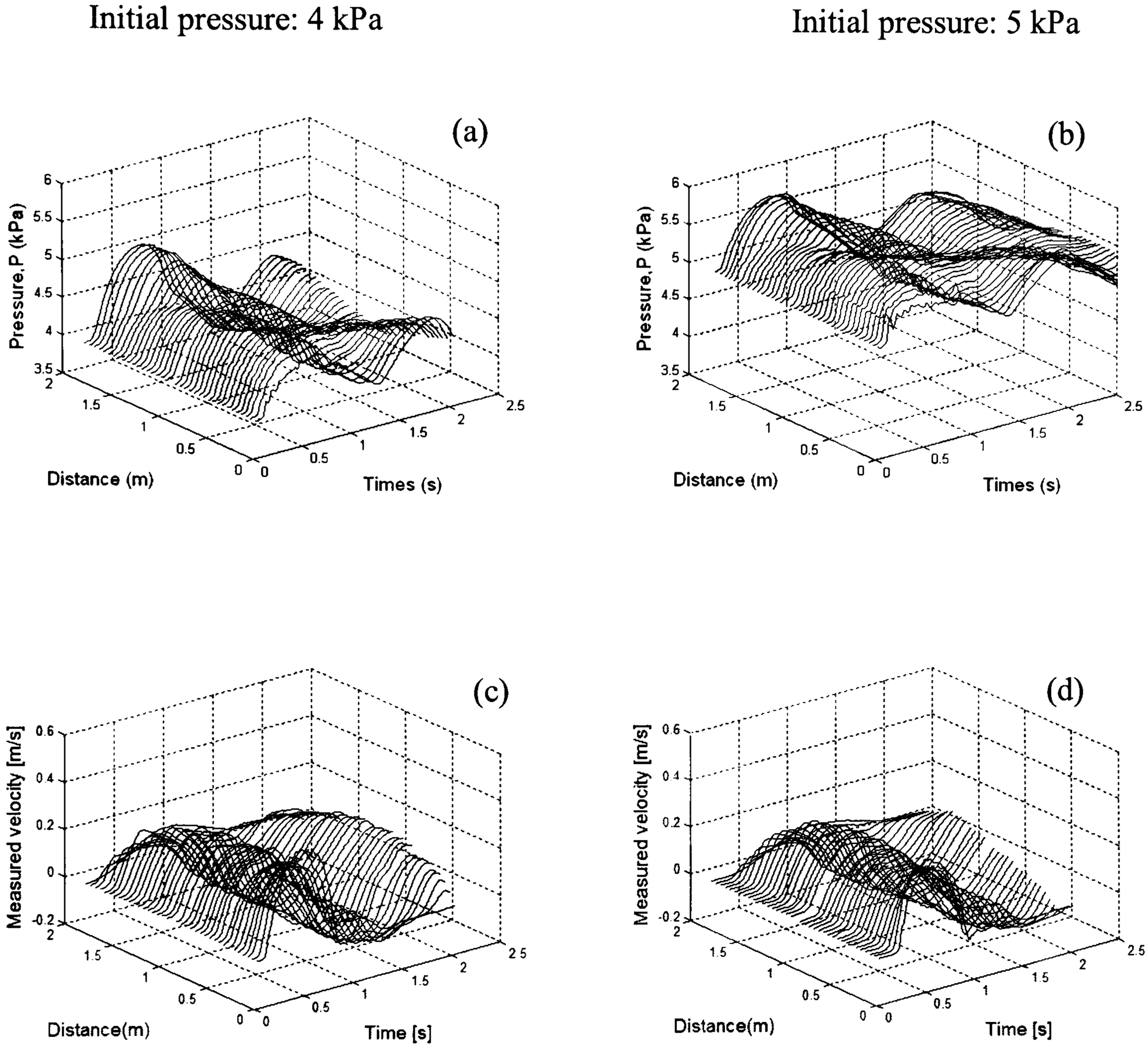

Figure 4.10 The measured pressure and velocity waveform in the space-time in 16 mm tube when the initial pressure is 4 kPa (a), (c) and 5 kPa (b), (d).

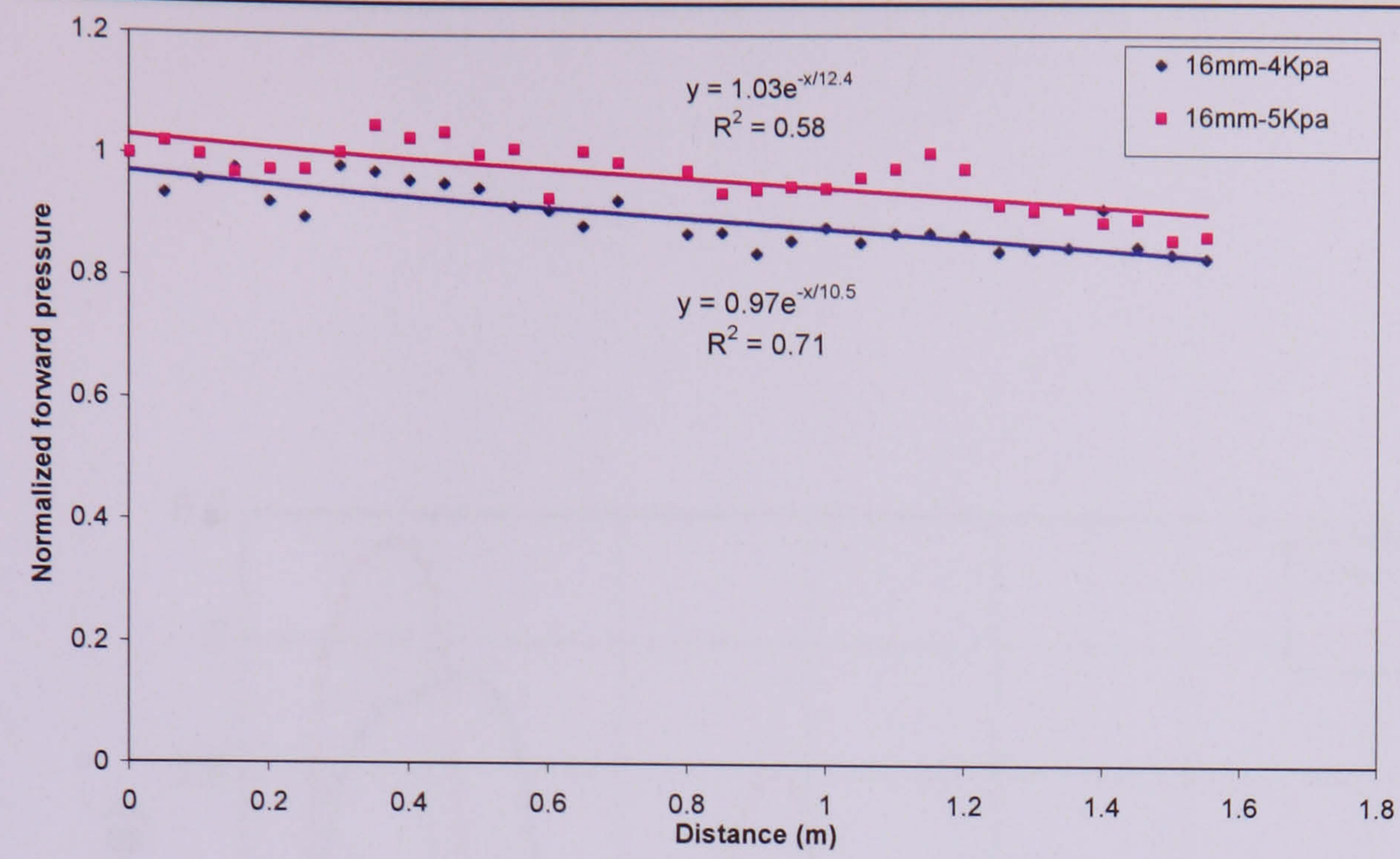

(a)

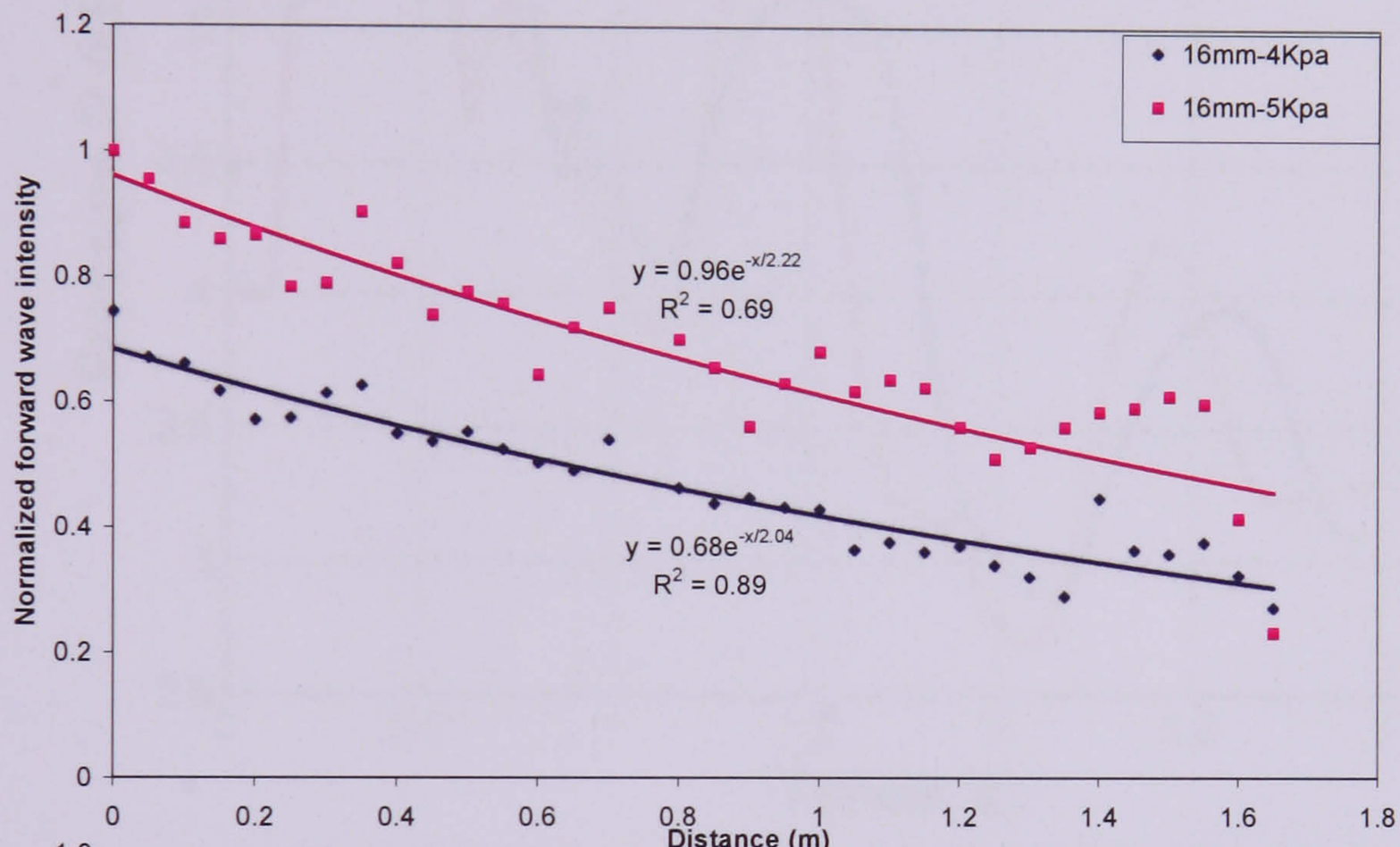

(b)

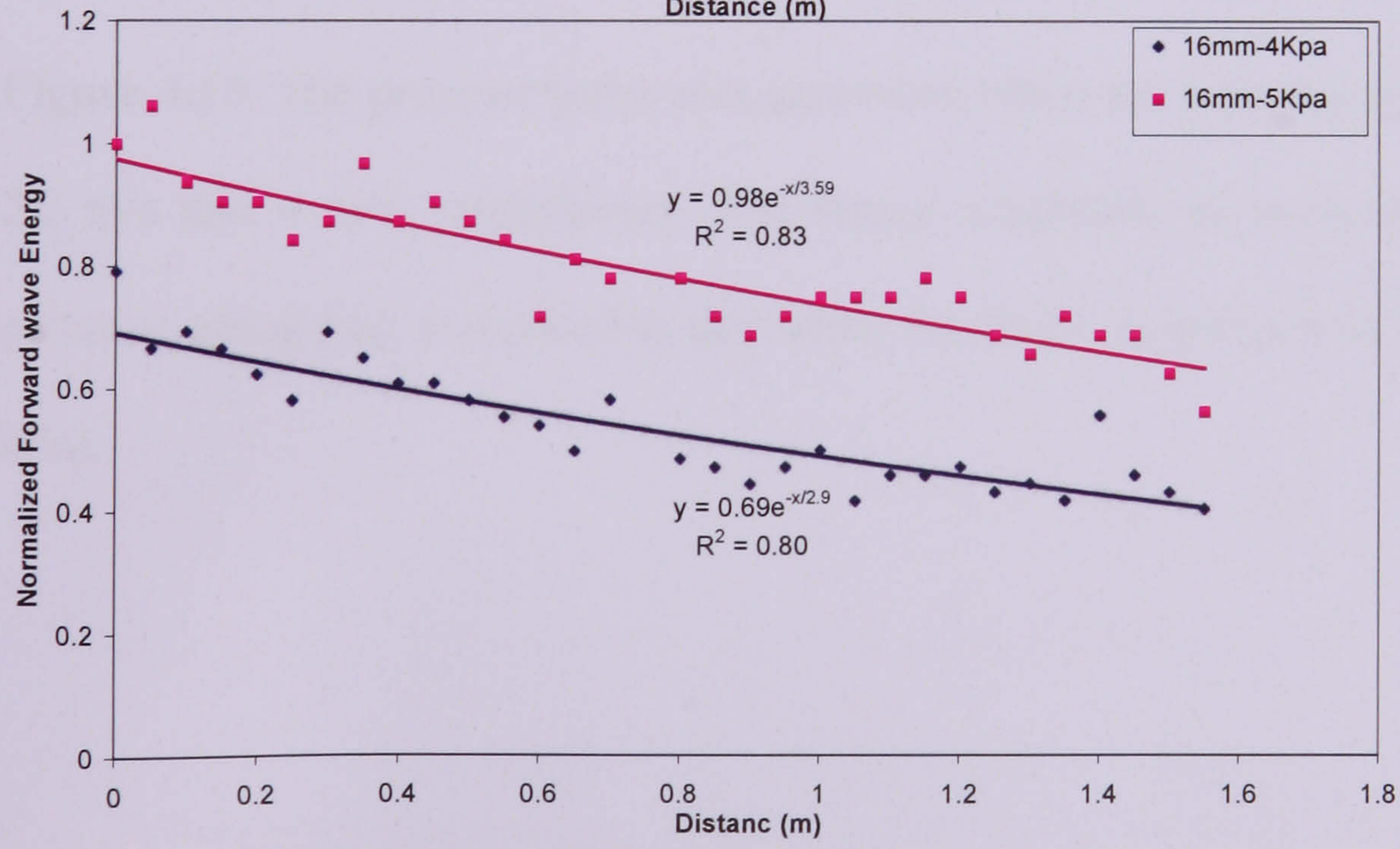

(c)

Figure 4.12 The normalized forward pressure (a), the normalized forward wave intensity (b) and the normalized forward wave energy (c) dissipated exponentially along the distance in 16mm tube with the initial pressure at 4kPa and 5kPa, respectively. The power of exponential regression line indicates that the greater dissipation occurs when initial pressure is 4kPa.

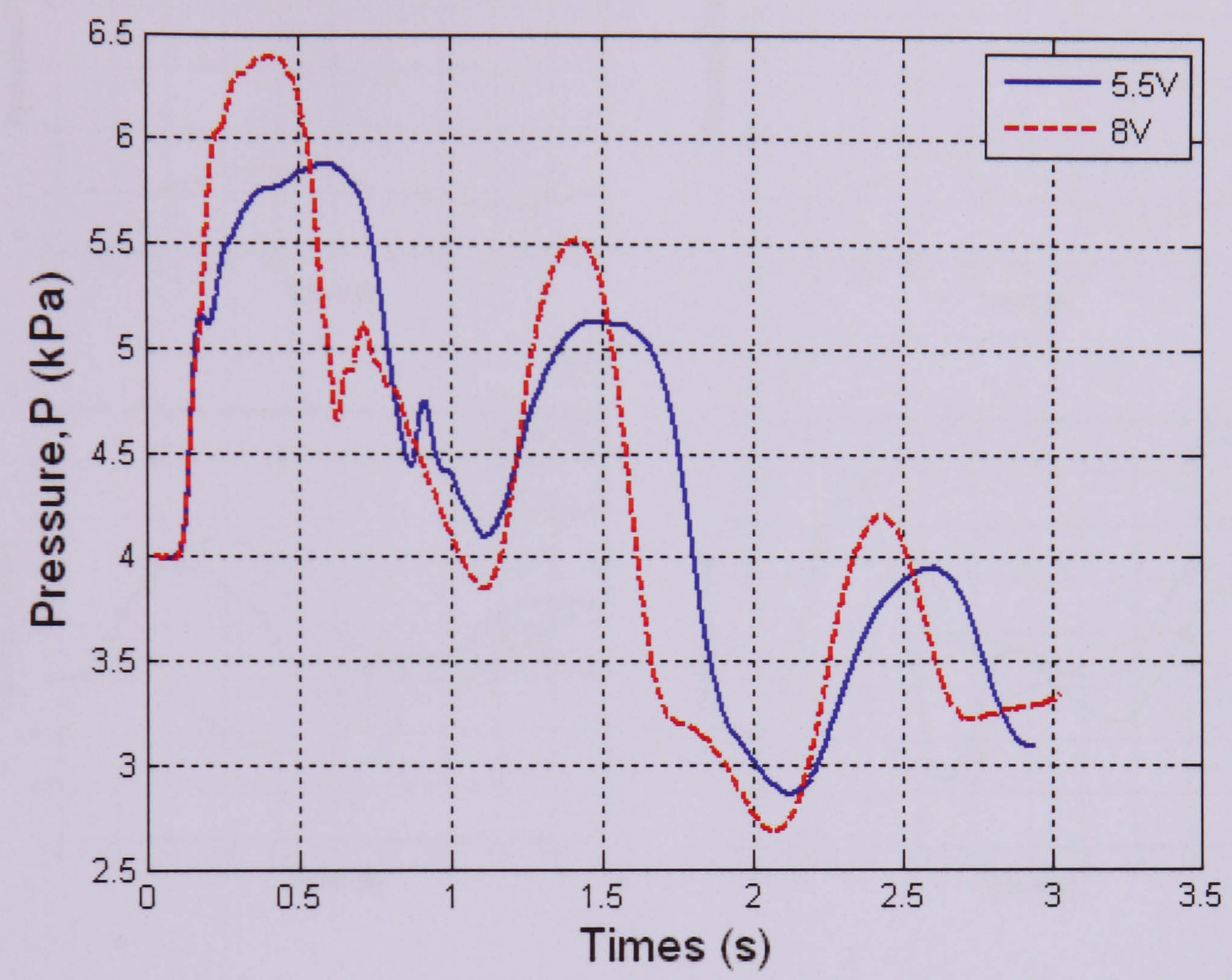

Figure 4.13. The pressure pulse was generated when the pumping speed of piston is 2.2 m/s and 4 m/s, respectively. The bigger amplitude of pulse occurs when the piston is going fast, compared to that when the piston is going slow (2.4 kPa vs. 1.9 kPa).

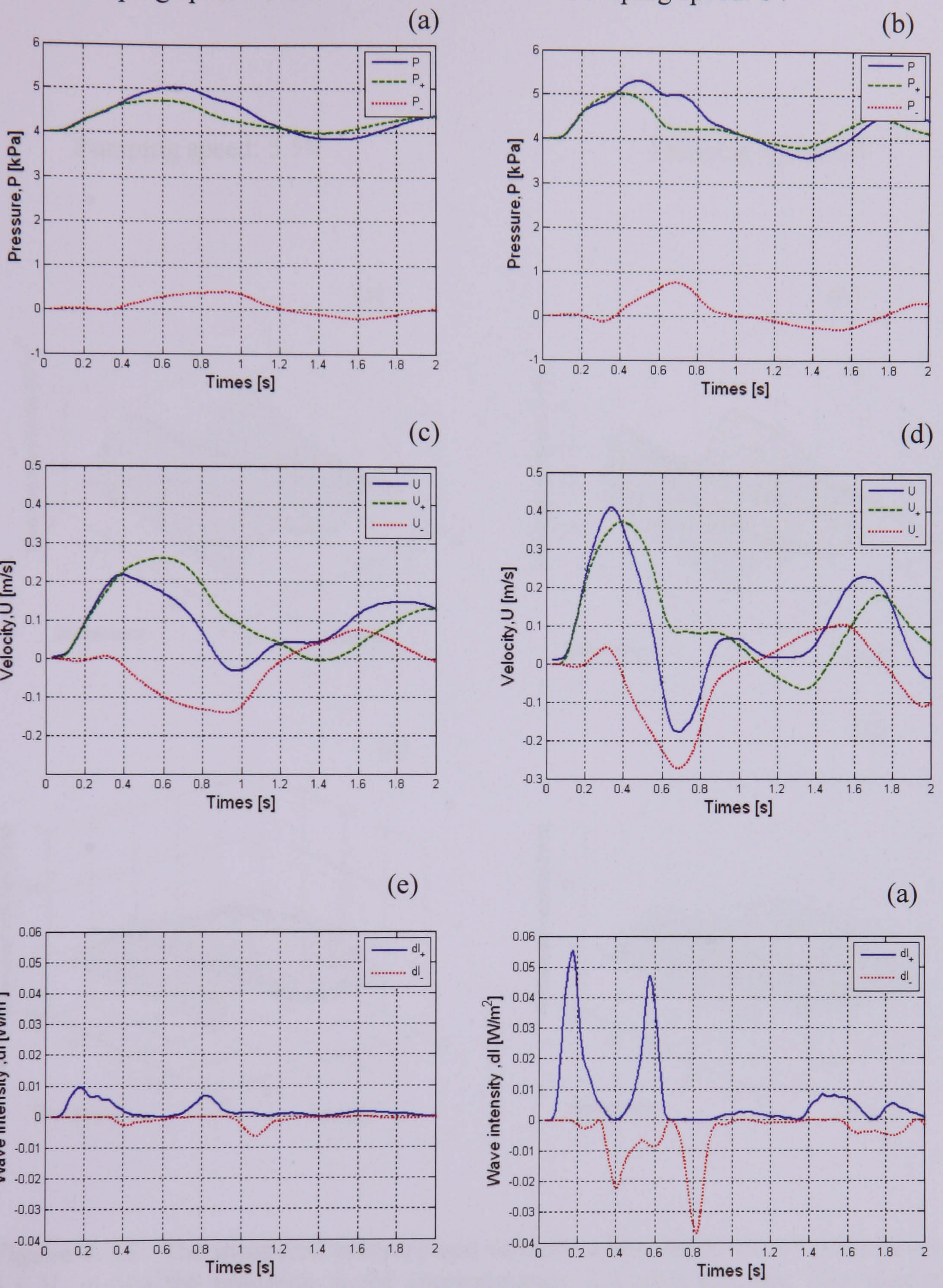

Figure 4.14 At the site of 150 cm away from inlet for 16 mm tube the measure, forward and backward pressure when the pumping speed is slow (Voltage is 5.5 V) (a) and fast (Voltage is 8 V) (b), respectively. At the same site the measured, forward and backward velocity when the pumping speed is slow (Voltage is 5.5 V) (c) and fast (Voltage is 8 V) (d), respectively. The forward and backward wave intensity when the pumping speed is slow (Voltage is 5.5 V) (e) and fast (Voltage is 8 V) (f), respectively.

Pumping speed: 5.5V

Pumping speed: 8V

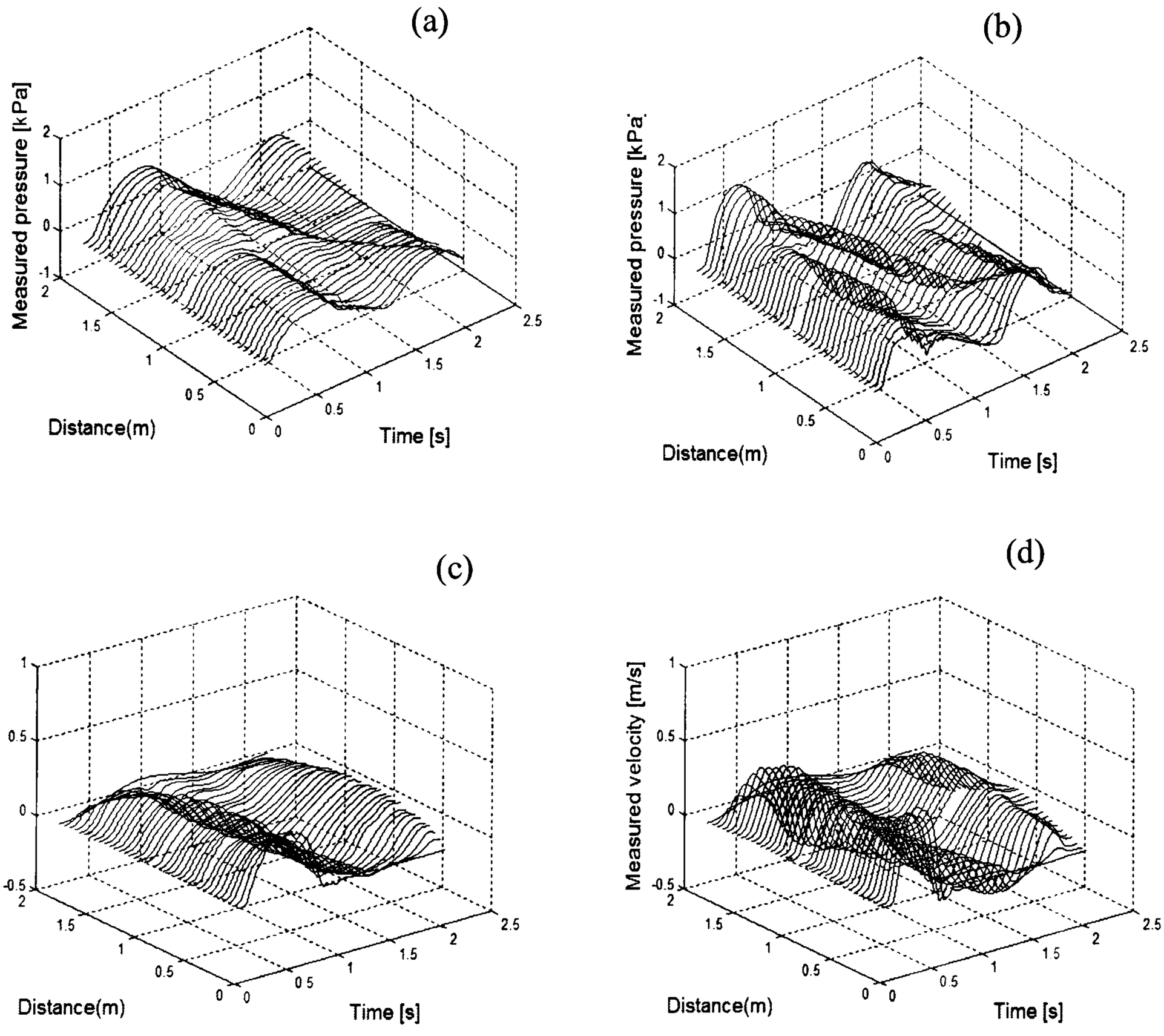

Figure 4. 15 . The measured pressure and velocity when the power of pump is set as 5.5 V, giving the pumping speed approximately 2.2 cm/s **(a), (c);** The measured pressure and velocity when the power of pump is set as 8 V, giving the pumping speed approximately 4 cm/s **(b), (d)**

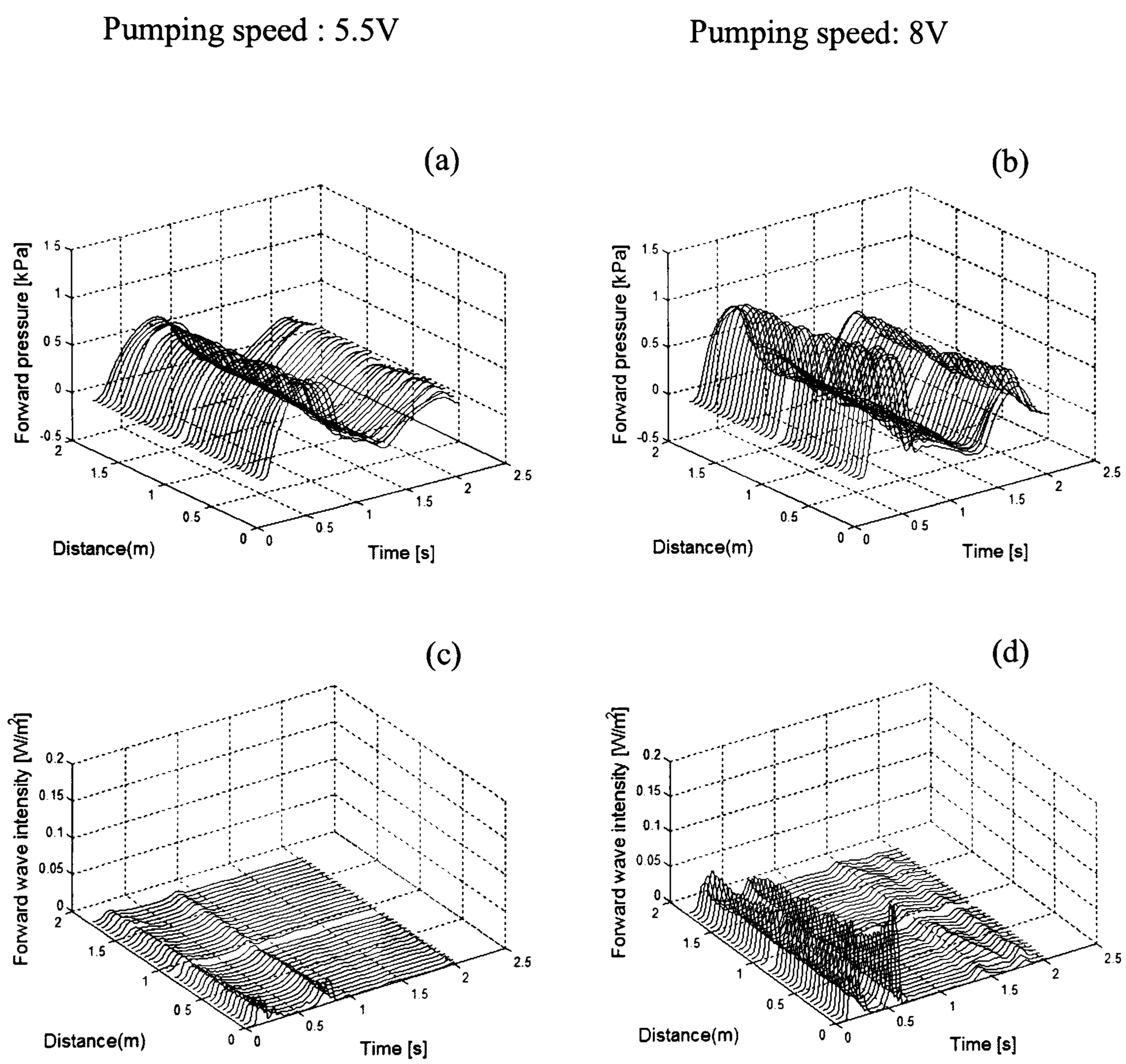

Figure 4. 16 The forward pressure waveforms in the space-time in 16 mm tube when the power of pump is set as 5.5 v (a) and 8 V(b), giving the pumping speed of piston is approximately 2.1 cm/s and 4 cm/s, respectively. The forward wave intensity waveforms in the space-time in the 16 mm tube when the power of pump is set as 5.5 v (a) and 8 V(b), giving the pumping speed of piston is approximately 2.2 cm/s and 4 cm/s, respectively.

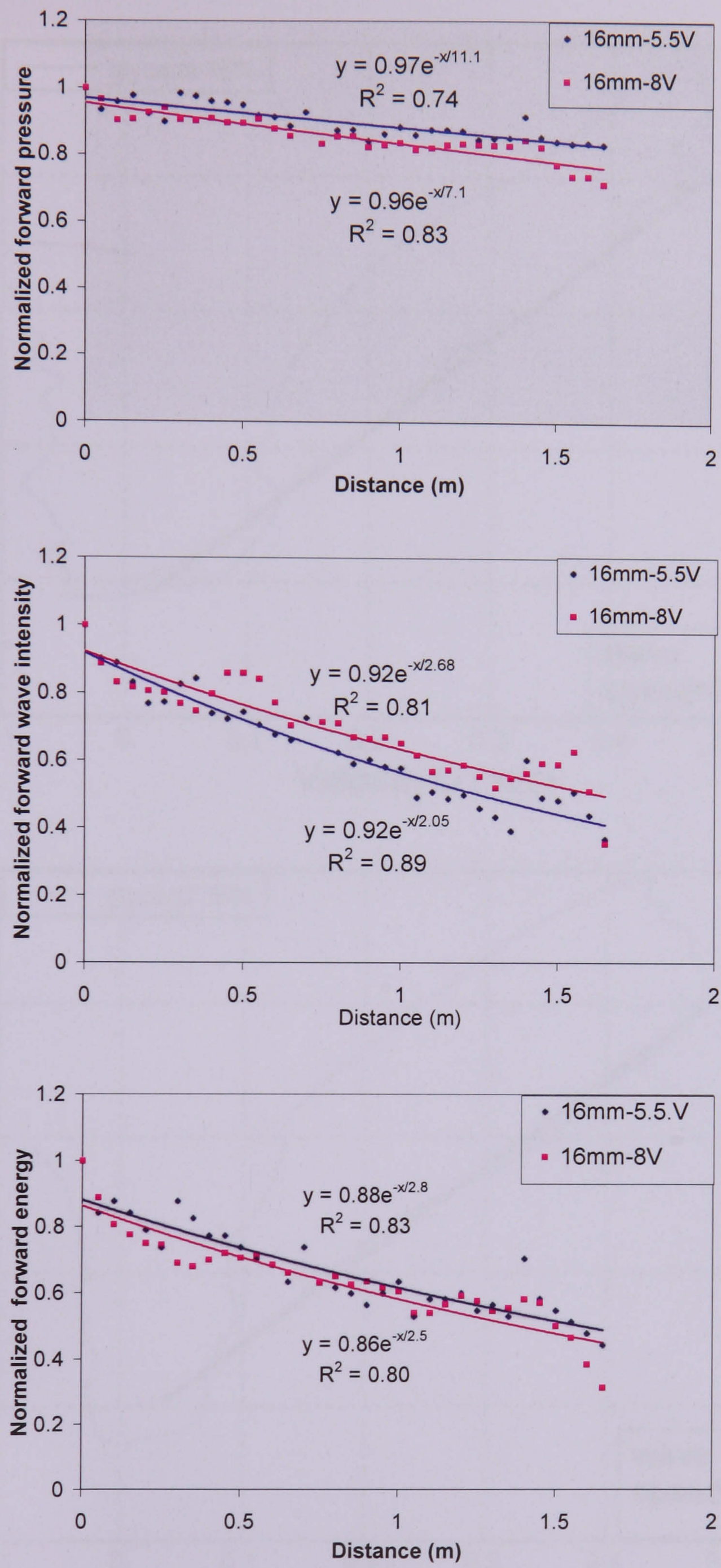

Figure 4.17 The normalized forward pressure **(a)**, forward wave intensity (b) and forward wave energy (c) dissipated exponentially along the distance in 16 mm tube when the pumping speed of piston is 2.2 cm/s and 4 cm/s (power is set up as 5.5V and 8V), respectively. The power of exponential regression line indicates that the greater dissipation occurs when the pumping speed is faster.

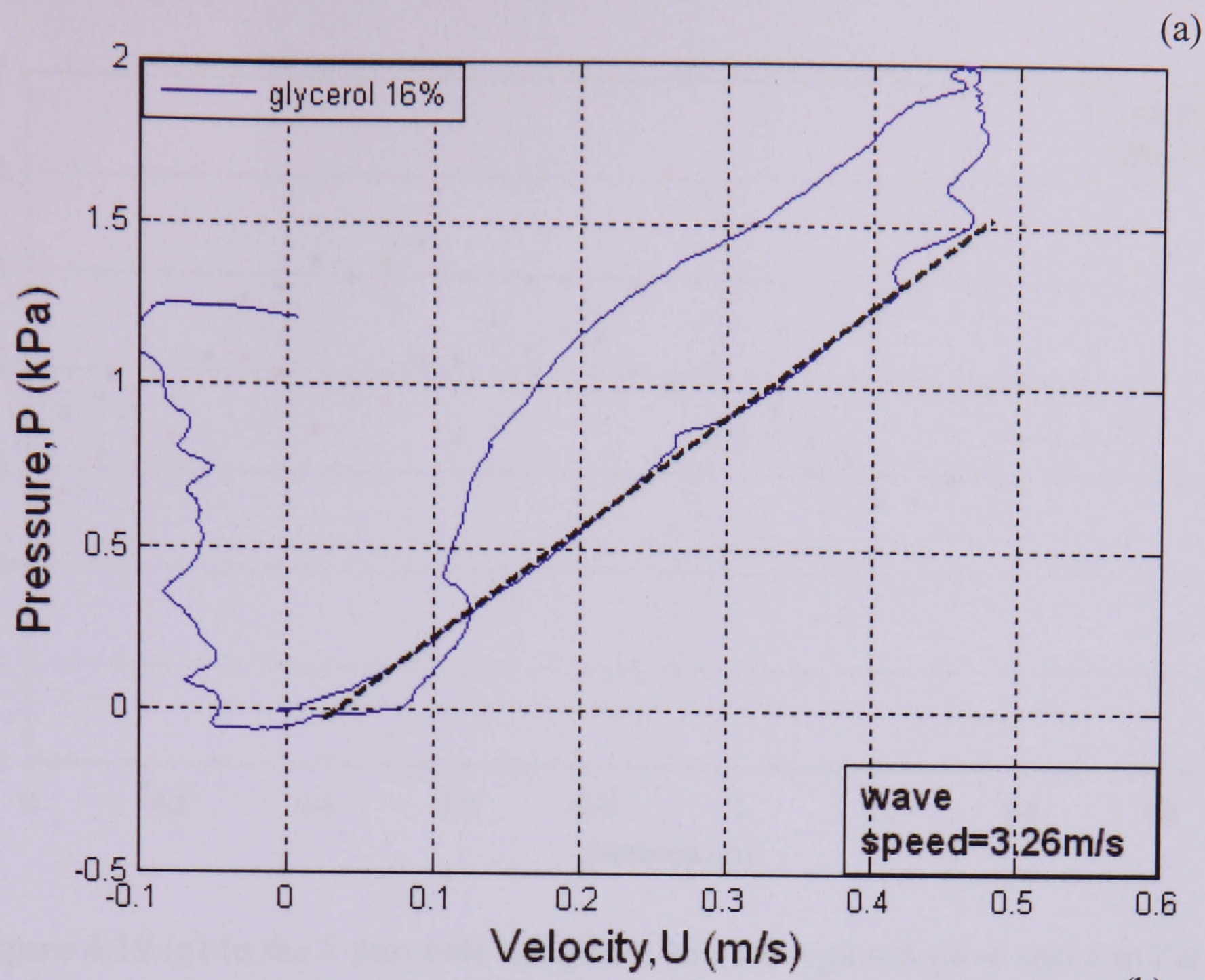

Figure 4.18. At 5 cm away from inlet of the 12 mm tube, wave speed was determined by PU-loop in the 16% glycerol-water solution **(a)** and 36% glycerol-water solution **(b)**. Bold dash lines indicate the linear relationship between pressure and velocity before the reflection wave arrived.

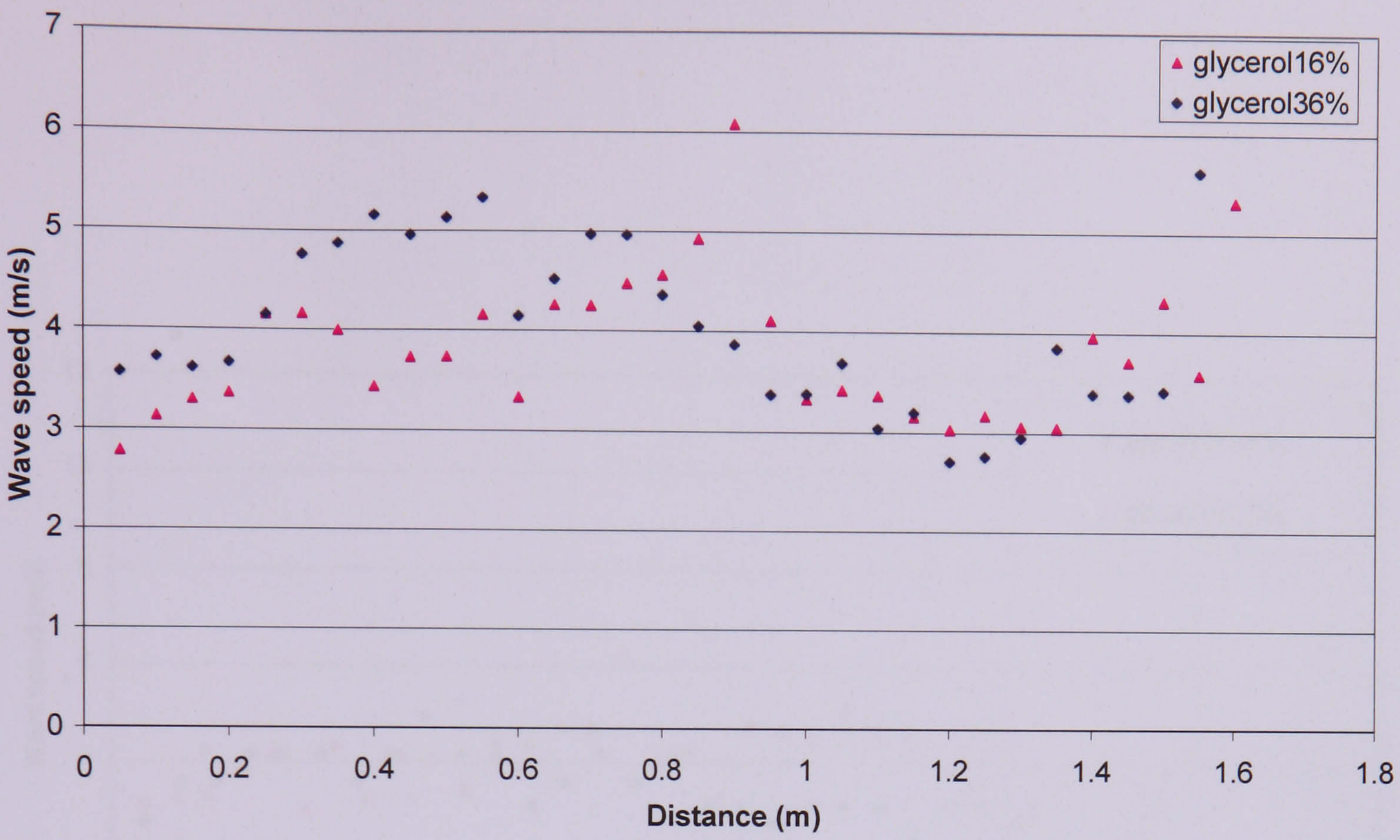

Figure 4.19 (a) In the 8 mm tube the global and the regional wave speed in the 16% of glycerol-water solution are similar to that in the 36% of glycerol-water solution. The average wave speed for 16% of the glycerol-water solution is approximately 3.83 ±0.73 m/s and for the 36% of the glycerol-water solution is approximately 4.02 ±0.82 m/s.

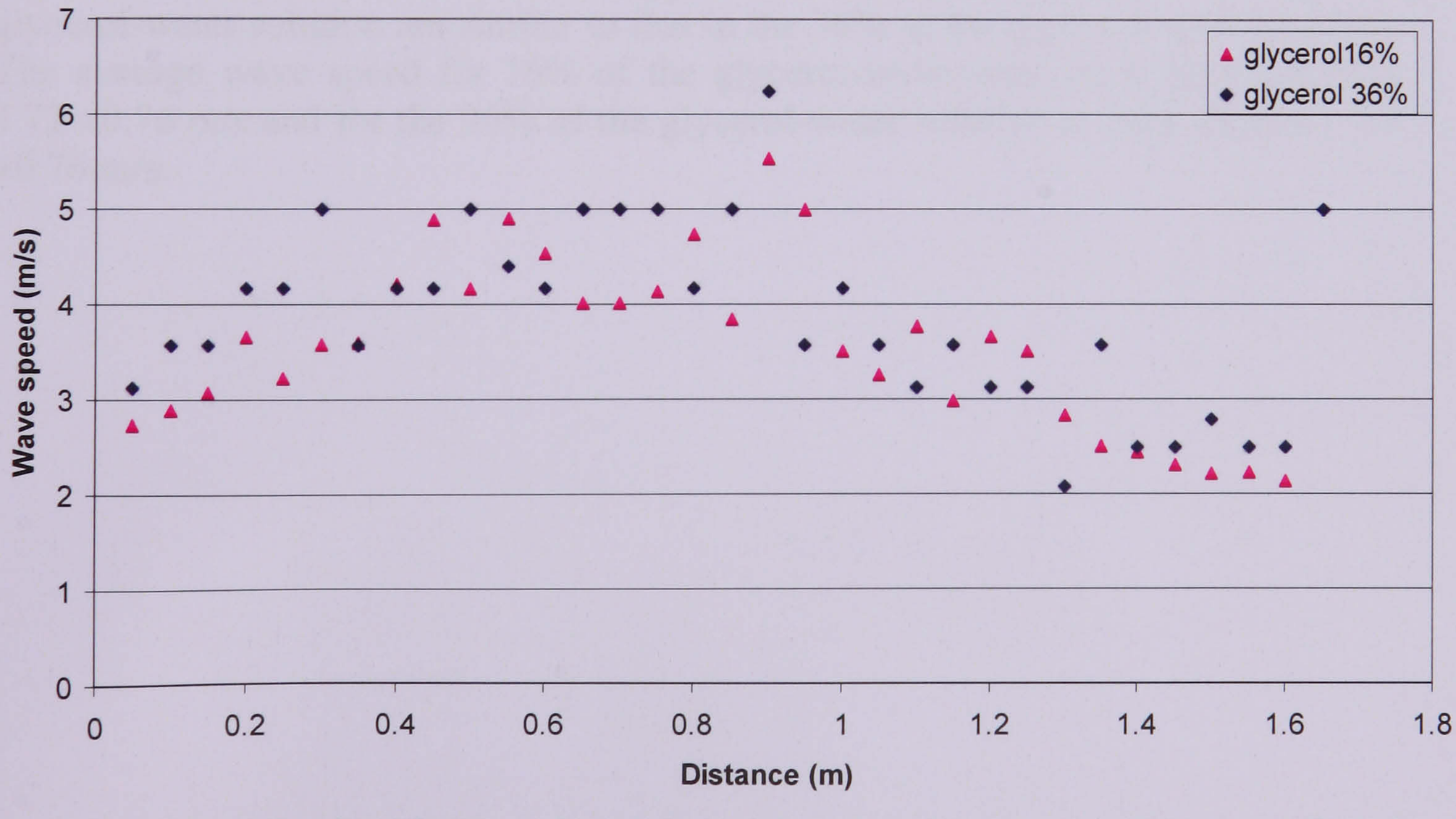

Figure 4.19 (b) In the 12 mm tube global and regional wave speed in the 16% of glycerol-water solution are similar to that in the 36% of glycerol-water solution. The average wave speed for 16% of the glycerol-water solution is approximately 3.88 ±0.76 m/s and for the 36% of the glycerol-water solution is approximately 3.85 ±0.96 m/s.

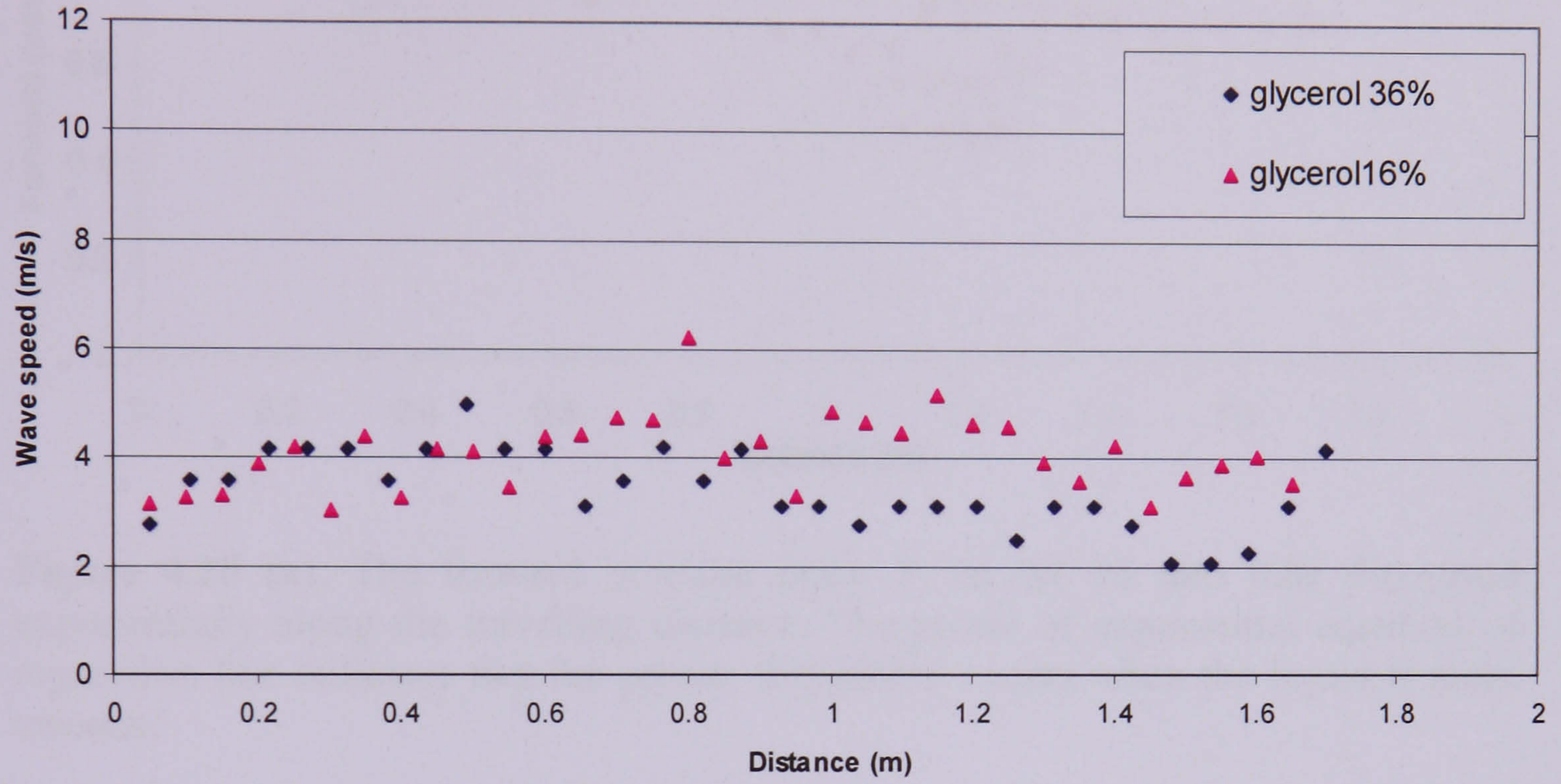

Figure 4.19 (c) In the 16mm tube the global and regional wave speed in the 16% of glycerol-water solution are similar to that in the 36% of the glycerol-water solution. The average wave speed for 16% of the glycerol-water solution is approximately 3.72 ±0.76 m/s and for the 36% of the glycerol-water solution is approximately 3.4 ±0.76 m/s.

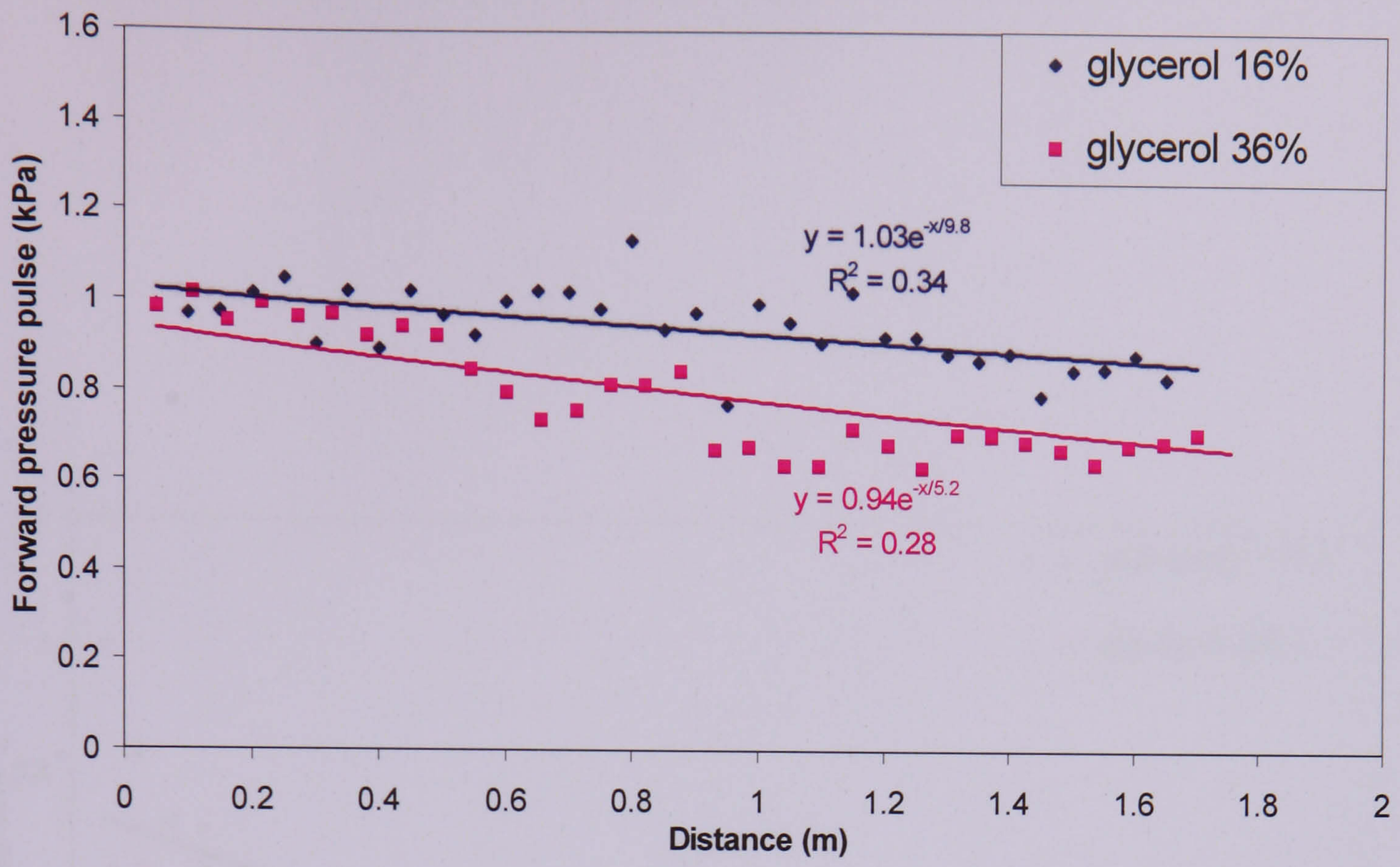

Figure 4.20 (a). The forward pressure pulse P_+ in the 16 mm tube dissipated exponentially along the travelling distance. The power of exponential equation of regression line indicates that the greater dissipation occurs when the liquid is more viscous.

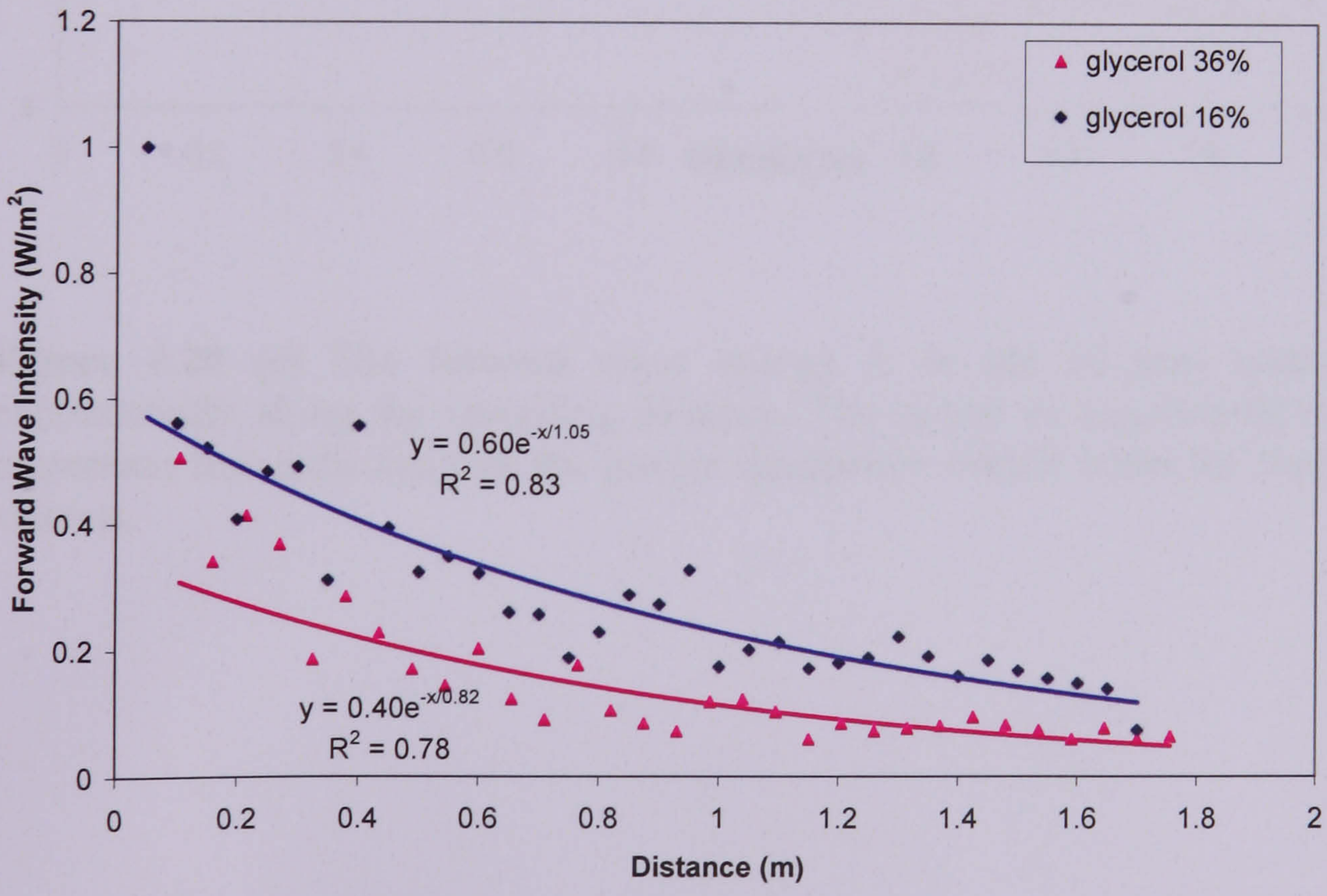

Figure 4.20 (b). The peak of forward wave intensity dI_+ in the 16 mm tube dissipated exponentially along the travelling distance. The power of exponential equation of regression line indicates that the greater dissipation occurs when the liquid is more viscous.

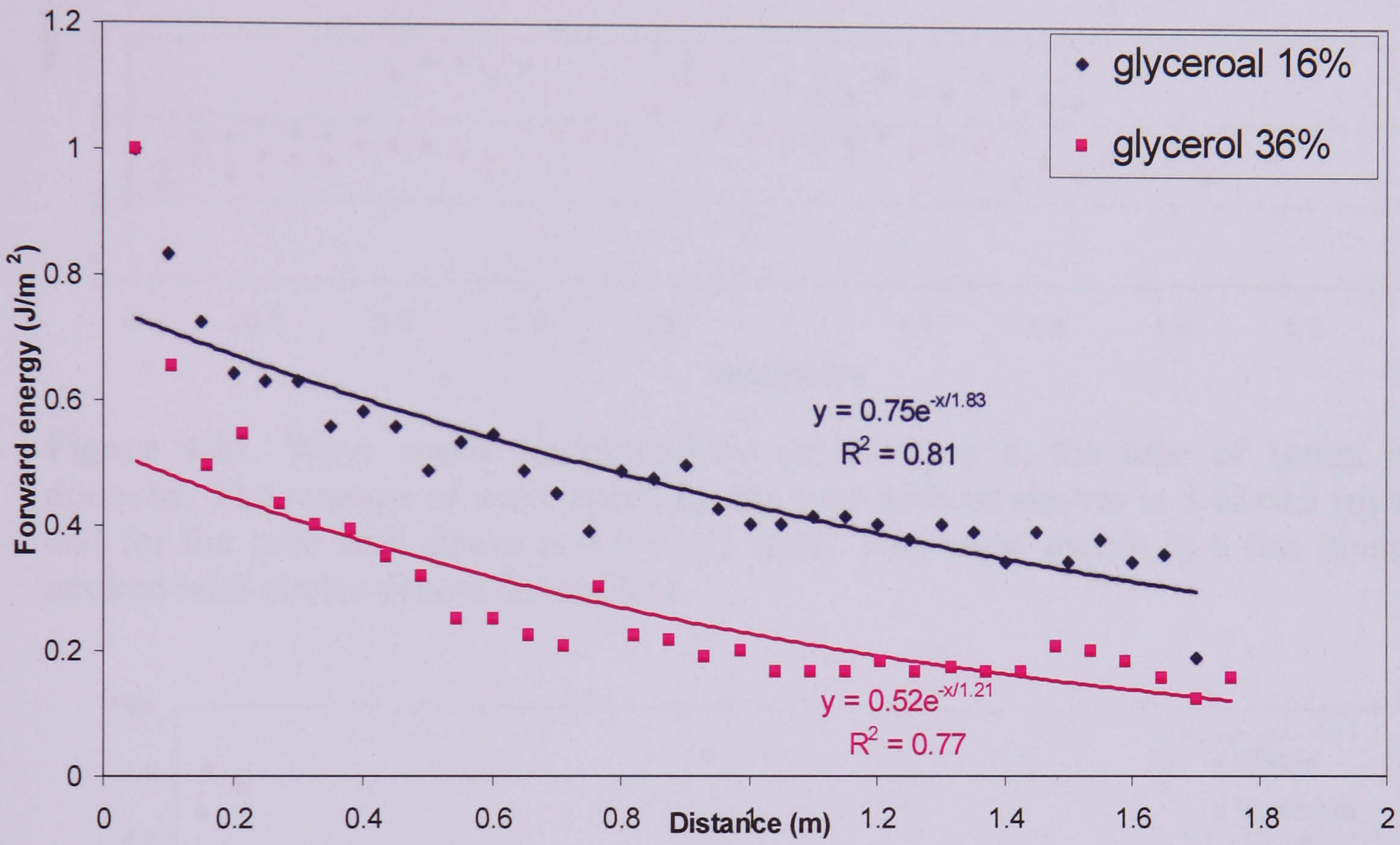

Figure 4.20 (c) The forward wave energy I_+ in the 16 mm tube dissipated exponentially along the travelling distance. The power of exponential equation of regression line indicates that the greater dissipation occurs when the liquid is more viscous.

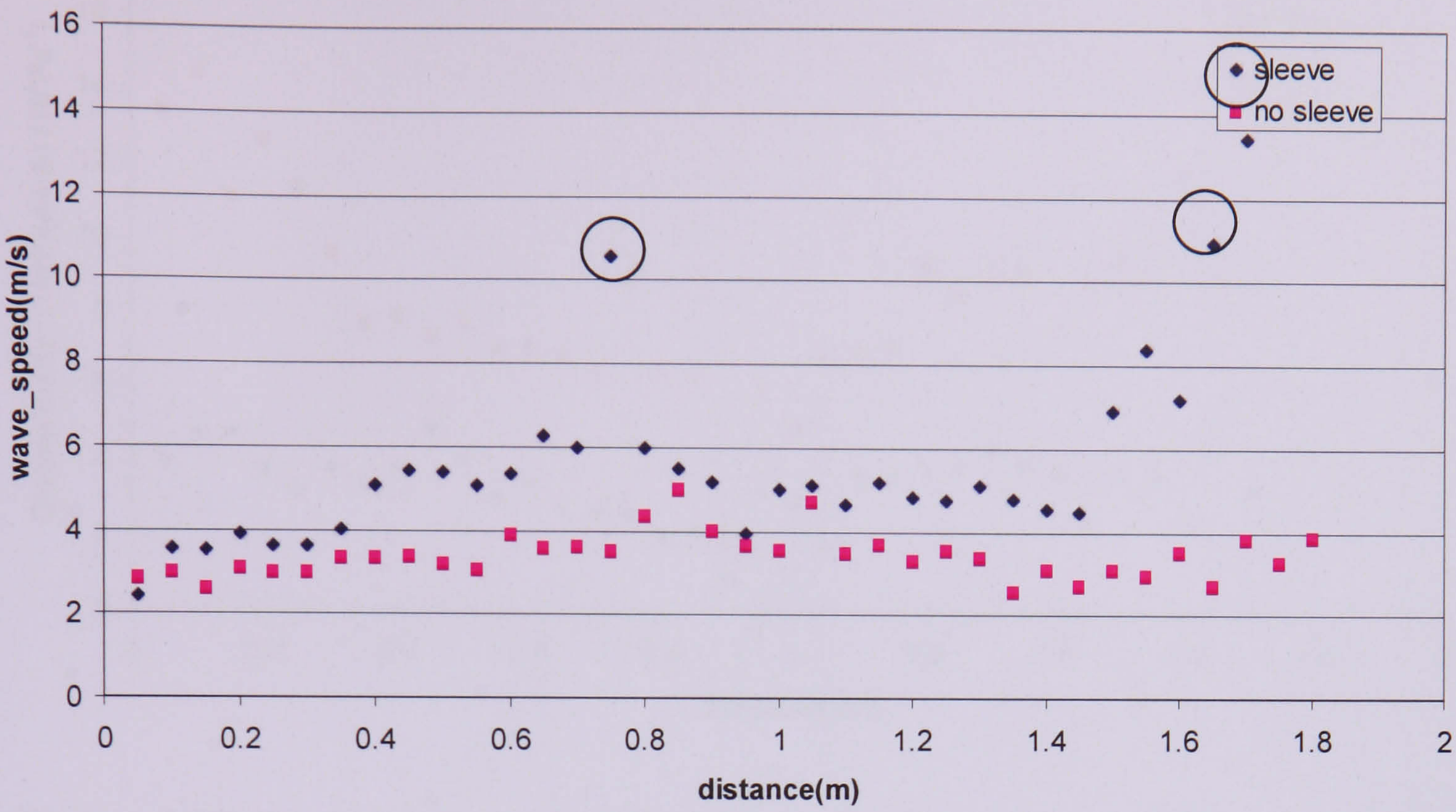

Figure 4.21. Wave speed determined by the PU-loop in the tube of 16mm in diameter. The average of wave speed for the tube without sleeves is 3.42±0.5 (m/s) and for the tube with sleeve is 4.9 ± 1.1 (m/s). The wave speeds in a few points marked with circles denote the outliers.

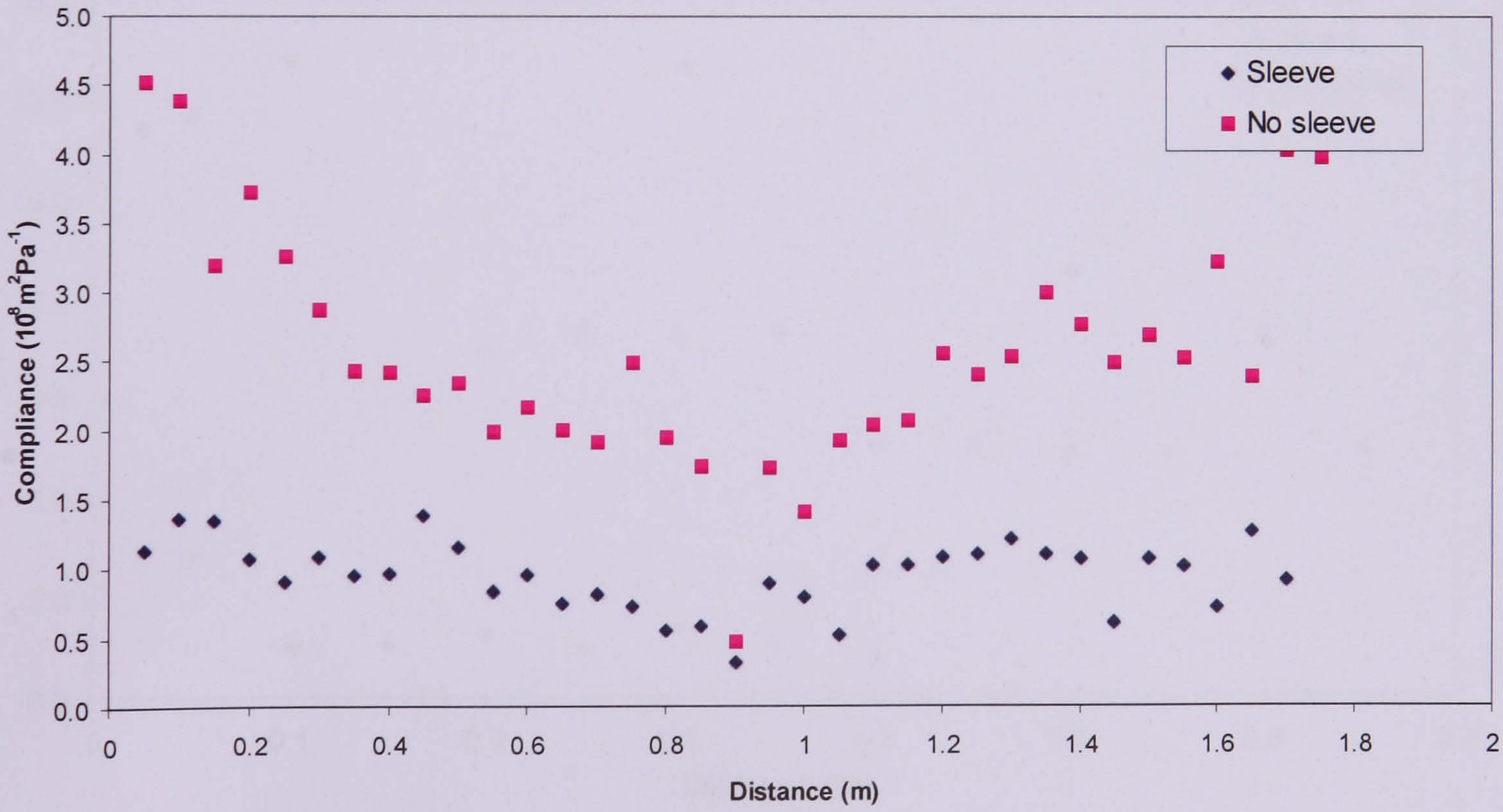

Figure 4.22 Local dynamic compliances in the 16 mm tubes with and without odified, which are established by the dynamic measured diameter and pressure.

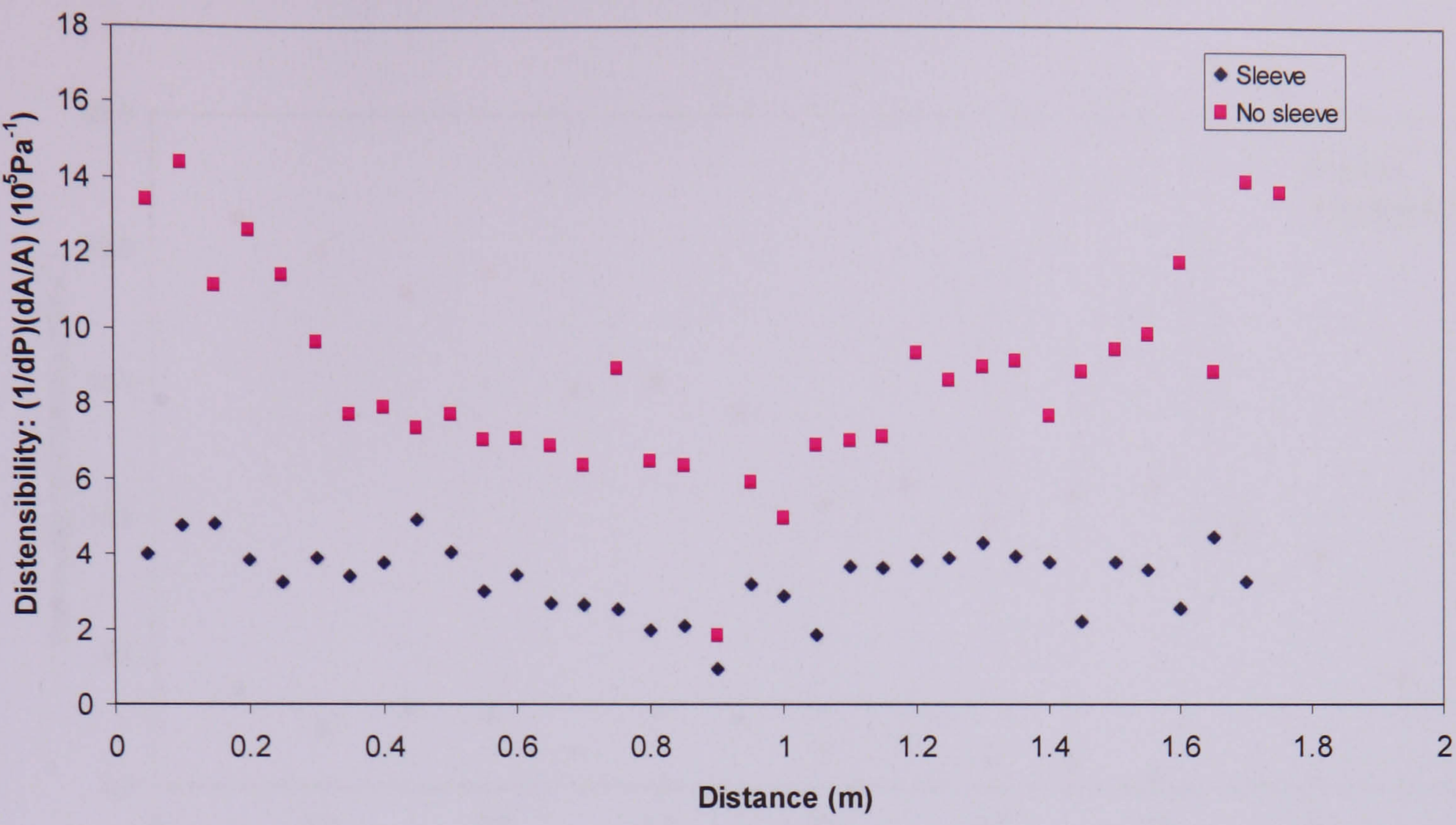

Figure 4.23 Local dynamic distensibilities in the 16 mm tubes with and without modified, which are established by the dynamic measured diameter and pressure and undisturbed cross-sectional area

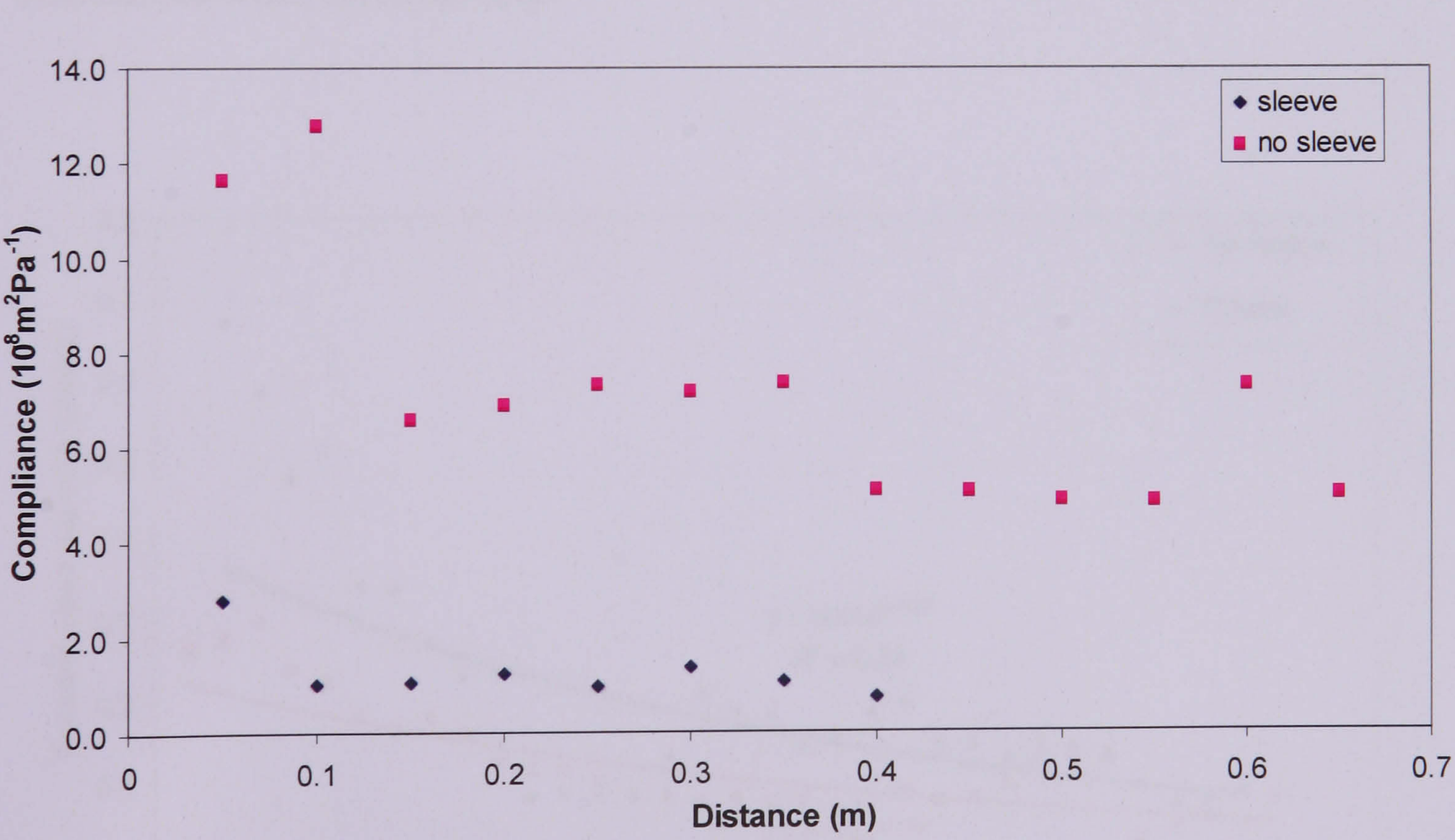

Figure 4.24 Local dynamic compliances in the 24 mm tubes with and without sleeves, which are established by the dynamic measured diameter and pressure.

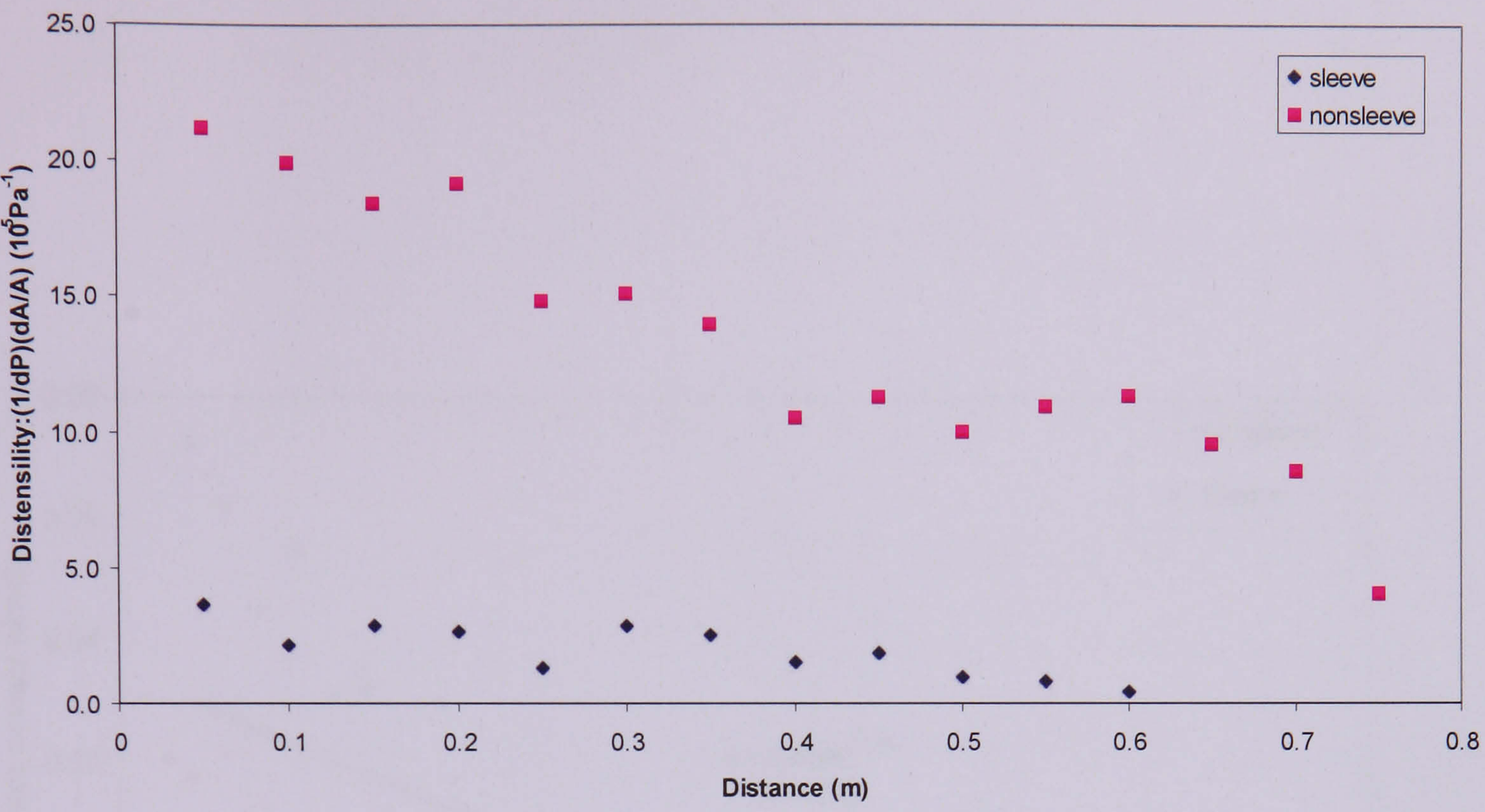

Figure 4.25, Local dynamic distensibilities in the 24 mm tubes with and without sleeve, which are established by the dynamic measured diameter, pressure and undisturbed cross-sectional area.

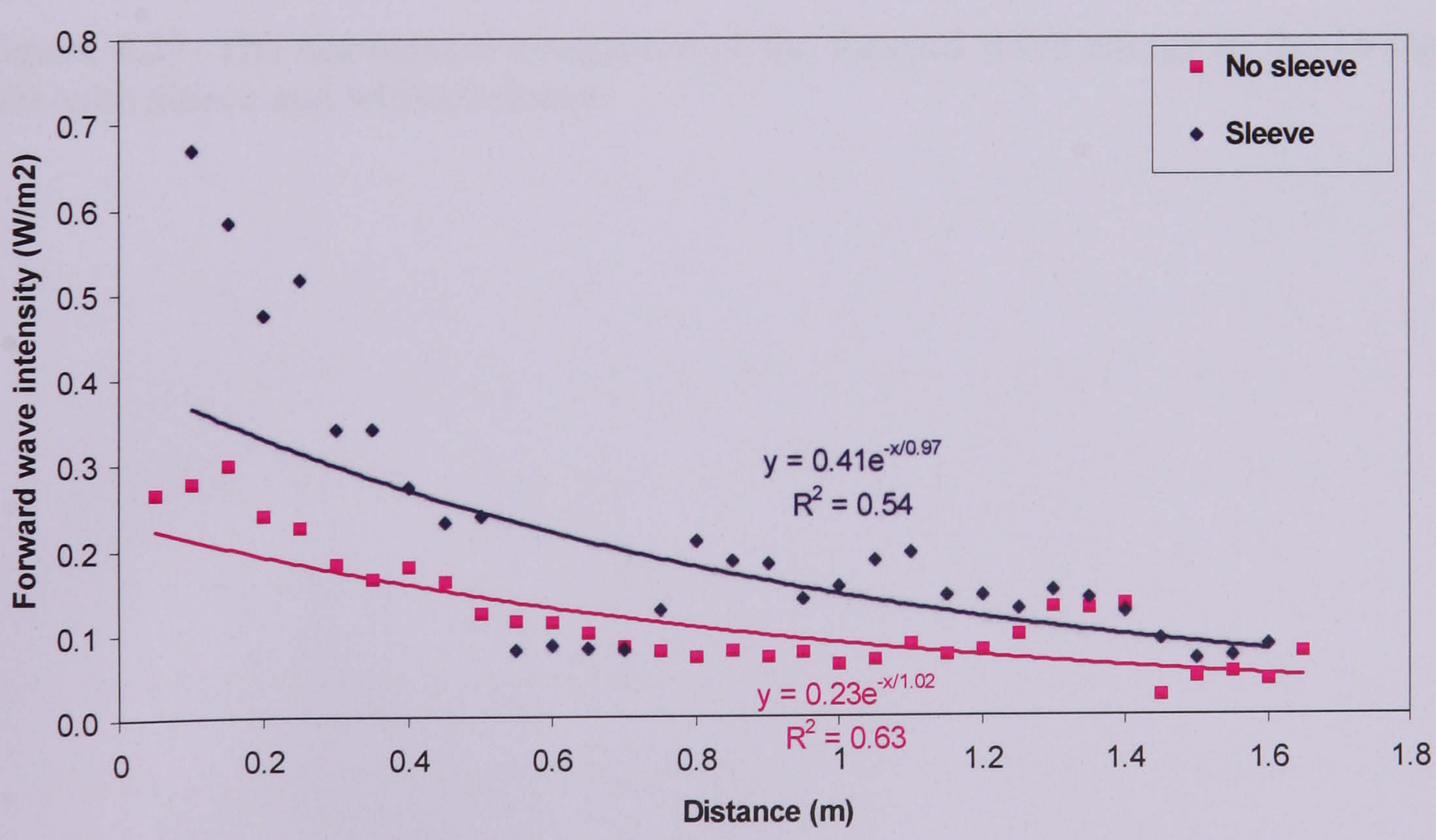

Figure 4.26, The normalized dissipation of the peak of forward wave intensity in the 16 mm tube with sleeve and without sleeve. The power of exponential equations of best fitting curve indicates that the degree of dissipation.

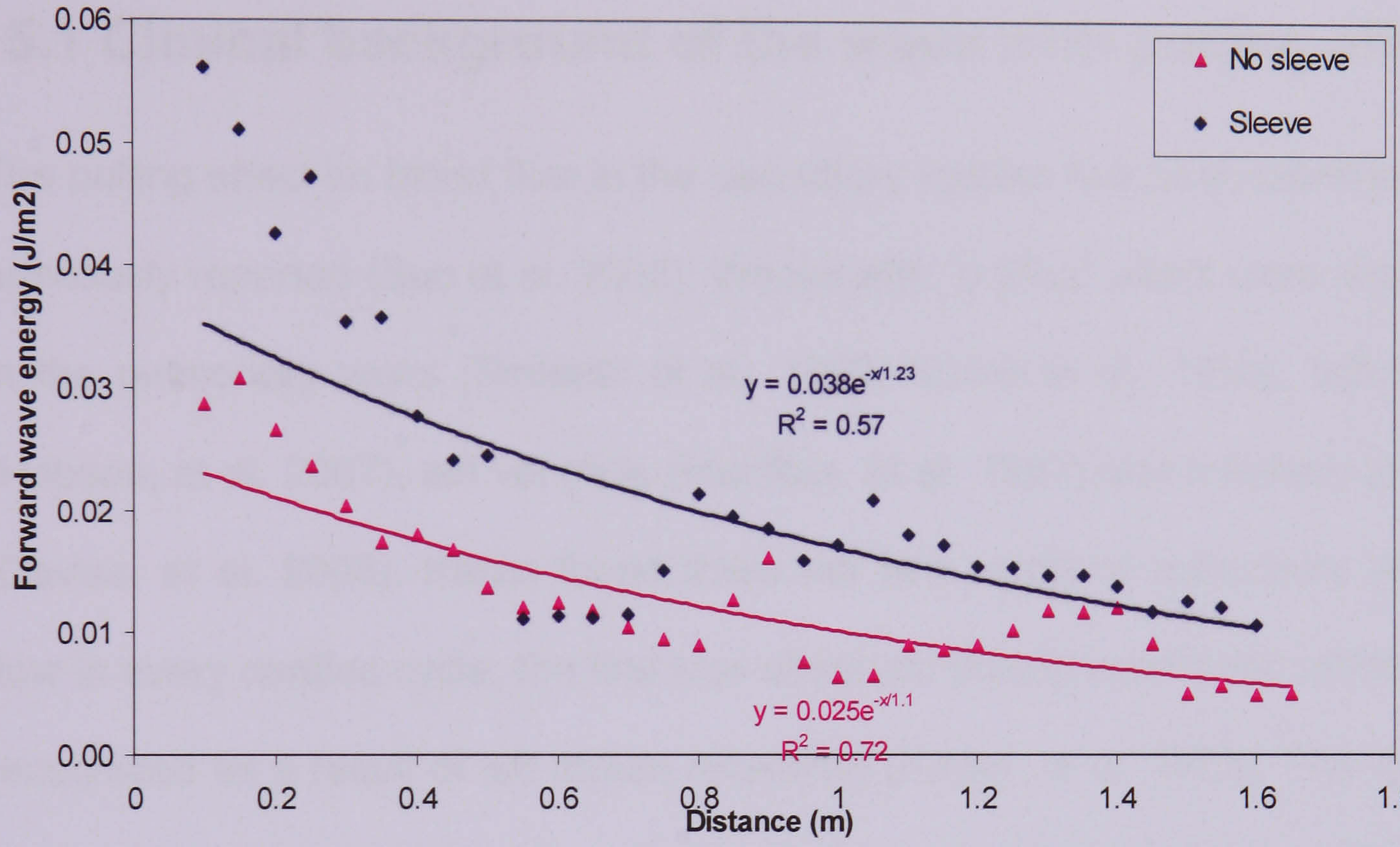

Figure 4.27, The normalized dissipation of the forward wave energy in the 16 mm tube with sleeve and without sleeve.

Chapter 5

Dissipation of waves during pulling and pushing actions

5.1 Clinical background of the wave with pulling effect

The pulling effect on blood flow in the circulatory system has been identified and previously reported (Sun et al. 2006). Waves with "pulling" effect were observed in the pulmonary veins (Smiseth et al., 1999, Karen et al., 1995), left atrium (Hobson, et al. 2007), left ventricle (MacRae, et al 1997) and coronary arteries (Davies, et al. 2006). Karen found there are two peaks of pulmonary venous flow in every cardiac cycle; the first was observed during ventricular systole and recognized as a result of left atrium relaxation (Karen, et al. 1985). The second peak, which was seen during ventricular diastole, was reckoned due to the rapid filling of the left ventricle. During ventricular diastole, the atrium acts as an open conduit through which blood flows directly from the pulmonary veins across the mitral valve into the left ventricle.

Davies demonstrated that the suction wave played more important role than did the pushing waves in the filling of coronary circulation of human (Davies, et al., 2006). Sun concluded that the increase of coronary flow during diastole resulted from the relaxation of left ventricle generating both forward and backward expansion waves (Sun, et al. 2000). The relaxation of the left ventricle during diastole produces waves with pulling effect, which suck a volume of blood from the aorta, and thus boost coronary flow.

Although waves with pulling effect are important in the cardiovascular system, as much as explored insofar, dissipation of such waves has not been thoroughly studied previously. This lack of knowledge is speculated to be the result of the general difficulty of measuring the dissipation in large arteries (Bertram *et al.* 1999), let alone in a complex branching system with short segments such as the venous or the coronary circulations.

The aim of this chapter is to investigate the dissipation of waves induced by pulling action in the time domain. It is also aimed to compare the propagation of waves with pushing and pulling effects in terms of wave speed, magnitude and wave energy dissipation.

5.2 Methods

5.2.1 Experiment setup

We used the experiment setup in section of 3.1.1, which is shown in **Figure 3.1**. The experimental setup consists mainly of a piston pump, water filled tank to support the tube, two reservoirs, and latex tubes. The pump generates a forward flow waveform in the shape of a single approximately half sinusoidal by moving the piston from bottom to top dead centre, which we term "pushing action". The pump can also generate a flow waveform in the backward direction by moving the piston from top to bottom dead centre, which we term "pulling action". We note that the initial experimental conditions, including displaced volume by the pump and the undisturbed pressure, are identical in these two actions for generating the forward and backward waveforms. The stroke of piston in either direction is 2 cm in length and internal diameter of cylinder is 5 cm, giving an approximately 40 ml of displaced volume. We used an 11 Watts

graphite brushes DC motor (Maxon 110937, A-max , Sachseln, Switzerland) to drive the pump. The motor used a constant DC power supply of 5.5 Volts. The characteristics of this motor reveal that speed of motor will reduce when the load increase for a fixed Voltage of power supply.

5.2.2 Instrumentation

Simultaneous measurements of pressure and flow were taken at the same measuring sites along the tube of 2 m in length at intervals of 5 cm. Two flexible (latex) tube sizes of 12 mm and 16 mm in diameter (unstretched) were used in this study with the initial undisturbed pressure of 4 kPa and 5 kPa. The tubes, reservoirs and pump are filled with water before the flow waveform was generated.

Pressure and flow were measured using a tipped catheter pressure transducer (Millar Instruments Inc., Houston, Texas, USA) and ultrasonic flow probe (Transonic System, Inc, Ithaca, NY, USA), respectively. The diameter of the 16 mm diameter tube was measured at the same positions of the pressure and flow using ultrasonic paired crystals (Sonometrics Corporation, London, Ontario, Canada).

All the data were acquired at a sampling rate of 500 Hz using programs written in Labview (National Instrument, Austin, TX, USA). The analysis procedure is carried out using programs written in Matlab (The Mathworks, Natick, MA, USA).

It is noticed that relative volumes (volume displaced by the pump against the total volume in the tube) in two sized tubes are varied. Relative in 16mm tube (9.8%) is much smaller than that in 12mm tube (17%).

5.3 Analysis

5.3.1 Waves with the pushing and pulling action

The concept of fluid wave is defined as the disturbance to the flow that travels through the fluid (Lighthill, 1978). Waves in tubes can be considered as the variation of the excess pressure, $p_e = p - p_0$, where, p_0 is the undisturbed pressure, p is the measured pressure and p_e is the excess pressure, which cause fluid acceleration (Lighthill, 1978). This type of wave has a pushing effect on the fluid, both the wave and the flow travel in the same direction (forward). If the measured pressure is lower than the undisturbed pressure, the variation of pressure herein can be expressed as, $\boldsymbol{p_s = p_0 - p}$, where p_s is the shortage pressure and this type of wave has a pulling effect. The shortage pressure will cause the deceleration of the fluid and flow will travel in the backward direction. Therefore, the disturbance (wave) at the inlet of any flexible tube will travel forward, regardless of the direction of the flow. A typical example of pressure and velocity waveforms for waves with pushing and pulling effects *in vitro* are presented in **Figure 5.1**.

5.3.2 Compression and expansion waves

A wave can be classified as compression or expansion according to its effect on pressure. A compression wave causes an increase but an expansion wave causes a decrease in pressure. For example, let us consider a wave with a pushing effect as a half-sinusoid in shape (**Figure 5.1 a & c**). The first half of the wave with a pushing action will be a compression wave as the pressure increases, which will be followed by an expansion wave when the pressure begins to decrease, as shown in **Figure 5.1a** (Shaded area indicates the

expansion wave**).** In contrast, the first half of the wave with a pulling effect will be an expansion wave (shaded area in **Figure 5.1b, d**) as the pressure decreases, which will be followed by a compression wave when the pressure begins to increases (**Figure 5.1b**). A comparison of the features of waves with pushing and pulling effects is presented in **Table 5.1.**

5.3.3 Wave intensity analysis (WIA)

The wave with either the pushing effect or the pulling effect can be analysed using WIA. The forward and backward pressure, velocity and wave intensity for both the wave with pushing and pulling effect can be established using WIA. Wave intensity (WI) with the either pushing effect or the pulling effect is always positive for the forward and negative for the backward directions (Parker and Jones, 1990). A typical WI curve in our experiments is shown in **Figure 5.1e, f**. The WI curve for a wave with either a pushing or a pulling effect has two peaks corresponding to the two halves of the wave generated by the piston. For a wave with pushing effect, the first peak represents the intensity of the compression wave and the second peak represents the intensity of the expansion wave (Shaded area). In contrast, for a wave with a pulling effect, the first peak represents the intensity of the expansion wave (shaded area) and the second peak represents the intensity of the compression wave.

The wave energy can be established by integration of the corresponding curve of WI over time.

The area under the peak of the compression wave intensity denotes compression wave energy, and under the peak of expansion wave intensity denotes expansion wave energy. As one of the main aims of this work is to

explore the dissipation of waves with pulling effect, dissipation of wave intensity and wave energy in this paper will be established using the expansion wave.

Meanwhile, we also use the PU-loop method to establish the local wave speed using the simultaneous measurements of pressure and velocity at the same sites for both the wave with pushing and pulling effect (Khir, et al. 2001). **Figure 5.2** shows typical examples of PU-loops measured for the waves with pushing (**a**) and pulling (**b**) effect.

5.4 Results

5.4.1 Wave speed

Local wave speed at each measurement sites was determined using the PU-loop method. Overall, local wave speed of waves with pulling effect is greater than those with pushing effect (**Table 4.2**). In the tube of 12 mm in diameter, the average speed of the wave with pulling effect is *38%* greater than that of the wave with pushing effect (*4.5±0.9* vs. *3.3±1 m/s)*. In the tube of the 16 mm in diameter, the average speed of the wave with pulling effect is 31% greater than that of the wave with pushing effect (*3.6±0.5m/s* vs. *2.7±0.6 m/s*). **Figure 5.3 a, b** show the variation of wave speed along the tubes of 12 mm and 16 mm in diameter.

Also and as expected, local wave speed in the smaller sized tubes was greater than that in the bigger sized tubes for the same wave with either pushing or pulling effect (**Figure 5.3 a, b** and **Table 5.2).** For example, the average local wave speed during the pulling effect in 12 mm tube is *28%* greater than that in the 16 mm tube (*4.5±0.9 vs. 3.6±0.5* m/s) and for the

pushing action in 12 mm tube is 23% greater than in the 16 mm tube (*3.5±1 vs. 2.7±0.6* m/s).

5.4.2 The amplitude of measured pressure and velocity

The measured pressure and velocity waveforms during the pulling and pushing effect in the time-space plane are shown in **Figure 5.4a, b, c, d.** The amplitude of the measured pressure of both the forward and backward flows resulting from the pushing and pulling actions, decrease at first, then begin to increase due to the arrival of the reflected wave. The amplitudes of the measured velocity of both the forward and backward flows resulting from the pushing and pulling actions decreases slowly at first, then begins to decrease sharply, also due to the arrival of the reflected wave.

Under the same initial experimental conditions, the pressure and velocity magnitudes resulting from the pulling action are greater than those resulting from the pushing action (**Figure 5.4a, b, c, d**). For example, at 25 cm away from inlet of the 12 mm tube, the pressure pulse of the wave with pulling effect is approximately *95%* greater than that of the wave with pushing effect (3.9 vs. 2.0 kPa). Similarly, the velocity amplitude of the wave with pulling effect is greater by *43%* than that of the wave with pushing effect (1.0 vs. 0.7 m/s) (**Figure 5.2a, b, c, d**).

5.4.3 The forward pressure: P_+

The amplitudes of P_+ for the waves with pushing and pulling effect dissipated exponentially along the travelling distance throughout the length of the tube (**Figure 5.4e, f**). The dissipation of P_+ for the wave with pulling effect is greater than that of the wave with pushing effect regardless of the tube size or the initial pressure (**Table 5.2, Figure 5.5**). For example, at 1 m away from inlet of 12 mm

diameter tube, P_+ dissipated approximately 21% (3.1 vs. 3.6 kPa) and 12% (1.5 vs. 1.7 kPa) compared with the P_+ at the inlet of the tube for the pulling and pushing actions, respectively.

In addition, the amplitudes of P_+ during the pushing and pulling effect in the smaller sized tubes dissipated more than those in the larger sized tubes (**Table 5.2**). For example, at 1 m away from inlet P_+ dissipated approximately 21% (3.1 vs. 3.9 kPa) in the 12mm tube and 12% (1.2 vs. 13 kPa) in the 16 mm tube for pulling action. At the same position P_+ dissipated approximately 12% in the 12mm tube and 9.7% in the 16 mm tube for pushing action.

5.4.4 Wave intensity and energy: dI_+ *and* I_+

The peak of forward wave intensity, dI_+, dissipated exponentially along the travelling distance (**Figure 5.4g, h**). Normalised dI_+ and I_+ of the expansion wave during either the pushing or the pulling effect dissipated along the travelling distance as an exponential function (**Figure 5.5b, c**). The power of the exponential equation of normalised dI_+ and I_+ indicates their dissipation. For example, in the 12mm tube the dissipation of normalised dI_+ and I_+ during the pulling action was greater than those during the pushing action (e.g. $e^{-x/0.71}$ vs. $e^{-x/1.13}$ and $e^{-x/1.09}$ vs. $e^{-x/1.33}$). Note the smaller the denominator of power, the greater the dissipation. A more physiologically relevant example, at 10 cm away from inlet of the 12 mm tube, dI_+ for the pulling and pushing actions dissipated approximately *13%* and *7%*, respectively. The degree of dissipation of dI_+ and I_+ of both during pushing and pulling effect are also presented in the **Table 5.2.**

It is noted that the best fitted curves for the separated forward pressure, forward wave intensity and wave energy during pulling and pushing actions start from unit (=1) based on the normalization value, which is illustrated at section 3.6 (**Figure 4.5 a, b and c**).

In addition, the dissipation of dI_+ and I_+ in the smaller sized tubes was greater than that in the bigger sized tube (**Table 5.2**). For example, at 1 m away from inlet in the 12 mm tube dI_+ and I_+ for the pulling action, the decay is approximately *80%* (0.38 vs. 1.94 W/m^2) and *66%* (0.031 vs. 0.0922 J/m^2), respectively, compared to that in the 16 mm tube, which is approximately *74%* (0.058 vs. 0.23 W/m^2) and *57%* (0.005 vs. 0.0 J/m^2).

The intensity of the expansion of the wave with pulling effect is greater than that with pushing effect. For example, at 25 cm away from inlet of the 12 mm tube the intensity of the expansion for the wave with pulling effect is approximately 6.7 times greater than that with pushing effect (0.87 vs. 0.13 W/m^2) (**Figure 5.1**).

The dissipation of dI_+ and I_+ for the wave with the pushing and pulling actions are presented in **Table 5.2.**

5.5 Discussion

Pulling (expansion) waves were observed in the pulmonary venous (Hellevik, et al. 1999) and left side of the circulatory system (MacRae, et al., 1997). Carabello (Carabello, et al., 2006) indicated the second peak of coronary flow waveform is a pulling wave, which is generated by the relaxation of the left ventricle. Further, it is thought that pulling waves generated due to left ventricular relaxation play a major role in shaping the pulsatile nature of

pulmonary venous flow, whose characteristics are being used clinically in several areas such as: (1) estimation of left ventricular filling pressure; (2) evaluation of left ventricular and left atria diastolic function and (3) grading the severity of mitral valve regurgitation (Tomotsugu, et al., 2003). Despite of the various observations of the pulling waves, only the dissipation of the pushing waves has been previously thoroughly investigated.

One of the reasons for this lack of knowledge is that flow with pulling waves exists mainly in areas in the circulations such as the pulmonary veins and the coronary system, where the arterial segments are short and the flow is affected by both the proximal and distal effects. This makes it difficult to distinguish a pure pulling wave, which would not be affected by flow from the opposite direction. Therefore, an *in vitro* set up with a backward half-sinusoidal waveform was produced at the inlet of latex tubes and used to investigate the dissipation of pulling waves. We have also used WIA to separate the waves and discern the decay of waves with pulling action in one direction, whilst excluding the effects of any other waves running in the opposite direction.

Although the experimental conditions such as low initial pressure and lack of restrictions surrounding the walls of the latex tube, do not present a close resemblance to the physiological conditions of the coronary circulation and pulmonary venous system, the behaviour of waves generated with the pulling action discussed in this paper are similar to those observed *in vivo*. For example, Sun observed that at the beginning of left ventricle relaxation, both pressure and velocity waveforms in the coronary artery decrease at first then begin to increase, which is very similar to the pressure and velocity waveforms generated by the pulling action in our experiments (Sun, et al. ,2000). Further,

the authors observed that an expansion wave was followed by a compression wave intensity, which is also similar to the wave intensity waveform calculated for the pulling action in our experiments (**Figure 5.1**). Furthermore, as can be calculated from **Table 5.2**, the magnitude of the forward pressure wave during the pushing and pulling action in 12 mm diameter tubes are dissipated by approximately 2% and 3%, respectively, when it runs for 10 cm. In our experiments, dissipation of short distance plays a minor role in determining the amplitude of pressure waveforms, regardless of the wave nature.

When a compression wave is produced by a pushing action in a static fluid system, the direction of wave propagation is consistent with flow direction (forward). However, when an expansion wave is produced by a pulling action in a static fluid system, the direction of wave propagation is opposite to that of the flow; the wave propagates in the forward but the flow runs in the backward direction (**Table 5.1**). Therefore, if a wave is generated at the inlet of static fluid system ($U = 0$) it will propagate forward regardless of its nature, and a distinction can be made between the compression and the expansion wave based on the direction of the flow. However, if an expansion wave is generated at the inlet of a dynamic fluid system where $U \neq 0$ both the wave and the flow could be still running in the forward direction, although the flow is being decelerated, $dU < 0$. In our experiments there are two mechanisms for the generation of the expansion wave in the forward direction, both of which result in decelerating the fluid. The first is by moving the piston backward and the second is when the piston starts to slow down. A similar observation was made in vivo and has been accepted as the mechanism for decelerating flow in the aorta due to the slowing down of ventricular contraction speed [Parker, 1988].

Under the same initial conditions in our experiments, the magnitude of the pressure and flow pulses for waves with the pulling action are much greater than those with the pushing action (**Figure 5.1**). Theoretically, these magnitudes should be of the same magnitude since the waveforms are produced by the same piston pump and in an identical way except for the direction of piston movement. Possible explanations to this phenomenon are:

(a) Effect of hydrostatic pressure

The piston of the pump and the forces acting on it are shown in **Figure 5.6.** When the piston moves forward to generate forward flow, it pushes against the hydrostatic pressure, P_L, which has to be overcome to allow the acceleration of the piston. On the other hand, when the piston moves backward to generate backward flow, the hydrostatic pressure, P_L, assists in pushing the piston backwards enhancing the driving force, F, in the backward direction.

The characteristics of the motor used in our experiments indicate that for a fixed voltage the angular speed decreases as the load increases. This information agrees with our observation that the time of the half-sinusoidal waveforms generated by the pulling action is slightly smaller than those generated by the pushing action (0.68 vs. 0.774 s in the 12 mm tube, **Figure 5.1**), which indicates that speed of motor for the pulling action is slightly faster than that for the pushing action. Therefore, although the driving force used for the pushing and pulling actions is the same, the total power acting on the piston when it is pushing forward is less than that when it is pulling backward. This difference might account for part of the difference of amplitude of pressure and velocity waveforms between the pushing and pulling actions.

(b) Effect of flux area

When the compression wave generated by the pushing action passes by the measurement sites, the velocity should be relatively smaller due to the enlargement of the cross-sectional area. In contrast, as the expansion wave generated by the pulling action passes by the measurement sites, the velocity should be relatively greater due to the reduction in the cross-sectional area (**Figure 5.6**). Therefore, the variation of diameter due to the nature of the wave might account for part of the difference between the magnitudes of velocity wave during the pushing and pulling actions.

To verify this hypothesis, we also simultaneously measured the pressure, flow and diameter waveforms during the pushing and pulling actions in the 16 mm diameter tube. The amplitudes of the pressure, velocity, the maximum diameter during the pushing action and minimum diameter for the pulling action are shown in **Table 5.3** and **Figure 5.7.** It is reasonable to assume a circular cross-section area of each tube and the ratio of the maximum to minimum cross-sectional area during the pushing and pulling actions is expressed as $R_a = \frac{D_{push}^{\ 2}}{D_{pull}^{\ 2}}$ where D_{push} and D_{pull} are the maximum and minimum diameter during the pushing and pulling actions, respectively. Meanwhile, the ratio of amplitude of velocity during the pushing (U_{push}) to the pulling (U_{pull}) action can be written as $R_u = \frac{U_{push}}{U_{pull}}$, R_a has an inverse relationship to R_u. As shown in **Table 5.3.** values of R_a are very close to those of $1/R_u$; for example at 50 cm away from inlet of the 16mm tube R_a is approximately 1.152 and $1/R_u$ is

approximately 1.11. This indicates that variation of cross-sectional area caused by the diameter change might account for the dissimilarity of velocity pulse during the pushing and pulling actions.

In our experiments, we observed that local wave speed is highest in the middle part of the tube and gradually declines toward both ends of the tube (**Figure 5.3**). A possible explanation is that the thickness of the wall of the tubes used in our experiments is not absolutely uniform due to the dipping method used in manufacturing these tubes. The smallest wall thickness we measured was about 0.15 mm at one end and gradually increases to the largest at the other end of approximately 0.2 mm. Further, these tubes are produced in 1 m length and each of the 2 meters tube were constructed by gluing the thicker ends of two tubes of 1 m using liquid latex. The overlapped part of connecting the two tubes was inevitably slightly stiffer and thicker than the other parts of the 2 m long tube. This variation in wall thickness and mechanical properties might be the source of difference in the local wave speed along the tube; giving the highest values around the middle of the tube. The variation of local wave speed along the tube length, which is associated with the changes of wall thickness, provides evidence to the sensitivity of PU-loop method to local changes in wall properties.

	Pushing Action				Pulling Action			
Wave Directions	F		B		F		B	
Wave Nature	CW	EW	CW	EW	EW	CW	EW	CW
dP	↑	↓	↑	↓	↓	↑	↓	↑
dU	↑	↓	↓	↑	↓	↑	↑	↓
dI	+	+	-	-	+	+	-	-
Flow Directions	F	F	B	B	B	B	F	F

Table 5.1. Flow direction and nature of the pushing and pulling waves.
F and B denote the direction of travel for either the wave or the flow. CW and EW indicate compression and expansion wave respectively. Upward arrows "↑" indicate an increase, downward arrows "↓" indicate a decrease and "+" indicates positive and "-" indicates negative.

Conditions			Pushing Action				Pulling Action			
Diameter	Thickness	Initial pressure	$\frac{P_+}{P_{+i}}$	$\frac{dI_+}{dI_{+i}}$	$\frac{I_+}{I_{+i}}$	C (m/s)	$\frac{P_+}{P_{+i}}$	$\frac{dI_+}{dI_{+i}}$	$\frac{I_+}{I_{+i}}$	C (m/s)
12mm	0.2mm	4 kPa	$e^{-x/7.9}$	$e^{-x/1.13}$	$e^{-x/1.33}$	3.3±1.0	$e^{-x/4.71}$	$e^{-x/0.71}$	$e^{-x/1.09}$	4.5±0.96
		5 kPa	$e^{-x/8.87}$	$e^{-x/1.21}$	$e^{-x/1.56}$	3.1±0.9	$e^{-x/4.59}$	$e^{-x/0.7}$	$e^{-x/1.21}$	4.2±1.2
16mm	0.2mm	4 kPa	$e^{-x/7.46}$	$e^{-x/1.36}$	$e^{-x/1.64}$	2.7±0.6	$e^{-x/8.2}$	$e^{-x/0.79}$	$e^{-x/1.37}$	3.6±0.5
		5kPa	$1.1e^{-x/9.8}$	$e^{-x/1.41}$	$e^{-x/1.5}$	2.4±0.7	$e^{-x/8.83}$	$e^{-x/0.75}$	$e^{-x/1.37}$	3.3±0.7

Table 5.2 The exponential equations for normalised values of forward pressure, $\frac{P_+}{P_{+i}}$, forward wave intensity, $\frac{dI_+}{dI_{+i}}$, and forward wave energy, $\frac{I_+}{I_{+i}}$, during the pushing and pulling actions measured in two sized tubes (12 mm and 16 mm diameter). Dissipation is expressed as an exponential function $e^{-x/\lambda}$, where x is the distance away from inlet and λ is the inverse of the power of the exponential decay, allowing for calculating the dissipation at any distance away from the inlet of the tube. C indicates the average wave speed of all measuring sites along the 2 m length tube at an initial pressure of 4 kPa and 5 kPa, respectively.

Table 5.3 The amplitudes of pressure, velocity and diameter variation for the pushing and pulling actions for 16 mm tube.

Position (cm)	Amplitude of pressure, ΔP (kPa)			Amplitude of velocity , ΔU (m/s)				Peak of diameter, D (mm)		
	Pushing	Pulling	Difference (%)	Pushing	Pulling	Difference (%)	$\frac{1}{R_u} = \frac{\Delta U_{pull}}{\Delta U_{push}}$	Pushing	Pulling	$R_a = \frac{D^2_{push}}{D^2_{pull}}$
25	1.1	1.58	43.636	0.34	0.39	14.706	1.15	19.4	17.7	1.2
50	1.09	1.59	45.872	0.34	0.38	11.765	1.11	19.15	17.9	1.14
75	1.04	1.54	48.077	0.36	0.39	8.333	1.08	19.1	18	1.125
100	0.97	1.49	53.608	0.38	0.43	13.158	1.13	19.04	18.05	1.11
125	1.27	2.05	61.417	0.36	0.38	5.556	1.06	19.43	17.66	1.21
150	1.51	2.43	60.927	0.27	0.28	3.704	1.03	19.95	17.28	1.33

Difference (%) means the percentage of difference between the pushing and pulling action with the respect to the pulling action. The amplitude of the pressure and velocity during the pushing action is the maximum value minus the undisturbed value and during the pulling action is the undisturbed value minus the minimum value. The peak of diameter during the pushing action is the maximum diameter and during the pulling action is the minimum value.

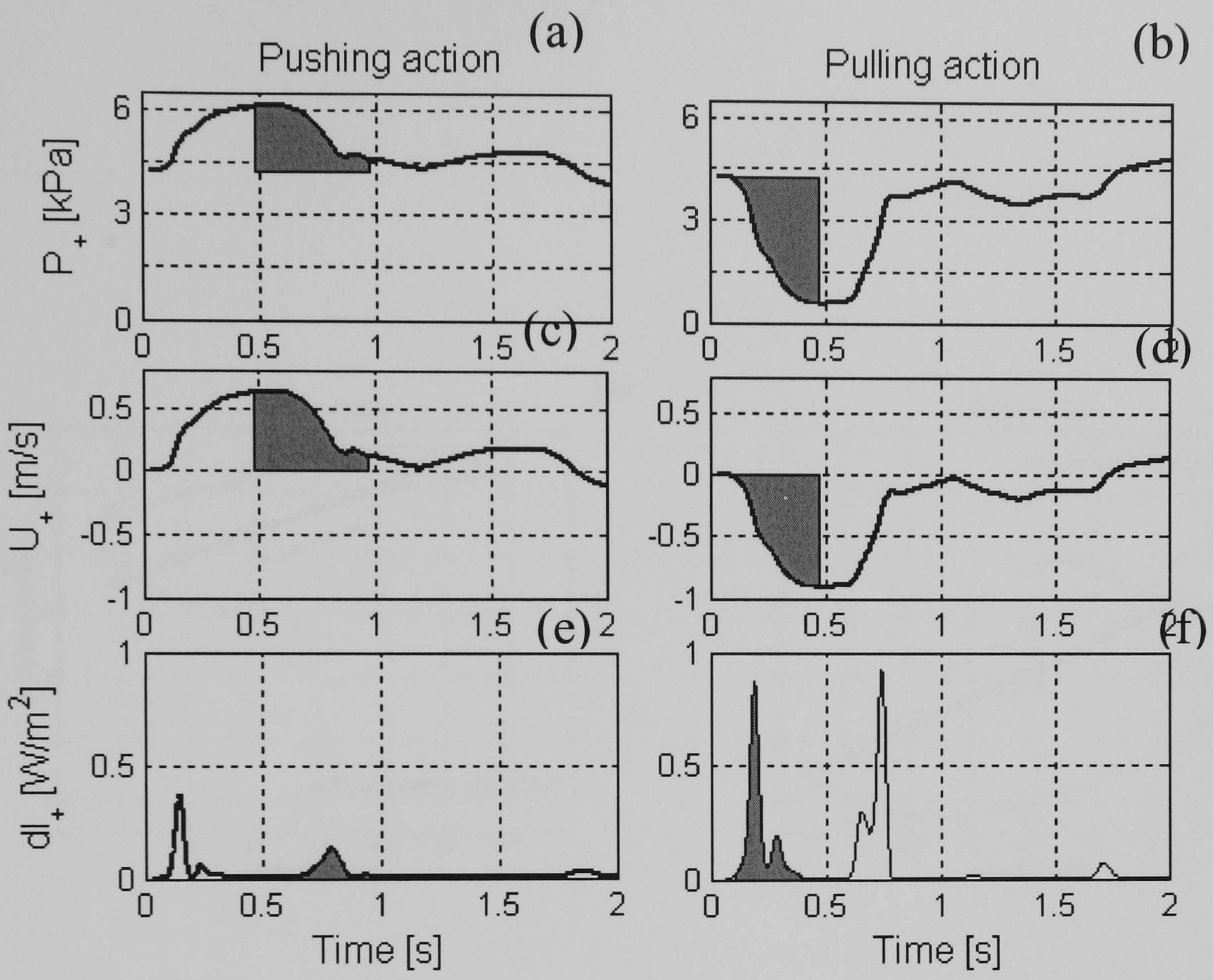

Figure 5.1 A typical calculated forward pressure (a, b), forward velocity (c,d) and forward wave intensity (e,f) waveforms during the pushing and pulling actions. Measurements were taken at 25 cm away from inlet in the 12 mm in diameter tube with initial pressure of 4 kPa. The shaded areas represent the expansion wave, which is identified by a decrease of pressure, occurs in the second half of the waveform with pushing action, but in the first half of the waveform with pulling action.

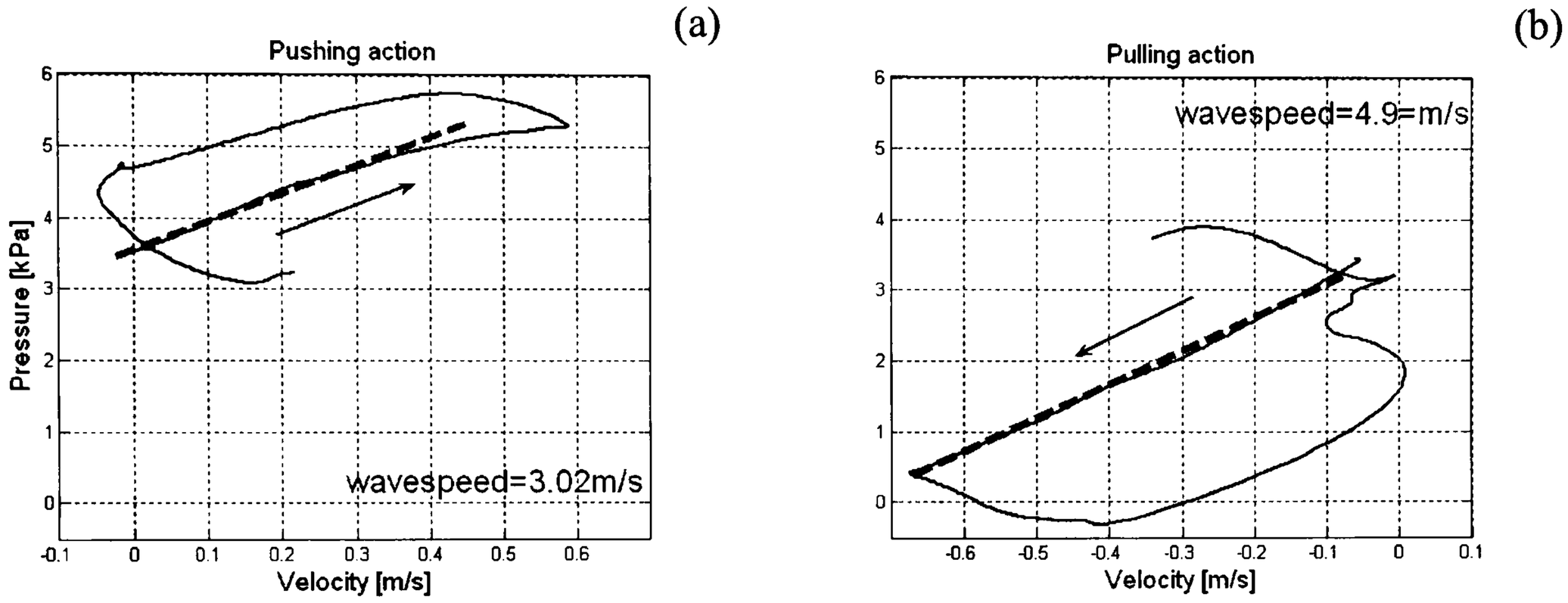

Figure 5.2 The PU-loop measured for the wave with pushing (a) and pulling effect (b). Pressure and velocity were measured were taken at 110cm away from the inlet of the 12mm in diameter tube at an initial pressure of 5kPa. Arrows indicate the direction of loop. The initial linear part of the each loop, whose slope is directly related to wave speed is marked by the bold dash lines. In this case, wave speed in the same tube is 3.02m/s for the pushing wave with and 4.9m/s for the pulling wave, respectively.

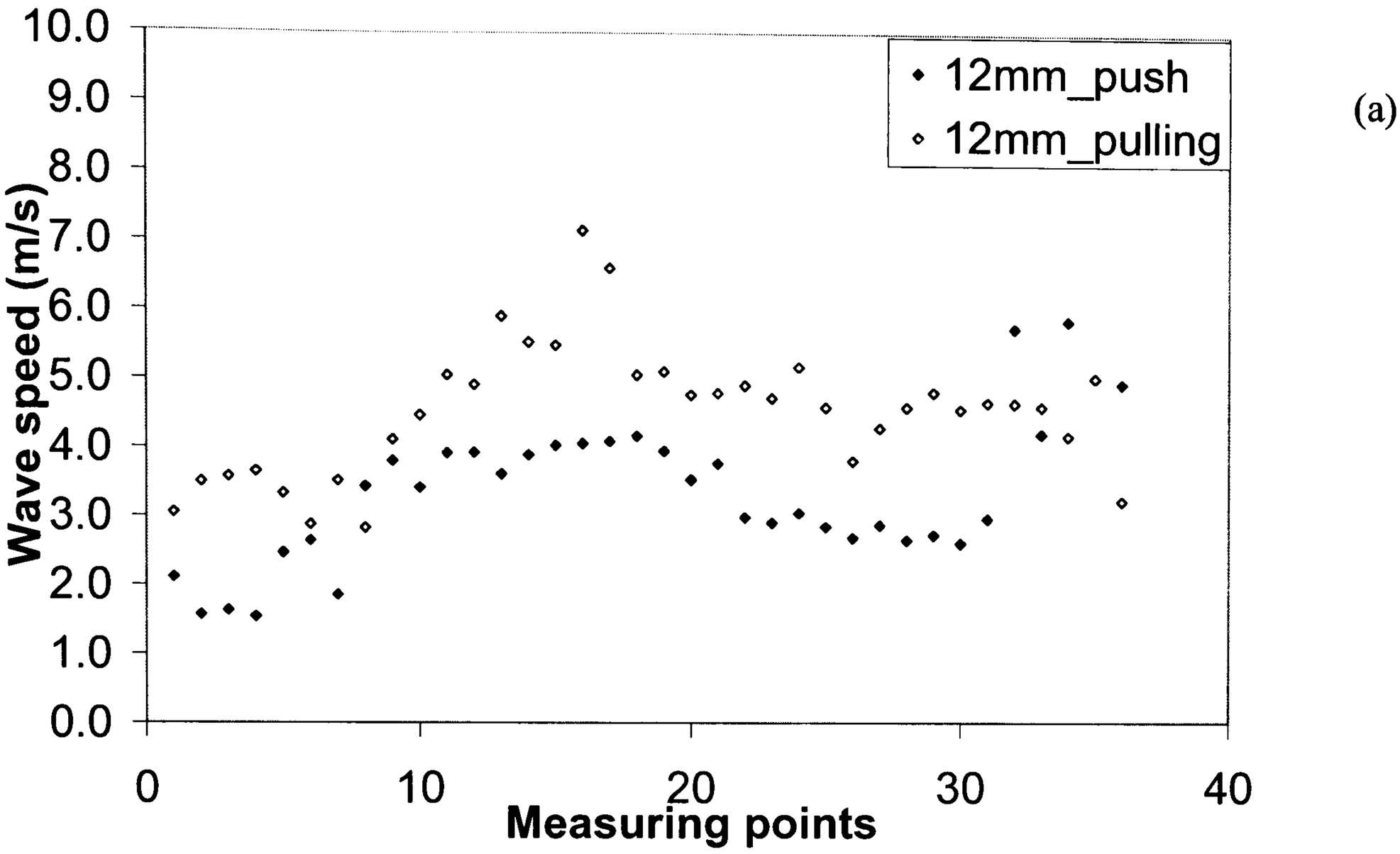

Figure 5.3 Local wave speed determined using the PU-loop method for the waves with pushing and pulling effects in 12mm tube (a) and in 16mm tube (b) with an initial pressure of 4kPa. Horizontal ordinate indicates the measuring sites and vertical ordinate indicates the local wave speed.

Pushing action wave

Pulling action wave

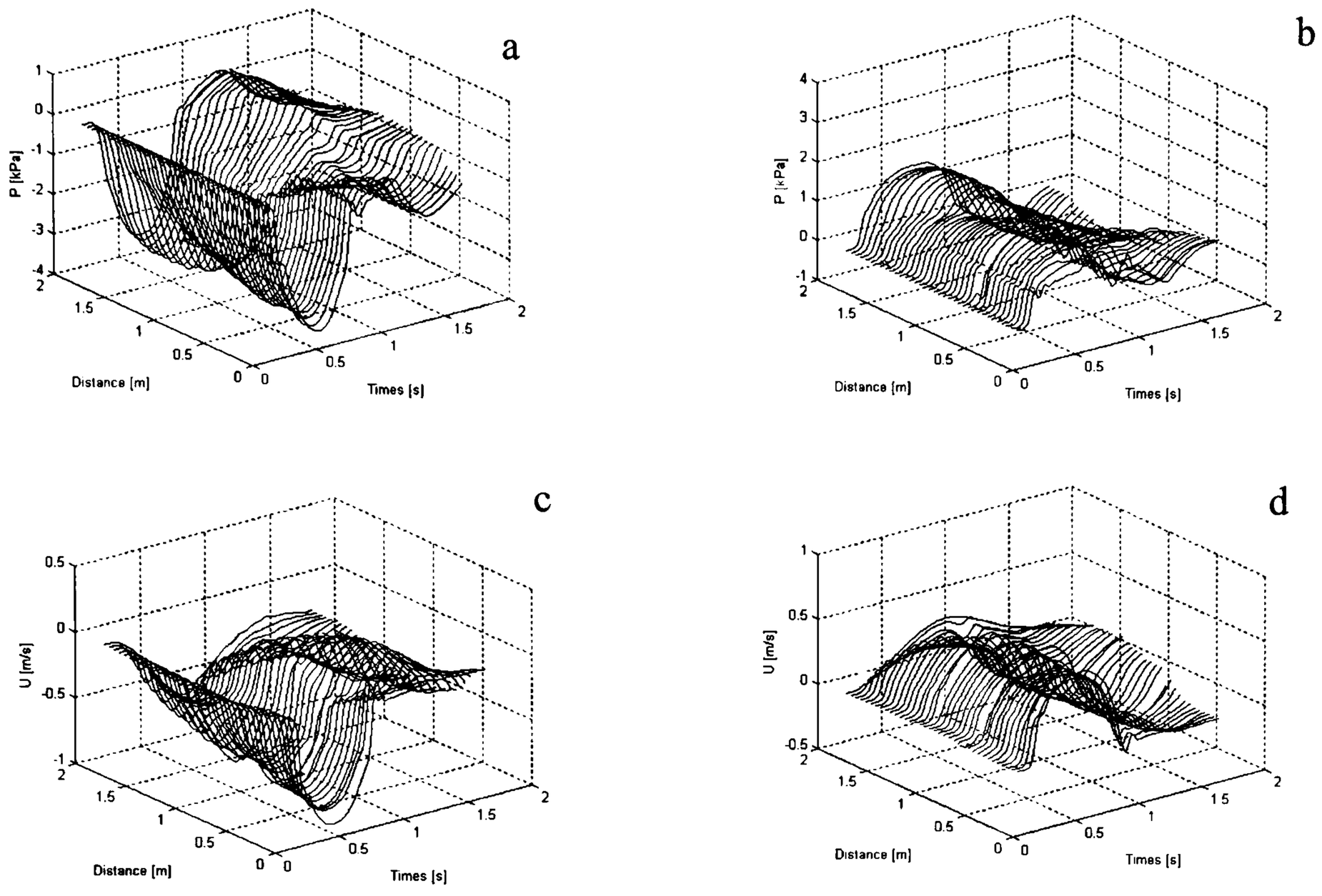

Figure 5.4 The measured pressure, velocity, the separated forward pressure and wave intensity during the pulling and pushing actions are shown. The measurements were taken at intervals of 5 cm along the 12 mm tube at initial pressure of 4 kPa.

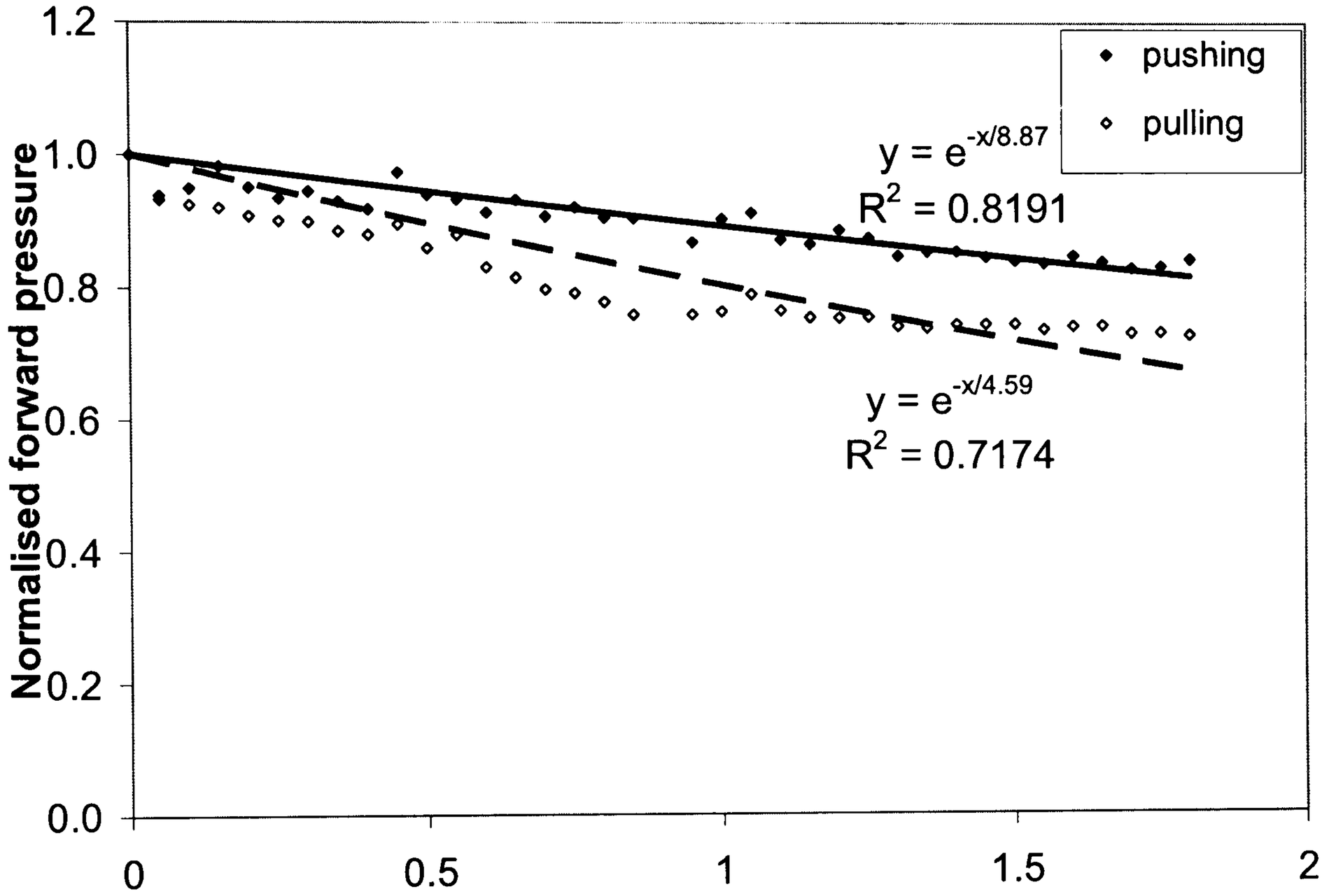

Figure 5.5 (a). The normalised forward pressure are plotted against the travelling distance in the tube of 12 mm in diameter with the initial pressure of 5 kPa. The corresponding power of exponent indicates greater dissipation during the pulling action than during the pushing action.

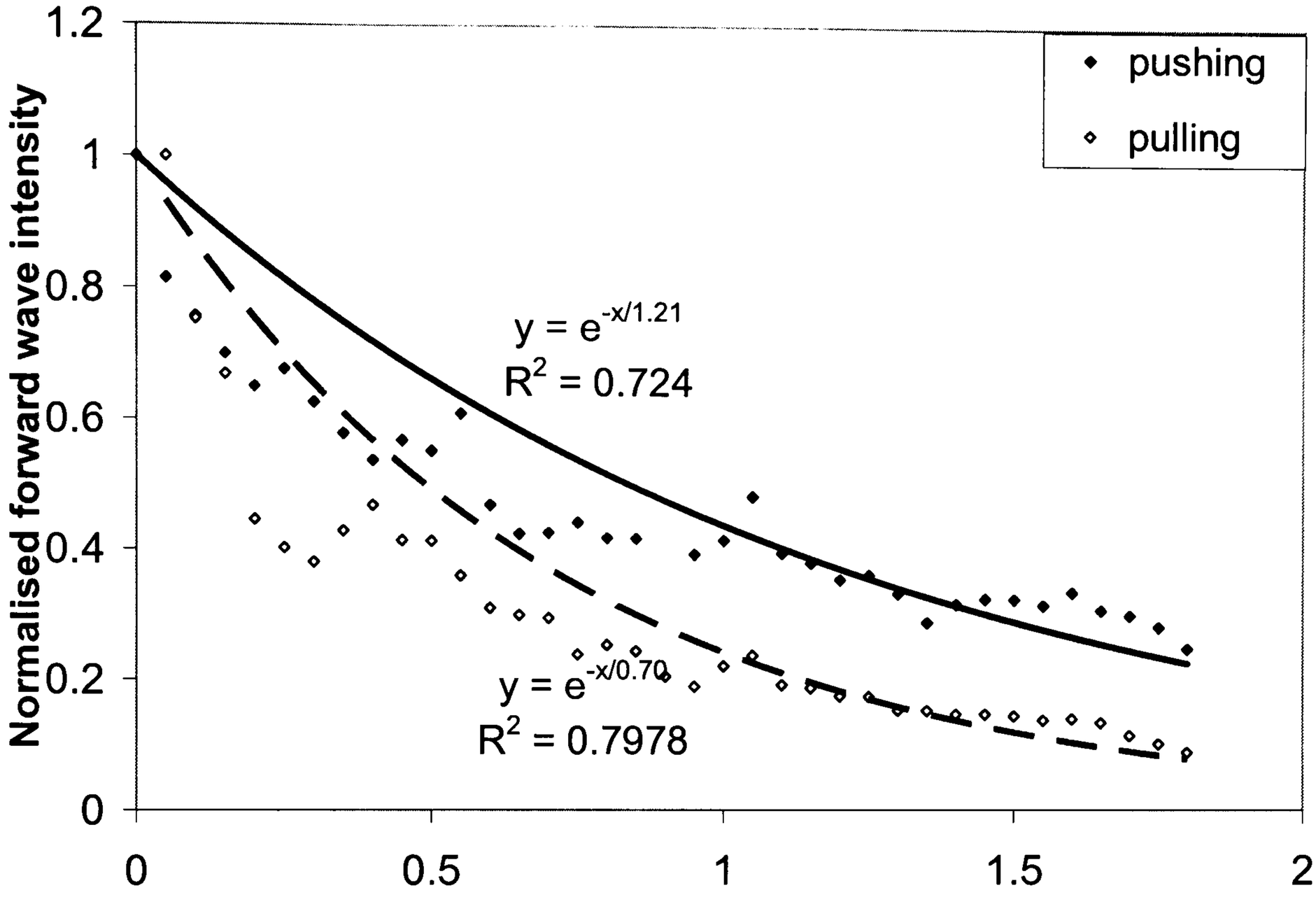

Figure 5.5 (b) The normalised forward wave intensity are plotted against the travelling distance in the tube of 12 mm in diameter with the initial pressure of 5 kPa. The corresponding power of exponent indicates greater dissipation during the pulling action than during the pushing action.

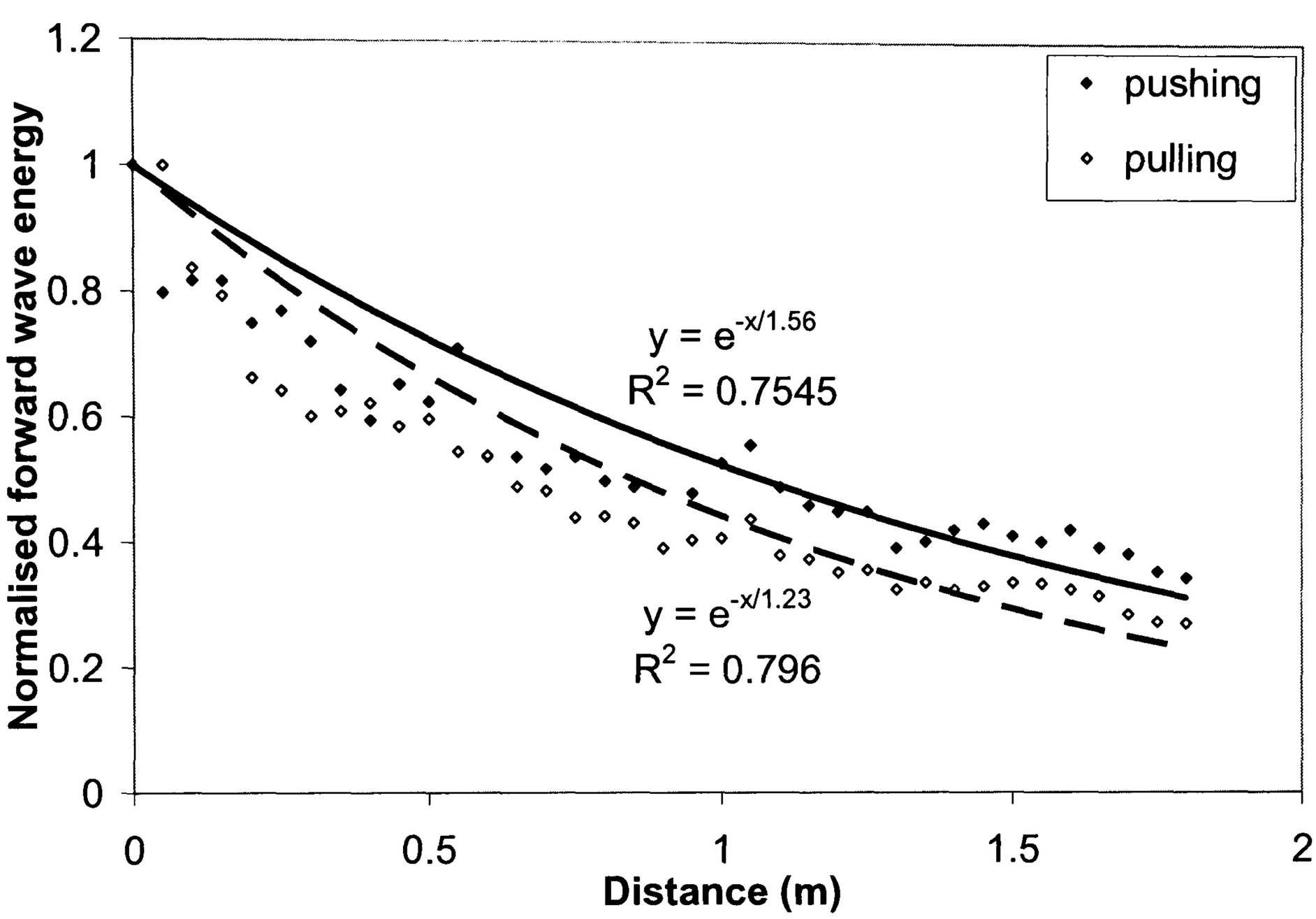

Figure 5.5 (c) The forward wave energy are plotted against the travelling distance in the tube of 12 mm in diameter with the initial pressure of 5 kPa. The corresponding power of exponent indicates greater dissipation during the pulling action than during the pushing action.

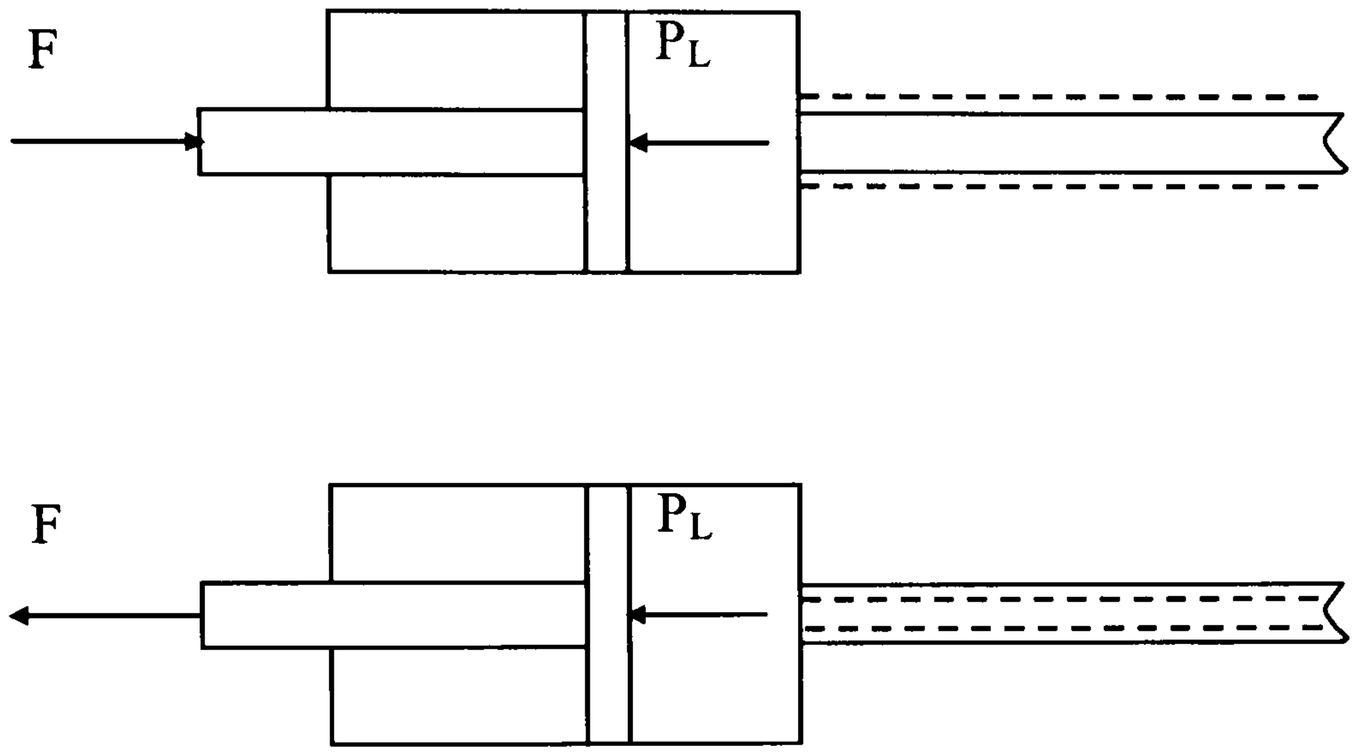

Figure 5.6 Sketch of piston and the applied forces; (a) piston is moving forward and (b) piston is moving backward. F is driving force and P_L is the hydrostatic pressure head acting on the piston. The dashed line indicates the change in tube wall's diameter during the pushing and pulling actions.

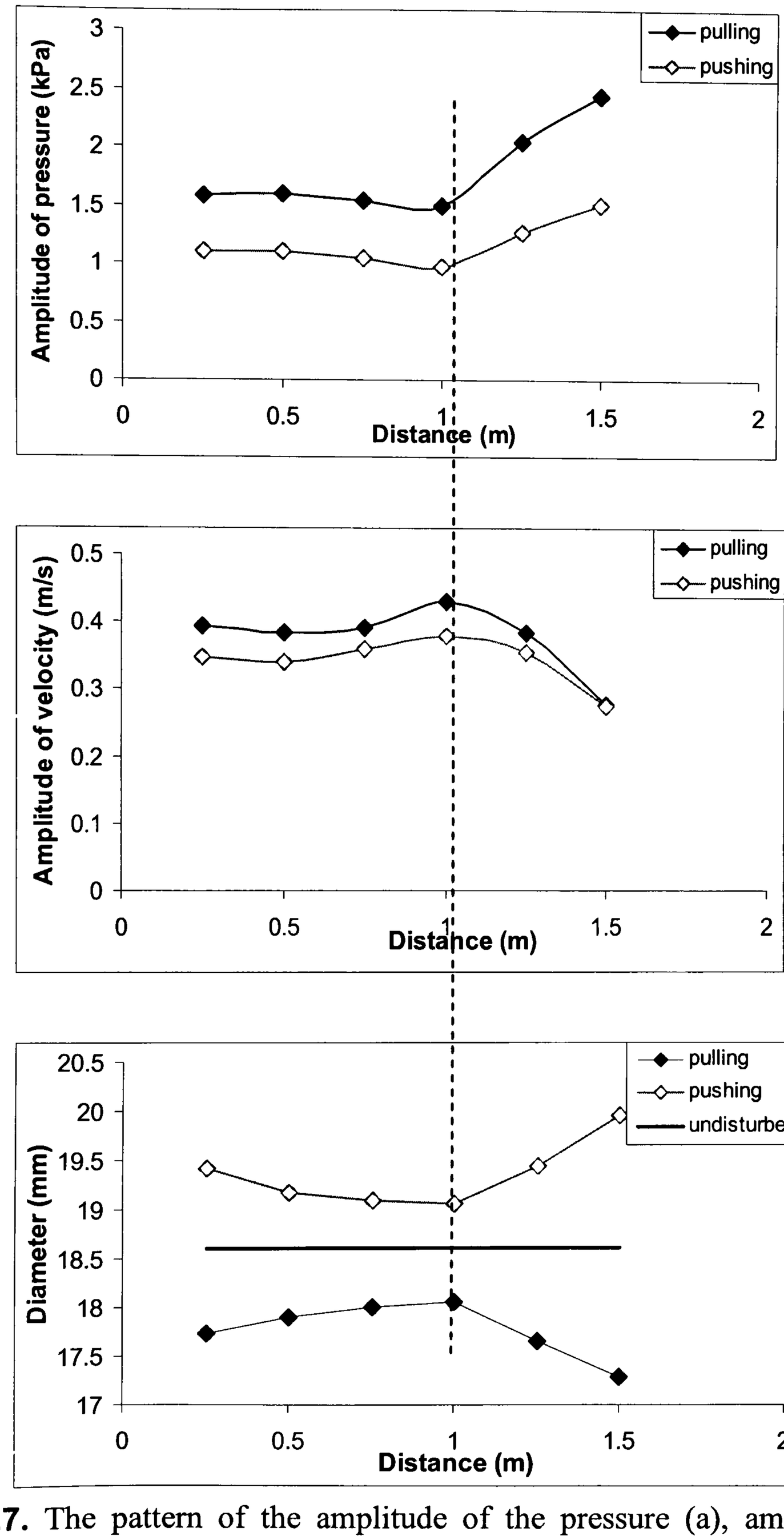

Figure 5.7. The pattern of the amplitude of the pressure (a), amplitude of the velocity (b), the maximum diameter for pushing action and minimum diameter for pulling action (c) were shown in the 16 mm tube. Vertical dash line indicates that the reflection wave start affecting the peak of wave. Solid dark line in the **Figure 5.7** (c) denotes the undisturbed diameter.

Chapter 6

Determination of wave speed and separation of waves using diameter and velocity

6.1 Introduction

The investigation of the relationship between pressure and diameter waveforms is often motivated by the need for the non-invasive measurement of local pressure waveform. The measurements using a pressure catheter inserted in the artery invasively might affect the local condition of geometry and flow. In addition, invasive measurement of pressure is not very suitable for routine examination (Hoeks, et al., 2004).

The relationship between pressure and diameter in the arteries appear non-linear (Pedley, 1980) although it is suggested by Sugawara that the carotid arterial pressure-diameter relationship could, in practise, be regarded as being linear (Sugawara, et al. 2000). There is also strong opinion for an exponential relationship between arterial cross-section and pressure (Meinders, et al., 2004), however, Hartley concluded that the diameter signals can replace pressure signals for calculating the augmentation index after studying arterial motion in mice using a non-invasive Doppler method(Hartley et al., 2003).

The arterial pressure and velocity is often assessed in frequency domain through impedance approach using the Fourier theory. Wave intensity analysis (WIA), which was originally introduced by Parker and Jones (1989), is a one-dimensional analysis and a time domain approach, which allows for studying wave propagation in arterial system and elastic tubes as a function of time and

space. Compared with impedance approach in frequency domain, WIA is more clinical intuitively since the findings are directly related to physiological events.

Wave intensity (WI) is defined as the flux of energy carried by the wave per cross sectional area and has the advantage of not assuming any periodicity or linearity in the system (Jones and Parker, 1992). WIA allows for separation of waveform into forward (incident) and backward (reflection) direction (Parker and Jones, 1990) and has been applied to different sites in the cardiovascular system, including waves in the aorta (Khir et al., 2005; Koh, et al., 1998), coronary arteries (Sun et al., 2003, David et al. 2006) and left and right ventricular (Zhang et al. 2005; Yi-Chun Sun et al., 2004). Accurate prediction of arrival time of reflection wave using backward WI and backward pressure waveform is of clinical significance and has been used to diagnosis ventricular hypertrophy and cardiac failure (Koh et al., 1998).

Due to the advantages of WI and the importance of non-invasive assessment of arterial waveform, Harada et al. (Harada et al. 2000) developed a non-invasive measurement system of wave intensity (WI) in arteries, which is based on the conversion of diameter change from the cuff-type manometer in the upper arm to pressure change. This technique has been applied in many investigations to the cardiovascular system such as carotid arterial wave intensity (Ohte et al. 2003) and assessments of the reflection pulse wave in patients (Nobuoka et al., 2001, Bleasdale et al., 2003). However, it is well known the pulse pressure is not constant throughout the arterial tree. Use of pulse pressure at one site as surrogate for pulse pressure at another arterial site may be erroneous (Van et al., 2001).

As is known, wave speed is one of key factors describing the wave propagation of blood flow in arteries and local wave speed is mainly related to the elastic property of arterial wall (Mcdonald, 1974). The conventional way to determine wave speed is based on foot-to-foot method. PU-loop method, is technique for the determination of local wave speed only using measurements of pressure and flow at the same site (Khir et al. 2001). This method has been proven to be sensitive to the changes of local property in the wall (Feng et al., 2008) and also has been used to determine the wave speed online (Harada et al. 2002). This chapter aims to determine the local wave speed only using simultaneous measurements of diameter and velocity rather than pressure and velocity.

With the exception of a recent PhD study on pulmonary arteries (O'Brien', 2003), no literatures show that the determination of WI and separation of wave forms into forward and backward direction directly using the diameter and velocity. This chapter aims to develop an algorithm to produce WI-type analysis, using the measurement of diameter and velocity, which could potentially be used non-invasively. The specific objectives of this investigating are: (1) to determine the wave speed using only simultaneous measurement of diameter and flow velocity; (2) separation of diameter, velocity and WI into forward and backward directions; (3) assessment of the agreement of timing determined by diameter and velocity with the corresponding time determined by pressure and velocity.

6.2 Theory

6.2.1 Separation of wave using diameter and velocity

Let assume a long tube with undisturbed diameter, D, it is well established that wave speed is a function of distensibility of tube wall (Pedley, 1980)

$$c^2 = \frac{AdP}{\rho dA} \tag{6.1}$$

Where, A and dA are the initial cross-sectional area and its change, respectively. Re-arrange (6.1) gives

$$dP = \rho c^2 \frac{dA}{A} \tag{6.2}$$

Given that $A = \frac{\pi}{4} D^2$ and $dA = \frac{\pi}{2} DdD$, where, dD is the change of the diameter of the tube, the following term can be introduced:

$$\frac{dA}{A} = \frac{2dD}{D} \tag{6.3}$$

Substitute (6.3) into (6.2) gives,

$$dP = \rho c^2 \frac{2dD}{D} \tag{6.4}$$

Because the change in pressure, dP, can be considered as the linear summation of the change in the pressure in the forward and backward direction, $\boldsymbol{dP = dP_+ + dP_-}$ (Jones and Parker, 1992). It is reasonable to assume that change in diameter, dD, to be considered as the linear summation of diameter changes due to changes in the forward and backward pressure changes,

$$\boldsymbol{dD = dD_+ + dD_-} \tag{6.5}$$

The water-hammer equation is

$$dP_{\pm} = \pm \rho c dU_{\pm} \tag{6.6}$$

Substitute (6.4) into (6.6), gives

$$dD_{\pm} = \pm\frac{D}{2c}dU_{\pm} \qquad \text{or} \quad dU_{\pm} = \pm\frac{2c}{D}dD_{\pm} \tag{6.7}$$

If we assume the change in the velocity waveform, *dU*, is the result of the algebraic summation of the changes in the forward and backward directions, we can write,

$$dU = dU_{+} + dU_{-} \tag{6.8}$$

Substitution $dU_{\pm}$ from equation (6.7) into (6.8) gives

$$dU = \frac{2c}{D}dD_{+} + (-\frac{2c}{D}dD_{-}) \tag{6.9}$$

The change in diameter resulting from the change in pressure in the forward and backward directions can be obtained by multiplying (6.5) by $(2c/D)$, adding and subtracting (6.9), and rearrange

$$dD_{\pm} = \frac{1}{2}(dD \pm \frac{D}{2c}dU) \tag{6.10}$$

To determine the change in velocity in the forward and backward directions we substitute (6.7) into (6.5) gives

$$dD = \frac{D}{2c}dU_{+} + (-\frac{D}{2c}dU_{-}) \tag{6.11}$$

The velocity differences in the forward and backward directions can be similarly determined by multiplying (6.5) by $(D/2c)$, adding (6.11), and multiplying (6.5) by $(D/2c)$, subtracting (6.11) and rearrange

$$dU_{\pm} = \frac{1}{2}(dU \pm \frac{2c}{D}dD) \tag{6.12}$$

The forward and backward diameter and velocity can be obtained by summation of changes in diameter and velocity in the forward and backward

directions.

$$D_+ = \sum_1^n dD_+ + D(0) \qquad U_+ = \sum_1^n dU_+ \tag{6.13}$$

$$D_- = \sum_1^n dD_- \qquad U_- = \sum_1^n dU_- \tag{6.14}$$

where, $D(0)$ is the undisturbed diameter of the tube.

A typical example of measured and separated diameters, as are shown in the **Figure 6.1b**, is used to compare with the measured and separated pressures at the same measuring site, **Figure 6.1a**.

6.2.2 Determination of wave intensity using diameter and velocity

Traditionally, wave intensity is determined by the change of pressure and velocity. To distinguish wave intensity determined by the pressure and velocity from that by the diameter and velocity, we use the terms, dI_{PU} and, dI_{DU}, respectively.

dI_{DU} can be established by multiplying the change of diameter by the changes of velocity ,

$$dI_{DU} = dDdU \tag{6.15}$$

Similar to dI_{PU}, dI_{DU} can also be separated into the forward and backward directions, which can then be determined by multiplying the change in diameter and velocity in respective direction; dI_{DU+} is wave intensity in the forward direction and dI_{DU-} is wave intensity in the backward direction.

$$dI_{DU+} = dD_+dU_+ = \frac{1}{4(D/2c)}(dD + \frac{D}{2c}dU)^2$$

$$dI_{DU-} = dD_-dU_- = -\frac{1}{4(D/2c)}(dD - \frac{D}{2c}dU)^2 \tag{6.16}$$

Where, $\frac{D}{2c}$ is the slope of dD over dU in the forward or backward directions.

An example of separated dI_{DU} is shown in **Figure 6.1 d**, which is used for comparison with the separated dI_{PU} based on the measurements of pressure and velocity at the same site, **Figure 6.1 c**.

6.2.3 DU-loop method

The separation of diameter, velocity and dI_{DU} waveforms into their forward and backward directions also requires knowledge of wave speed. We hypothesised that in the absence of reflected wave, D and U are related linearly with the slope of $\frac{D}{2c}$ based on the relationship of the change of diameter and velocity shown in equation (6.7). The DU-loop (Diameter and velocity loop) is made by plotting velocity and diameter in the same coordinates, **Figure 6.2b**. DU-loop shows that the relationship of diameter and velocity in the beginning of DU-loop is linear due to the absence of reflected wave. Therefore, the slope of linear part of DU-loop during the beginning, when the reflection wave has not arrived, can be used to determine wave speed by the factor of, $D/2c$. The wave speed determined by PU-loop is also shown in the **Figure 6.2a**, which is used to compare with the wave speed determined by DU-loop.

6.3 Method

6.3.1 Experimental setup

The experimental setup was shown in **Figure 6.3**, which is composed of an Intra-Aorta-Ballon Pump (IABP), artificial heart (BCM), tank with water inside, two reservoirs, and latex tubes (two sizes: 16mm in diameter with 2m in length;

24mm in diameter with 1m in length).

BCM (Cardialcare, Minneapolis, MN, U.S.A) is a flexible diaphragm pulsatile left ventricle assist device (LVAD), which can be operated using a IABP. As shown in **Figure 6.3**, the inlet of BCM was connected with the left reservoir and the outlet of BCM was connected with inlet of latex tube. In this work, the BCM was operated by IABP and generates an approximate half-sinusoidal wave. The heart rate was 80bpm and augmentation of scale was arranged as level 1.

6.3.2 Instrumentation

The simultaneous measurements of pressure, flow and diameter were taken at the same position at intervals of 15 cm along each tube. Pressure, flow and diameter are measured using tipped catheter pressure transducer (Millar Instruments, INC, Houston, Texas, 77023, USA), ultrasonic flow probe (Transonic System, Inc, Ithaca, NY, USA) and ultrasonic paired crystals (Sonometric Cooperation, 500 Nottinghill London, ONT, N6K 3P1, Canada) ,respectively. All the data were acquired at a sampling rates of 500Hz using in-house program written in Labview (National Instrument, Austin, TX, USA). The analysis was carried out using programs written in Matlab (The Mathworks, Natick, MA, USA).

6.3.3 Analysis

Regression line and Student's t-test analyses are used to assess the correlation of wave speed determined by the PU-loop and DU-loop. We also examined the correlations of arrival of time of reflection wave determined by the backward pressure, P-, and the backward diameter, D-, as well as by dI_{PU-} and dI_{DU-}.

The relationship of timing of key points, t_1, t_2, t_3 and t'_1, t'_2, t'_3, determined by these two methods is also assessed. The terms t_1, t_2 are the timing of peak of dI_{PU+} for compression and expansion wave, respectively, and the term t_3 is the timing of first peak of $dI_{PU\pm}$. Similarly, t'_1, t'_2, t'_3 indicate the timing of corresponding points for dI_{DU-}. p_1, p_2, p_3 and p'_1, p'_2, p'_3 indicate the peak values in the corresponding points (t_1, t_2, t_3 and t'_1, t'_2, t'_3,) for $dI_{PU\pm}$ and $dI_{DU\pm}$,respectively, **Figure 6.1**. In addition, the relationship of peak values at key points between these two methods is assessed. All the statistical analyses were carried out using commercial program SPSS13 (SPSS Inc. 233 S. Wacker Drive, 11th Floor, Chicago, IL, US). In addition, Bland-Altman method was used to assess the agreement of these two methods (Bland and Altman, 1986).

6.4 Results

6.4.1 Wave speed determined by PU-loop and DU-loop

Wave speed determined by PU-loop is slightly greater than that determined by DU-loop (**Table 6.1**). For example, the wave-speed determined by PU-loop at 150 cm in 16 mm tube is 16% greater than by DU-loop (3.53 vs. 2.94 m/s), **Figure 6.2**. In 16 mm tube, the average wave speed determined by PU-loop is 6.5% greater than by DU-loop (3.7±0.38 vs. 3.46±0.35 m/s). In 24 mm tube, the average wave speed determined by PU-loop is 10.9% greater than by DU-loop (3.38±0.45 vs. 3.02±0.57 m/s). The regression line and Student's t-test show that wave speed determined by PU-loop and DU-loop are correlated well with r=0.786 and P<=0.005 (**Figure 6.4 a**).

The agreement of wave speed determined by the two methods is also assessed using Bland-Altman method (**Figure 6.4b**). The results show that mean of difference between these two methods is 0.26 m/s, which indicated that wave speed determined by PU-loop is slightly above that determined by DU-loop. The difference of wave speed between these two methods is within the range of mean±2SD (0.26±0.56 m/s).

6.4.2 Arrival time of reflected waves (T_{rw})

The measured pressure, P, and its separated forward pressure, P_+ and backward pressure, P_-, shown in **Figure 6.5a**, are very similar in shape to the corresponding diameters, shown in **Figure 6.5b**. Before the arrival of reflected wave arriving, the forward pressure (green solid line, **Figure 6.5a**) is expected to be superimposed to the measured pressure waveform (blue solid line **Figure 6.5a**), and likewise the forward diameter is also as the same as the measured diameter during only incident wave occurring (**Figure 6.5b**). The arrival time of reflected wave, T_{rw} determined by the backward pressure (red solid line, **Figure 6.5a**), is very close to that determined by the backward diameter (red solid line, **Figure 6.5b**). The measured pressure and diameter increase sharply with the arrival of reflected wave (indicated with dotted circle). Similar to the forward and backward wave intensity determined by the pressure and velocity, dI_{PU}, the forward and backward diameter wave intensity determined by the diameter and velocity, dI_{DU}, also has two peaks; first one represents the compression wave and the second one represents expansion wave (**Figure 6.5e, f**). Furthermore, the forward and backward velocity determined by the measured pressure and velocity are almost identical in shape to those determined by the measured

diameter and velocity (**Figure 6.5c, d**).

All figures of **Figure 6.5** show that T_{rw} established using the measured pressure and velocity are very similar to that determined using diameter and velocity.

Table 6.2 lists T_{rw} at each measurement sites in the tube of 16 mm in diameter and in the tube of 24 mm in diameter. The results show that there is a small difference between T_{rw} determined by dI_{PU-} (T_{rw}_dI_{-}) and by dI_{DU-} (T_{rw}_dI_{DU-}) as well as by P_{-} (T_{rw}_P_{-}) and D_{-} (T_{rw}_D_{-}). The greatest percentage of difference of T_{rw} between the two methods is 1.6% and the average percentage of difference is 0.241±0.78.

Regression line (y = 0.995x + 0.003) (**Figure 6.6a)** indicates that the T_{rw} determined by these two methods are highly correlated with each other (r=0.9996, and significance P<0.005).

The agreement between these two methods determining T_{rw} was assessed by Bland-Altman method. The result shows that average of difference of T_{rw} determined by these two methods is –0.00213 m/s with the upper limit (+2SD) of 0.018m/s and lower limit (-2SD) of –0.014m/s. We consider that the agreement limit (-0.014~0.018 m/s) is small enough and provide confidence that the T_{rw} determined using these two methods highly agree with each other without bias (**Figure 6.6b**).

6.4.3 Timing of key points

Timing of peak of dI_{PU+} for compression wave, t_1, and for expansion wave, t_2, are very close to the corresponding timing of dI_{DU+}, t'_1 and t'_2, respectively. For example, at 40 cm away from inlet for 24 mm tube t_1 is

approximately *3.24 s* and t'_1, is *3.23 s*. Similarly, timing of the first peak of dI_{PU-}, t_3, is also close to the corresponding timing of dI_{DU-}, t'_3, **Figure 6.1 c, d.**

The correlation of t_1, t_2, t_3 and t'_1, t'_2, t'_3 is assessed using regression line and equation. Regression line, y = 1.001x –0.003, for the timing at three points determined by these two methods is nearly identical to the identity line, y=x. In addition, the correlation coefficients (r=0.9999 and significance P<0.005) further provide evidence that the timing of these key points determined by these two methods are highly correlated (**Figure 6.7a**).

Likewise, the assessment of timing at three points determined by these two methods highly agreed with each other according to Bland-Altman method. The average of difference between two methods is –0.0014±0.009 m/s with upper limit (+2SD) is 0.017m/s and lower limit (-2SD) is –0.02m/s (**Figure 6.7b**).

6.4.4 Comparison of P and *D*

The separated forward pressure determined by pressure and velocity is very similar to the separated forward diameter determined by diameter and velocity in shape (**Figure 6.1 a, b and Figure 6.5 a, b).** The amplitudes of forward pressure determined by the pressure and velocity are correlated well to the amplitude of forward diameter determined by diameter and velocity. In the 16 mm tube, for example, the amplitudes of forward pressure determined by pressure and velocity are correlated with the amplitudes of forward diameter determined by the diameter and velocity with r=0.86 (**Figure 6.8**).

6.4.5 Peak values at key points

The peak values of dI_{PU+} for compression wave, p_1, and for expansion wave, p_2, are correlated well with the corresponding values of dI_{DU+}, **Figure**

6.9. The value of first peak of dI_{PU-}, p_3 is also correlated with the corresponding value of dI_{DU-}, p'_3, **Figure 6.10**.

6.5 Discussion

WIA provides a novel perspective on wave propagation along the ventricular-arterial system. The separation consideration of instantaneous pressure and flow transients associated with forward and backward traveling wave-fronts allows for the assessment of the contribution of generation by the ejecting left ventricle and of reflected waves from peripheral arteries in quantity (Jones et al., 2000). In general, the measurement of pressure waveforms requires an invasive approach. Niki et al. investigated carotid artery WI non-invasively using the measured diameter waveform of carotid arteries although the diameter waveform was scaled using systolic and diastolic blood pressure measured with the cuff-type manometer applied to the upper arm (Niki et al. 2002). Use of maximum and minimum value of the pressure waveforms examined at other measuring sites is questionable since both morphology and values of the pressure waveform changes with the locations in the arterial system (Nichols and O'Rourke ,1998).

There are a few techniques such as the Penaz method and arterial tonometry can be used to measure the arterial pressure wave non-invasively. The Penaz method is used in non-invasive recordings of finger blood pressure with the Figapres or Portapres (Imholz et al. 1998). Arterial tonometry measures the force that is needed to flatten a superficial artery. Most accurate tonometry measurements are done at the radial artery as the vessel can be compressed against the bone. Zambanini et al. (2005) studied the wave energy in carotid,

brachial and radial arteries non-invasively using applanation tonometry to record the pressure waveform. They also separate the wave into forward and backward direction using WIA. To date, no investigation is not found to separate waveforms into forward and backward directions directly using measuring diameter changes and velocity with the exception of diameter-velocity analysis in pulmonary arteries by O'Brien (O'Brien, 2003).

O'Brien (2003) derived the equation from the conservative of mass and momentum to express the relation of changes in diameter and in velocity:

$$dU = \pm 2c \; d\ln D \tag{18}$$

The wave intensity in the form of diameter and velocity are separated into the forward and backward directions:

$$dI_{D\pm} = \pm\frac{c}{2}(d\ln D \pm \frac{1}{2c}dU)^2 \tag{19}$$

O'Brien's analysis method is similar to the method we proposed in section 2. The wave intensity based on the measurements in our experiment, which is analyzed using O'Brien's method were compared to those, which were analyzed using our method, **Figure 6.11**. The comparison of these two methods indicates that the shape of wave intensity determined using O'Brien's method is similar to those using our method. The timing of reflected wave determined using these two methods are very close. The unit determined using equation (19) is "m/s", which is different from unit of wave intensity derived using our method "m^2/s" and also the peak values of wave intensity determined using our method is different from those determined using O'Brien's method.

6.5.1 Significance of DU-loop determining wave speed

It is known that the properties and dimensions in the ascending aorta are dissimilar to those in the peripheral arteries [Nichols and O'Rourke, 2005]. Also, the wave speed is related to the properties of the arterial wall. Hence determination of wave speed using the measurements at one point is significant to hemodynamic study as it provides direct information about arterial distensibilities. PU-loop method allows for determination of wave speed using measurements of pressure and velocity only at one point, however, there is needed for the measurement of pressure invasively. Local wave speed is determined by the DU-loop rather than PU-loop allows for the wave speed established only using the measurements at one point non-invasively. The wave speed determined by DU-loop is slightly smaller than that by PU-loop, which might be caused by the viscoelastic property of tube wall. For example, in **Figure 6.12** shown the relationship between pressure and diameter of 16 mm tube, in which the hysteresis loop is made. It is noticeable that hysteresis loop in 16 mm tube is smaller than that in 24 mm tube, **Figure 6.13**. Therefore, the difference of wave speed determined by the PU-loop and DU-loop in 24 mm tube is bigger than that in 16 mm tube probably related to the bigger hysteresis area at the 24 mm than at the 16 mm tube.

6.5.2 Importance of WI determined by diameter and velocity

With aged arteries or hypertension, wave speed is increased, resulting in the earlier arrival of reflected waves from periphery to the heart (Nichols, 2005). Increase of wave speed and early return of reflected wave can result in the increase of aortic systolic pressure, which can increase left ventricle after-load (O'Rourke et al. 2004). Also, early return of reflected wave to the heart can

affect the augmentation index (Murgo, et al. 1980), which is an independent predictor of cardiovascular disease including mortality (Nichols and Edwards, 2001).

The arrival time of reflected wave can be obtained using four methods: (1) using input impedance to calculate the distance to the apparent reflection site (Westerhof, 1972); (2) measurement of time from the initial pressure upstroke to inflection point of pressure waveform, through which the time that wave running downstream and being reflected back can be obtained (Murgo, 1980); (3) reflection time can be obtained using WIA through detecting the onset on separated backward pressure or wave intensity waveform (Parker et al., 1990); (4) detecting of end of the initial linear part of the PU-loop during systole, which is mark of arrival time of reflected waves (Khir et al, 2007). The methods for detecting reflection time mentioned above required the measurement of pressure waveform, which is usually taken invasive. The technique developed in this chapter to determine the arrival time of reflected waves only required the measurement of diameter and velocity non-invasively. High agreement between the arrival times of reflected wave, T_{rw}, determined by dI_{PU} and by dI_{DU} provides evidence of validation of this technique on measuring T_{rw}.

The agreement of T_{rw} in the pulmonary arteries of dogs determined by diameter and velocity and by pressure and velocity (O'Brien, 2003) is not as high as it is found in this chapter. This is speculated to be due to the strong viscoelasticity and non-linearity of pulmonary wall.

Blood vessels are usually composed of materials, including elastin, collagen and smooth muscles. Normally, the property of is viscoelasticity and

the relationship between stress and strain of blood vessel is non-linear (Caro, 1978; Milno, 1989; Bia, et al., 2003; Shau, et al., 1999). Therefore, it is suggested that the viscoelasticity and non-linearity of arterial wall should be considered when the method proposed in this chapter is applied to arteries system.

There is strong opinion for an exponential relationship between arterial cross-section and pressure (Meinders, et al. 2004) although the relationship between pressure and diameter in carotid arteries are thought to be linear (Sugawara, et al. 2000; van Bortel, et al. 2001). Similar to WIA, the method proposed in this chapter not having any assumption on elastic and linearity of vessel wall can accommodate both viscoelastics and non-linearity effects.

The value of wave intensity analysis also lies in that it can be used for assessment of dynamic ventricular-arterial interaction (Ramsey and Sugawara, 1997). Knowledge of amplitude and timing of forward compression and expansion wave intensity as well as backward wave intensity benefits understanding of contribution of wave energy ejected by ventricle and reflected by peripheral arteries (Jones, et al. 1994; 1992). The accurate prediction of timing of compression and expansion wave and backward wave non-invasively by measurement diameter and velocity is of clinical significance for understanding of cardiac-arteries interaction. The timings at the key points determined by $dI_{PU\pm}$ and $dI_{PU\pm}$ are correlated well with each other indicates the method proposed in this chapter also can be used to assess the timing of compression and expansion waves. The fact of peak values at these points determined by the two methods are correlated well further provides evidence for the validation of this method on the study for the wave propagation in flexible

tubes. The high correlation of timing and peak value between these two methods in this study suggested that it is worth to do further investigation in order to prove the application of this method in vivo.

Table6 1. Wave speed determined by PU-loop and DU-loop

Diameter of tube	Measuring sites (cm)	ws_pu (m/s)	ws_du (m/s)	mean (m/s)	Diff (%)
16 mm	0.15	3.30	3.00	3.15	9.22
	0.30	3.26	2.99	3.12	8.21
	0.45	3.73	3.43	3.58	8.01
	0.60	3.85	3.39	3.62	12.05
	0.75	4.26	3.76	4.01	11.88
	0.95	4.34	3.98	4.16	8.39
	1.05	3.94	3.75	3.85	4.87
	1.20	3.59	3.56	3.57	0.99
	1.35	3.25	3.65	3.45	-12.33
	1.50	3.34	3.45	3.40	-3.33
	1.65	3.65	3.65	3.65	0.09
	mean*	3.68	3.51	3.60	4.75
	STD	0.39	0.31	0.32	
24 mm	0.10	3.25	2.78	3.02	14.28
	0.25	2.91	2.65	2.78	9.12
	0.40	4.00	3.87	3.94	3.27
	0.55	3.38	2.81	3.10	16.86
	mean*	3.39	3.03	3.21	10.88
	STD	0.46	0.57	0.50	

Note:
Measuring site is the distance the measurement was taken from the inlet.
Ws_pu (m/s) is the wave speed determined by PU-loop
Ws_du (m/s) is the wave speed determined by DU-loop
Mean* is the average wave speed along the length of tube
STD is the Standard Deviation.
Mean (m/s) is the average value of wave speed determined by PU-loop and DU-loop for each measurement.
Diff (%) is the percentage of difference of wave speed determined by PU-loop and DU-loop

Table 6. 2, Arrival time of reflected waves determined by P_- and D_-

Diameter of tube	Measuring sites (m)	$T_{rw}\_D_-$ (s)	$T_{rw}\_P_-$ (s)	Mean (s)	Diff (s)	*Diff(%)*
16 mm	0.15	1.00	0.98	0.99	0.01	1.20
	0.30	0.88	0.89	0.89	-0.01	-0.80
	0.45	0.81	0.79	0.80	0.02	1.60
	0.60	0.72	0.72	0.72	0.00	-0.20
	0.75	0.57	0.58	0.57	-0.01	-1.00
	0.95	0.47	0.47	0.47	0.00	0.40
	1.05	0.41	0.40	0.40	0.01	0.90
	1.20	0.32	0.32	0.32	0.00	-0.25
	1.35	0.22	0.21	0.22	0.01	0.70
	1.50	0.13	0.13	0.13	-0.01	-0.50
	1.65	0.11	0.12	0.11	-0.01	-0.50
24 mm	0.15	0.40	0.39	0.39	0.01	0.70
	0.30	0.34	0.33	0.33	0.01	0.90
	0.45	0.21	0.21	0.21	0.01	0.70
	0.60	0.11	0.11	0.11	0.00	-0.20

Note: T_{rw}-D_- is arrival time of reflected waves determined by D_-.
T_{rw}-P_- is arrival time of reflected waves determined by P_-.
Mean is the average of arrival time of reflected waves determined by P_- and D_-.
Diff is the difference of T_{rw}-D_- and T_{rw}-P_-.
Diff (%) is the percentage of difference between the arrival time of reflected waves determined by P_- and by D_-. $Diff(\%) = \frac{T_{rw}\_D_- - T_{rw}\_P_-}{T_{rw}\_D_-} * 100\%$

Table 6. 3, Arrival time of reflected waves determined by $T_{rw}\_dI_{DU-}$ and $T_{rw}\_dI_{PU-}$

Diameter of tube	Measuring sites (m)	$T_{rw}\_dI_{DU-}$ (s)	$T_{rw}\_dI_{PU-}$ (s)	Mean (s)	Diff (s)	*Diff(%)*
16 mm	0.15	1.00	0.99	0.99	0.01	1.20
	0.30	0.87	0.87	0.87	0.00	-0.40
	0.45	0.80	0.80	0.80	0.00	0.20
	0.60	0.71	0.71	0.71	0.00	0.00
	0.75	0.57	0.57	0.57	-0.01	-0.70
	0.95	0.47	0.47	0.47	0.01	0.50
	1.05	0.40	0.40	0.40	0.00	0.30
	1.20	0.32	0.32	0.32	0.00	0.35
	1.35	0.22	0.22	0.22	0.00	0.00
	1.50	0.12	0.13	0.12	-0.01	-0.70
	1.65	0.09	0.11	0.10	-0.02	-1.50
24mm	0.15	0.40	0.39	0.40	0.01	1.20
	0.30	0.33	0.32	0.33	0.00	0.30
	0.45	0.23	0.21	0.22	0.02	1.60
	0.60	0.11	0.10	0.10	0.00	0.40

Note:

$T_{rw}\_dI_{DU-}$ is arrival time of reflected waves determined by the onset of dI_{DU-}
$T_{rw}\_dI_{PU-}$ is arrival time of reflected waves determined by the onset of dI_{PU-}
Mean is the average of arrival time of reflected waves determined by dI_{DU-} and dI_{PU-}.
Diff is the difference of arrival time of reflected waves determined by dI_{DU-} and dI_{PU-}.
Diff (%) is the percentage of difference between the arrival time of reflected waves determined by $T_{rw}\_dI_{DU-}$ and by $T_{rw}\_dI_{PU-}$. $Diff\,(\%) = \frac{T_{rw\_dI_{DU-}} - T_{rw\_dI_{PU-}}}{T_{rw\_dI_{DU-}}} * 100\%$

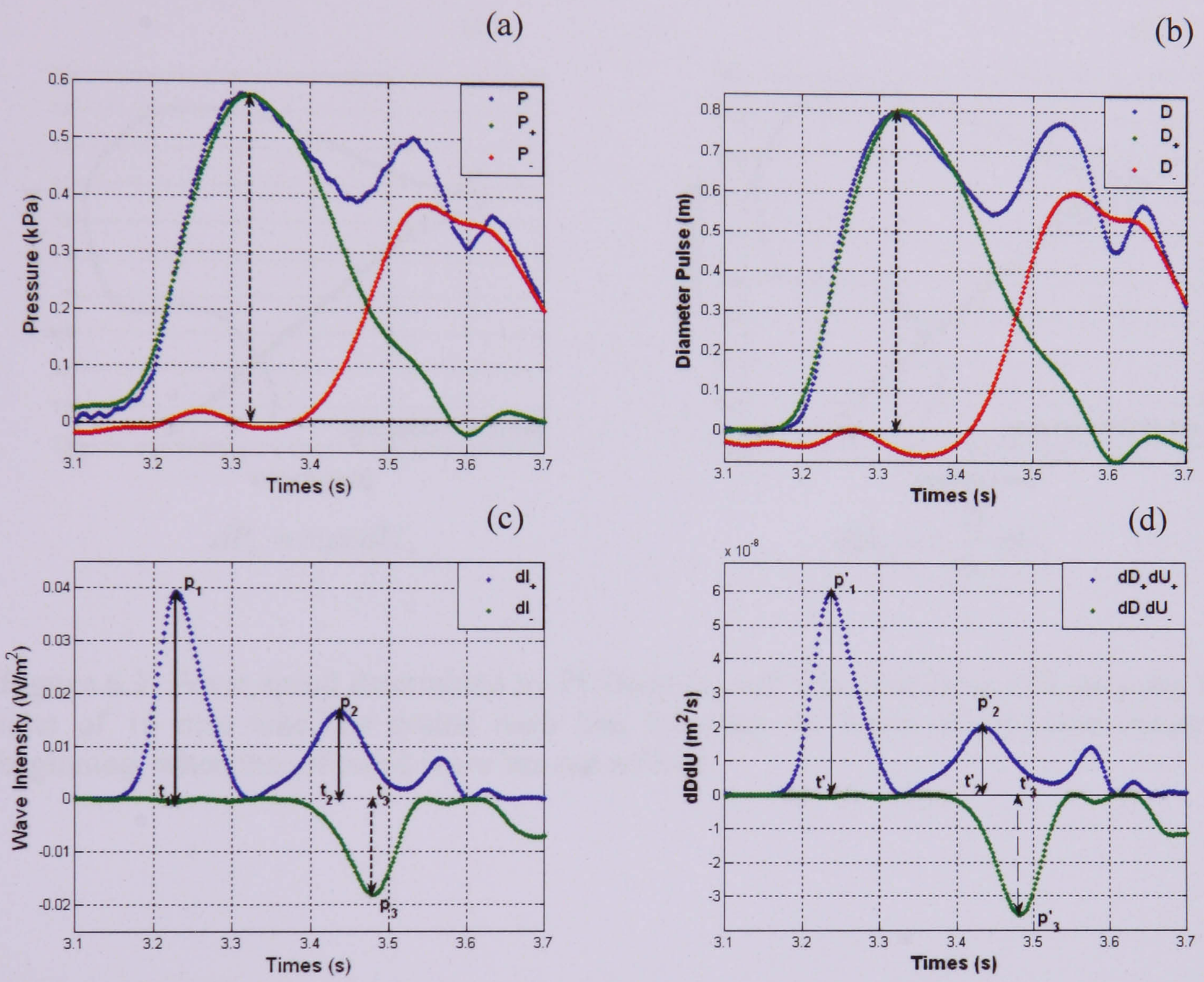

Figure 6.1 (a) The measured, forward and backward pressure at 40 cm away from inlet of 24 mm tube, where vertical double arrow indicates the peak of forward pressure. (b) The measured, forward and backward diameter at same measuring site and vertical double arrow indicates the peak of forward diameter. (c) $dI_{PU\pm}$ at the same measuring site, where the p_1, p_2 indicate that the peak values of dI_{PU+} for compression and expansion wave and p_3 indicates the peak value of dI_{PU-} for the first peak. t_1, t_2, t_3 indicate the corresponding timing at p_1, p_2, p_3. (d) $dI_{DU\pm}$ at the same measuring site, where p'_1, p'_2, p'_3 indicates the peak values of dI_{DU+} for compression and expansion wave and the first peak value of dI_{DU-}. t'_1, t'_2, t'_3 indicate the corresponding timing at p'_1, p'_2, p'_3.

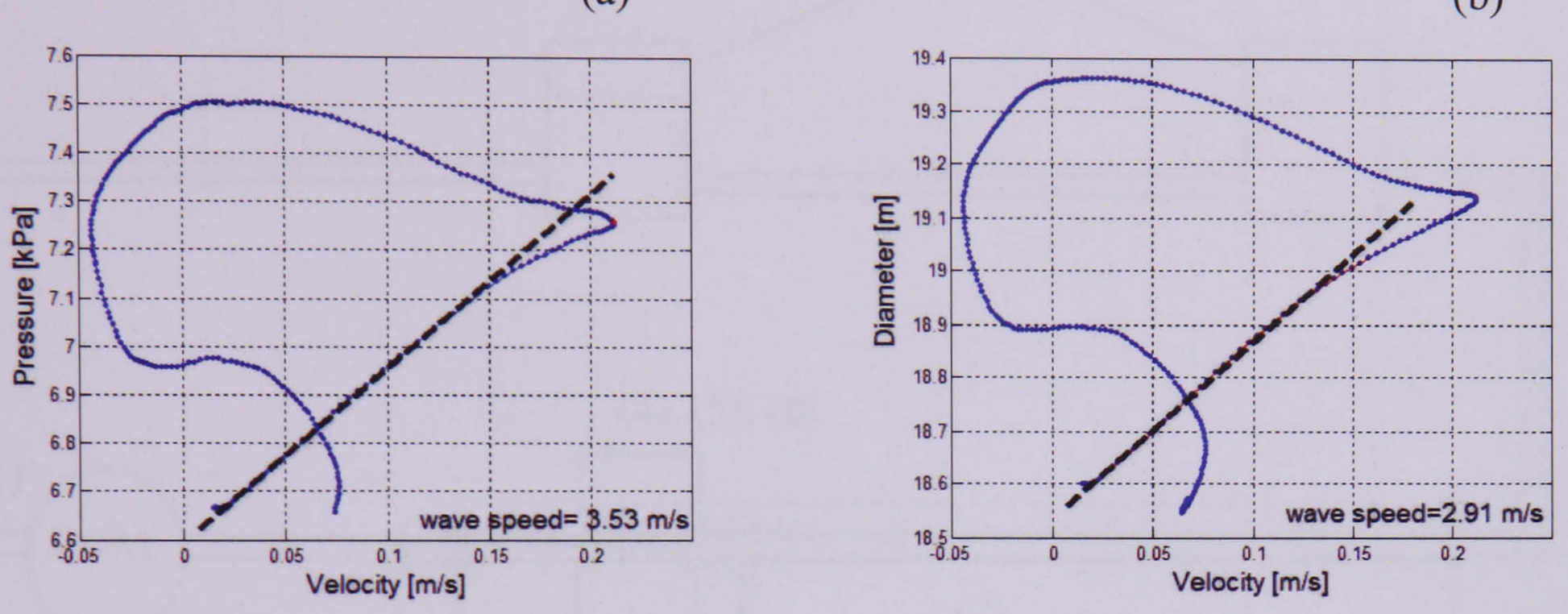

$$dP_{\pm} = \pm \rho c dU_{\pm}$$

$$dD_{\pm} = \pm \frac{D}{2c} dU_{\pm}$$

Figure 6.2 Wave speed determined by PU-loop (a) and DU-loop (b) at 150 cm away from inlet of 16 mm tube.The dotted dash line indicates the slope of DU-loop during the beginning, when the reflected wave has not arrived.

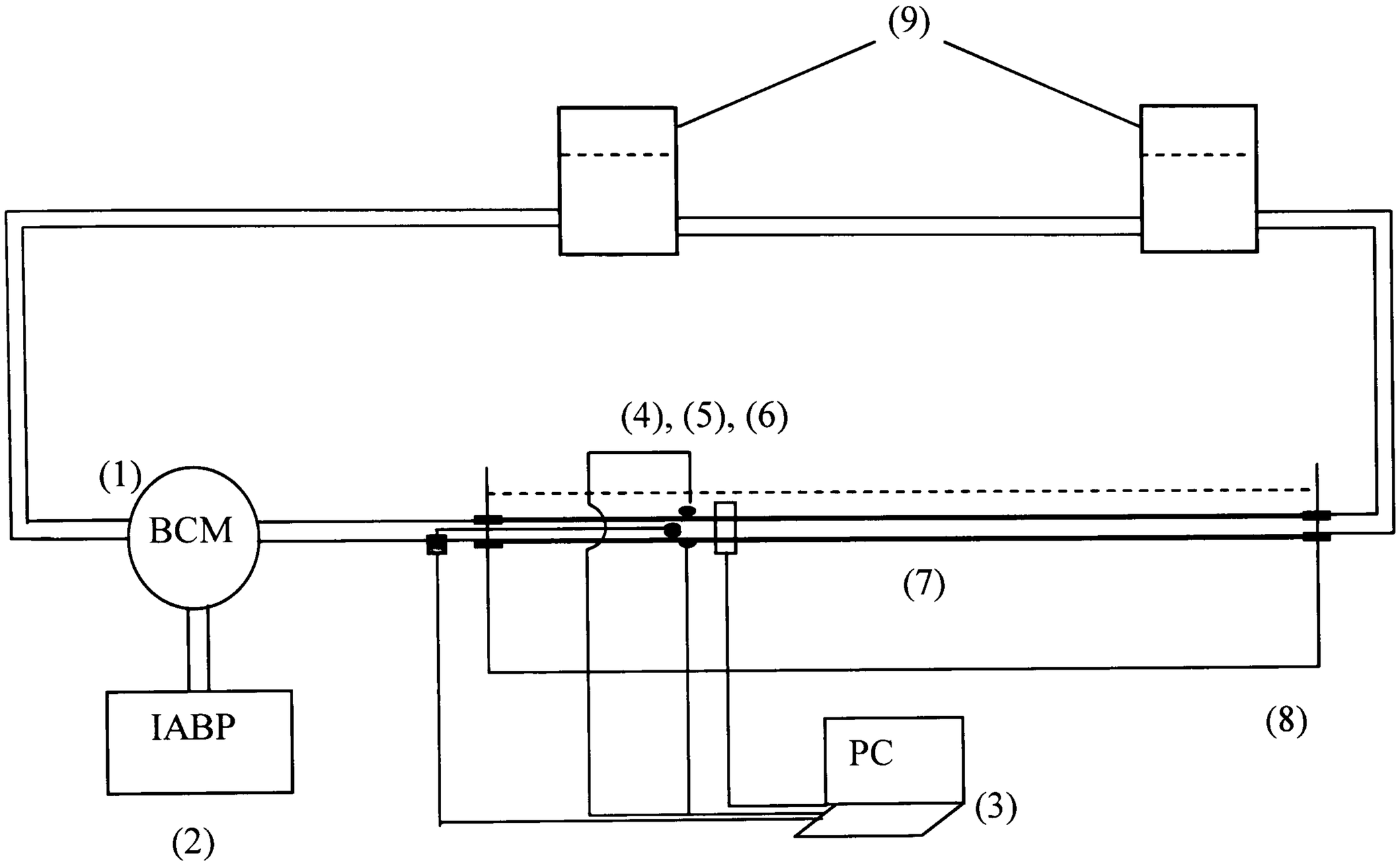

Figure 6.3 Experiment setup : (1) Artificial pump (BCM) , (2) IABP (Intra-arotic balloon pump), (3) Personal computer, (4) Catheter tipped pressure transducer, (5) Paired crystals, (6) Ultrasonic flow probe, (7) Latex tubes, (8) Tank with water to support tube ,(9) Reservoirs

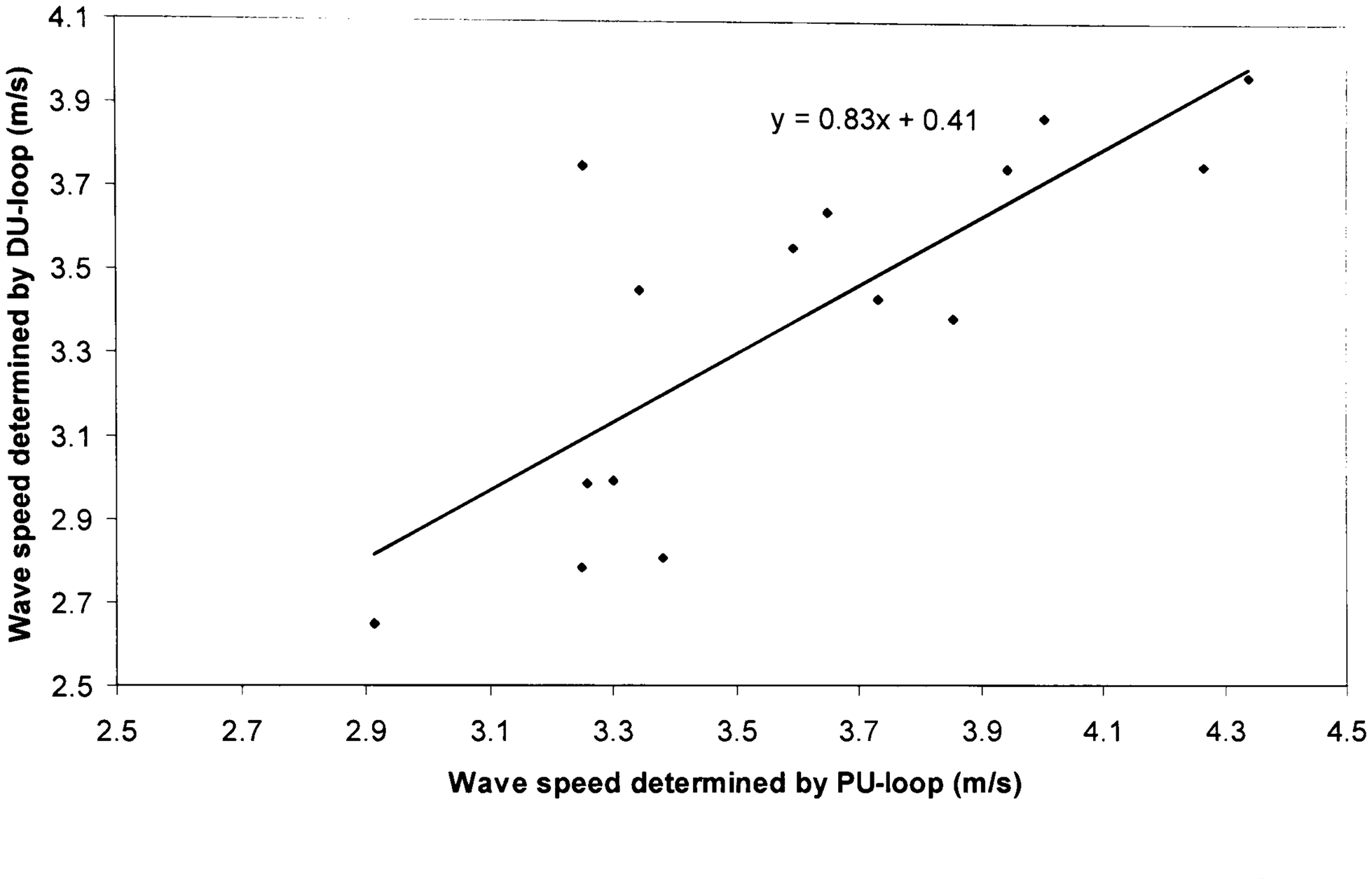

Figure 6.4 (a) Correlation of wave speed determined by PU-loop and DU-loop. The correlation coefficient r=0.79.

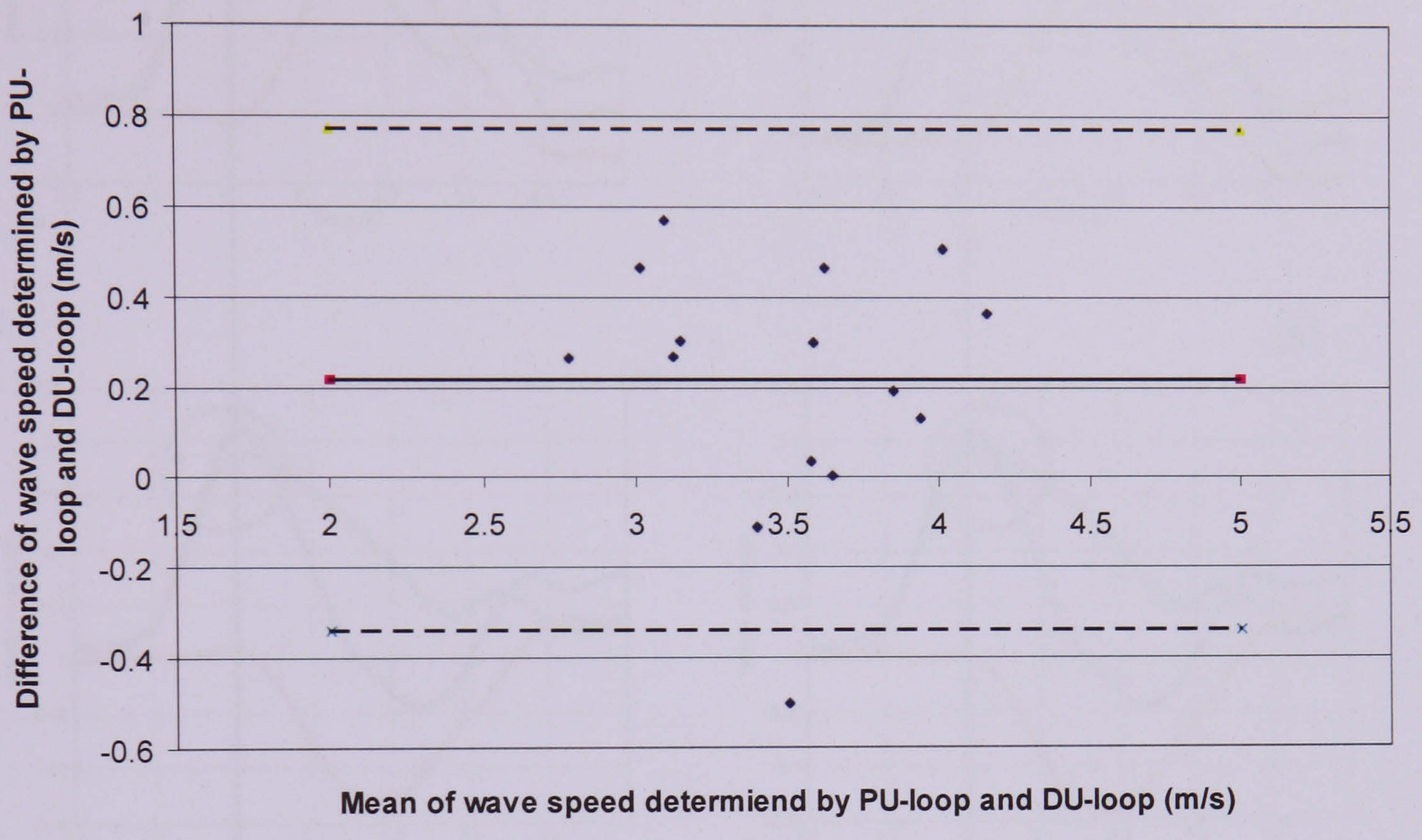

Figure 6.4 (b) The agreement between the wave speed determined by PU-loop and DU-loop are assessed by Bland-Altsman method. Solid horizontal line indicates the mean of difference of wave speed determined by the two methods; Upper horizontal dash line indicates the upper limit with mean+2SD and lower horizontal dash line indicates the lower limit with the mean-2SD.

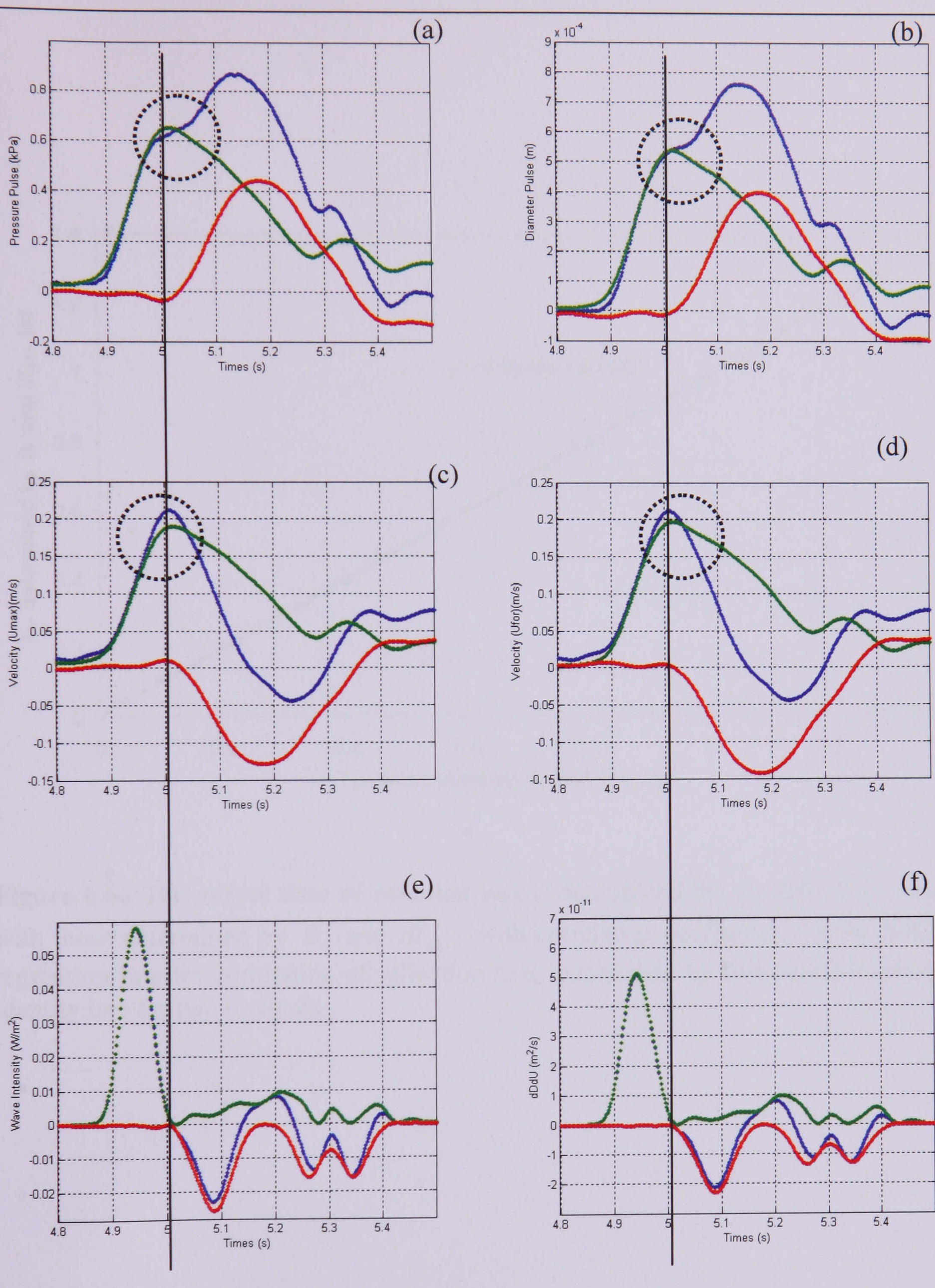

Figure 6.5 Left Panel: Measured, separated forward and backward pressure (a), velocity (c) and wave intensity dI_{PU} and $dI_{PU\pm}$ (e); Right Panel: (b) Measured, separated forward and backward diameter (b), velocity (d) and dI_{DU} and $dI_{DU\pm}$ (f). Data is measured in 16 mm tube at 150 cm away from inlet.

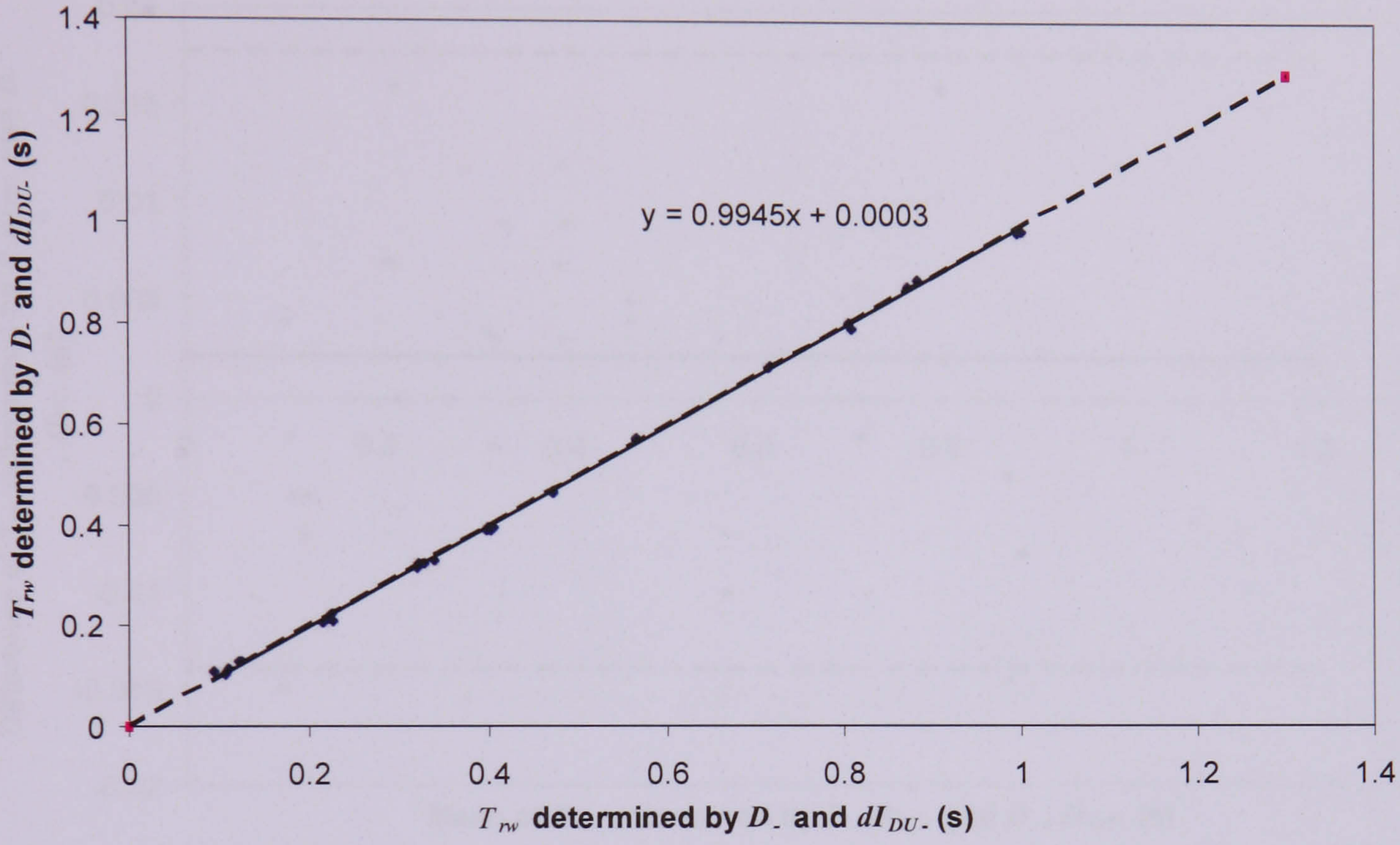

Figure 6.6a The arrival time of reflected waves determined by P_- and dI_{PU-} are agreed with those determined by D_- and dI_{DU-} with correlation coefficient r=0.99. Solid line is regression line for correlation of reflection time established by two methods. Dash line is identity line for two methods.

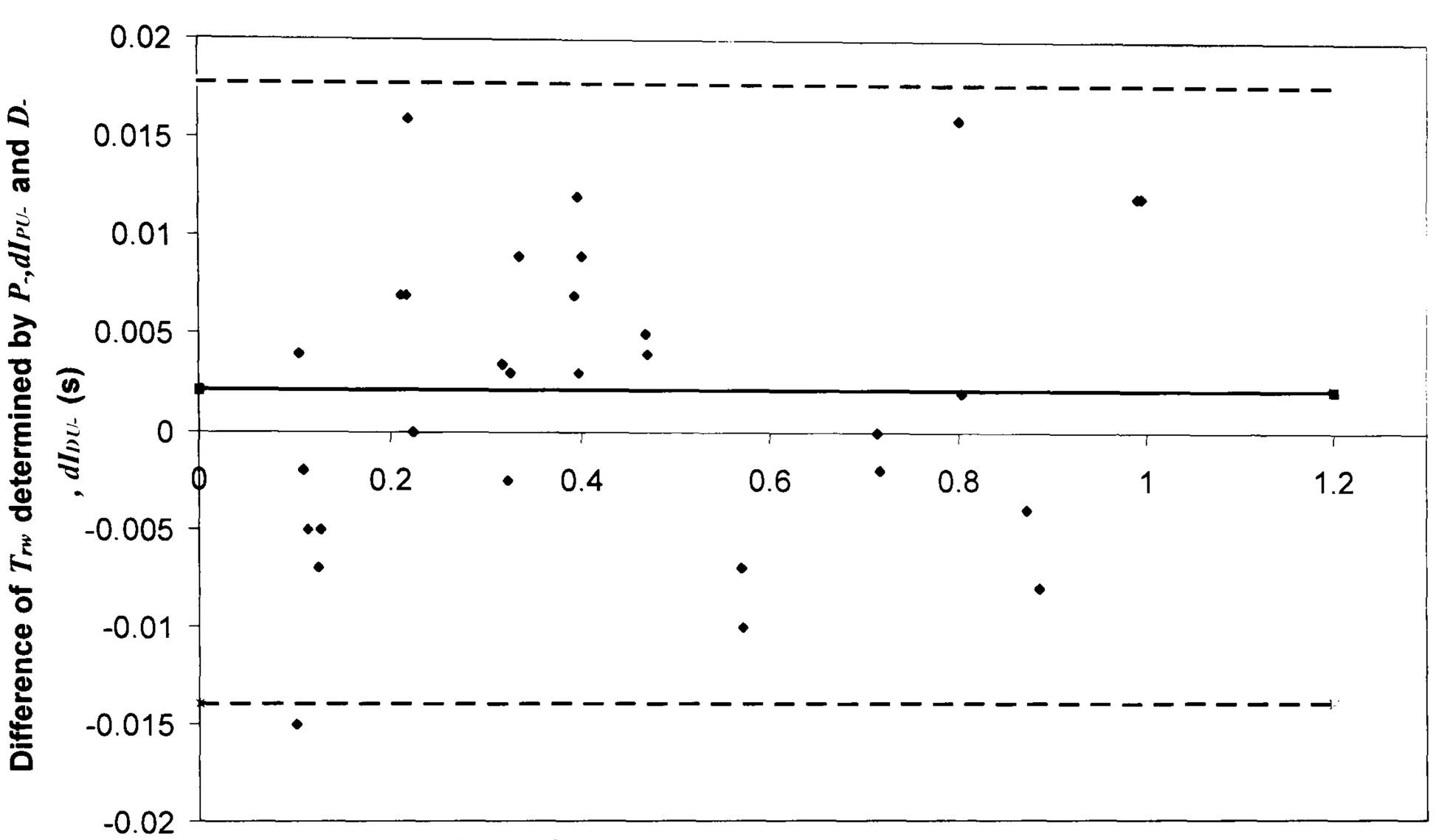

Figure 6.6b, The arrival time of reflected waves determined by P_- and dI_{PU-} are agreed with those determined by D_- and dI_{DU-} without bias. Solid horizontal line indicates the mean of difference of the arrival time of reflected waves, T_{rw}, determined by the two methods; Upper horizontal dash line indicates the upper limit with mean+2SD at 0.018 (s) and lower horizontal dash line indicates the lower limit with the mean-2SD at –0.014(s).

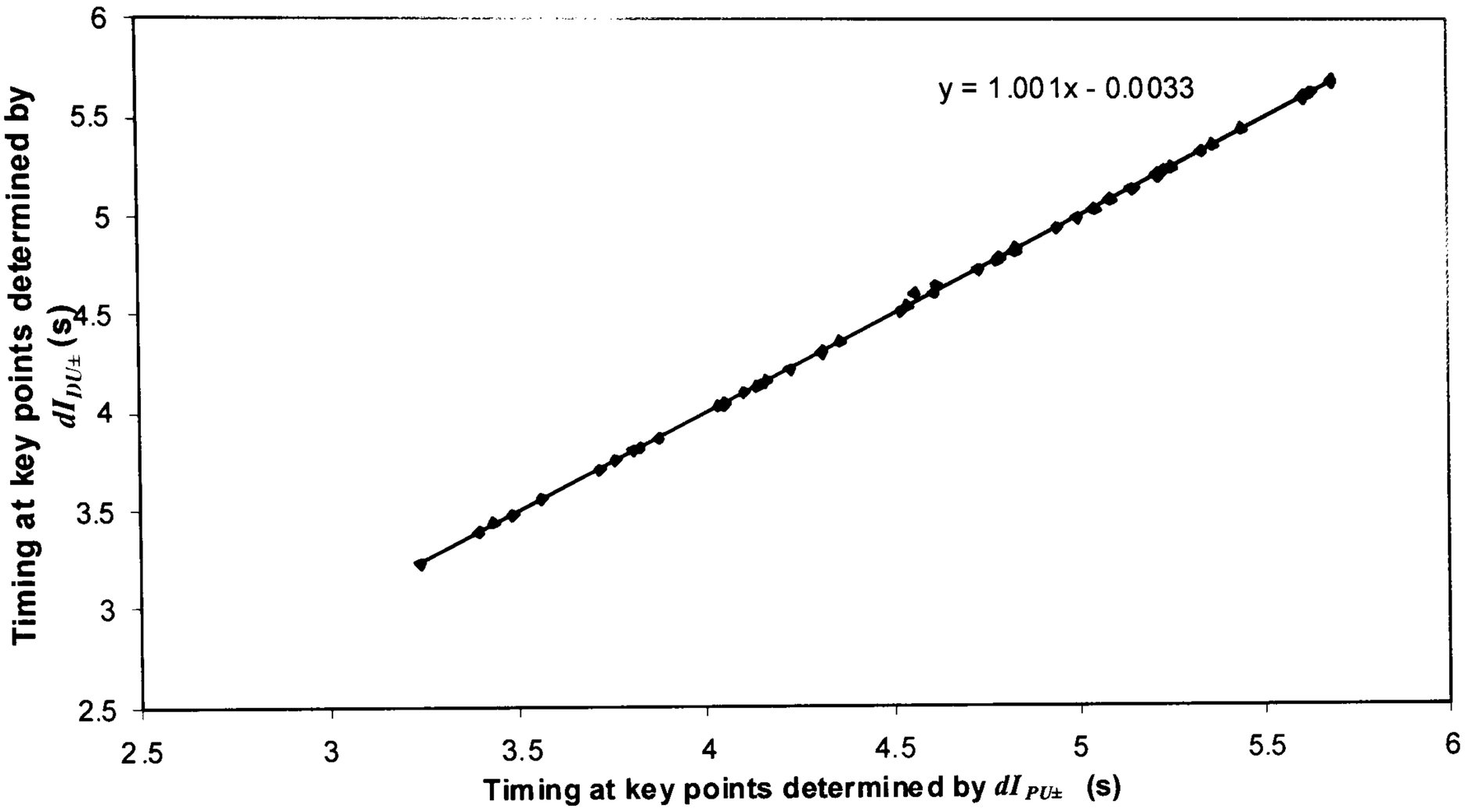

Figure 6.7a. The time of peak of dI_{PU+} for compression and expansion waves, t_1, t_2 and the first peak of dI_{PU-}, t_3 against the time of peak of dI_{DU+} for compression and expansion waves, t'_1, t'_2 and of the first peak of dI_{DU-}, t'_3. Correlation coefficient r=0.99.

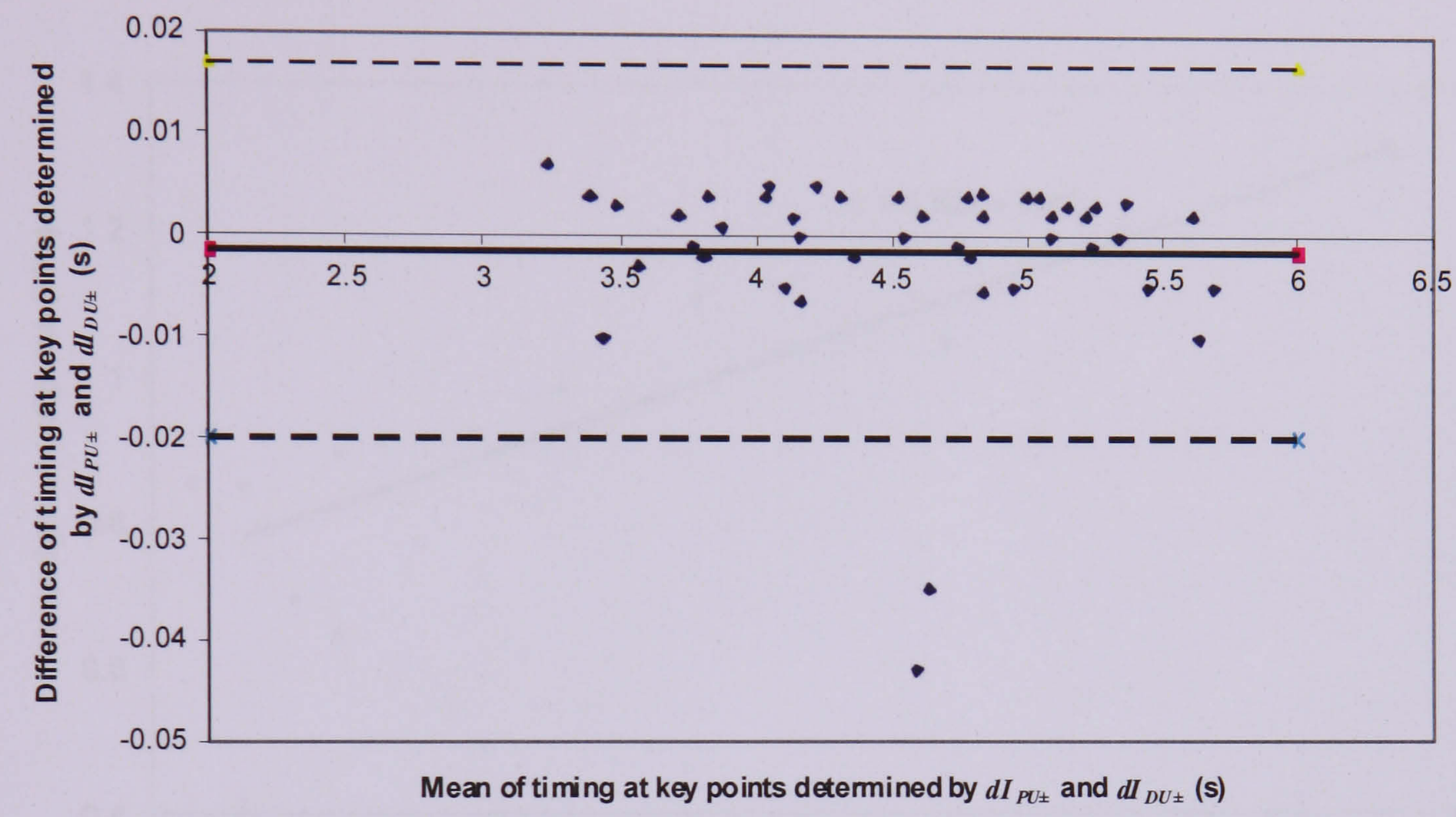

Figure 6.7b, The relationship of the time of peak of dI_{PU+} for compression and expansion waves, t_1, t_2 and the first peak of dI_{PU-}, t_3 and the time of peak of dI_{DU+} for compression and expansion waves, t'_1, t'_2 and of the first peak of dI_{DU-}, t'_3 is assessed using Bland-Altsman method. Solid horizontal line indicates the mean of difference of the time at key points determined by the two methods; Upper horizontal dash line indicates the upper limit with mean+2SD at 0.017 (s) and lower horizontal dash line indicates the lower limit with the mean-2SD at –0.02(s).

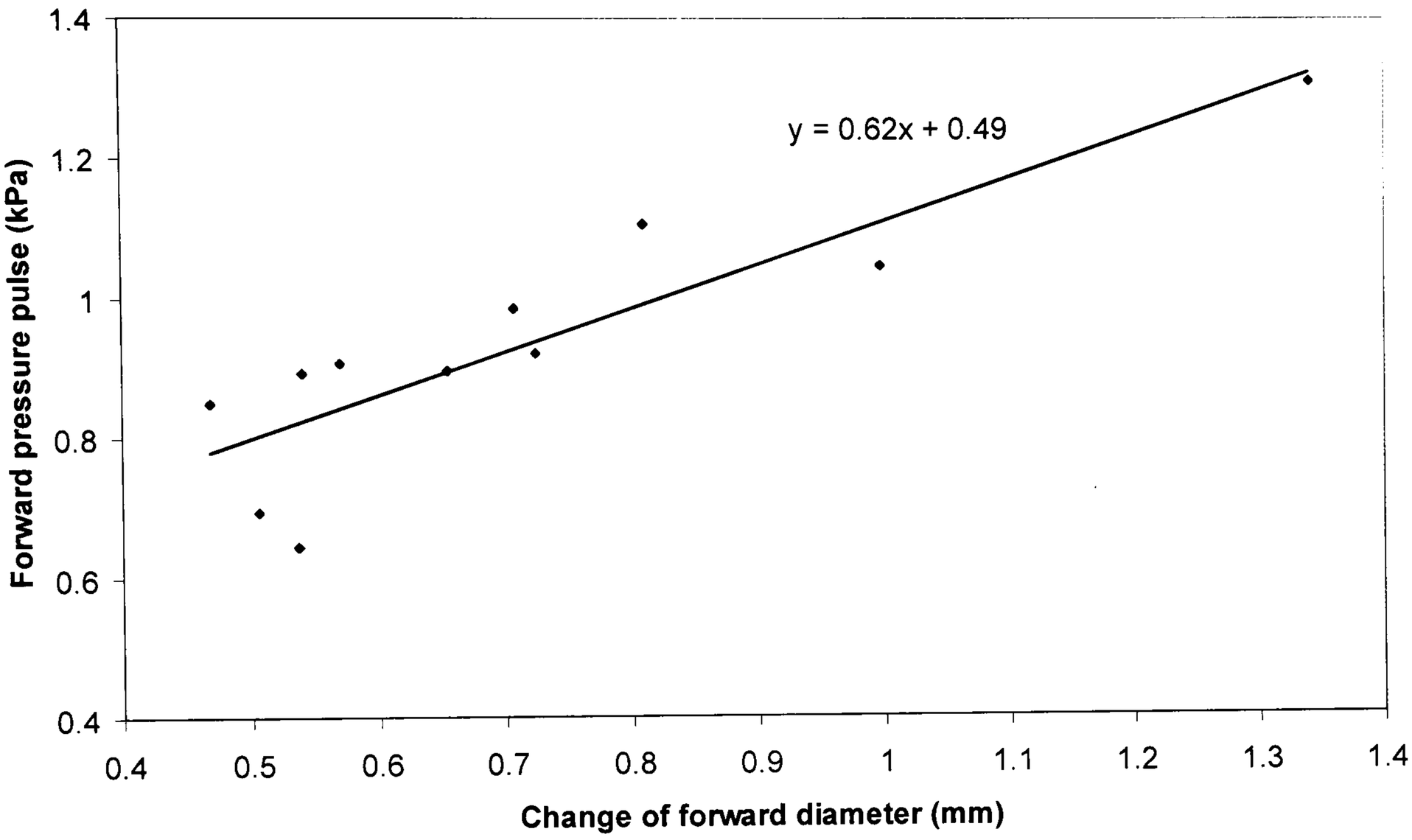

Figure 6.8 Relationship between the amplitude of forward pressure and forward diameter in the16 mm in diameter tube. r=0.86.

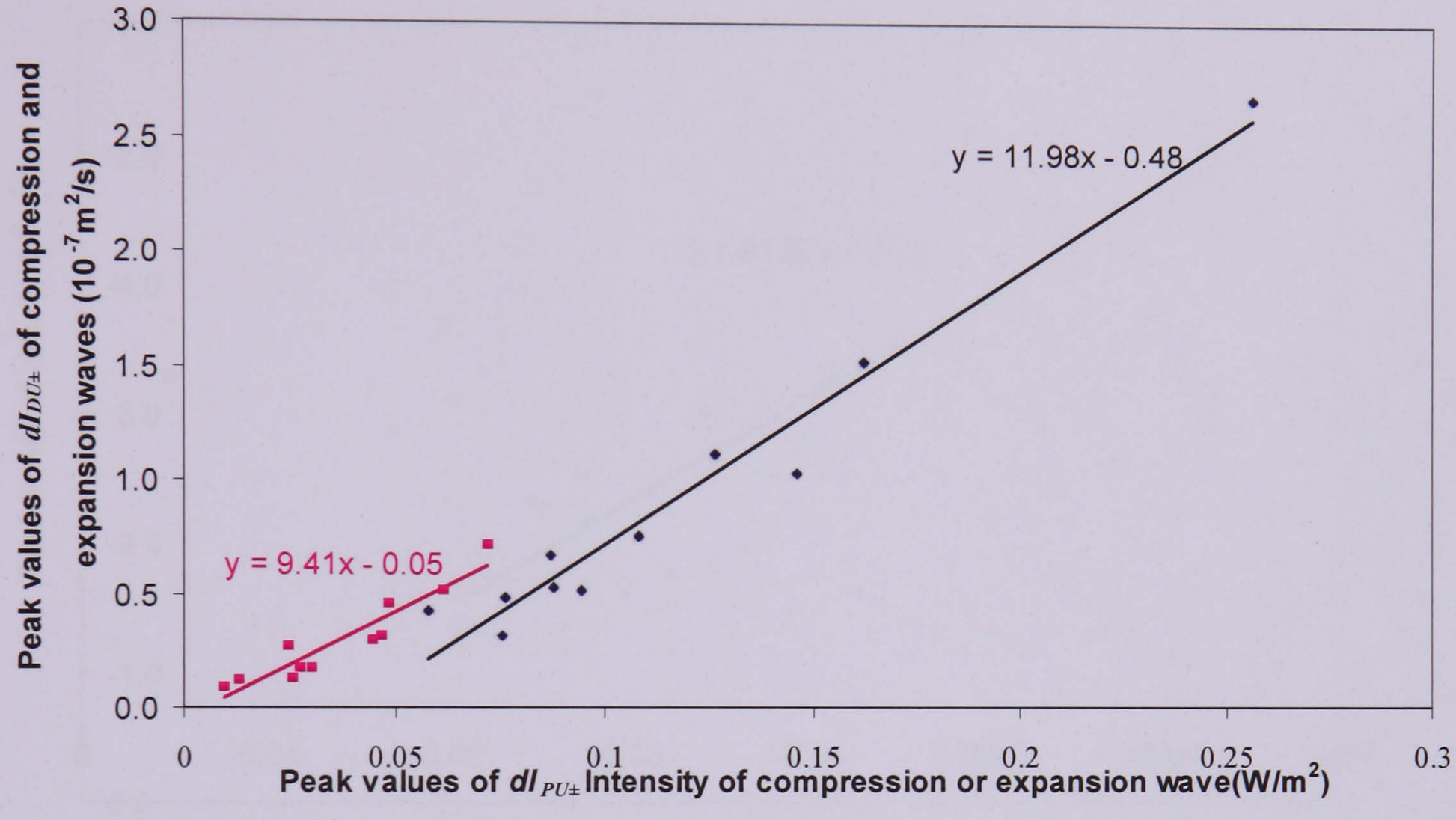

Figure 6.9 Relationship between the values at the peak of dI_{PU+} for compression and expansion waves and the values at the peak of dI_{DU+} for compression and expansion waves. Blue squares indicate the values for the compression waves and correlation coefficient for the relationship between compression waves r=0.98; and pink squares indicates the values for the expansion waves and correlation coefficient for the relationship between expansion waves r=0.94.

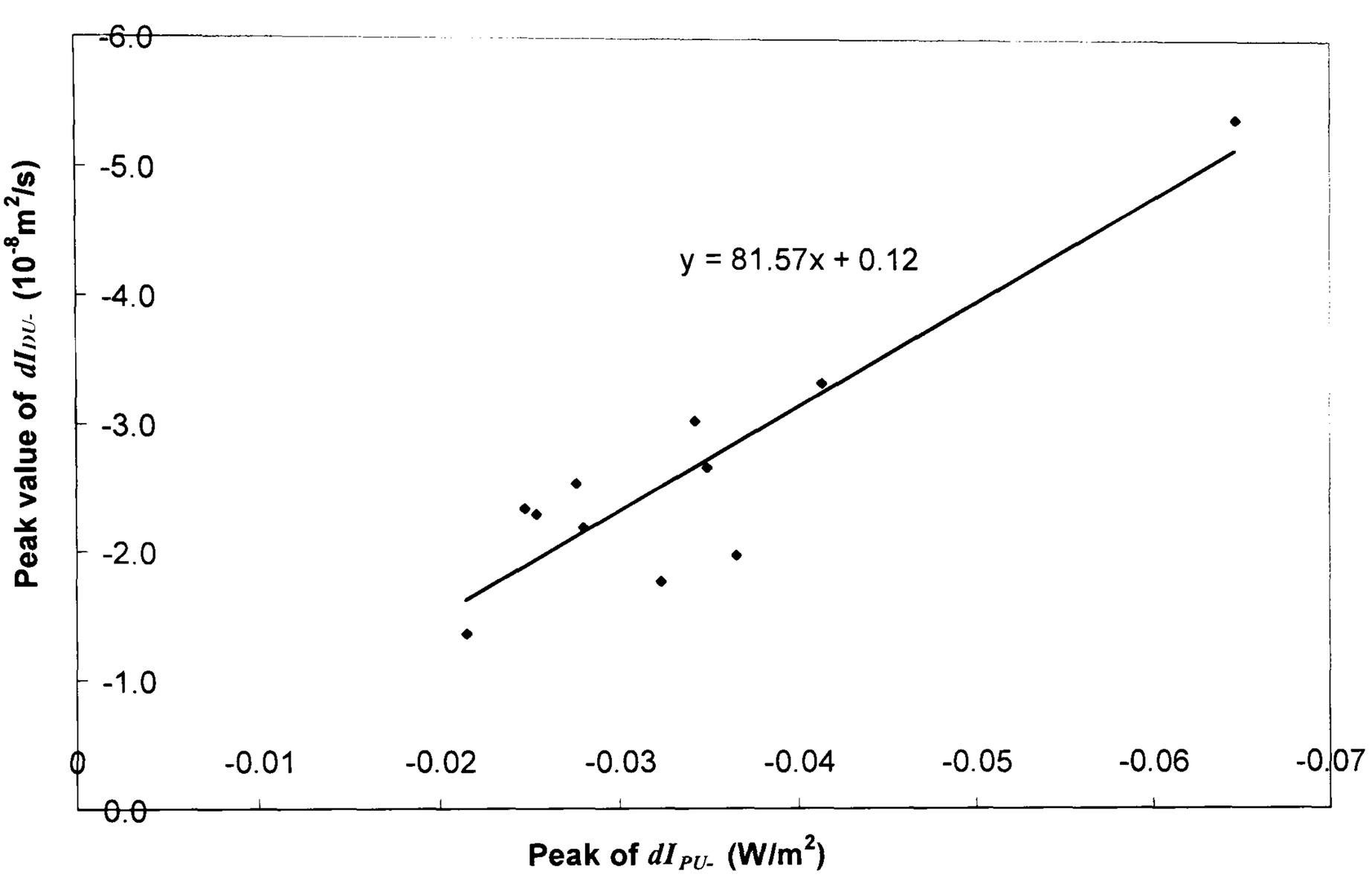

Figure 6. 10 The relationship of the first peak of dI_{PU-} **and** dI_{DU-}.

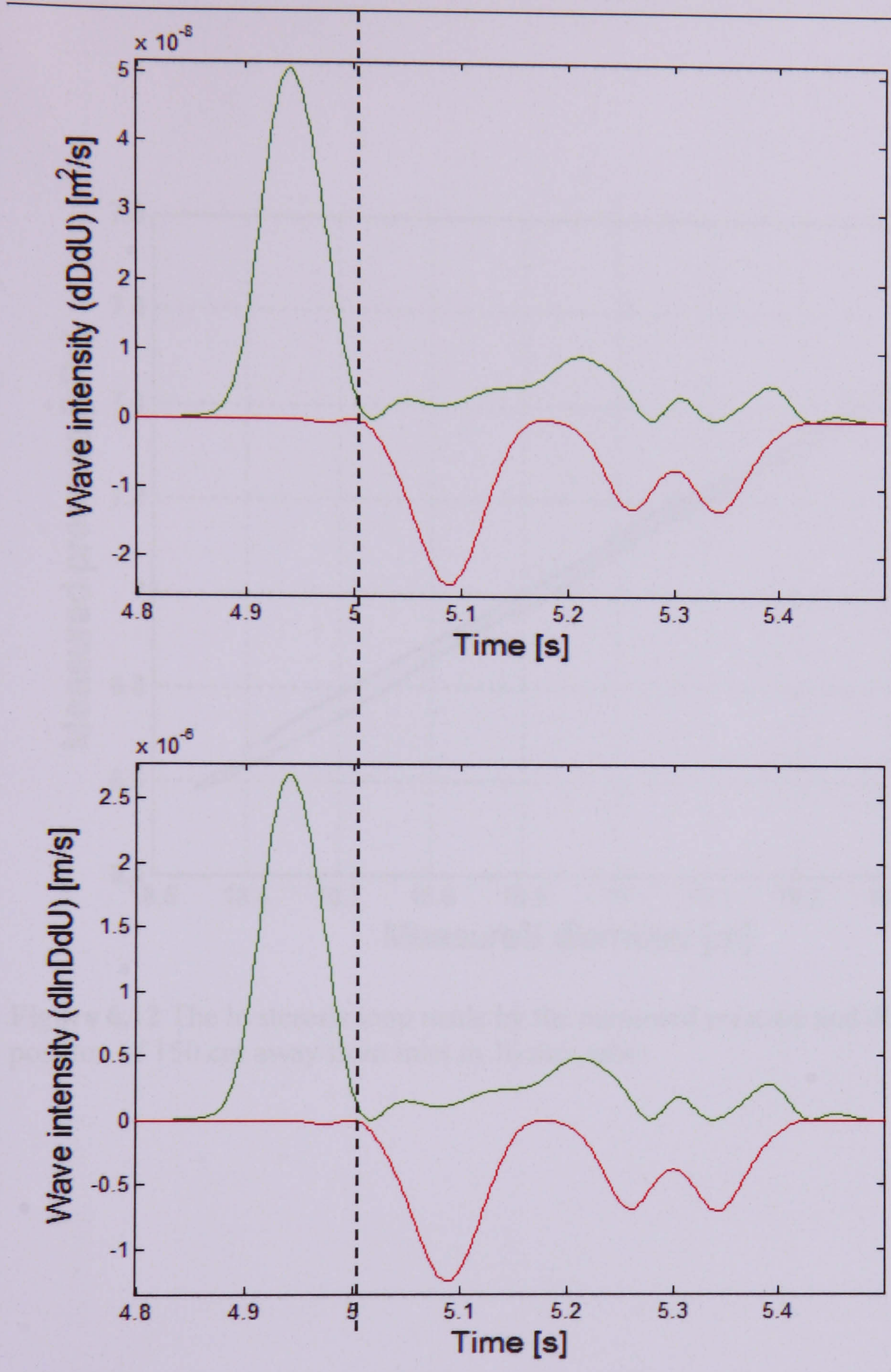

Figure 6.11, Separated wave intensity determined by diameter and velocity at the 150 cm away from inlet in 16 mm tube. (a) Wave intensity calculated using O'Brien's method; (b) Wave Intensity calculated using the method proposed in this paper. Green curve is forward intensity and red curve is backward wave intensity. Vertical dash line indicates the arrival time of reflected wave.

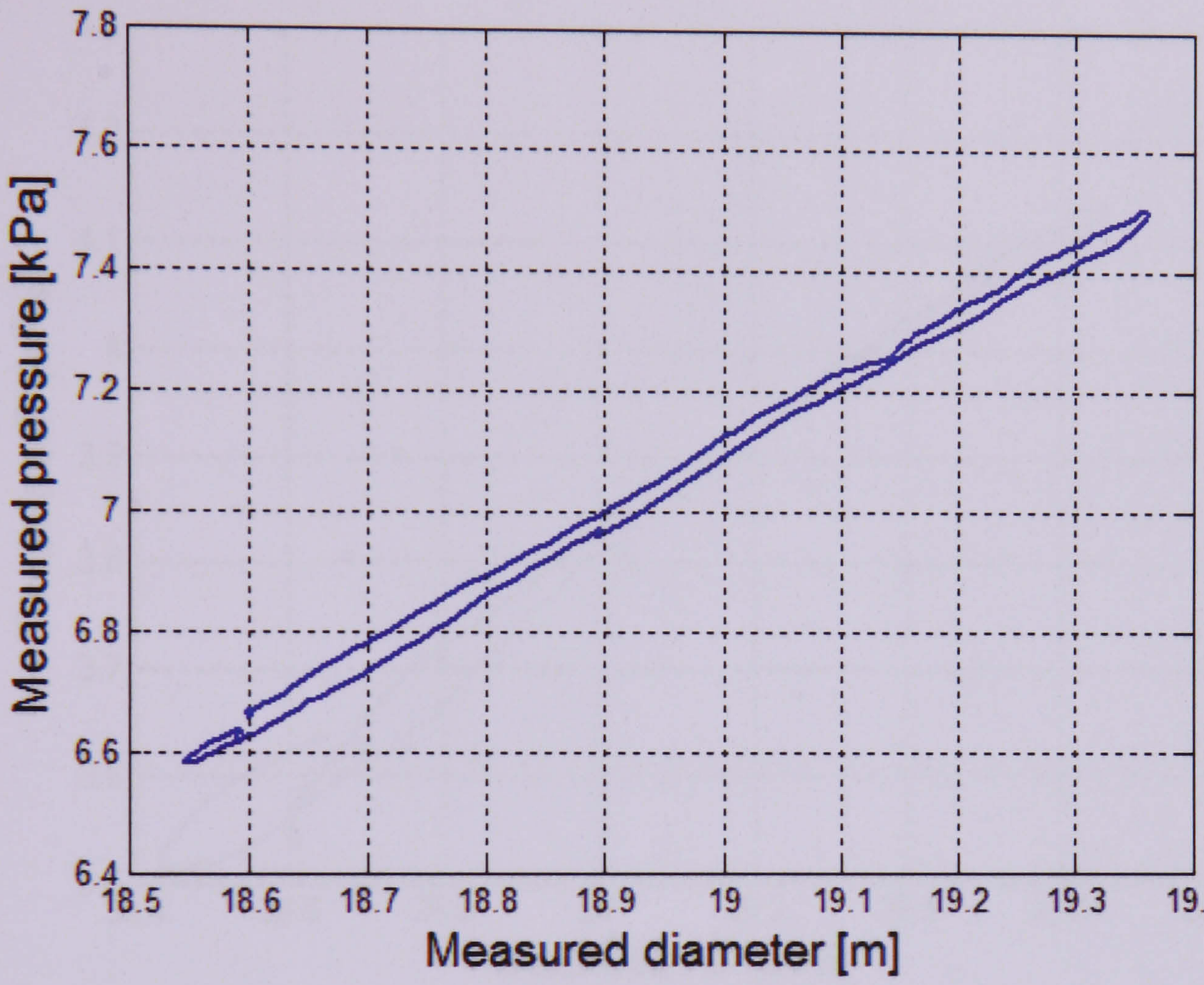

Figure 6.12 The hysteresis loop made by the measured pressure and diameter at the position of 150 cm away from inlet in 16 mm tube.

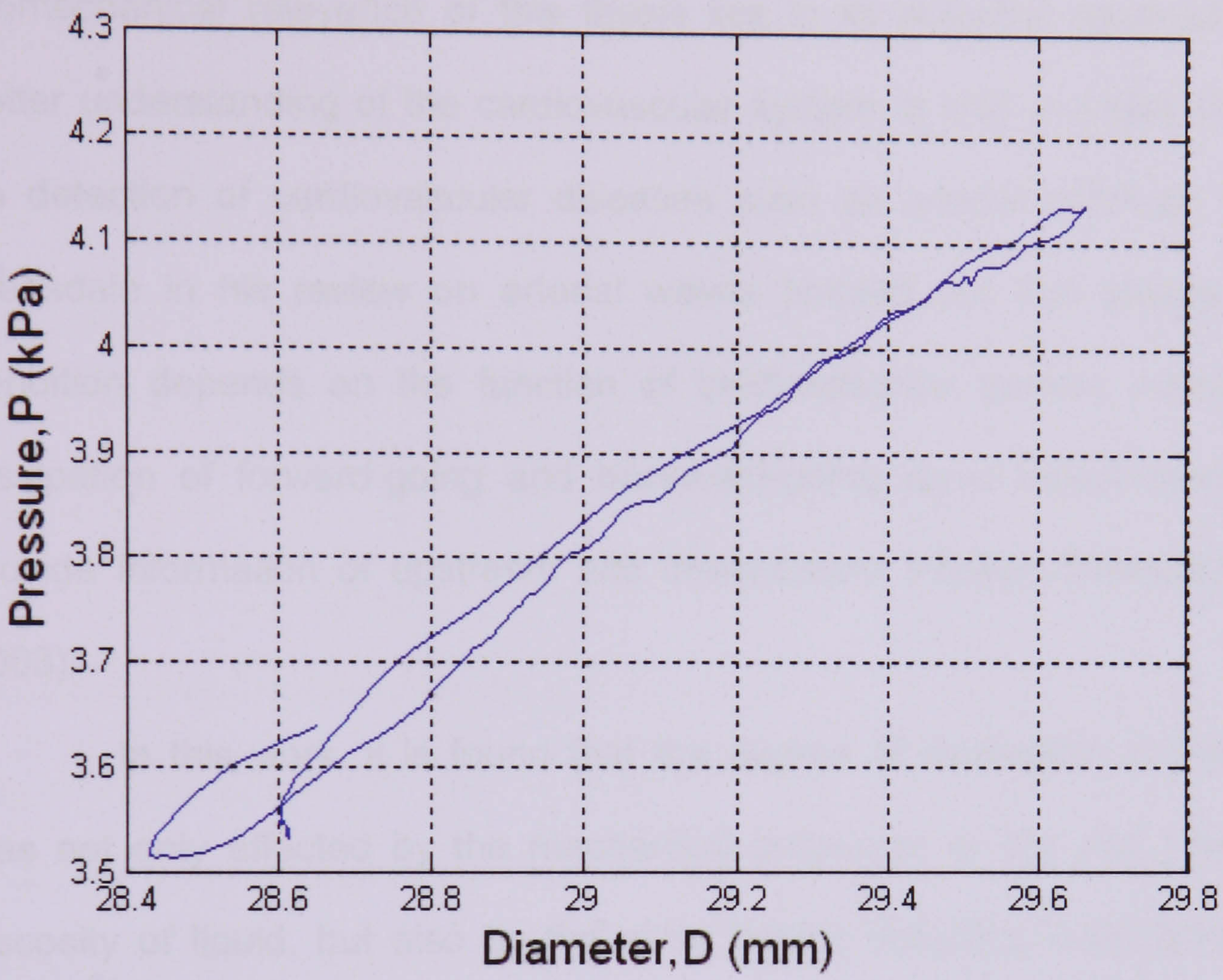

Figure 6.13 The hysteresis loop made by the measured pressure and diameter at the position of 15 cm away from inlet in 24 mm tube.

Chapter 7

Discussion and Conclusion

Biomechanical relevance of this thesis lies in its potential application to the better understanding of the cardiovascular system. It also provides information on detection of cardiovascular diseases such as arterial stiffness. Recently, Bleasdale in his review on arterial waves pointed out that patient's clinical condition depends on the function of cardiovascular system. Knowledge of dissipation of forward-going and backward-going wave independently would provide information of upstream and downstream arteries (Bleasdale, et al. , 2003).

In this work, it is found that the degree of dissipation in flexible tube was not only affected by the mechanical properties of the wall property and viscosity of liquid, but also by the other factors including initial pressure and pumping speed (Chapter 4), as well as direction of wave in relation to direction of flow (Chapter 5). Also, the pressure and velocity pulse are affected by these factors. It is known that walls of aorta in human become gradually stiffer and tapered towards the peripheral arteries. In this research, it is found that stiffer tubes and smaller sized tubes resulted in greater dissipation, from which we may extrapolate that blood wave energy could dissipate more in the peripheral arteries than in the large arteries. Also, we found with higher pumping speed, wave energy dissipated more, which could imply that the higher heart rates might induce greater wave dissipation in the arterial system.

Blood waves are reflected in the periphery of the arterial tree. The observed propagation coefficient is consequently affected by the reflecting properties of

the whole arterial system and by local physical conditions (Minor, 1989). In this research, the technique of separation of wave into the forward and backward directions using WIA allows us to investigate the dissipation of waves in the forward and backward directions independently, excluding the effect of reflection wave. Therefore, in our research degree of dissipation in either forward or backward directions was only affected by the local physical condition.

To date, the propagation of wave during the pulling action has not been explored although it is very important in the cardiovascular system (Davies, 2006). In this research, the propagation of waves during the pulling action has been compared with that during the pushing action using parameters, such as the pressure and velocity pulse, wave speed and the dissipation. Also, a mechanism for the different propagation behaviour of waves during the pulling and pushing action has been suggested. Introduction of this unexplored topic could bring in further information about the behaviour of the flow in different locations in the cardiovascular system.

Wave intensity analysis allows for the separation of wave into their forward and backward directions using the measured pressure and velocity. However, the measurement of pressure is normally taken invasively. The method of separation of waves proposed in this research using the measured diameter and velocity provides a potential non-invasive technique for the separation of waves into their forward and backward directions. The arrival times of reflected waves detected by the backward pressure and backward diameter are very close, further confirming the validation of the new method introduced in this thesis. The derivation of the equation (6.11) is based on the water-hammer equation and the relationship of wave speed and distensibility,

which does not make any assumption of linearity of tube wall and also accommodates the convective effect. The difference between measurement of wave speed determined by PU-loop and DU-loop might be caused by the viscoelastic property of tube wall.

There are a few conclusions withdrawn from this research:

1. Dissipation of wave in flexible tube in time domain can be investigated in the forward and backward directions independently using the WIA.
2. The amplitudes of separated forward and backward pressure dissipated exponentially along the travelling distance. Similarly, the wave intensity and wave energy also dissipated along the travelling distance as an exponential equation.
3. The degree of wave dissipation in flexible tube is not only affected by the wall property and viscosity of liquid but also by the experimental conditions, including the initial pressure and the pumping speed. The smaller the tube size the greater the dissipation, and the dissipation is greater when the initial pressure is lower. Also, the greater dissipation is associated with faster speed of pumping.
4. The pressure and velocity pulses are also affected by the initial experimental conditions and wall property. It is found: (a) the stiffer the tube wall the greater the pressure and velocity pulse; (b) the faster the pumping speed the greater the pressure and velocity pulse; (c) the lower the initial pressure the greater the pressure and velocity pulse.

5. Local wave speed in flexible tubes is flow-direction and wave-nature dependant; greater with expansion than compression waves. Wave dissipation has an inverse relationship with vessel diameter and dissipation of the expansion wave in a backward flow induced by a pulling action is greater than that of a forward flow induced by a pushing action. Under the same initial experimental conditions the amplitude of pressure waveforms generated in the forward direction during the pushing action are smaller than those generated in the backward direction during the pulling action. Amplitude of velocity during the pulling action is greater than that in the pushing action due to reduced diameter resulting from the expansion wave.
6. The algorithm derived in this thesis for determining wave speed and wave intensity only using measurement of diameter and velocity at one point could potentially be non-invasively. Wave speed determined by DU-loop is slightly less than that determined by PU-loop. The timing of peak of forward compression and expansion wave intensity based on pressure and velocity highly agreed with the corresponding timing based on diameter and velocity. Therefore, we concluded that the new technique can be used to determine wave speed and wave intensity using measurement of diameter instead of pressure.

Future Work

In this thesis, the dissipation of waves has been investigated when the properties of tube wall and dimension are uniform along the travelling length. Segers suggested that the tapering of aorta is one of factor affecting the wave reflection indices (Segers, 2000). Also, we have not study the effect of gravity on wave dissipation. Therefore, further work should be done in the areas as follows:

(1) Dissipation of waves will be investigated in the tapered tube rather than uniform tube.

(2) Effect of gravity on wave dissipation will also be investigated in the future.

(3) To investigate the source of wave dissipation, the relationship between the energy stored in the wall and wave intensity will be investigated in vitro and in vivo.

Lists of publications

(1) Feng J, Long Q, Khir AW.Wave dissipation in flexible tubes in the time domain: in vitro model of arterial waves. J Biomech. 2007;40(10):2130-8. Epub 2006 Dec 12.

(2) Feng J, Khir AW.Determination of wave intensity in flexible tubes using measured diameter and velocity Conf Proc IEEE Eng Med Biol Soc. 2007;2007:985

(3) Feng J, Khir AW.A new approach to investigate wave dissipation in viscoelastic tubes: application of Wave Intensity Analysis, Conf Proc IEEE Eng Med Biol Soc. 2005;3(1):2260-2263.

(4) Feng J, Khir AW The Compression and expansion waves of the forward and backward flows: an in-vitro arterial model, Institute of Mechanical Engineering, Part H: Journal of Engineering in Medcine, DOI: 10.1243/09544119JEIM339

(5) Khir AW, Swalen MJ, Feng J, Parker KH. Simultaneous determination of wave speed and arrival time of reflected waves using the pressure-velocity loop. Med Biol Eng Comput.2007 Dec;45(12):1201-10. Epub 2007. Aug

(6) Feng J, and Khir A. W., Determination of Wave speed and separation of wave using diameter and velocity (in progress).

References

ANLIKER, M., HISTAND, M.B. and OGDEN, E., 1968a. Dispersion and attenuation of small artificial pressure waves in the canine aorta. *Circulation research,* **23**(4), pp. 539-551.

ANLIKER, M., MORITZ, W.E. and OGDEN, E., 1968b. Transmission characteristics of axial waves in blood vessels. *Journal of Biomechanics,* **1**(4), pp. 235-246.

ANLIKER, M., WELLS, M.K. and OGDEN, E., 1969. The transmission characteristics of large and small pressure waves in the abdominal vena cava. *IEEE transactions on bio-medical engineering,* **16**(4), pp. 262-273.

ANLIKER, M., YATES, W.G. and OGDEN, E., 1971. Transmission of small pressure waves in the canine vena cava. *The American Journal of Physiology,* **221**(2), pp. 644-651.

ASMAR, R., RUDNICHI, A., BLACHER, J., LONDON, G.M. and SAFAR, M.E., 2001. Pulse pressure and aortic pulse wave are markers of cardiovascular risk in hypertensive populations. *American Journal of Hypertension: Journal of the American Society of Hypertension,* **14**(2), pp. 91-97.

BENETOS, A., WAEBER, B., IZZO, J., MITCHELL, G., RESNICK, L., ASMAR, R. and SAFAR, M., 2002. Influence of age, risk factors, and cardiovascular and renal disease on arterial stiffness: clinical applications. *American Journal of Hypertension : Journal of the American Society of Hypertension,* **15(12)**, pp. 1101-1108.

BERGEL, D.H., 1961a. The static elastic properties of the arterial wall. *The Journal of physiology,* **156**(3), pp. 445-457.

BERGEL, D.H., 1961b. The dynamic elastic properties of the arterial wall. *The Journal of physiology,* **156**(3), pp. 458-469.

BERTRAM, C.D., 1980. Energy dissipation and pulse wave attenuation in the canine carotid artery. *Journal of Biomechanics,* **13**(12), pp. 1061-1073.

BERTRAM, C.D. and SHE, J., 1995. Analysis of the effects of measurement errors on the evaluation of propagation coefficients, in rubber tubes and canine aorta in vivo. *Technology and health care: official journal of the European Society for Engineering and Medicine*, 3(3), pp. 161-184.

BERTRAM, C.D., GOW, B.S. and GREENWALD, S.E., 1997. Comparison of different methods for the determination of the true wave propagation coefficient, in rubber tubes and the canine thoracic aorta. *Medical engineering & physics,* **19**(3), pp. 212-222.

BERTRAM, C.D., PYTHOUD, F., STERGIOPULOS, N. and MEISTER, J.J., 1999. Pulse wave attenuation measurement by linear and nonlinear methods in nonlinearly elastic tubes. *Medical engineering & physics,* **21**(3), pp. 155-166.

BIA, D., AGUIRRE, I., ZOCALO, Y., DEVERA, L., CABRERA FISCHER, E. and ARMENTANO, R., 2005. Regional differences in viscosity, elasticity and wall buffering function in systemic arteries: pulse wave analysis of the arterial pressure-diameter relationship. *Revista espanola de cardiologia,* **58**(2), pp. 167-174.

BLAND, J.M. and ALTMAN, D.G., 1986. Statistical methods for assessing agreement between two methods of clinical measurement. *Lancet,* **1**(8476), pp. 307-310.

BLEASDALE, R.A., MUMFORD, C.E., CAMPBELL, R.I., FRASER, A.G., JONES, C.J. and FRENNEAUX, M.P., 2003. Wave intensity analysis from the common carotid artery: a new noninvasive index of cerebral vasomotor tone. *Heart and vessels,* **18**(4), pp. 202-206.

BLEASDALE, R.A., PARKER, K.H. and JONES, C.J., 2003. Chasing the wave. Unfashionable but important new concepts in arterial wave travel. *American journal of physiology. Heart and circulatory physiology,* **284**(6), pp. H1879-85.

CARABELLO, B.A., 2006. Understanding coronary blood flow: the wave of the future. *Circulation,* **113**(14), pp. 1721-1722.

CARO, C.G., 1978. The mechanics of circulation. London: Oxford University Press.

DAVIES, J.E., WHINNETT, Z.I., FRANCIS, D.P., MANISTY, C.H., AGUADO-SIERRA, J., WILLSON, K., FOALE, R.A., MALIK, I.S., HUGHES, A.D., PARKER, K.H. and MAYET, J., 2006. Evidence of a dominant backward-propagating

"suction" wave responsible for diastolic coronary filling in humans, attenuated in left ventricular hypertrophy. *Circulation,* **113**(14), pp. 1768-1778.

DAVIES, J.E., WHINNETT, Z.I., FRANCIS, D.P., WILLSON, K., FOALE, R.A., MALIK, I.S., HUGHES, A.D., PARKER, K.H. and MAYET, J., 2006. Use of simultaneous pressure and velocity measurements to estimate arterial wave speed at a single site in humans. *American journal of physiology. Heart and circulatory physiology,* **290**(2), pp. H878-85.

EULAR, L., 1775. Principia pro motu sanguinis per arterias determinado: Opera Posthuma Mathematica et Physica Anno 1844 detecta, 2 ediderunt PH Fuss et N Fuss Petropoli; *Apund Eggers et Socios,*.

FENG, J. and KHIR, A.W., 2007. Determination of wave intensity in flexible tubes using measured diameter and velocity. *Conference proceedings: Annual International Conference of the IEEE Engineering in Medicine and Biology Society. IEEE Engineering in Medicine and Biology Society. Conference,* **2007**, pp. 985-988.

FENG, J., LONG, Q. and KHIR, A.W., 2007. Wave dissipation in flexible tubes in the time domain: in vitro model of arterial waves. *Journal of Biomechanics,* **40**(10), pp. 2130-2138.

FENG, J., and KHIR, A.W., 2008. The compression and expansion waves of the forward and backward flows: An In vitro arterial model, *Journal of Engineering in Medicine, Proceedings of the Institution of Mechanical Engineers – Part H (In press)*

FLEWITT, J.A., HOBSON, T.N., WANG, J.,JR, JOHNSTON, C.R., SHRIVE, N.G., BELENKIE, I., PARKER, K.H. and TYBERG, J.V., 2007. Wave intensity analysis of left ventricular filling: application of windkessel theory. *American journal of physiology. Heart and circulatory physiology,* **292**(6), pp. H2817-23.

FUNG, Y.C., 1981. Biomechanics: Mechanical Properties of Living Tissues. Spring-Verlag New York.

GOW, B.S. and TAYLOR, M.G., 1968. Measurement of viscoelastic properties of arteries in the living dog. *Circulation research,* **23**(1), pp. 111-122.

GREENWALD, S.E., NEWMAN, D.L. and MOODIE, T.B., 1985. Impulse propagation in rubber-tube analogues of arterial stenoses and aneurysms. *Medical & biological engineering & computing,* **23**(2), pp. 150-154.

HARADA, A. and ET AL., 2000. Development of a Non-invasive Real-time Measurement System of Wave Intensity, 2000, IEEE Ultrasonic Symposium.. *IEEE Ultrasonic Symposium, .*

HARADA, A., OKADA, T., NIKI, K., CHANG, D. and SUGAWARA, M., 2002. On-line noninvasive one-point measurements of pulse wave velocity. *Heart and vessels,* **17**(2), pp. 61-68.

HELLEVIK, L.R., SEGERS, P., STERGIOPULOS, N., IRGENS, F., VERDONCK, P., THOMPSON, C.R., LO, K., MIYAGISHIMA, R.T. and SMISETH, O.A., 1999. Mechanism of pulmonary venous pressure and flow waves. *Heart and vessels,* **14**(2), pp. 67-71.

HISTAND, M.B. and ANLIKER, M., 1973. Influence of flow and pressure on wave propagation in the canine aorta. *Circulation research,* **32**(4), pp. 524-529.

HOBSON, T.N., FLEWITT, J.A., BELENKIE, I. and TYBERG, J.V., 2007. Wave intensity analysis of left arterial mechanics and energetic in anesthetized dogs. *American journal of physiology. Heart and circulatory physiology,* **292**(3), pp. H1533-40.

HORSTEN, J.B., VAN STEENHOVEN, A.A. and VAN DONGEN, M.E., 1989. Linear propagation of pulsatile waves in viscoelastic tubes. *Journal of Biomechanics,* **22**(5), pp. 477-484.

IMHOLZ, B.P., WIELING, W., VAN MONTFRANS, G.A. and WESSELING, K.H., 1998. Fifteen years experience with finger arterial pressure monitoring: assessment of the technology. *Cardiovascular research,* **38**(3), pp. 605-616.

JONES, C.J., PARKER, K.H., HUGHES, R. and SHERIDAN, D.J., 1992. Nonlinearity of human arterial pulse wave transmission. *Journal of Biomechanical Engineering,* **114**(1), pp. 10-14.

JONES, C.J., SUGAWARA, M., KONDOH, Y., UCHIDA, K. and PARKER, K.H., 2002. Compression and expansion wavefront travel in canine ascending aortic flow: wave intensity analysis. *Heart and vessels,* **16**(3), pp. 91-98.

JONES, C.J.H. and PARKER, K.H., 1994. Arterial wave intensity: physical meaning and physiological significance. ***Recent progress in cardiovascular mechanics***. Harwood academic publishers, pp. 129-148.

JONES, E., ANLIKER, M. and CHANG, I.D., 1971. Effects of viscosity and constraints on the dispersion and dissipation of waves in large blood vessels. II. Comparison of analysis with experiments. *Biophysical journal,* **11**(12), pp. 1121-1136.

JONES, E., ANLIKER, M. and CHANG, I.D., 1971. Effects of viscosty and constraints on the dispersion and dissipation of waves in large blood vessels. I. Theoretical analysis. *Biophysical journal,* **11**(12), pp. 1085-1120.

KEREN, G. and MARON, B.J., 1995. Patterns of pulmonary venous and transmitral flow velocity in patients with hypertrophic cardiomyopathy. *Journal of the American Society of Echocardiography : official publication of the American Society of Echocardiography,* **8**(4), pp. 494-502.

KEREN, G., SHEREZ, J., MEGIDISH, R., LEVITT, B. and LANIADO, S., 1985. Pulmonary venous flow pattern--its relationship to cardiac dynamics. A pulsed Doppler echocardiographic study. *Circulation,* **71**(6), pp. 1105-1112.

KHIR, A.W., O'BRIEN, A., GIBBS, J.S. and PARKER, K.H., 2001. Determination of wave speed and wave separation in the arteries. *Journal of Biomechanics,* **34**(9), pp. 1145-1155.

KHIR, A.W. and PARKER, K.H., 2005. Wave intensity in the ascending aorta: effects of arterial occlusion. *Journal of Biomechanics,* **38**(4), pp. 647-655.

KHIR, A.W., SWALEN, M.J., FENG, J. and PARKER, K.H., 2007. Simultaneous determination of wave speed and arrival time of reflected waves using the pressure-velocity loop. *Medical & biological engineering & computing,* **45**(12), pp. 1201-1210.

KHIR, A.W., ZAMBANINI, A. and PARKER, K.H., 2004. Local and regional wave speed in the aorta: effects of arterial occlusion. *Medical engineering & physics,* **26**(1), pp. 23-29.

KOH, T.W., PEPPER, J.R., DESOUZA, A.C. and PARKER, K.H., 1998. Analysis of wave reflections in the arterial system using wave intensity: a novel method for

predicting the timing and amplitude of reflected waves. *Heart and vessels,* **13**(3), pp. 103-113.

KORTEWEG, D.J., 1878. Ueber die Fortpflanzungsgeschwindigkeit des Schalles in elastischen Röhren. *Annalen der Physik und Chemie Ser,* **3**, pp. 525-542.

LATHAM, R.D., RUBAL, B.J., WESTERHOF, N., SIPKEMA, P. and WALSH, R.A., 1987. Nonhuman primate model for regional wave travel and reflections along aortas. *The American Journal of Physiology,* **253(2 Pt 2),** pp. H299-306.

LATHAM, R.D., SIPKEMA, P., WESTERHOF, N. and RUBAL, B.J., 1988. Aortic input impedance during Mueller maneuver: an evaluation of "effective length". *Journal of applied physiology (Bethesda, Md.: 1985),* **65**(4), pp. 1604-1610.

LATHAM, R.D., WESTERHOF, N., SIPKEMA, P., RUBAL, B.J., REUDERINK, P. and MURGO, J.P., 1985. Regional wave travel and reflections along the human aorta: a study with six simultaneous micromanometric pressures. *Circulation,* **72**(6), pp. 1257-1269.

LAURENT, S., BOUTOUYRIE, P., ASMAR, R., GAUTIER, I., LALOUX, B., GUIZE, L., DUCIMETIERE, P. and BENETOS, A., 2001. Aortic stiffness is an independent predictor of all-cause and cardiovascular mortality in hypertensive patients. *Hypertension,* **37**(5), pp. 1236-1241.

LEAROYD, B.M. and TAYLOR, M.G., 1966. Alterations with age in the viscoelastic properties of human arterial walls. *Circulation research,* **18**(3), pp. 278-292.

LIGHTHILL, J., 1978. Waves in fluids. Cambridge: Cambridge University Press.

MACRAE, J.M., SUN, Y.H., ISAAC, D.L., DOBSON, G.M., CHENG, C.P., LITTLE, W.C., PARKER, K.H. and TYBERG, J.V., 1997. Wave-intensity analysis: a new approach to left ventricular filling dynamics. *Heart and vessels,* **12**(2), pp. 53-59.

MAXWELL, J.A. and ANLIKER, M., 1968. The dissipation and dispersion of small waves in arteries and veins with viscoelastic wall properties. *Biophysical journal,* **8**(8), pp. 920-950.

MCDONALD, D.A., 1974. Blood Flow in Arteries. Edward Arnold Ltd.

MCDONALD, D.A., 1968. Wave attenuation in visco-elastic arteries. *Hemorheology.* Oxford: A.L.Copley, Pergamon Press, pp. 113-125.

MEINDERS, J.M. and HOEKS, A.P., 2004. Simultaneous assessment of diameter and pressure waveforms in the carotid artery. *Ultrasound in medicine & biology,* **30**(2), pp. 147-154.

MILNOR, W.R., 1989. *Hemodynamics*. Baltimore, Maryland, USA.: Williams&Wilkins.

MILNOR, W.R. and BERTRAM, C.D., 1978. The relation between arterial viscoelasticity and wave propagation in the canine femoral artery in vivo. *Circulation research,* **43**(6), pp. 870-879.

MILNOR, W.R. and NICHOLS, W.W., 1975. A new method of measuring propagation coefficients and characteristic impedance in blood vessels. *Circulation research,* **36**(5), pp. 631-639.

MORITZ, W.E. and ANLIKER, M., 1974. Wave transmission characteristics and anisotropy of canine carotid arteries. *Journal of Biomechanics,* **7**(2), pp. 151-154.

MURGO, J.P., WESTERHOF, N., GIOLMA, J.P. and ALTOBELLI, S.A., 1981. Effects of exercise on aortic input impedance and pressure wave forms in normal humans. *Circulation research,* **48**(3), pp. 334-343.

MURGO, J.P., WESTERHOF, N., GIOLMA, J.P. and ALTOBELLI, S.A., 1980. Aortic input impedance in normal man: relationship to pressure wave forms. *Circulation,* **62**(1), pp. 105-116.

NEWMAN, D.L., GREENWALD, S.E. and DENYER, H.T., 1981. Impulse propagation in normal and stenosed vessels. *Cardiovascular research,* **15**(4), pp. 190-195.

NICHOLS, W.W. and O'ROURKE, M.F., 2005. McDonald's Blood Flow in Arteries Theoretical, experimental, and clinical principles. Arnold, London, Sydney, Auckland.

NICHOLS, W.W. and O'ROURKE, M.F., 1998. McDonald's blood flow in arteries: theoretical, experimental and clinical principles. New York: Arnold, Oxford University Press, Inc.

NICHOLS, W.W., 2005. Clinical measurement of arterial stiffness obtained from noninvasive pressure waveforms. *American Journal of Hypertension : Journal of the American Society of Hypertension,* **18**(1 Pt 2), pp. 3S-10S.

NICHOLS, W.W. and EDWARDS, D.G., 2001. Arterial elastance and wave reflection augmentation of systolic blood pressure: deleterious effects and implications for therapy. *Journal of cardiovascular pharmacology and therapeutics,* **6**(1), pp. 5-21.

NIKI, K., SUGAWARA, M., CHANG, D., HARADA, A., OKADA, T., SAKAI, R., UCHIDA, K., TANAKA, R. and MUMFORD, C.E., 2002. A new noninvasive measurement system for wave intensity: evaluation of carotid arterial wave intensity and reproducibility. *Heart and vessels,* **17**(1), pp. 12-21.

NIKI, K., SUGAWARA, M., UCHIDA, K., TANAKA, R., TANIMOTO, K., IMAMURA, H., SAKOMURA, Y., ISHIZUKA, N., KOYANAGI, H. and KASANUKI, H., 1999. A noninvasive method of measuring wave intensity, a new hemodynamic index: application to the carotid artery in patients with mitral regurgitation before and after surgery. *Heart and vessels,* **14**(6), pp. 263-271.

NOBUOKA, S., AONO, J., NAGASHIMA, J., ANDO, H., ADACHI, H., IMAI, Y., SHIBAMOTO, M., TANAKA, H., MIYAKE, F. and MURAYAMA, M., 2001. Assessment of reflection pulse wave in patients with cardiomyopathy: evaluation of noninvasive measurement of wave intensity. *Acta Cardiologica,* **56**(5), pp. 283-287.

OHTE, N., NARITA, H., SUGAWARA, M., NIKI, K., OKADA, T., HARADA, A., HAYANO, J. and KIMURA, G., 2003. Clinical usefulness of carotid arterial wave intensity in assessing left ventricular systolic and early diastolic performance. *Heart and vessels,* **18**(3), pp. 107-111.

O'Brien A., 2003, Pulmonary hemodynamics. PhD thesis. Imperial College, London.

O'ROURKE, M.F., 1967. Steady and pulsatile energy losses in the systemic circulation under normal conditions and in simulated arterial disease. *Cardiovascular research,* **1**(4), pp. 313-326.

O'ROURKE, M.F. and PAUCA, A.L., 2004. Augmentation of the aortic and central arterial pressure waveform. *Blood pressure monitoring,* **9**(4), pp. 179-185. .

O'ROURKE, M.F., STAESSEN, J.A., VLACHOPOULOS, C., DUPREZ, D. and PLANTE, G.E., 2002. Clinical applications of arterial stiffness; definitions and reference values. *American Journal of Hypertension : Journal of the American Society of Hypertension,* **15**(5), pp. 426-444.

PARKER, K.H., JONES, C.J., DAWSON, J.R. and GIBSON, D.G., 1988. What stops the flow of blood from the heart? *Heart and vessels,* **4**(4), pp. 241-245.

PARKER, K.H. and JONES, C.J.H., 1990. Forward and backward running waves in the arteries: analysis using the method of characteristics. *Transactions of the ASME. Journal of Biomechanical* Engineering, 112(3), pp. 322-6.

PEDLEY, T.J., 1980. The fluid mechanics of large blood vessels. Cambridge: Cambridge: C.U.P.

PYTHOUD, F., STERGIOPULOS, N., BERTRAM, C.D. and MEISTER, J.J., 1996. Effects of friction and nonlinearities on the separation of arterial waves into their forward and backward components. *Journal of Biomechanics,* **29**(11), pp. 1419-1423.

PYTHOUD, F., STERGIOPULOS, N. and MEISTER, J.J., 1996. Separation of arterial pressure waves into their forward and backward running components. *Journal of Biomechanical Engineering,* **118**(3), pp. 295-301.

RAMSEY, M.W. and SUGAWARA, M., 1997. Arterial wave intensity and ventriculoarterial interaction. *Heart and vessels,* **Suppl 12**, pp. 128-134.

RENEMAN, R.S., MEINDERS, J.M. and HOEKS, A.P., 2005. Non-invasive ultrasound in arterial wall dynamics in humans: what have we learned and what remains to be solved. *European heart journal,* **26**(10), pp. 960-966.

REUDERINK, P., SIPKEMA, P. and WESTERHOF, N., 1988. Influence of geometric taper on the derivation of the true propagation coefficient using a three point method. *Journal of Biomechanics,* **21**(2), pp. 141-153.

REUDERINK, P.J., HOOGSTRATEN, H.W., SIPKEMA, P., HILLEN, B. and WESTERHOF, N., 1989. Linear and nonlinear one-dimensional models of pulse

wave transmission at high Womersley numbers. *Journal of Biomechanics,* **22**(8-9), pp. 819-827.

SCHOFIELD, R.S., SCHULER, B.T., EDWARDS, D.G., ARANDA, J.M.,JR, HILL, J.A. and NICHOLS, W.W., 2002. Amplitude and timing of central aortic pressure wave reflections in heart transplant recipients. *American Journal of Hypertension : Journal of the American Society of Hypertension,* **15**(9), pp. 809-815.

SCHULTZ, D.J., TUNSTALL-PEDOE, D.S., LEE, F.J., FUNNING, A.J. and BELHOUSE, B.J., 1969. Velocity distribution and transition in the arterial system. *In Ciba symposium on Circulatory and Respiratory and Mass Transport.* Chuichill, London: Wolstenholme GEW and Knight J Eds,.

SEGERS, P. and VERDONCK, P., 2000. Role of tapering in aortic wave reflection: hydraulic and mathematical model study. *Journal of Biomechanics,* **33**(3), pp. 299-306.

SHAU, Y.W., WANG, C.L., SHIEH, J.Y. and HSU, T.C., 1999. Noninvasive assessment of the viscoelasticity of peripheral arteries. *Ultrasound in medicine & biology,* **25**(9), pp. 1377-1388.

Sherwin, S.J., Franke, F., Peiro, J., Parker, K., 2003, One-dimensional modeling of a vascular network in spece-time variables, *Journal of Engineering Mathematics*, **47**, 217-250.

SMISETH, O.A., THOMPSON, C.R., LOHAVANICHBUTR, K., LING, H., ABEL, J.G., MIYAGISHIMA, R.T., LICHTENSTEIN, S.V. and BOWERING, J., 1999. The pulmonary venous systolic flow pulse--its origin and relationship to left atrial pressure. *Journal of the American College of Cardiology,* **34**(3), pp. 802-809.

SUGAWARA, M., NIKI, K., FURUHATA, H., OHNISHI, S. and SUZUKI, S., 2000. Relationship between the pressure and diameter of the carotid artery in humans. *Heart and vessels,* **15**(1), pp. 49-51.

SUN, Y., BELENKIE, I., WANG, J.J. and TYBERG, J.V., 2006. Assessment of right ventricular diastolic suction in dogs with the use of wave intensity analysis. *American journal of physiology. Heart and circulatory physiology,* **291**(6), pp. H3114-21.

SUN, Y.H., ANDERSON, T.J., PARKER, K.H. and TYBERG, J.V., 2004. Effects of left ventricular contractility and coronary vascular resistance on coronary dynamics. *American journal of physiology. Heart and circulatory physiology,* **286**(4), pp. H1590-5.

SUN, Y.H., ANDERSON, T.J., PARKER, K.H. and TYBERG, J.V., 2000. Wave-intensity analysis: a new approach to coronary hemodynamics. *Journal of applied physiology (Bethesda, Md.: 1985),* **89**(4), pp. 1636-1644.

TABATA, T., THOMAS, J.D. and KLEIN, A.L., 2003. Pulmonary venous flow by Doppler echocardiography: revisited 12 years later. *Journal of the American College of Cardiology,* **41**(8), pp. 1243-1250.

TAYLOR, M.G., 1959. Wave travles in arteries. PhD edn. University of London: University of London.

UEDA, H., HAYASHI, T., TSUMURA, K., YOSHIMARU, K., NAKAYAMA, Y. and YOSHIKAWA, J., 2004. The timing of the reflected wave in the ascending aortic pressure predicts restenosis after coronary stent placement. *Hypertension research : official journal of the Japanese Society of Hypertension,* **27**(8), pp. 535-540.

URSINO, M. and ARTIOLI, E., 1992. Wave propagation in the silicon tube: comparison of the two-point and three-point pressure methods. *Bio-medical materials and engineering,* **2**(3), pp. 155-169.

URSINO, M., ARTIOLI, E. and GALLERANI, M., 1994. An experimental comparison of different methods of measuring wave propagation in viscoelastic tubes. *Journal of Biomechanics,* **27**(7), pp. 979-990.

URSINO, M., ARTIOLI, E. and GALLERANI, M., 1993. Wave propagation with different pressure signals: an experimental study on the latex tube. *Medical & biological engineering & computing,* **31**(4), pp. 363-371.

VAN BORTEL, L.M., BALKESTEIN, E.J., VAN DER HEIJDEN-SPEK, J.J., VANMOLKOT, F.H., STAESSEN, J.A., KRAGTEN, J.A., VREDEVELD, J.W., SAFAR, M.E., STRUIJKER BOUDIER, H.A. and HOEKS, A.P., 2001. Non-invasive assessment of local arterial pulse pressure: comparison of applanation tonometry and echo-tracking. *Journal of hypertension,* **19**(6), pp. 1037-1044.

VAN DEN BOS, G.C., WESTERHOF, N. and RANDALL, O.S., 1982. Pulse wave reflection: can it explain the differences between systemic and pulmonary pressure and flow waves? A study in dogs. *Circulation research,* **51**(4), pp. 479-485.

VERBEKE, F., VAN BIESEN, W., PEETERS, P., VAN BORTEL, L.M. and VANHOLDER, R.C., 2007. Arterial stiffness and wave reflections in renal transplant recipients. *Nephrology, dialysis, transplantation : official publication of the European Dialysis and Transplant Association - European Renal Association,* **22**(10), pp. 3021-3027.

WANG, J.J. and PARKER, K.H., 2004. Wave propagation in a model of the arterial circulation. *Journal of Biomechanics,* **37**(4), pp. 457-470.

WANG, Z., JALALI, F., SUN, Y.H., WANG, J.J., PARKER, K.H. and TYBERG, J.V., 2005. Assessment of left ventricular diastolic suction in dogs using wave-intensity analysis. *American journal of physiology. Heart and circulatory physiology,* **288**(4), pp. H1641-51.

WESTERHOF, N., SIPKEMA, P., VAN DEN BOS, G.C. and ELZINGA, G., 1972. Forward and backward waves in the arterial system. *Cardiovascular research,* **6**(6), pp. 648-656.

WOMERSLEY, J.R., 1957. Oscillatory flow in arteries: the constrained elastic tube as a model of arterial flow and pulse transmission. *Physics in Medicine and Biology,* **2**(2), pp. 178-187.

ZAMBANINI, A., CUNNINGHAM, S.L., PARKER, K.H., KHIR, A.W., MCG THOM, S.A. and HUGHES, A.D., 2005. Wave-energy patterns in carotid, brachial, and radial arteries: a noninvasive approach using wave-intensity analysis. *American journal of physiology. Heart and circulatory physiology,* **289**(1), pp. H270-6.